Wave attenuation over the Oesterdam tidal flat nourishment

Wind-wave transformation in the intertidal zone

Master Thesis

Yahia Kala

Deltares

TU Delft Delft University of Technology

ERASMUS +: ERASMUS MUNDUS MOBILITY PROGRAMME

Master of Science in

COASTAL AND MARINE ENGINEERING AND MANAGEMENT

CoMEM

WAVE ATTENUATION OVER THE OESTERDAM TIDAL FLAT NOURISHMENT

Delft University of Technology
4 July 2016

Yahia Kala

The Erasmus+: Erasmus Mundus MSc in Coastal and Marine Engineering and Management is an integrated programme including mobility organized by five European partner institutions, coordinated by Norwegian University of Science and Technology (NTNU).

The joint study programme of 120 ECTS credits (two years full-time) has been obtained at two or three of the five CoMEM partner institutions:

- Norges Teknisk- Naturvitenskapelige Universitet (NTNU) Trondheim, Norway
- Technische Universiteit (TU) Delft, The Netherlands
- Universitat Politècnica de Catalunya (UPC). BarcelonaTech. Barcelona, Spain
- University of Southampton, Southampton, Great Britain
- City University London, London, Great Britain

During the first three semesters of the programme, students study at two or three different universities depending on their track of study. In the fourth and final semester an MSc project and thesis has to be completed. The two-year CoMEM programme leads to a multiple set of officially recognized MSc diploma certificates. These will be issued by the universities that have been attended by the student. The transcripts issued with the MSc Diploma Certificate of each university include grades/marks and credits for each subject.

Information regarding the CoMEM programme can be obtained from the programme coordinator:

Øivind A. Arntsen, Dr.ing.
Associate professor in Marine Civil Engineering
Department of Civil and Transport Engineering
NTNU Norway
Telephone: +4773594625 Cell: +4792650455 Fax: + 4773597021
Email: oivind.arntsen@ntnu.no

CoMEM URL: https://www.ntnu.edu/studies/mscomem

CoMEM Thesis

This thesis was completed by:
Yahia Kala

Under supervision of:
Prof. dr. ir. A.J.H.M. Reniers (TU Delft, Chair)
Dr. ir. J. van der Werf (Deltares)
Ir. P.L.M. de Vet (TU Delft, Deltares)
Dr. ir. B. Hofland (TU Delft, Deltares)

As a requirement to attend the degree of
Erasmus+: Erasmus Mundus Master in Coastal and Marine Engineering and Management (CoMEM)

Taught at the following educational institutions:

Norges Teknisk- Naturvitenskapelige Universitet (NTNU)
Trondheim, Norway

Technische Universiteit (TU) Delft
Delft, The Netherlands

University of Southampton,
Southampton, Great Britain

At which the student has studied from August 2014 to July 2016.

إلى أمي وأبي الأعزاء

To my dear mother and father

SUMMARY

The Oesterdam tidal flat nourishment is a hook-shaped nourishment that was constructed in November 2013 in the Kom area of the Eastern Scheldt. One of the objectives of the nourishment is to increase the design life of the Oesterdam in the face of increasing wave loads due to structural erosion of the intertidal flats. A study is conducted in order to examine the available hydrodynamic and morphological data, validate an existing hydrodynamic model, and estimate projections of design wave loads.

The morphological development of the Oesterdam nourishment is examined from bathymetric surveys. In order to estimate the post-nourishment erosion rates, trend analysis is done on bathymetric surveys done over 2.5 years. The nourishment is estimated to erode at an average rate of 1.3 to 2.1 cm /year. Several limitations in the trend analysis, including summer seasonal bias and the lack of surveys, contribute to uncertainty in the estimated trends. Projections of erosion at the Oesterdam flat up until the year 2080 are presented.

A Delft3D FLOW/WAVE model is used in order to simulate the water levels, waves, and currents in the Eastern Scheldt and in the Kom, including over the Oesterdam nourishment. Measured water level data, pressure data and current data are used to partially validate model results. The results show generally good agreement in calculated wave pressures, while a small structural underestimation in wave periods and current velocities is noted. The dominant processes of wave transformation are deemed to be local wind-wave generation, whitecapping, and bottom friction. The nourishment hook has a noticeable wave damping effect at lower water levels when there is more interaction with the bed.

The Delft3D FLOW/WAVE model, in conjunction with projected erosion rates, is used to estimate future design wave loads on the Oesterdam. Load functions, which are combinations of wave height and wave period, are used to examine the changes in wave loads over time. At the design water level of 4 m and the design wind speed of 30-32 m/s, the wave loads show a noticeable decrease with the nourishment compared to the no-nourishment scenario. However, wave growth over the nourishment shows that the nourishment hook plays no role in the wave height at the toe of the Oesterdam. Therefore, the part of the nourishment at the foot of the dam is the cause of the lower design wave loads.

Recommendations for future work include further validation of the Delft3D model for more extreme measured conditions, the simulation of morphological changes on an annual basis, and the continued use of pressure transducers mindful of their limitations. In addition, a detailed safety assessment of the Oesterdam, with the effects of long term erosion taken into account, is recommended.

ACKNOWLEDGMENTS

The thesis was completed at TU Delft and Deltares. I would like to thank the following people for their help in providing data and expert advice:

- Jan van het Westende (RWS)
- Jan de Bel (RWS)
- Mariska Bijleveld (RWS)
- Edwin Paree (HZ)
- Matthijs Boersema (HZ)
- Erik Arnold (Royal Haskoning)
- Ivo Wenneker (Deltares)
- Robert 't Hart (Deltares)
- Caroline Gautier (Deltares)

Special thanks to my committee members Lodewijk de Vet, Ad Reniers, Jebbe van der Werf, and Bas Hofland for their guidance throughout the thesis project. Last but not least, I would like to thank my CoMEM colleagues Ana, Stuart, Alejandra, Gerald, John, and Dennis for their support throughout the program.

Yahia Kala
Delft, June 20, 2016

Cover image sources: www.rijksoverheid.nl, https://beeldbank.rws.nl, Rijkswaterstaat, Edwin Paree

CONTENTS

LIST OF FIGURES

LIST OF TABLES

1

INTRODUCTION

The Eastern Scheldt is a tidal basin located in the southwestern delta region of the Netherlands. The basin in its present form consists of a rather complicated set of channels, flats, marshes, and structures. At the inlet, a large open storm surge barrier regulates water levels during storm conditions. On the perimeter of the basin, dikes and other structures protect the hinterland from high waters caused by tide and storm surge. An overview of the basin features is shown in Figure 1.1.

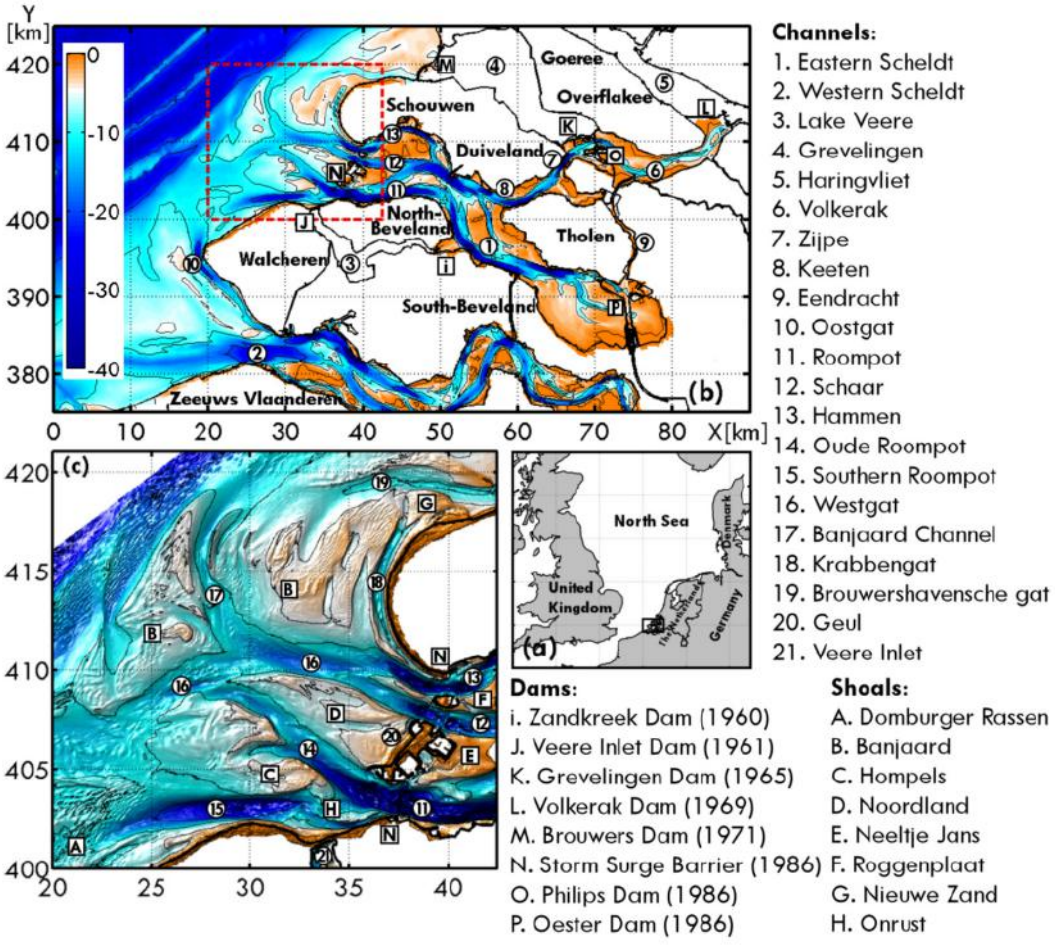

FIGURE 1.1: OVERVIEW OF ZEELAND AND THE DUTCH DELTA REGION. TAKEN FROM EELKEMA (2013)

As a result of the construction of the storm surge barrier and several closure dams, the Eastern Scheldt has been experiencing a problem called 'sand hunger' for several decades. This phenomenon is responsible for the long term erosion of the tidal flats and thus increased exposure of the dikes and closure dams to wave loads. This thesis focuses on the wave exposure of one particular closure dam: the Oesterdam.

The Oesterdam is located in the southeastern bulb of the Eastern Scheldt, called the 'Kom'. The Kom contains several tidal flats and marshes. One tidal flat in particular, the Oesterdam flat, was nourished with sand in November 2013. The nourishment was carried out in order to increase intertidal habitat and reduce the wave load on part of the Oesterdam. The nourishment project (including post-monitoring and analysis) is part of a larger network of projects and studies in the delta region. Figure 1.2 gives a simple overview of the projects carried out at the Oesterdam and the parties involved.

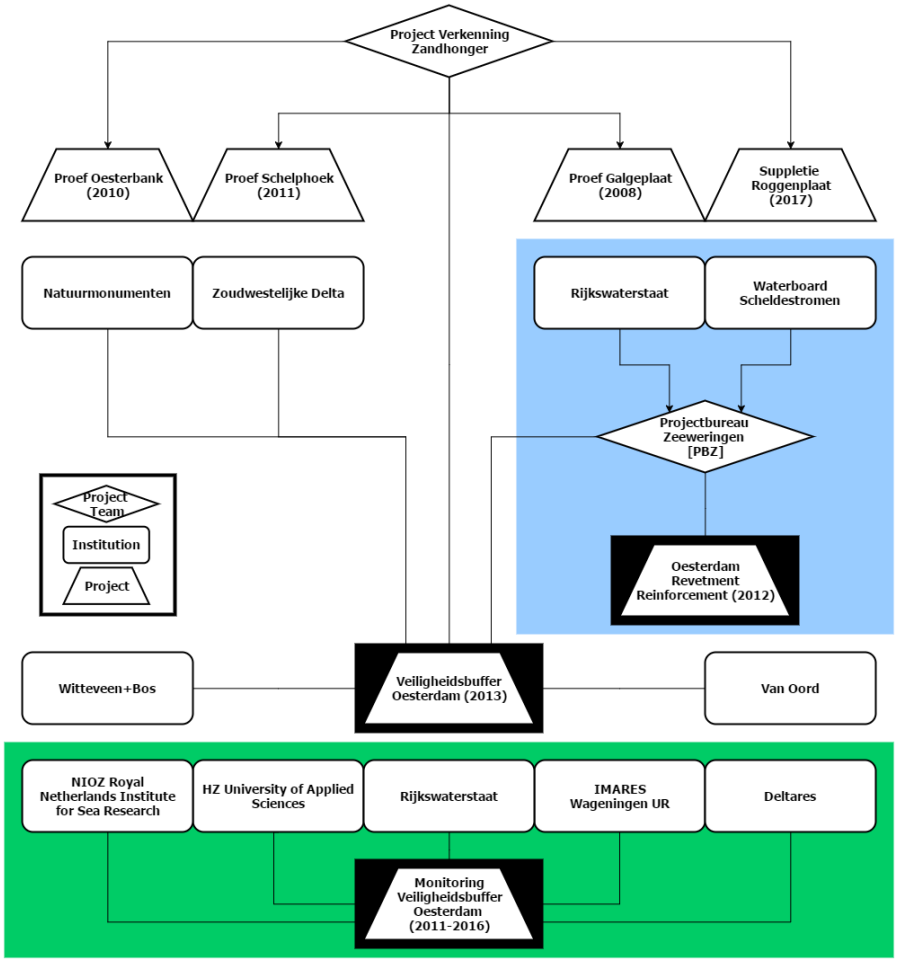

FIGURE 1.2: INSTITUTIONS, PROJECT TEAMS, AND PROJECTS RELATED TO THE OESTERDAM NOURISHMENT (VAN ZANTEN, 2012; BOERSEMA ET AL., 2014).

In short, the Oesterdam nourishment is the result of Project Veiligheidsbuffer Oesterdam, which itself is part of both Project Zeeweringen and Project Verkenning Zandhonger. The first project is a partnership between Rijkswaterstaat and the water board Scheldestromen, aimed at reinforcing the dike and dam revetments in the region. The second project (commissioned by Rijkswaterstaat) aims to investigate different ways to address the problems caused by sand hunger in the Eastern Scheldt.

The nourishment has implications for both projects due to its multi-functional design. Project Verkenning Zandhonger has several pilot projects in the Eastern Scheldt, the largest of which is the Oesterdam nourishment. An even larger nourishment is planned for the Roggenplaat in 2017/2018 (Boersema et al., 2015a).

A set of monitoring campaigns have been carried out to examine the physical and biological impacts of the Oesterdam nourishment. One measurement campaign was completed before the nourishment (T0: 2011) and two took place after the nourishment construction (T1: 2014 and T2: 2015/16) (Boersema et al., 2014, 2015b, 2016).

1.1. PROBLEM STATEMENT

Monitoring campaigns T0, T1, and T2 were carried out to help answer several questions related to the physical and biological impacts of the nourishment. One of the main questions yet to be answered is whether or not the Oesterdam nourishment has a significant impact on the wave exposure of the Oesterdam. Rijkswaterstaat estimates that the design life will be extended by 25-30 years based on measured erosion rates. However, the effect of the nourishment on the wave load has not been investigated. A need has been identified to determine the impact of the nourishment on waves propagating towards the dam.

In order to explore the effect of the nourishment during different environmental conditions, a hydrodynamic/wave model is needed to simulate design storm conditions at the site. However, there must be confidence in the results in order to apply the insights in practice. Specifically, the wave characteristics near the dam must be well represented. In order to build confidence in the model results, the model must be calibrated and validated at the site using measured data.

Two recent studies have attempted to perform this calibration and validation using Delft3D, one of which was focused on the Oesterdam nourishment (Das, 2010; Pezij, 2015). However, in both studies, wave heights over the intertidal flats were not successfully validated. It was speculated that problems in the data were a factor. This problem must be resolved in order to have confidence in the numerical model results and to estimate the design loads.

1.2. RESEARCH QUESTIONS

Three research questions and sub-questions that are explored. The research questions fall into three categories: morphology, operational wave conditions, and design wave conditions.

1. What are the insights gained from the morphological data collected from 2012-2016?
   - 1.a) What are the historical trends in morphological development of the tidal flats in the Eastern Scheldt?
   - 1.b) How has the nourishment developed since November 2013?
   - 1.c) What are the erosion trends, and what is the strength of those trends?
2. What is the wave attenuation impact of the nourishment hook in measured environmental conditions?
   - 2.a) What is the applicability of pressure transducers for the measurement of waves at the study site?
   - 2.b) What is the applicability of the selected hydrodynamic model at the study site, under a range of measured hydrodynamic conditions?
   - 2.c) What are the governing physical processes that affect wave transformation in the Kom and over the nourishment?

3. What is the effect of the Oesterdam tidal flat nourishment on the projected design storm wave loads from 2020 to 2080?
   - 3.a) Under design conditions, what are the main mechanisms of wave damping?
   - 3.b) How does the long term erosion of the tidal flats near the Oesterdam affect the wave loads?
   - 3.c) What is the sensitivity of the absolute values and relative changes in wave loads over time to changes in the erosion projections?

1.3. APPROACH

The approach to answer the main research question is split into four parts. Data analysis and numerical modelling are used to understand and represent the physical processes at the site. Processed water level, wave, and current data are used to calibrate and validate the numerical model in operational conditions. Projections of erosion are used with a calibrated numerical model to calculate projections of wave loads. Figure 1.3 gives an overview of the approach.

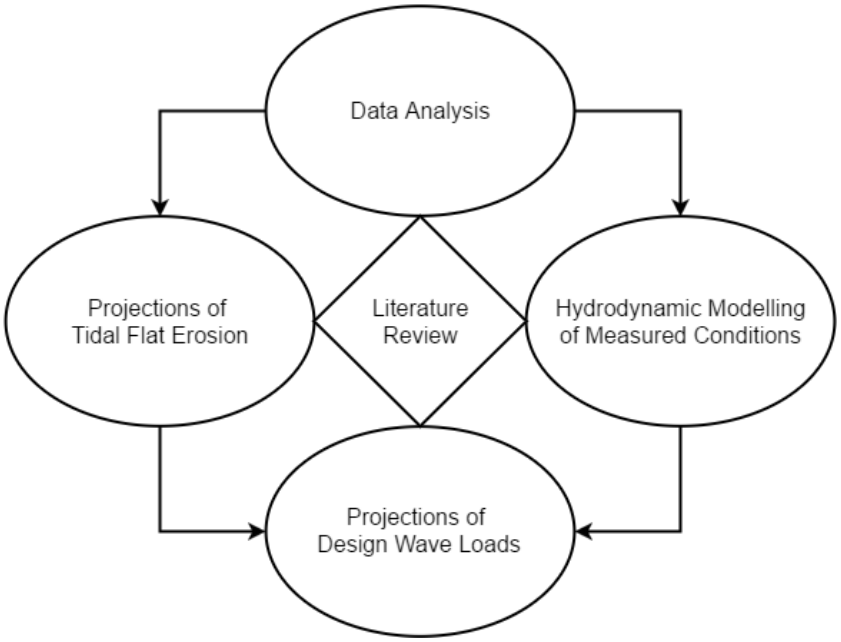

FIGURE 1.3: APPROACH FOLLOWED IN THE THESIS WORK.

1.4. SCOPE

The thesis focuses on the exploration of wave generation, dissipation, and transformation processes in the Kom. Due to time constraints, the following limitations in the scope are made:

- Morphological development is not analyzed using a numerical model, but by extrapolating linear trends from the literature and from new measurements.
- A safety assessment of the Oesterdam is not conducted, but the failure mechanisms of the structure are taken into consideration in the calculation of design wave loads.

2

LITERATURE REVIEW

A literature review is presented as a primer for the contents of the thesis work. First, a brief overview of coastal wave processes is given. Second, methods of wave measurement are outlined, with associated limitations. Third, literature on the Eastern Scheldt and the Kom is summarized. Fourth, relevant information on the Oesterdam is presented. The design standard, failure mechanisms, and calculation of design wave loads are included.

2.1. COASTAL WAVES

2.1.1. THEORIES

The main wave theories for surface gravity waves are linear wave theory, higher order stokes wave theory, and cnoidal wave theory (Holthuijsen, 2007). For small amplitude waves in deep water, linear wave theory offers an accurate representation of sea waves as harmonic waves. Steep waves (H/L » 0.1) behave nonlinearly and are better represented by higher order stokes theories. In shallower water (d/L <0.05), the assumptions of linear wave theory break down and the waves are better represented by cnoidal wave theory. Figure 2.1 gives a visual on the applicability of different wave theories for different values of relative depth and wave steepness. Each wave theory offers expressions for orbital motion of water particles under waves (kinematics), dynamic pressure (dynamics), and the relationship between wave period, water depth, and wave length.

One aspect of wave theory relevant to the thesis is the dynamic wave pressure in the water column induced by oscillations in the water surface. This is in addition to the hydrostatic pressure caused by the still water level (SWL). In general, deep water waves induce a dynamic pressure that decreases exponentially with depth, with negligible dynamic pressure at depths below half of the wavelength. In shallower water, the dynamic wave pressure approaches hydrostatic. Therefore, the same wave height with a shorter wave period will generally induce a lower dynamic pressure felt at some depth below SWL, except in very shallow water. Longer waves (in shallow water) such as tidal waves induce a pressure that is more or less hydrostatic. Figure 2.2 shows an illustration between dynamic wave pressure and depth. The derivation of the equations is included in Holthuijsen (2007) and CEM (2008).

2.1.2. WAVE SPECTRA

A useful way to describe a sea surface is as the sum of an infinite independent harmonic wave components, each with a different amplitude and frequency (or wavelength). This can be described by the random phase/amplitude model (Holthuijsen, 2007). From this model, the sea state at a particular point in space and time can be described in the frequency domain by a wave spectrum. The

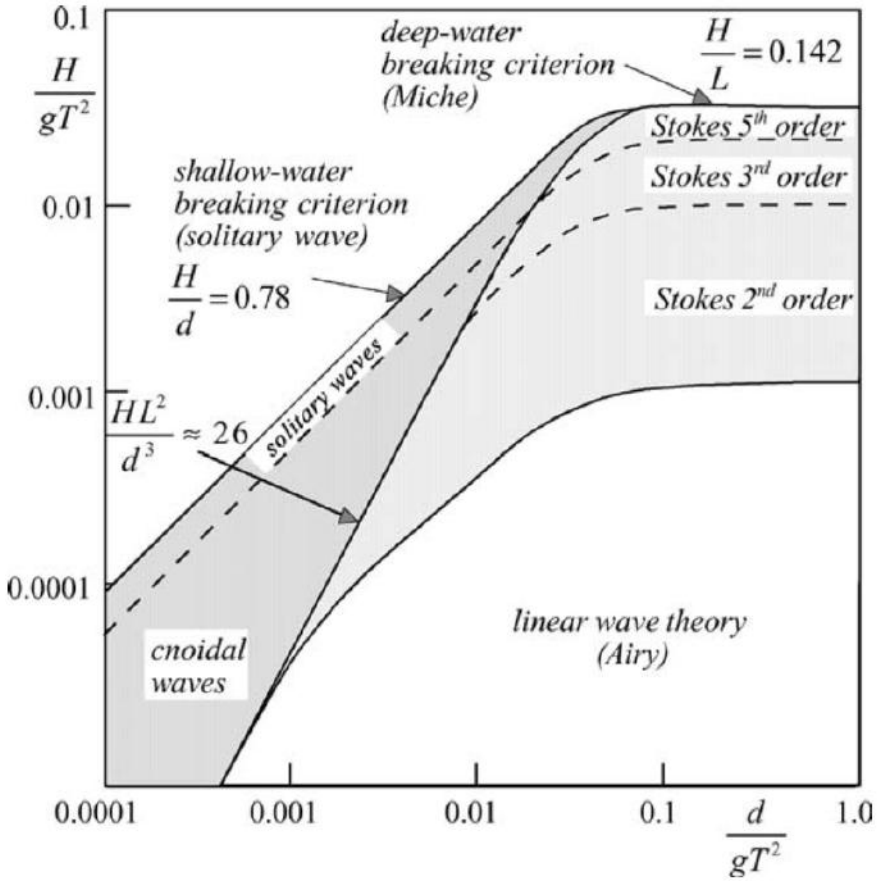

FIGURE 2.1: APPLICABILITY OF WAVE THEORIES FOR A RANGE OF RELATIVE DEPTH AND WAVE STEEPNESS. TAKEN FROM HOLTHUIJSEN (2007).

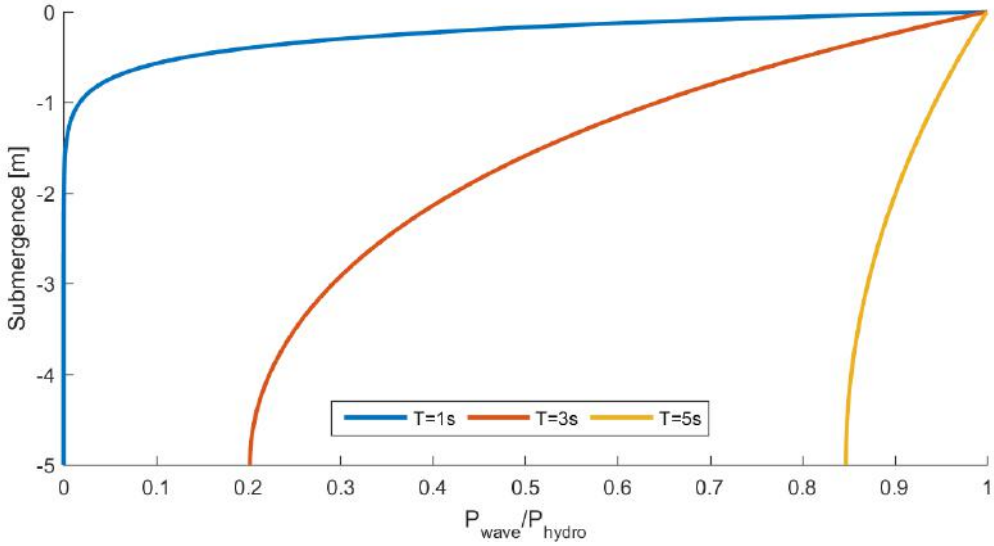

FIGURE 2.2: DYNAMIC WAVE PRESSURE OF A SURFACE WAVE FELT BELOW THE STILL WATER LINE (LWT). THE PRESSURE IS NORMALIZED BY THE HYDROSTATIC PRESSURE $p = \rho g H_s$.

wave spectrum is most often described for the variance of a sea surface, called the variance density spectrum. Other times, the variance density is multiplied by the specific weight of water (ρg) to obtain the wave energy spectrum. In this thesis, the terms variance density spectrum, surface spectrum, and wave energy spectrum are used interchangeably. In addition, a pressure spectrum at a certain depth can be obtained by transforming the surface spectrum using equations that relate the sea surface elevation to dynamic wave pressure.

An important aspect of wave spectra is the connection between the wave characteristics and the spectral shape. For young waves (duration limited) or fetch-limited waves, the spectrum is wide with a high spectral peak period. For larger fetches, fully-developed waves show a more narrow-banded spectrum with a higher spectral peak. For swell waves, the spectrum is much more narrow-banded and in the lower frequency range. Figure 2.3 illustrates some of the wind-wave spectra observed in the JONSWAP project.

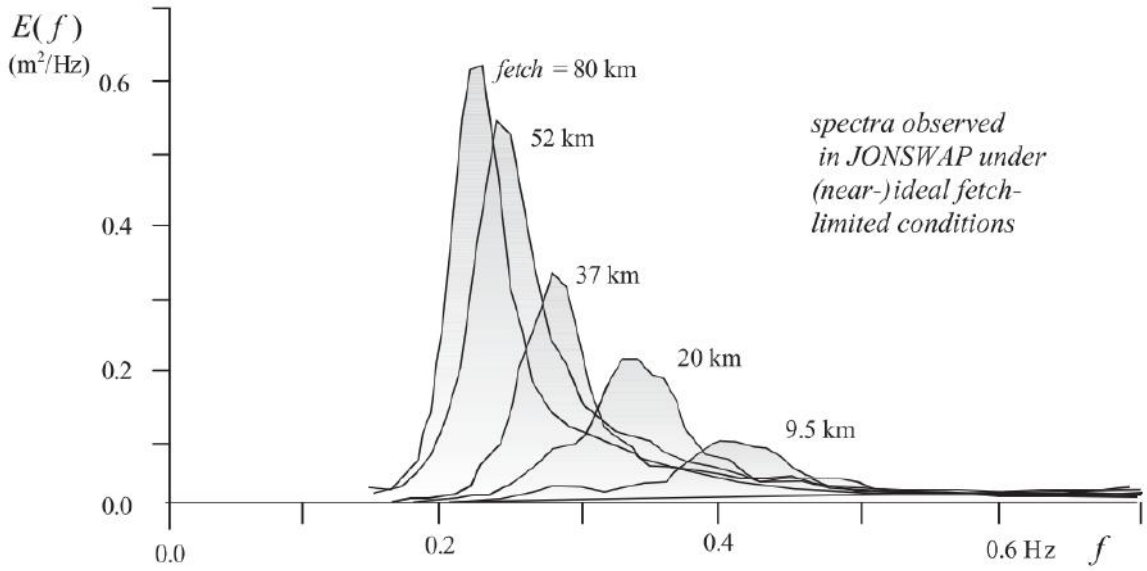

FIGURE 2.3: WAVE SPECTRA OBSERVED IN THE JONSWAP PROJECT, EACH WITH A DIFFERENT FETCH. TAKEN FROM HOLTHUIJSEN (2007) AND HASSELMANN ET AL. (1973).

2.1.3. PROPAGATION

As waves propagate from deep water into shallow water, two processes affect the wave height and direction: refraction and shoaling. Refraction is the process by which wave crests, travelling at an oblique angle with the bottom contours, bend due to the differential water depth (and thus differential propagation speed). Analytical solutions have been derived for simple straight and parallel bottom contours (CEM, 2002). In an irregular wave train, different frequencies within the train react differently, which causes the peak or mean spectral frequency change. Refraction may also be induced by ambient currents and can affect the wave height.

Shoaling occurs when the group velocity of the waves slows down as waves approach shallower water. As the group velocity decreases, the wave height of the propagating waves increases due to the principle of conservation of energy. A detailed elaboration is found in Holthuijsen (2007).

2.1.4. GROWTH AND TRANSFORMATION

Wind waves are thought to be generated through several mechanisms described by Miles (1957), Janssen (1991), and Phillips (1957). A positive feedback loop exists where instabilities in the water surface are amplified by overhead winds. Most of the energy transfer occurs on the high frequency side of the spectral peak (Holthuijsen, 2007). In shallow water, Young & Verhagen (1996) presents a family of growth curves representing the evolution of the wave field with increasing fetch.

An important transformation process in deep and intermediate water is quadruplet wave-wave interactions. Resonance between multiple waves (triads or quadruplets) act to transfer energy from one frequency band to another. While triads only occur in shallow water, quadruplet interactions may occur in both deep and intermediate waters. Quadruplet interactions, which are interactions between groups of four waves, are responsible for stabilizing the wave spectrum and generally lowering the peak frequency. More information can be found in Hasselmann et al. (1985).

2.1.5. DISSIPATION

Whitecapping is the process of wave breaking due to excessive steepness, generally understood to be the point where the wave height is about 14% of the wave length. Very steep waves eventually become unstable and break. The physics of whitecapping is poorly understood and mathematical formulations aim to simply represent the total dissipative effect on the wave spectrum (Cavaleri et al., 2007). Often, the rate of whitecapping dissipation is represented by characteristics of the entire wave spectrum (Komen et al., 1984). In general, the rate of whitecapping dissipation is positively related to the frequency band. Figure 2.4 shows the relative contributions of growth, transformation, and dissipation for a sea state in a sheltered harbour.

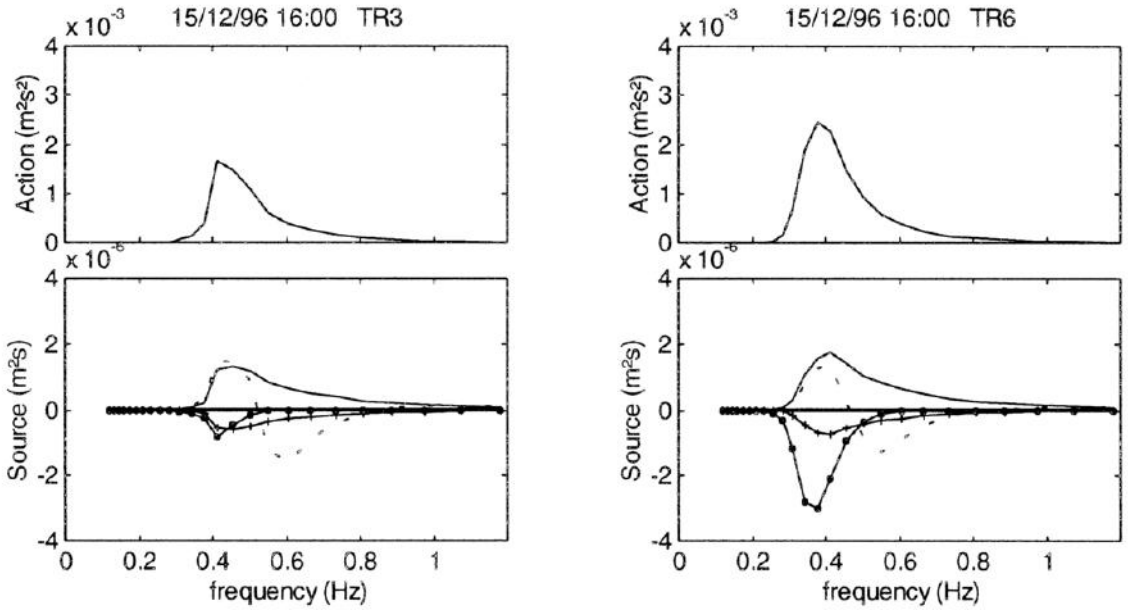

FIGURE 2.4: WAVE TRANSFORMATION IN MANUKAU HARBOR. THE UPPER PANELS ARE THE COMPUTED ACTION DENSITY SPECTRA. THE BOTTOM PANELS ARE THE COMPUTED SOURCE TERMS. THE LEFT PANEL SHOWS AN OFFSHORE POINT, WHILE THE RIGHT PANEL SHOWS A NEARSHORE POINT. SOURCE TERMS COMPUTED USING THE SWAN MODEL. (-) = WIND GROWTH, (+) = WHITECAPPING, (–) = QUADS, (-O-) = BOTTOM FRICTION. TAKEN FROM GORMAN & NEILSON (1999).

In shallower water where waves start to feel the bottom, friction plays a role in dissipating wave energy. This can be an important process in areas with extensive shallow foreshores where wave propagation and growth are limited by continuous interaction with the bed over large distances. Formulations for dissipation due to bed friction take into account the roughness of the bed (usually expressed as a coefficient), the wavelength (or orbital velocity near the bed), and other parameters (Cavaleri et al., 2007). In very shallow water, depth-induced wave breaking occurs when the ratio of wave height to water depth exceeds a certain value, usually approximated as 0.6-0.8 Salmon & Holthuijsen (2011).

2.1.6. NUMERICAL MODELS

Spectral wave models make up the bulk of the literature on the numerical modelling of coastal waves. These models generally work by taking an Eulerian approach to solving the spectral energy balance or action balance equation (Komen et al., 1994; Booij et al., 1999). Examples are the WAM model and the SWAN model. Spectral models are formulated around changes in the wave spectrum at different locations along a computational grid. Processes such as wind-wave growth, whitecapping, quadruplet interactions, bottom friction, and depth-induced breaking are incorporated as source/sink terms (see Figure 2.4).

Another approach to wave modelling, particularly in shallow water, is to solve the Navier Stokes equations and compute the free surface elevation. These models focus on shallow water applications where the assumptions of linear wave theory break down and the pressure distribution in the water column deviates from hydrostatic (Stelling & Zijlema, 2003). XBeach (non-hydrostatic), SWASH, and REEF3D are examples of such models. At the time of writing, none of these models simulate wind-wave generation.

2.2. MEASUREMENT OF WAVES

There are many ways to measure waves in coastal environments. These range from the use of wave buoys, step gauges or poles, or pressure transducers. The preferred method of measurement depends on the type of environment and the budget that is available. Below, two broad categories of wave measurement devices are presented: surface instruments and underwater sensors. All of the instruments described have general limitations when it comes to the measurement of breaking or highly nonlinear waves, whether in deep or shallow water.

2.2.1. SURFACE INSTRUMENTS

Wave buoys are floating objects which move with the water surface and record oscillations. They often have pitch and roll sensors in order to compute the 2-dimensional wave spectra at selected time intervals. While wave buoys are a common method of wave measurement, they have some limitations such as survivability during large storms and excessive lateral movement (Pandian et al., 2010).

Step gauges, or more generally wave poles, are instruments that are installed on the bed and protrude above the water surface. Oscillations in the surface elevation are recorded via sensors throughout the pole. While these are static instruments, they may overestimate wave heights when there is a large amount of splashing (Wenneker, 2014).

2.2.2. UNDERWATER SENSORS

Acoustic Doppler current Profilers (ADCPs), in addition to measuring currents, may also measure wave heights if they have high frequency measurement intervals. When configured with an upward-looking direction, the surface elevation can be profiled. The efficacy of wave height measurement has been demonstrated for shallow and deep water (Pandian et al., 2010).

Pressure transducers are one of the least expensive devices applied to wave measurement. They are deployed in the water column, typically less than a few meters below the still water line, and record the pressure induced by the overlying water over time. This pressure is converted to surface elevation by means of a transfer function, which is usually taken from linear wave theory. This particular method is explored due to the availability of data at the study site. In the presence of waves, dynamic pressure is felt in the water column as an exponential function of depth. This relationship between dynamic pressure and depth is most simply represented by the Linear Wave Theory:

$$S_p(f) = \left(\rho g K_p\right)^2 S(f) \tag{2.1}$$

Where:

$S_p(f)$ = Pressure spectrum [Pa^2/Hz]

$S(f)$ = Wave (variance density) spectrum [m^2/Hz]

K_p = Linear transfer function [−]

ρ = Density of water [kg/m^3]

g = Gravity constant [m/s^2]

$$K_p = \frac{\cosh \frac{2\pi(z+d)}{L}}{\cosh \frac{2\pi d}{L}} \tag{2.2}$$

Where:

d = Water depth [m]

z = Instrument elevation above the still water line [m]

L = Wave length [m]

There is a known issue with the use of the inverse transfer function (to go from pressure to wave height) in areas of large relative instrument depth (z/L). When the instrument relative depth is more than a value of 0.2-0.5 (Wenneker, 2014), the dynamic wave pressure is so low that it is indistinguishable from instrument noise. The result is an over-prediction of wave height due to the amplification of instrument noise. Efforts have been made to calibrate the transfer function for specific locations and wave conditions, but other measurements from wave buoys or step gauges are required.

Bishop & Donelan (1987); Wenneker (2014); Lee & Wang (1984) describe several ways to tackle this problem, the most popular of which is to use a minimum value ($K_{p,min}$) which would be applied for the entire spectrum. How and where to apply this minimum value depends on the depth of the instrument, the expected noise level, and the expected wave conditions. Approaches range from using an arbitrary value ($K_{p,min} = 1/3$), an arbitrary frequency ($K_{p,min} = K_p(f = 0.4Hz)$) or an arbitrary relative instrument depth ($K_{p,min} = K_p(|z|/L = 0.2)$). The most defensible solutions involve calibrating the $K_{p,min}$ value using other wave measurement devices such as step gauges or wave

buoys. However, this calibration would only be valid for a particular environment. Figure 2.5 shows how the inverse transfer function varies as a function of frequency or relative instrument depth.

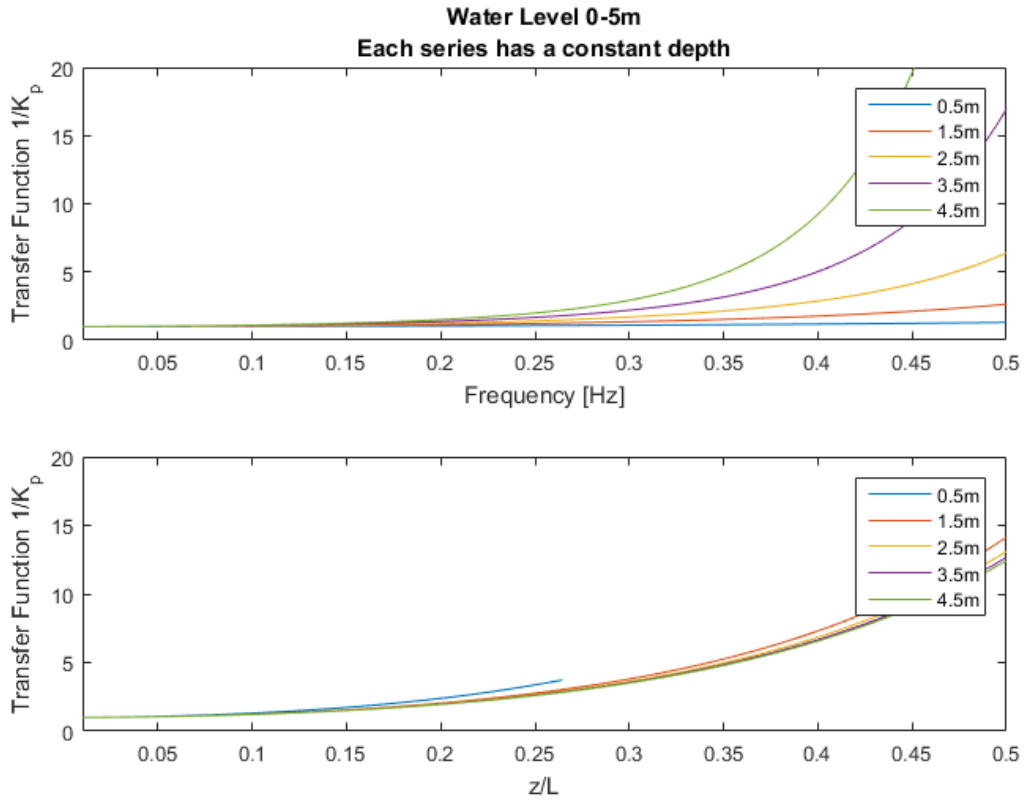

FIGURE 2.5: LINEAR WAVE THEORY INVERSE TRANSFER FUNCTION (FOR CONVERTING TO PRESSURE TO WAVE HEIGHT) AS A FUNCTION OF RELATIVE INSTRUMENT DEPTH AND FREQUENCY.

It is clear from Figure 2.5 that the calculated wave height is very sensitive to the choice of $K_{p,min}$ for environments with significant high frequency wave energy and for instruments installed in deep water. The slope of the curves increase exponentially at higher wave frequencies or relative instrument depths. It is also clear that the pressure box instrument must be placed as close to the water surface as possible in order to minimize sensitivity to $K_{p,min}$.

2.3. THE EASTERN SCHELDT

The Eastern Scheldt, in its present day form, is a tidal basin with negligible freshwater influence. Formerly connected with the Western Scheldt, the basin is now closed off by dams and polders on the inland side with a storm surge barrier at the inlet. The storm surge barrier is an open barrier, but disrupts the propagation of waves, tidal flows, and sediment exchange in and out of the basin. Table 2.1 gives an overview of the characteristics of the basin. The defining characteristics of the basin when it comes to waves are listed below.

- Sheltered from ocean waves, and thus fetch-limited
- Strong presence of subtidal and intertidal foreshores
- Macrotidal range with strong currents in the inlet and main channels

TABLE 2.1: DIMENSIONS AND TIDAL CHARACTERISTICS OF THE EASTERN SCHELDT (DE BOK, 2001).

Parameter	Eastern Scheldt	Kom	Units
Surface area (with flats)*	3.4×10^8	9.2×10^7	m^2
Average depth at NAP*	8.8	4.3	m
Inlet cross sectional area (NAP)	17,900	-	m^2
Mean tidal range	3	3.45	m
Tidal prism (1999)	9.32×10^8	3.17×10^8	m^3
Basin length*	<45	<13	km
Tidal period	12.42	-	hours
Tidal wavelength (λ)*	415	290	km

*Calculation performed based on 2013 vaklodingen data

The southeastern bulb of the Eastern Scheldt, dubbed the 'Kom', is the focus of the thesis. The Kom consists of many tidal flats, shallow foreshores and some marshes, which are delineated in Figure 2.6. Some of the morphological features are old drowned villages. For example, Kouwerve, Duvenee, and Loodijke are some of the drowned villages the area. In addition, the Kreekrakplaat and Yerseksche Oesterbank contain many sub-features such as sand banks and more drowned villages.

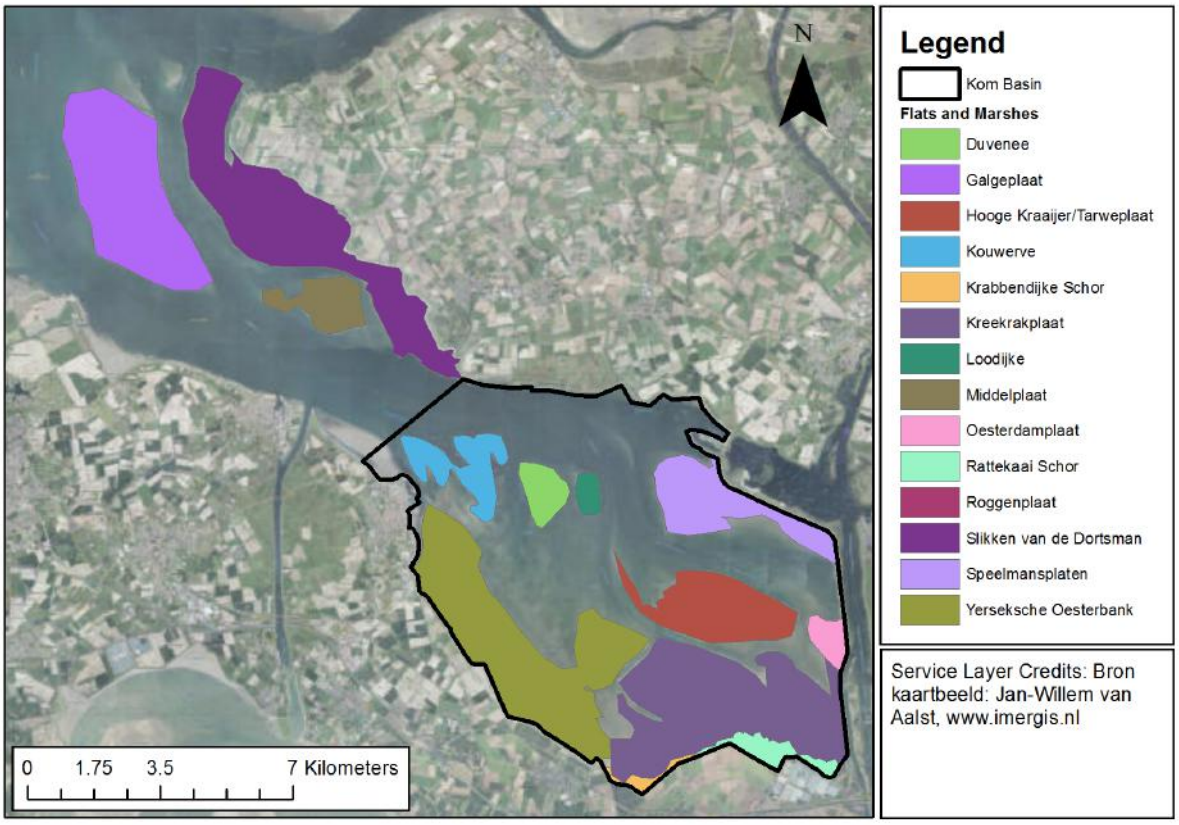

FIGURE 2.6: TIDAL FLATS AND MARSHES IN THE KOM.

2.3.1. HISTORICAL DEVELOPMENT

The Eastern Scheldt is in its present form largely due to human interventions over the past century. The historical development of what is now known as the Eastern Scheldt tidal basin is examined by De Bok (2001), De Graaf (2012), De Ronde et al. (2013), Eelkema (2013), among others. This section describes the main points relevant to the thesis. Figure 2.7 summarizes the human interventions in the 1900s.

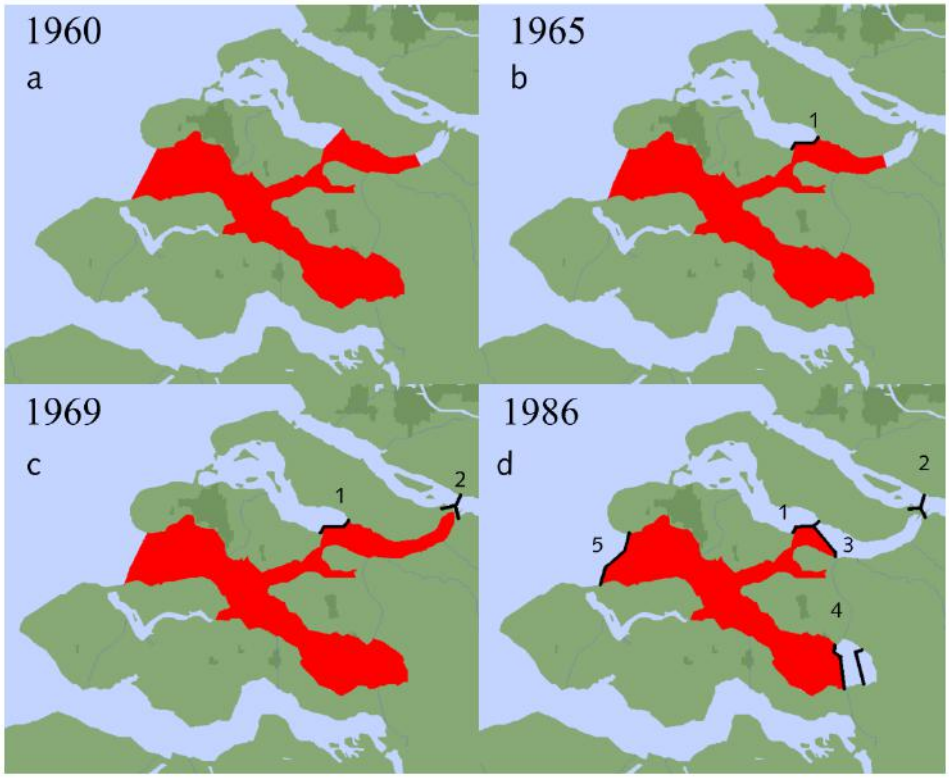

FIGURE 2.7: DEVELOPMENT OF THE EASTERN SCHELDT BASIN DUE TO THE DELTA WORKS. 1. GREVELINGENDAM. 2. VOLKERAK DAM. 3. PHILIPSDAM. 4. OESTERDAM. 5. STORM SURGE BARRIER. TAKEN FROM DE BOK (2001).

The Delta works had an important impact on the morphological equilibrium state of the Eastern Scheldt, which caused a phenomenon called sand hunger. Due to the constriction of the inlet size by the storm surge barrier, the tidal flows in and out of the basin became weaker. Both the tidal range and tidal prism were reduced, with smaller flow velocities unable to import as much sediment from the North Sea. Following the construction of the Oesterdam and Philipsdam, the tidal range was partially recovered due to reflection, while the tidal prism was further reduced. Figure 2.8 shows the changes in the tidal range and prism over time. Figure 2.9 shows the change in flood and ebb tidal velocities.

The cumulative impact of the Delta Works resulted in sediment demand from the tidal channels, as they were over-sized. Put simply, the weakened tidal flows in the channels are unable to transport enough sediment to build up the flats following wave-induced erosion caused by storms. As a result, unbalanced erosive/accretive forces cause a structural erosion in the intertidal areas. Table 2.2 shows estimates of annual erosion in some intertidal areas following the completion of the Delta works.

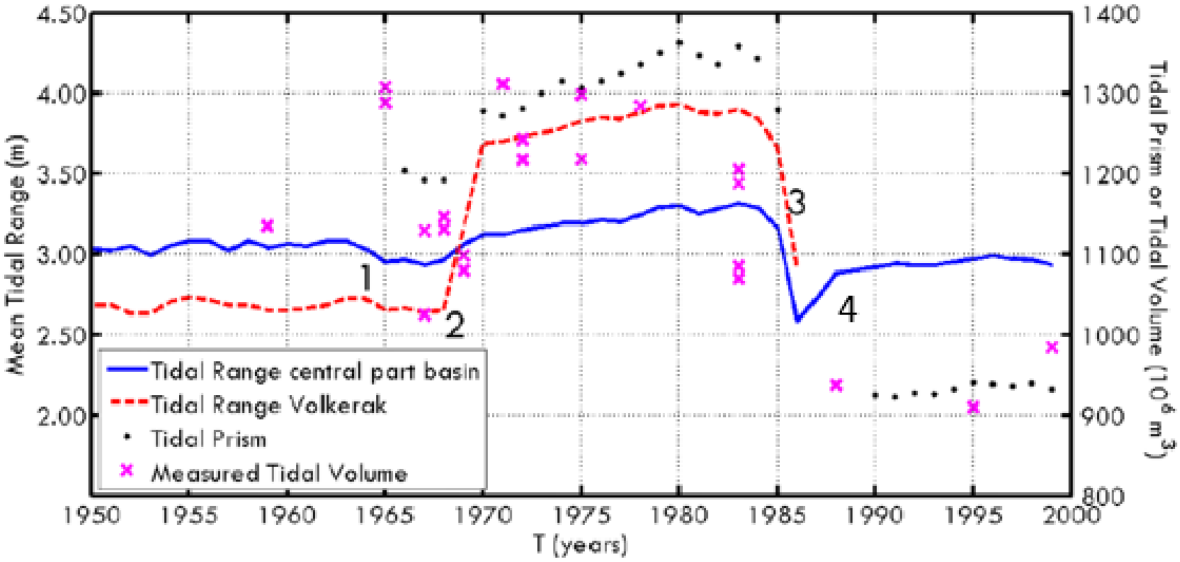

FIGURE 2.8: CHANGES IN MEAN TIDAL RANGE AND TIDAL PRISM IN THE EASTERN SCHELDT. NUMBERS INDICATE THE COMPLETION OF THE (1) GREVELINGENDAM, (2) VOLKERAK DAM, (3) STORM SURGE BARRIER, AND (4) OESTERDAM AND PHILIPSDAM. TAKEN FROM DE BOK (2001); PEZIJ (2015)

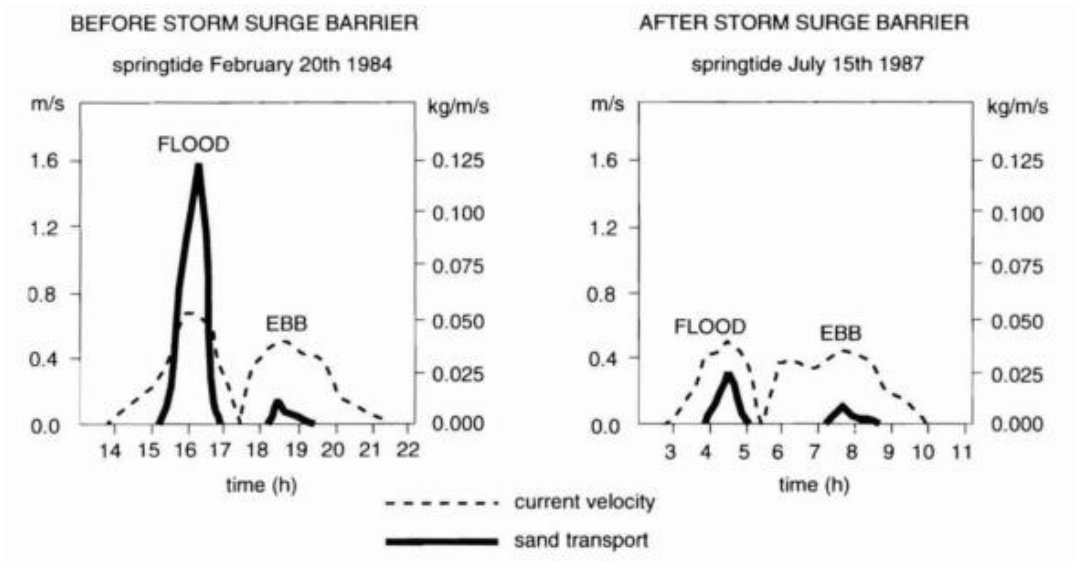

FIGURE 2.9: EASTERN SCHELDT INLET. CHANGES IN SEDIMENT IMPORT DURING FLOOD TIDE AND EXPORT DURING EBB TIDE BEFORE AND AFTER THE CONSTRUCTION OF THE STORM SURGE BARRIER. TAKEN FROM LOUTERS ET AL. (1998); PEZIJ (2015).

2.3.2. THE OESTERDAM NOURISHMENT

Project Veiligheidsbuffer Oesterdam came out of an initiative between Rijkswaterstaat, Projectbureau Zeeweringen, and other agencies which set out to build non-traditional solutions to the flood defense problems in the Eastern Scheldt. In April 2011, a multi-agency team was formed, which included Natuurmonumenten, to secure funding and come up with a plan for a project at the Oesterdam (Boersema et al., 2015b).

TABLE 2.2: INTERTIDAL EROSION RATES IN THE EASTERN SCHELDT, ESTIMATED FROM RTK PROFILE SURVEYS FROM 1990-2010. OBTAINED FROM DE GRAAF (2012) AND SANTINELLI & DE RONDE (2012).

Name	Average Erosion Rate [cm/yr]
Dortsman	1.3
Galgeplaat	0.6
Krabbendijke	0.2
Rattekaai	0
Roggenplaat	1
Neeltje Jans	1

In October 2011, a pre-nourishment monitoring campaign was initiated. In November 2013, the nourishment was constructed using 350,000 to 450,000 m^3 of sand dredged from the Wemeldinge and Lodijksche Gat, two channels just outside of the Kom. The average elevation of the flat was raised by 0.45m. In addition, several oyster reefs were built to stabilize the bed. The post-nourishment monitoring campaign took place from 2013 to 2016, at the time of this writing (Boersema et al., 2015b, 2016). The collected data includes sediment samples, bathymetric surveys, wave and current measurements, and visual observations.

Figure 2.10 shows the location and layout of the nourishment. The hook shape was designed to flood during high tide to facilitate water and sediment movement from the southern to northern part of the flat. In addition, several small ponds were designed along the hook (visible as dark circles) in order to observe any differences in biological development over time. The front of the dam foot was also nourished, covering the riprap toe berm and part of the copper slag block revetment, both of which are visible at low tide on the adjacent dam sections. The area between the foot and the hook was not nourished.

2.3.3. PRESENT DAY HYDRODYNAMICS

The tide in the Eastern Scheldt is semi-diurnal. Tidal propagation into the basin depends on the relative importance of friction and basin length (Bosboom & Stive, 2015). The tide in the Eastern Scheldt behaves like a standing wave, with almost a 90 degree phase difference between the water level and flow velocity at the inlet (Bosboom & Stive, 2015; De Bok, 2001). It cannot strictly be considered a standing wave, since the incident and reflected wave is attenuated by bottom friction.

Basins that are much shorter than the resonance length ($L << \lambda/4$) are classified as 'short' basins. Short tidal basins exhibit a constant oscillating water level known as 'pumping mode' (Bosboom & Stive, 2015). However, the water level in the Eastern Scheldt is not spatially constant, which shows that the basin is not short enough to exhibit pumping mode. While De Bok (2001) classifies the Eastern Scheldt as a short basin, this is simply based on the basin being shorter than the resonance length.

Waves in the Eastern Scheldt, save for the area close to the storm surge barrier, are dominated by locally generated wind-waves. van Leeuwen et al. (2014) did a study that looked at the wave penetration from the North Sea through the storm surge barrier. Using their schematized implementation of the barrier in SWAN, they determined that the frequency-dependent transmission coefficient through the barrier is:

FIGURE 2.10: OESTERDAM NOURISHMENT LOCATION AND LAYOUT, WITH CONSTRUCTED OYSTER REEFS.

$$K_t(f) = \begin{cases} 1 & f < 0.11 \\ -5.77f + 1.63 & 0.11 <= f < 0.24 \\ 0.25 & f >= 0.24 \end{cases} \tag{2.3}$$

Where:

K_t = Wave transmission coefficient [−]

f = Wave frequency [Hz]

Several studies have been conducted which have looked at the hydrodynamic characteristics of different parts of the Eastern Scheldt. Das (2010) used the numerical model Delft3D to model waves in deep water and over the Galgeplaat tidal flat. Pezij (2015) also used Delft3D but applied it to the Oesterdam nourishment. In both studies, the default settings in Delft3D for wave breaking, bottom roughness, and whitecapping were used[1]. In both models, there was a discrepancy between measured and modelled wave heights over the intertidal flats. It is not known whether the discrepancy was caused by an over-prediction in the model or by unreliable data.

[1] Both authors also used an alternative whitecapping formulation from Van der Westhuysen et al. (2007) with almost no differences in result

2.4. THE OESTERDAM

There are many names applied to coastal structures with similar or identical purposes. Closure dams are generally described as water-retaining structures which partially or completely block the flow of water from one side to the other. There are many types of closure dams which can be made of mattresses, sand, clay, stones, or caisson structures (Verhagen et al., 2012). They may be classified according to the surrounding hydrologic conditions, as shown in Figure 2.11. Examples include the Afsluitdijk, the Grevelingendam, the Philipsdam, and the Saemangeum dike (South Korea) (Verhagen et al., 2012).

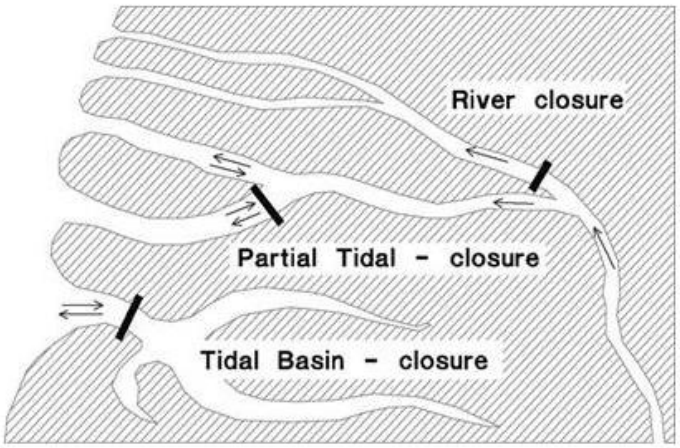

FIGURE 2.11: TYPES OF CLOSURE DAMS NAMED AFTER HYDROLOGIC CONDITIONS. TAKEN FROM VERHAGEN ET AL. (2012).

The Oesterdam is a tidal basin closure dam. It is located on the East side of the Kom and shelters a the Bergs diep, a part of the Scheldt-Rhine canal (see Figure 1.1 and Figure 2.7). The Oesterdam resembles a coastal dike in that it is a sloping structure with a berm and a revetment. A representative cross section of the Oesterdam is shown in Figure 2.12.

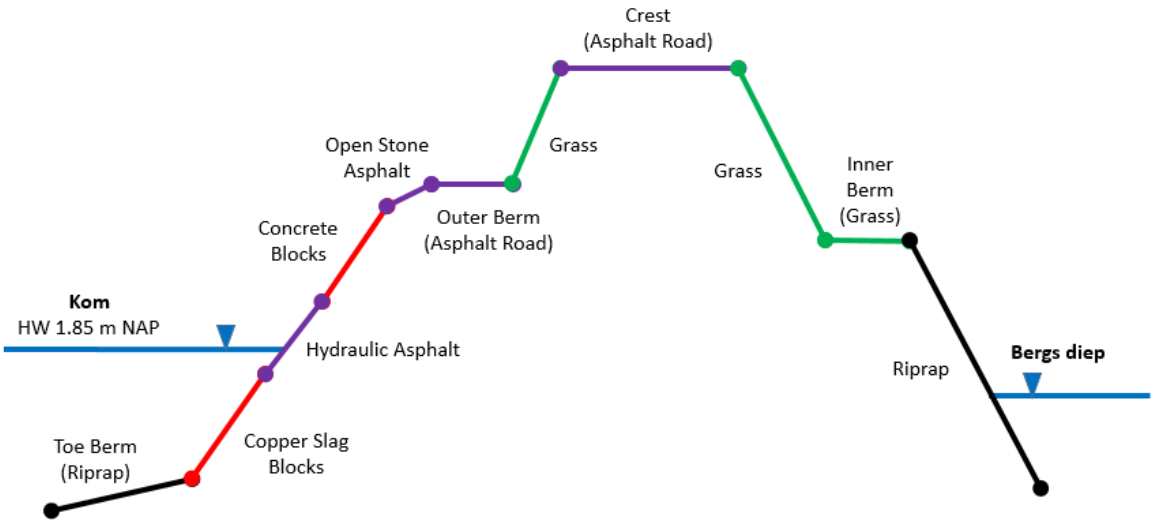

FIGURE 2.12: A SIMPLIFIED SCHEMATIC OF A CROSS SECTION OF THE OESTERDAM (NOT TO SCALE).

2.4.1. DESIGN STANDARD

The Oesterdam is a category-b flood defense that links dike ring of Tholen & St. Philipsland with that of South Beveland[2]. In the Zeeland region, the safety standard for dikes and dams is the ability to withstand a 1/4000 year storm, defined by a wind speed and/or water level with that return period. The design wind speeds for the 1/4000 year storm are reported in Royal Haskoning & Svasek Hydraulics (2011). The wave characteristics are then calculated based on the wind speed and water level. For all failure mechanisms, the highest water level usually gives the most conservative results, which are then used for design (ARCADIS, 2009). Table 2.3 summarizes the normative design conditions that apply to the Oesterdam.

TABLE 2.3: DESIGN WIND SPEED AND WATER LEVEL AT THE OESTERDAM

Code	Wind Direction [Deg]	Wind Speed [m/s]	Water Level [m NAP]*
1	270	33	4
2	285	32	4
3	300	31	4
4	315	28	4

*The actual maximum in the Kom is 3.95m due to the closure regime of the storm surge barrier

2.4.2. FAILURE MECHANISMS

The main failure mechanisms for closure dams depend on their construction type. The Oesterdam resembles a sea dike in that it is a sloping earth structure. The failure mechanisms of the Oesterdam that are explored in the literature are: overtopping, copper slag block failure, hydraulic asphalt failure, concrete block failure, and open stone asphalt failure. These are discussed in more detail below.

WAVE OVERTOPPING

Overtopping is a process by which wave run-up reaches the crest of a structure and passes over it. On sloping structures, waves usually break somewhere on the slope and significant volumes of splash may travel over the crest. For lower overtopping rates during a storm (typically reported as l/s/m), pedestrians and vehicles may be put in danger. For higher overtopping rates, slope failure may occur on the lee side where overtopped waves run down with high velocities. The deterministic equations for overtopping described in Pullen et al. (2007) are shown here (Equations (2.4) and (2.5)).

The amount of run-up and overtopping on a structure depends on the wave height, wave period, wave direction (relative to the structure) and structural geometry. Empirical formulas have been derived based on laboratory experiments in order to calculate overtopping. The standard equations used in the Netherlands for safety assessments of dikes and similar structures are described in Van der Meer (2002) and Pullen et al. (2007).

[2]Category-b defenses are structures that link dike rings, which are category-a defenses. More information on flood risk management in the Netherlands is found in Slomp (2012).

$$\frac{q}{\sqrt{gH_{m0}^3}} = \frac{0.067}{\sqrt{\tan\alpha}}\gamma_b\xi_{m-1,0}\cdot\exp\left(\frac{-4.3R_c}{\xi_{m-1,0}H_{m0}\gamma_b\gamma_f\gamma_\beta\gamma_v}\right) \tag{2.4}$$

$$\frac{q_{max}}{\sqrt{gH_{m0}^3}} = 0.2\cdot\exp\left(\frac{-2.3R_c}{H_{m0}\gamma_f\gamma_\beta}\right) \tag{2.5}$$

Where:

q	= Overtopping discharge	[$m^3/s/m$]
H_{m0}	= Significant wave height	[m]
g	= Gravitational constant	[m/s^2]
$\tan\alpha$	= Slope angle	[−]
$\xi_{m-1,0}$	= Surf/Iribarren number	[−]
R_c	= Crest freeboard above SWL	[m]
γ_b	= Berm influence factor	[−]
γ_f	= Friction/roughness influence factor	[−]
γ_β	= Wave angle influence factor	[−]
γ_v	= Vertical wall influence factor	[−]

Correction factors are applied to overtopping calculations to account for structures with different roughness, slope, the presence of a berm, and the presence of an vertical wall. Table 2.4 shows the sensitivity of overtopping to various parameters. The program PC-Overslag (and web-based version PC-Overtopping) implements the equations from Van der Meer (2002), including correction factors and support for variable slopes. ARCADIS (2009) applied a value of 1.0 l/m/s to the Oesterdam in order to assess the required crest height, but a higher threshold value may be acceptable during design storm conditions due to an evacuation scheme and due to the residual strength of the dam (Table 2.5). The overtopping assessment by De Graaf (2012) indicates that the overtopping during design conditions already exceeds the 1.0 l/m/s limit.

TABLE 2.4: RELATIONSHIP BETWEEN HYDRAULIC AND DIKE PARAMETERS AND RUN-UP/OVERTOPPING

Parameter	Effect on Overtopping
Water level ⋀	⋀
Wave height ⋀	⋀
Wave period ⋀	⋀
Water depth at toe ⋀	⋀
Obliqueness (wave angle) ⋀	⋁
Berm height ⋀	⋁
Berm width ⋀	⋁
Dike slope (tan) ⋀	⋀
Crest height ⋀	⋁
Slope roughness ⋀	⋁

TABLE 2.5: LIMITS FOR OVERTOPPING FOR DAMAGE TO THE DEFENSE CREST OR REAR SLOPE. TAKEN FROM PULLEN ET AL. (2007).

Hazard Type	Limit q [l/s/m]
Embankment Seawalls/sea dikes	
No damage if crest and rear slope are well protected	50-200
No damage to crest and rear face of grass-covered embankment of clay	1-10
No damage to crest and rear face of embankment if not protected	0.1
Promenade or revetment seawalls	
Damage to paved or armored promenade behind seawall	200
Damage to grassed or lightly protected promenade or reclamation cover	50

BLOCK REVETMENT STABILITY

Wave loads on block revetments impose a differential pressure which causes uplift forces on individual blocks. Wave impacts may also damage the surface of blocks, or cause washout of the underlayer material (usually gravel or geotextile). The stability of block revetments under wave loads comes from interlocking of adjacent blocks (due to geometry and/or friction) and the weight of the blocks. A general formula for block stability is given by Pilarczyk (2003).

$$\frac{H_s}{\Delta_m D} \leq F \frac{\cos(\alpha)}{\xi_p^b} \tag{2.6}$$

Where:

Hs = Significant wave height [m]
Δ_m = Relative density of material [−]
D = Thickness of blocks [m]
Ψ_u = Empirical stability upgrading factor (1 for riprap, >1 for other systems) [−]
F = Empirical stability factor, ranges from 3-8 [m]
b = Empirical exponent (0.67-1) [−]

In the Netherlands, the standard method for safety assessments for block revetments is the use of Steentoets (Breteler, 2014). Steentoets is an excel-based program that uses a set of checks for block stability, filter stability, and other block-related failure mechanisms.

ASPHALT REVETMENT STABILITY

Asphalt or other impervious revetments are usually designed for upper parts of sloping hydraulic structures due to their relative strength compared to blocks. However, due to their vulnerability to fatigue, they are constructed at an elevation that would only be reached under extreme storm surge during a design storm. The two main failure mechanisms for asphalt revetments are differential pore pressure and wave impacts, with wave impacts usually being the dominant mechanism.

Wave impacts on asphalt cause a stress on the material that may cause failure if it exceeds the failure stress. The stress on the revetment is dependent upon the stiffness ratio of the revetment and subsoil. Repeated wave impacts during storm cause fatigue, which effectively reduces the failure stress. This is represented by the Miner sum, which exceeds 1 when failure occurs:

$$\sum \frac{n_i}{N_{f,i}} \leq 1 \tag{2.7}$$

Where:

n_i = Number of load repetititions that occur during a storm
$N_{f,i}$ = Number of load repetations that lead to failure
$N_f = k_f \sigma^{-a_f}$
k_f, a_f = Fatigue parameters of asphalt, from physical tests
σ = Tension stress on the asphalt [MPa]

In the Netherlands, the standard method of computation of asphalt stability is the use of the GOLFKLAP program (De Looff et al., 2006). The program computes the miner sum for a specified storm and asphalt material properties. Design charts for hydraulic asphalt and open stone asphalt have been presented in Davidse et al. (2010) based on GOLFKLAP computations for aged asphalt (Appendix C). The aging process of asphalt is accounted for by using material properties from aged asphalt, measured using samples from old revetments.

A critical assumption in the design and safety assessment of asphalt revetments is the assumption of asphalt recovery following storm-induced fatigue. There exists a minimum recovery period beyond which the asphalt revetment 'recovers' from any storm-induced fatigue. Typical asphalt revetments are designed to be exposed to wave loads only several times per year, but the Oesterdam revetment lies partially below MHW. Despite this, the assumption was made in the original design of the hydraulic and open stone asphalt revetments (Van der Vliet, 2010).

3

DATA ANALYSIS

Processed hydrodynamic and morphological data was used to derive insights into the hydrodynamic processes and morphological changes at the Oesterdam. The wave damping effect of the Oesterdam nourishment hook was explored using wave measurement points inside and outside the hook. Current measurements were used to examine the character of the tidal flows on the nourishment. Finally, a trend analysis was done on the collected RTK bathymetry data in order to estimate average erosion rates in different parts of the nourishment.

3.1. DATA COLLECTION

Much of site data was provided by Rijkswaterstaat. Wind, wave, and water level data from measurement stations in the Eastern Scheldt was collected from online databases[1]. Figure 3.1 shows the locations of the measurement stations used in the analysis.

Three wave and current monitoring campaigns were conducted at the Oesterdam: one before the nourishment (T0 2011) and two afterwards (T1 2014 and T2 2015/2016). In each campaign, ADCP devices and pressure transducers (or pressure boxes) were deployed to measure currents and waves respectively. Between each deployment, some instruments were placed in the same locations but most were not. Figure 3.2 shows the measurement locations for all three deployments.

RTK bathymetric surveys of the Oesterdam flat from 2012-2016 were also provided by RWS. The 2013 bathymetry of the Eastern Scheldt was taken from the vaklodingen dataset. The data was used for trend analysis and for hydrodynamic model input. The dates of each RTK survey, before and after the nourishment, are listed on the next page.

[1] waterberichtgeving.rws.nl and live.waterbase.nl

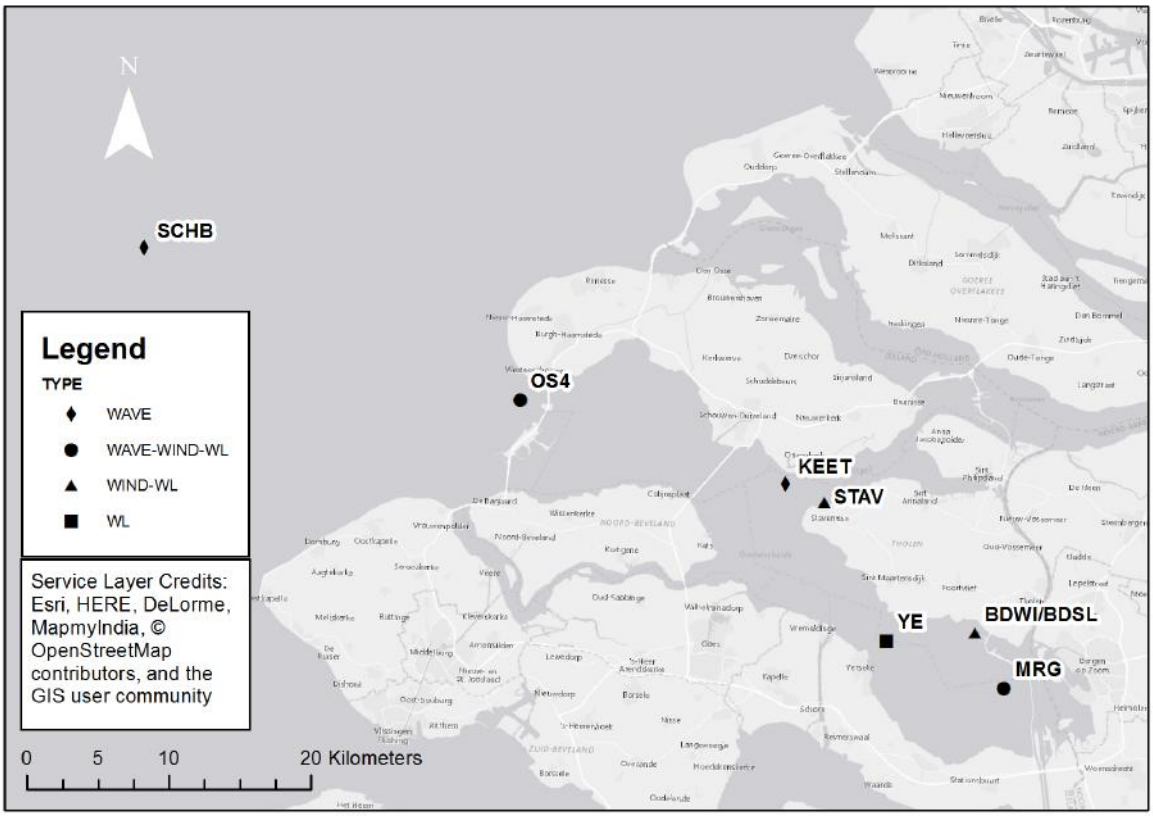

FIGURE 3.1: RIJKSWATERSTAAT WIND, WAVE, AND WATER LEVEL MEASUREMENT STATIONS. SCHB, OS4, AND KEET ARE WAVE BUOYS WHILE A STEP GAUGE/POLE IS USED AT MRG.

- Pre-nourishment
  1. January 18, 2012 [winter]
  2. June 5, 2012 [summer]
  3. November 2, 2012 [fall]
  4. March 27, 2013 [spring]
- Post-nourishment
  1. November 20, 2013 [fall]
  2. February 18, 2014 [winter]
  3. May 14, 2014 [spring] (nourishment foot re-profiled in March 2014)
  4. August 14, 2014 [summer]
  5. November 8, 2014 [fall]
  6. April 3, 2015 [spring]
  7. October 29, 2015 [fall]
  8. April 11, 2016 [spring]

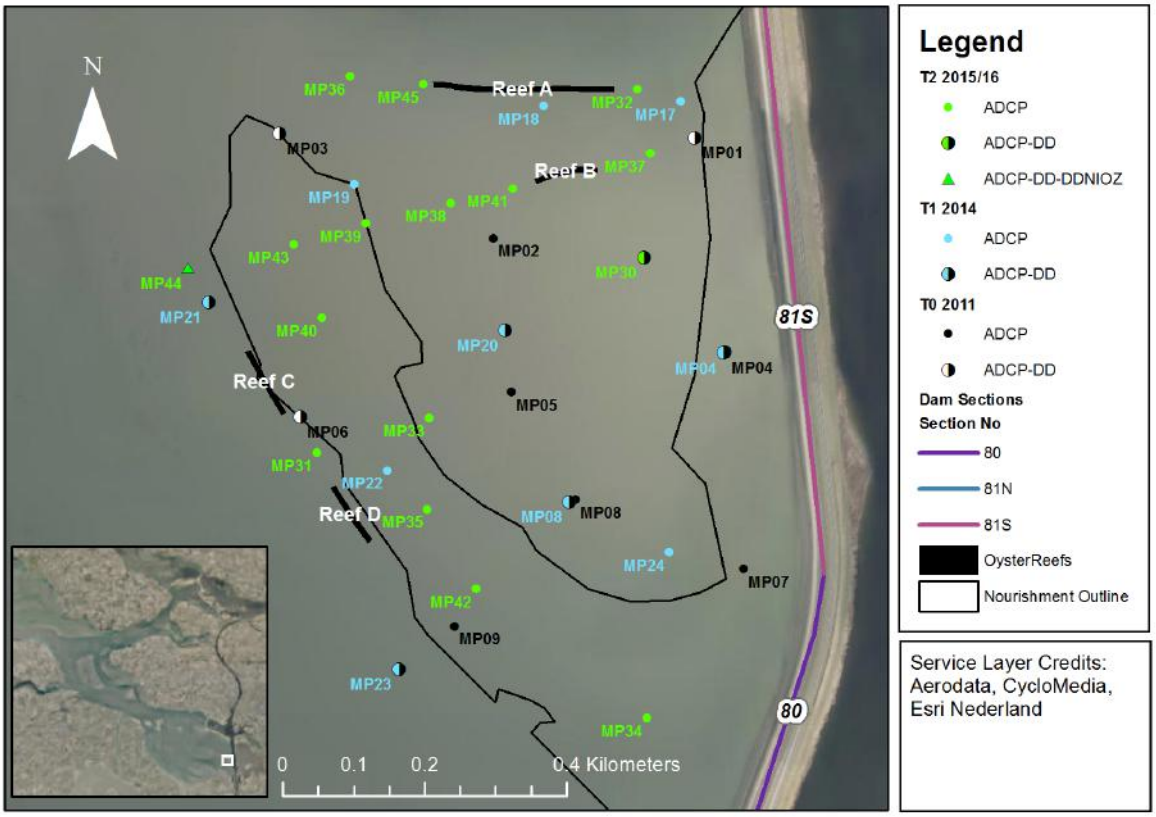

FIGURE 3.2: WAVE AND CURRENT MEASUREMENT LOCATIONS AT THE OESTERDAM FROM THE T0, T1, AND T2 DEPLOYMENTS. MP44 IS THE ONLY LOCATION WHERE TWO DIFFERENT PRESSURE BOXES WERE USED.

3.2. WIND, WATER LEVEL, AND WAVES IN THE EASTERN SCHELDT

The wind data analyzed from the Oosterschelde 4 (OS4), Stavenisse (STAV), Marollegat (MRG), and Bergsdiepsluis (BDWI) stations showed some differences in magnitude and direction. As visualized in Figure 3.3, some spatial variability in the wind field exists across the Eastern Scheldt. This is an important factor when selecting wind data for model input.

Wave heights at the Marollegat show some correlation with the wind speed, and the highest waves correspond to northwestern wind directions (Figure 3.4). As reported in De Graaf (2012), wind that comes from the northwesterly direction is associated with the highest waves despite the fact the strongest winds come from the southwest. The wave periods showed no relationship with wind speeds or directions. Figure 3.5 shows the measured wave spectrum at the Marollegat station. The spectrum shows the characteristic gradual high frequency tail seen in fetch-limited environments.

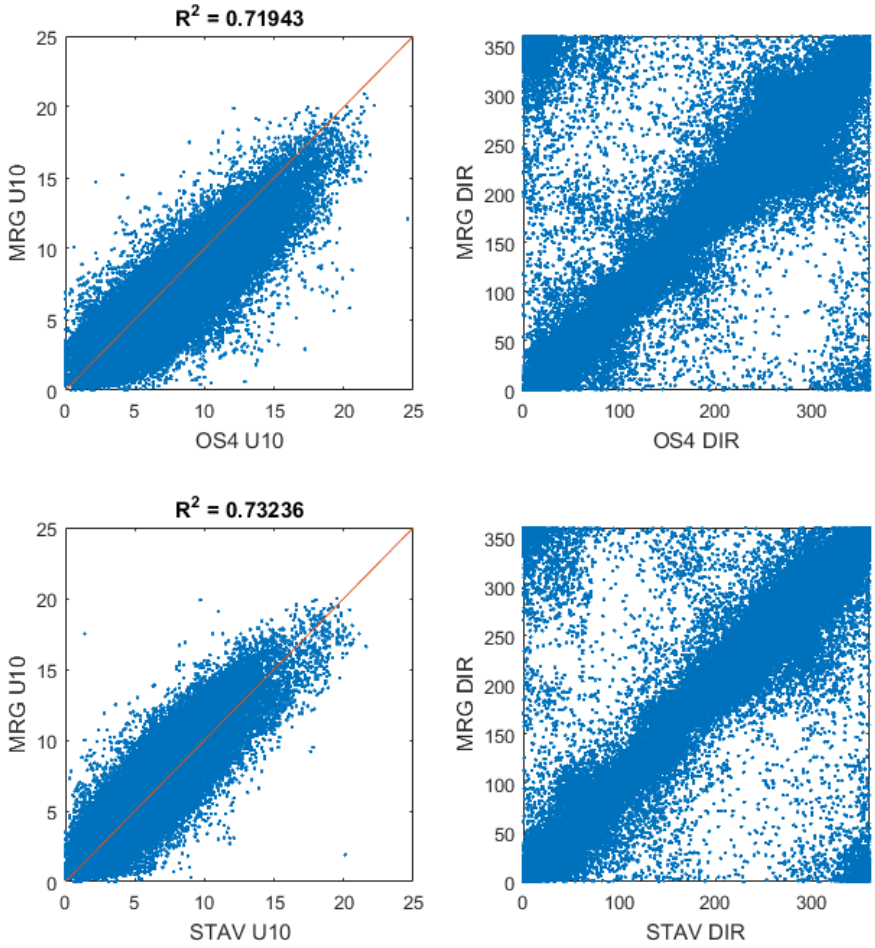

FIGURE 3.3: MAROLLEGAT WINDS CORRELATED WITH STAVENISSE (BOTTOM PANELS) AND OOSTERSCHELDE 4 (TOP PANELS). WIND SPEEDS ARE ON THE LEFT, WIND DIRECTION ON THE RIGHT.

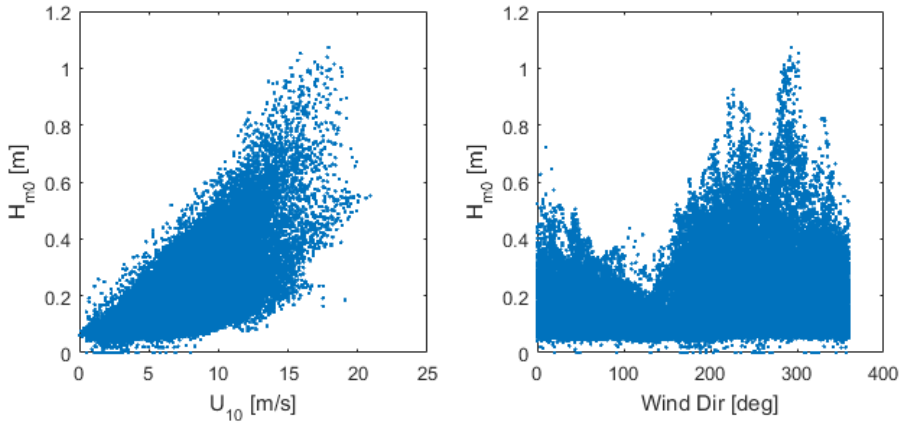

FIGURE 3.4: RELATIONSHIP BETWEEN WIND AND WAVE DATA COLLECTED AT MAROLLEGAT. WIND SPEED ON THE LEFT, AND WIND DIRECTION ON THE RIGHT.

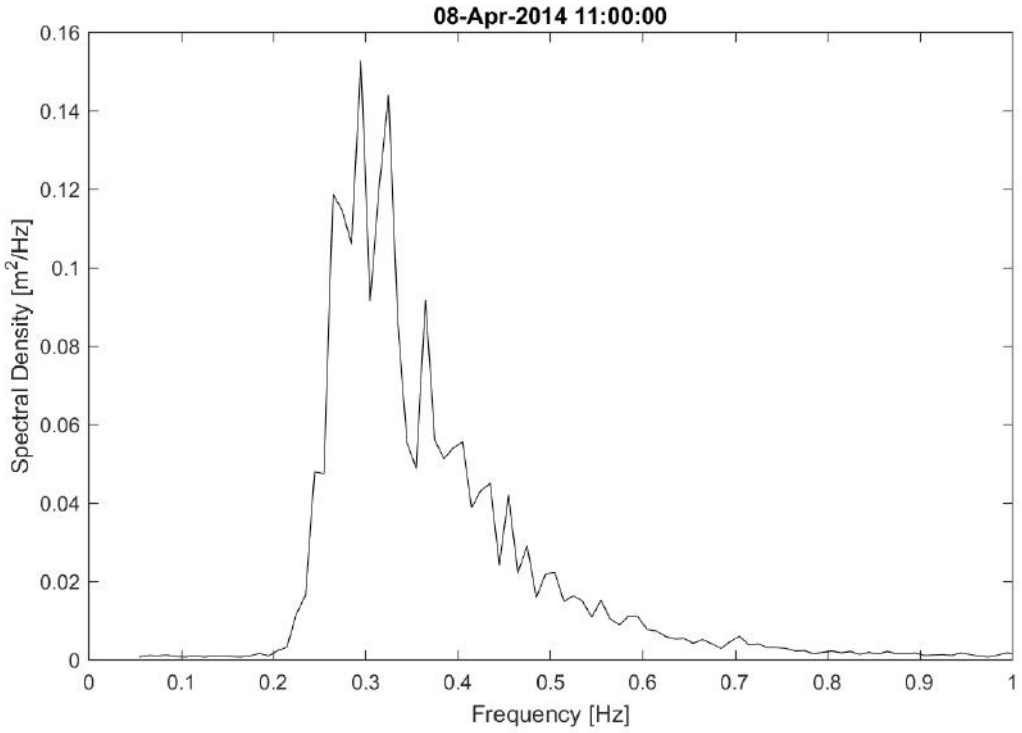

FIGURE 3.5: MEASURED SURFACE SPECTRUM AT THE MAROLLEGAT STATION DURING A PEAK WAVE EVENT ON APRIL 8, 2014 AT 11AM.

3.3. PRESSURE BOX DATA

The pressure box instruments were installed in their respective locations with heights of 5-20 cm over the bed. For the T0 and T1 deployments, GE PTX 600 pressure boxes were used, henceforth referred to as the RWS boxes. In the T2 deployment, a NIOZ OSSI pressure box was used alongside two RWS pressure boxes. This was done in order to assess the accuracy of the RWS pressure boxes.

A spectral approach was used to process the data. The spectral approach is preferred over the zero-crossing approach due to the ability to calculate spectral moments and for better comparison with model results. When the two approaches were compared, it was observed that wave heights that were calculated with the spectral approach were slightly higher than with the zero-crossing approach, due to the slightly different implementation of the transfer function. The Linear Wave Theory transfer function (excluding currents or non-linear effects) was used to convert pressure to wave height with a limit governed by $|z|/L = 0.2$[2]. Note that in Pezij (2015), a hydrostatic transfer function was used, which is known to underestimate wave heights at higher frequencies.

The choice of $|z|/L = 0.2$ is based on the recommendation of Wenneker (2014) and from observations of converted wave spectra. Most of the time, no obvious signs of high-frequency noise amplification were apparent in the estimated wave spectra using the $|z|/L = 0.5$ limit. The choice is highly subjective in the absence of surface wave data. Therefore, the following approach is taken:

- For the purposes of data analysis, the pressure data is converted to wave data using the LWT transfer function with a limit governed by $|z|/L = 0.2$. A comparison of different limits on the transfer function is included in Appendix A.

[2] Relative submergence of the instrument.

- For the purposes of calibration and validation of the numerical model, the model results are converted to pressure data, which avoids the subjectivity of having to choose a limit on the transfer function. Comparisons are made between pressure moments P_{m0} (the equivalent to H_{m0}). The mean wave periods from the estimated (using $|z|/L = 0.5$) and modelled surface spectra are also compared[3].

A drawback of this approach is that the high frequency tail of the model spectra (which would produce very little pressure) cannot be directly validated. However, it can be inferred from surface spectra observations at the MRG station and in the literature whether or not the high-frequency tails in the (surface spectra) model results are realistic. In addition, estimated wave spectra (using transfer function limits of $|z|/L = 0.5$), which at certain time points do not contain amplified noise, can also be used to infer this. However, in general, the measured pressure spectra showed signs of interference with multiple high frequency peaks and irregular shapes rather than the smooth gradual shape shown in Figure 2.3. In any case, the high frequency tail is only important for the wave parameters at the surface, and not important for sediment transport insofar as there is negligible interaction with the bottom. More discussion can be found in Chapter 4 and Chapter 7.

3.3.1. TIDAL MODULATION OF WAVES

The waves over the Oesterdam nourishment show the similar sensitivity to wind speed and direction that are observed from the MRG station (Figure 3.6). However, other influences are important at this location. The wave data measured at the nourishment show a sensitivity to water depth. Outside of the nourishment hook, one can analyze the effect of the tide on the wave characteristics. While the waves are seldom depth-limited, a relationship exists between wave period and water depth.Figure 3.7 shows that the wave periods increase with water depth while the wave heights show no discernible relationship with water depth.

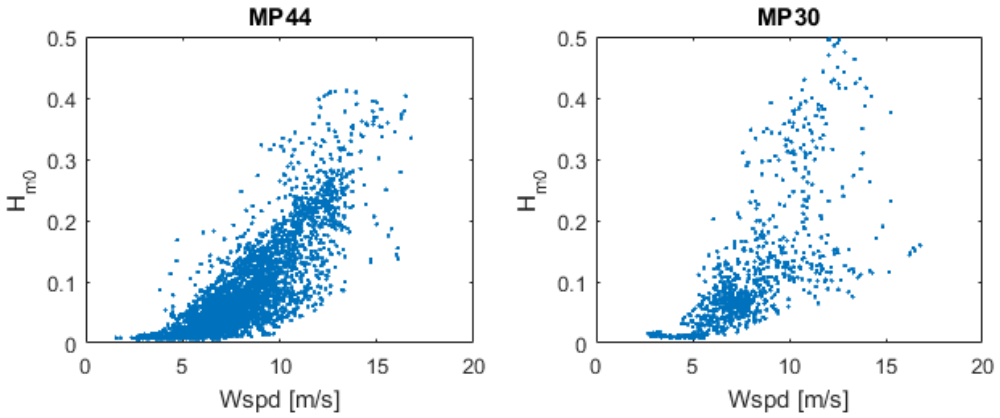

FIGURE 3.6: RELATIONSHIP BETWEEN MRG WIND AND PRESSURE BOX WAVE HEIGHTS. LEFT: MP44. RIGHT: MP30.

[3]Mean periods calculated from the pressure spectra were ignored, as they showed a strong low-frequency bias during small wave events where spectra are essentially white noise.

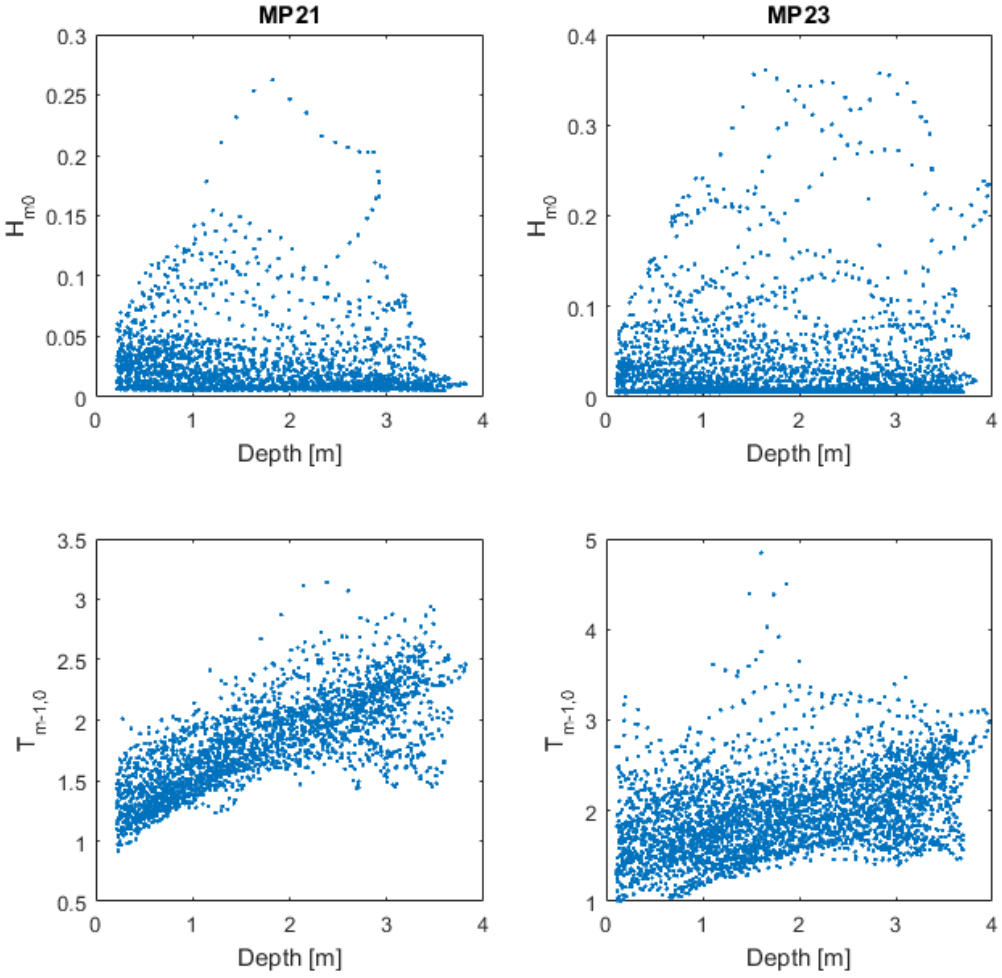

FIGURE 3.7: TIDAL MODULATION OF WAVES AT NOURISHMENT. TOP: WAVE HEIGHTS. BOTTOM. WAVE PERIODS. LEFT: MP21. RIGHT: MP23.

3.3.2. EFFECT OF THE NOURISHMENT HOOK

During the T1 period, the MP20/21 devices were deployed at the same time. The MP08/23 devices were deployed a few weeks later. During the T2 period, the MP30 and MP44 devices were also deployed at the same time. This allows for an analysis of the effect of the nourishment hook. Figure 3.8 shows a schematic of a cross section of the nourishment hook with the MP device locations.

Figure 3.9 shows the wave attenuation/growth over the hook for a range of water depths. The figure shows a weak general trend for wave attenuation at shallower water depths and wave growth for deeper depths. The wave growth could be due to shoaling and wind-wave growth over a distance of 300-400m. It is important to note that most of the data showed relative depths (d/L) between 0.05 and 0.5, which would be classified as intermediate depth.

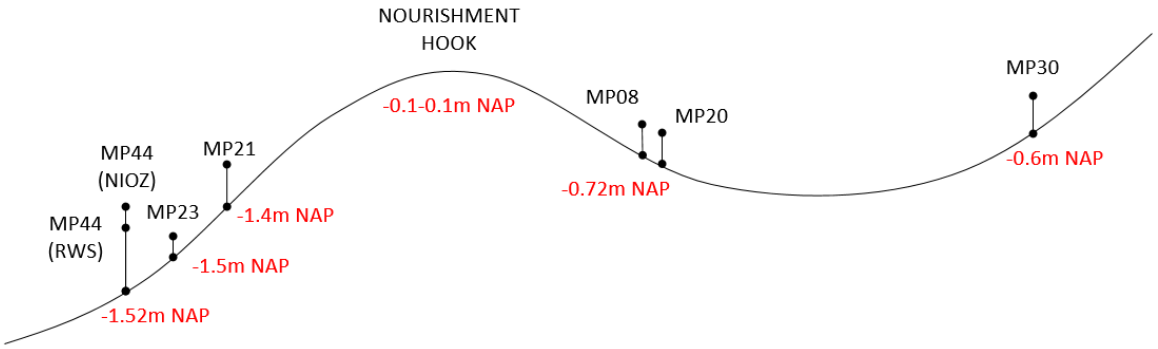

FIGURE 3.8: SCHEMATIZED CROSS SECTION OF NOURISHMENT HOOK (NOT TO SCALE).

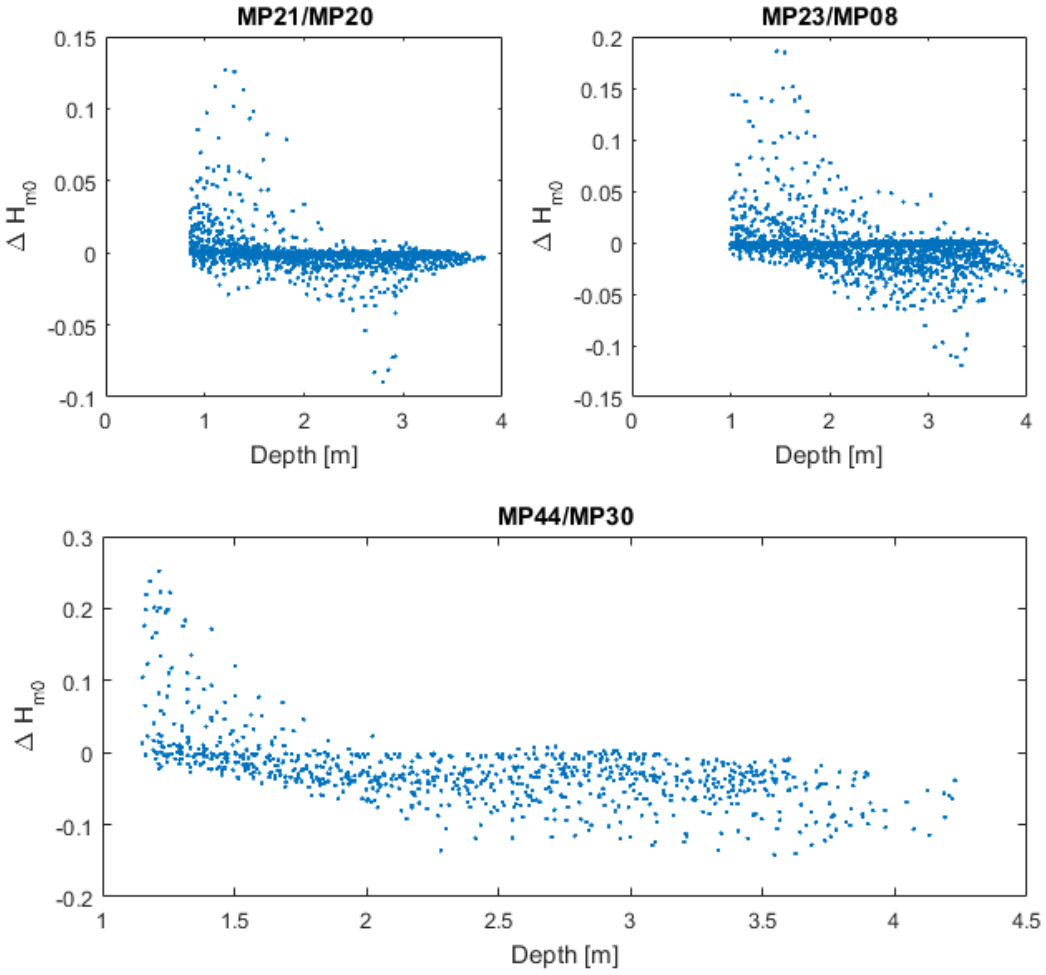

FIGURE 3.9: WAVE ATTENUATION/GROWTH OVER THE NOURISHMENT HOOK. POSITIVE VALUES INDICATE ATTENUATION, NEGATIVE VALUES INDICATE GROWTH.

3.3.3. RWS AND NIOZ PRESSURE BOXES

At the MP44 location, two pressure boxes were deployed in order to gain insight on instrument accuracy. One was provided by RWS (4 Hz) and the other by NIOZ (5 Hz). Figure 3.10 shows a comparison of the pressure measured by the two instruments. It can be observed that, despite the fact that the NIOZ sensor is located higher in the water column than the RWS sensor, the measured dynamic pressures are lower. In order from most likely to least likely, several possible conclusions can be drawn from this:

1. Measurement error in the recorded elevation of each pressure box.
2. Interference or damage to the RWS or NIOZ sensors during deployment.
3. Structural overestimation of dynamic pressure by the RWS box, or structural underestimation by the NIOZ box.
4. Errors during data processing.

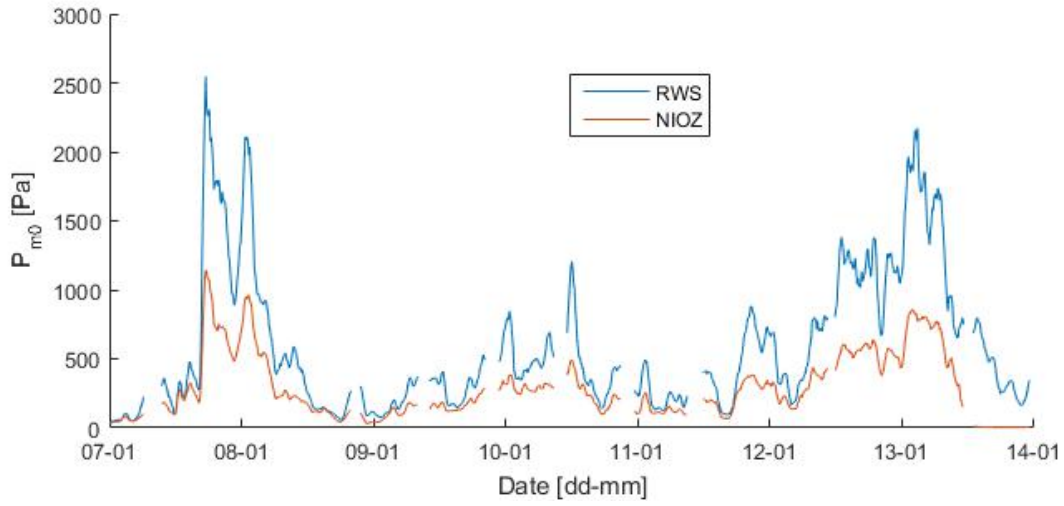

FIGURE 3.10: PROCESSING RESULTS FROM THE NIOZ AND RWS PRESSURE BOXES FOR THE T2 CAMPAIGN IN 2016.

The use of the NIOZ pressure box has raised more questions of instrument accuracy rather than answer them. A better experiment would be to install a different type of wave measuring device appropriate for shallow water. This could be a step gauge or high-frequency acoustic sensor. However, these types of instruments are more expensive than pressure transducers. The NIOZ pressure box data is not further analyzed in this thesis.

3.4. ADCP CURRENT DATA

The relationship between current speeds and tidal phase is plotted in the figure below. In addition, the depth-averaged current direction as a function of the tidal phase is also plotted. It can be seen that, during flood tide, the currents flow predominantly in the southeast direction, while they flow in the west-northwest direction during ebb tide. The current speeds during flood and ebb tide show no indication of flood or ebb dominance, except at MP20 and MP21 where a flood dominance is observed (additional plots shown in Appendix A). The reason may be that the MP20/21 locations are closer to the Marollegat channel.

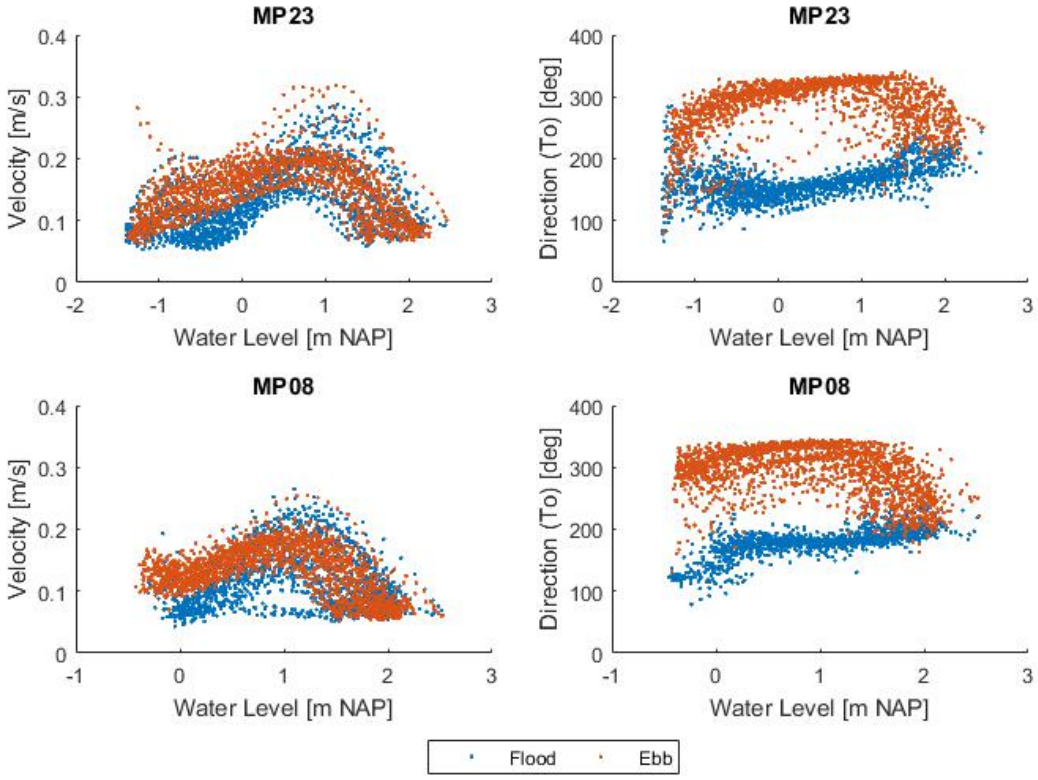

FIGURE 3.11: FLOOD AND EBB TIDAL CURRENTS AT THE MP23 AND MP08 LOCATIONS. DIRECTIONS ARE TOWARDS (OPPOSITE TO THE WIND/WAVE CONVENTION).

3.5. DEVELOPMENT OF THE NOURISHMENT

Bathymetric surveys on the Oesterdam flat were carried out 2-4 times per year from 2012 to 2016. The surveys were conducted by the use of RTK measurements along transects over the flat and nourishment area. RTK surveys were conducted in parallel transects using a GPS pole. The data was processed in ArcGIS for the calculation and visualization of bed level changes over time. Figure 3.12 shows the difference in the measured bathymetry from May 14, 2014 to October 29, 2015. Pezij (2015) noted the development of an ebb-tidal channel just east of the nourishment hook, which has since widened. More recently, the ebb channel appears to be developing into a more pronounced meandering shape.

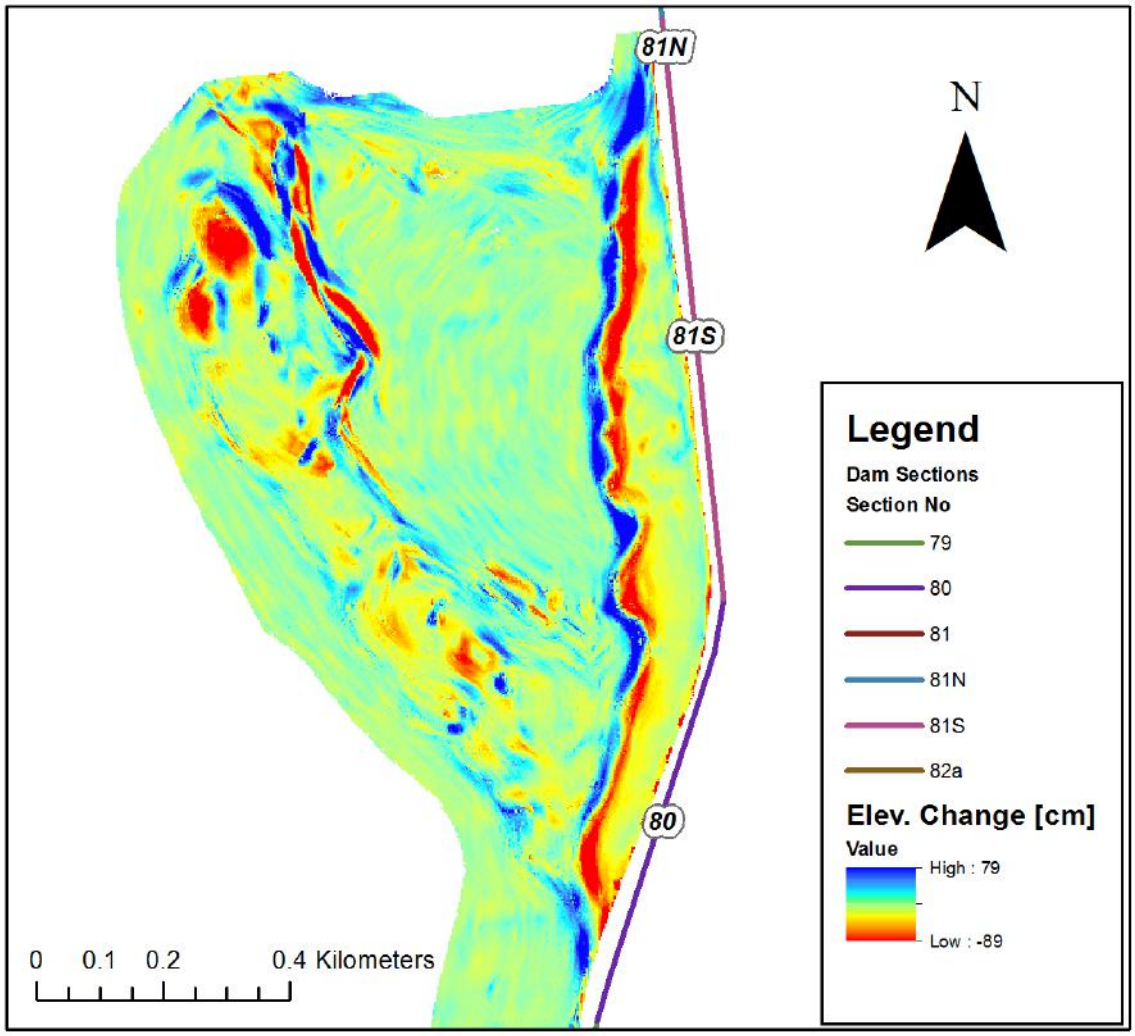

FIGURE 3.12: EROSION AND SPREADING OF THE NOURISHMENT FROM MAY 14, 2014 TO OCTOBER 29, 2015. BLUE INDICATES ACCRETION, RED INDICATES EROSION.

3.5.1. VISUAL OBSERVATIONS

Two site visits were conducted. The first was on March 5, 2016 and the second was on May 12, 2016. During both visits, the most significant observation was the formation of a second ebb channel and the sedimentation (and widening) of the old ebb channel that had previously formed. The second ebb channel formed west of the old channel, on top of the nourishment hook. What is not immediately apparent in Figure 3.12 is that many of the original ponds (shown in Figure 2.10) experienced sedimentation, and in some cases, became completely dry at low tide.

Another interesting observation was the damage to the Oyster reef at the northwest side of the hook (Reef C). Considerable damage was observed at this reef, unlike all of the other reefs. In fact, very little damage was observed at Reef D. In addition, the sediment around Reef D looked considerably finer than the sediment surrounding Reef C. More wave exposure at the northern part of the hook is likely to explain this difference.

3.6. TREND ANALYSIS OF AVERAGE BED ELEVATION

The average elevation of the flat and each element, before and after the nourishment, was calculated. Linear trends were fitted to the data in order to calculate how fast the nourishment hook, the foot, and the sheltered area were changing relative to the average change over the entire flat. Because the nourishment foot was re-profiled in March 2014, only surveys 3-8 were used for that particular trend analysis. Figure 3.13 shows the definition of the nourishment elements. Figure 3.14 shows the results of the calculated bed level change. Table 3.1 shows the calculated post-nourishment erosion rates.

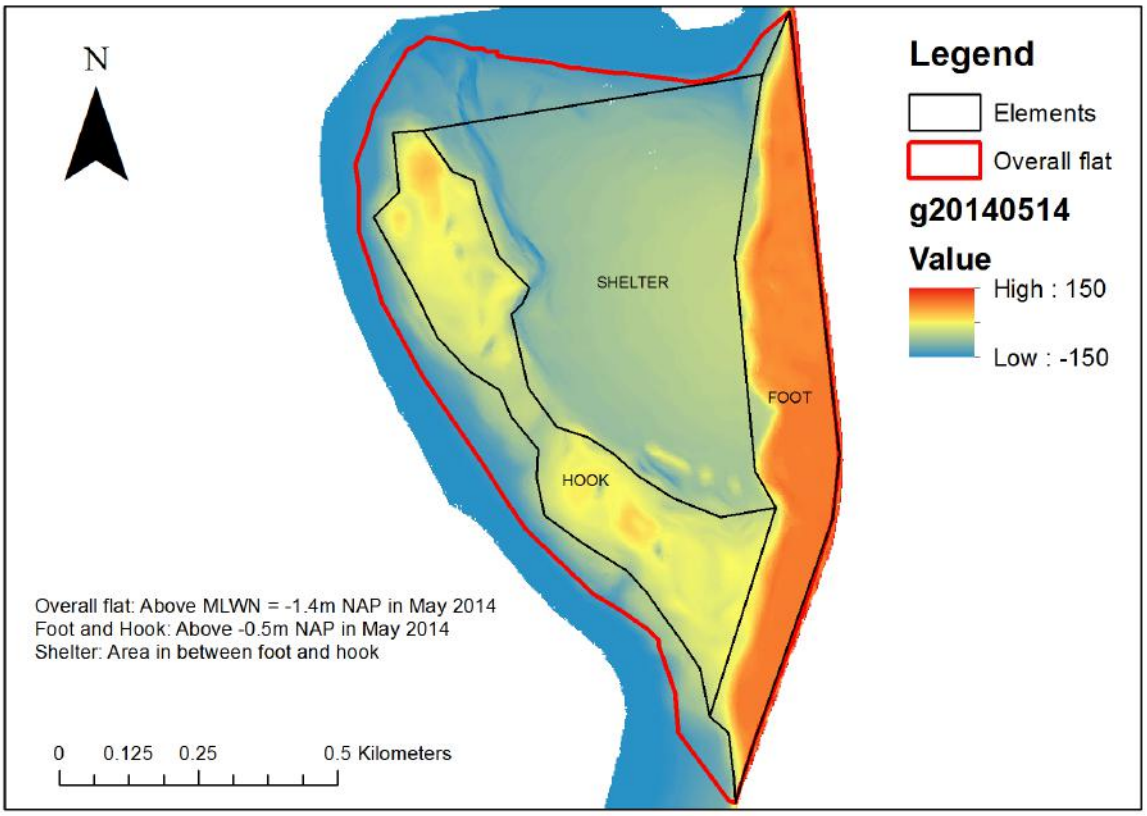

FIGURE 3.13: NOURISHMENT ELEMENTS DEFINED FOR TREND ANALYSIS OF EROSION FROM 2014 TO 2016.

TABLE 3.1: EROSION RATES ESTIMATED FROM TREND ANALYSIS POST-NOURISHMENT.

Element	Average [cm/yr]	Lower Bound* [cm/yr]	Upper Bound* [cm/yr]
Overall Flat	1.69	1.3	2.1
Foot	4.49	3.44	5.54
Hook	4.02	3.46	4.57
Shelter	0.78	0.4	1.16

*Calculated based on the 95% confidence interval, or twice the standard error of the average rate.

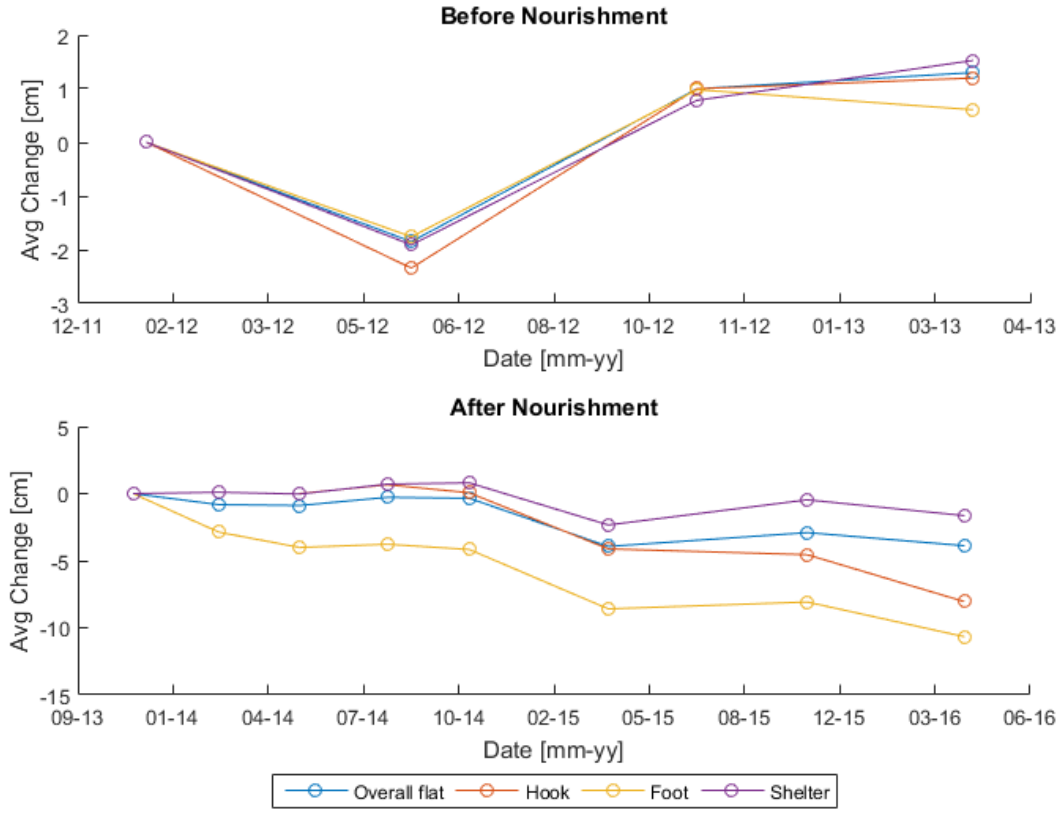

FIGURE 3.14: AVERAGE MEASURED BED LEVEL CHANGE AT THE OESTERDAM FLAT. THE HOOK, FOOT, AND SHELTER.

Before the nourishment, four RTK surveys were conducted at the Oesterdam. Linear regression and the calculation of 95% confidence intervals resulted in a statistically insignificant positive (accretive) trend. Errors in the RTK data may explain this, along with the lack of data points. Based on this, an estimate of the pre-nourishment erosion rate cannot be made from the RTK data.

After the nourishment, the overall flat and each defined element were all calculated to have statistically significant erosive trends. However, with only 5-7 data points the trends may not represent the real situation well. The hook and foot eroded much faster than the sheltered area in between, as expected. The results of this analysis show an average post-nourishment erosion rate of approximately 1.3-2.1 cm/year, using the 95% confidence interval. This is close to the estimate by De Graaf (2012) of 0.5 to 2 cm/year, which was based on vaklodingen data and RTK measurements on other flats.

3.6.1. LIMITATIONS

The RTK surveys before and after the nourishment were not conducted at consistent time points throughout the year. Due to the lack of surveys, all of them were used for the trend analysis. However, a seasonal bias may have skewed the results. For example, the pre-nourishment surveys show an apparent accretion at the flat, but the first survey was done during the winter, when stormy weather is expected to temporarily erode parts of the flat. The following surveys were done in other parts of the year, when presumably most of the eroded sediment is recovered. In the post-nourishment surveys, the winter survey was only done in the beginning, which means there may be a summer bias in the trend, thus underestimating the erosion rate.

Taking out the winter surveys might improve the trend analysis but the number of surveys is already very small. There would have to be at least 30 surveys (done at consistent time points) to extract a reliable estimate of the real erosion rates (Wigley et al., 2006).

4

HYDRODYNAMIC MODELLING OF MEASURED CONDITIONS

A Delft3D FLOW/WAVE model was used to simulate measured conditions throughout the Eastern Scheldt and at the Oesterdam nourishment. The model was validated in the deeper parts of the basin and partially validated at the Oesterdam nourishment using pressure data. Modelled currents were compared to ADCP data and the effect of currents on the waves was explored. A sensitivity analysis was conducted in order to gain more insight into the sensitivity of the wave parameters at the nourishment to different model input parameters. The application of the Delft3D model is discussed in this section.

4.1. MODEL SELECTION

In Pezij (2015), a coupled Delft3D FLOW/WAVE model was set up for the Eastern Scheldt and the Kom. At the time of writing, the Delft3D WAVE module uses SWAN version 40.72AB. SWAN is a spectral wave model that simulates the processes of wind-wave growth, wave propagation (shoaling and refraction), wave dissipation (whitecapping, friction, and depth-inducted breaking), and transformation (triads and quadruplets). The SWAN computations are coupled with the FLOW model at specified intervals in order to account for wave-induced currents and wave-current interaction. More information on Delft3D and SWAN can be found in Deltares (2014a), Deltares (2014b), and The SWAN Team (2008).

Other numerical models such as XBeach (Roelvink et al., 2015) and SWASH (TU Delft, 2016) were considered for application in the Kom. These numerical models are similar in that they are wave-resolving with the capability to simulate long-wave generation in the surf zone, a process that is important for wave run-up and dune erosion. This process and other shallow water processes may be important for the assessment of run-up and overtopping at a structure, especially in the presence of a shallow foreshore (Oosterlo, 2015). However, under both operational and design conditions, the waves at the Oesterdam are usually not depth-limited due to the limited fetch for wave growth. In addition, these models currently do not simulate wind-wave growth, which is the most important wave-related process in the Kom. Therefore, if one of these models are used, they must be in combination with SWAN or another wind-wave model.

The Delft3D FLOW/WAVE model was chosen for the thesis work. This was done for three reasons. First, the problem of calibration in shallow water identified by Pezij (2015) and Das (2010) could be explored in further detail. Second, coupling SWAN results with XBEACH or SWASH would be

difficult with the complex bathymetry in front of the Oesterdam. Third, it is believed that wind-wave generation is still an important process at the Oesterdam and using the other models over part of the domain would neglect additional wave growth.

4.2. MODEL SETUP

The model setup was obtained from Pezij (2015). Most of the default settings were used for both the FLOW and WAVE setup. For the SCALOOST FLOW model, the storm surge barrier was implemented as a series of porous plates with a calibrated transmission coefficient of 2.6 from Pezij (2015). The bottom roughness was calibrated to a manning's n = 0.029 $m^{1/3}/s$. The storm surge barrier was not implemented in the WAVE module as it was determined to have no effect on the simulated waves at Marollegat. Table 4.1 details the model parameters and settings. Detailed descriptions of the default parameters in Delft3D FLOW and WAVE (SWAN) are found in Deltares (2014a) and The SWAN Team (2008).

4.2.1. GRIDS

The five FLOW and WAVE computational grids were obtained from Pezij (2015). The bathymetry is based on the 2013 Vaklodingen survey of the Eastern Scheldt. At the Oesterdam, the bathymetry was imported from the RTK measurements in November 2013 (for T1) and October 2015 (for T2). Figures 4.1 and 4.2 show the grids used in the modelling.

The FLOW and WAVE simulations were split into the SCALOOST and Kom model domains. First, the SCALOOST model, consisting of only the SCALOOST grids, was used to generate flow and wave boundary conditions for the Kom model (referred to as the Oesterdam model in Pezij (2015)). NESTHD was used to generate flow boundary conditions for the Kom FLOW model. An output point at Yerseke (YE, see Figure 3.1) was used to create the wave boundary for the Kom model. In the Kom model, a nested wave grid is used within the Kom wave grid while only one flow grid is used. The third wave grid has a resolution of 10x10m and covers the Oesterdam flat.

4.2.2. BOUNDARY CONDITIONS

Offshore flow boundary conditions for 2013/2014 (T1) were obtained from the DCZMv6-ZUNOv4 North Sea model. However, the model results were not available for January 2016. The 2013/2014 North Sea model time series was converted to astronomical tidal forcing in MATLAB using T-TIDE. This allowed for the simulation of the January 2016 time period. One limitation of this approach is that storm surges are neglected. Offshore wave boundary conditions were created using data from the Schouwenbank (SCHB) wave buoy. For the SCALOOST model, wind from the Stavenisse station was used as input. For the Kom model, wind from the Marollegat station was used as input.

TABLE 4.1: MODEL PARAMETERS IN SCALOOST AND KOM SIMULATIONS.

Parameter	Value	Units
FLOW		
Time Step	0.125	mins
Courant Number	<10	
Wind Drag Coefficients:		
. Breakpoint 1 (0 m/s)	0.000623	[−]
. Breakpoint 2 (100 m/s)	0.00723	[−]
. Breakpoint 3 (100 m/s)	0.00723	[−]
Bed Roughness Formulation	Manning	
. Bed Roughness	0.029	$m^{1/3}/s$
Horizontal Eddy Viscosity	1	m^2/s
Additional Keywords:		
. Cstbnd = #YES#		
. Filppl = #barrier_scaloost.ppl# (SCALOOST only)		
. Energy loss coefficient (ppl)	2.6	[−]
. Upwppl = #Y# (SCALOOST only)		
WAVE		
Computational Mode	Stationary	
Coupling Interval	30	mins
Frequency Range	0.05-2	Hz
Number of Frequency Bins	24	
Number of Directional Bins	36	
Whitecapping Formulation	Komen (delta=0)	
Quadruplets	On (defaults)	
Triads	On (defaults)	
Diffraction	Off	
Bed Friction Formulation	JONSWAP	
. Bed Friction Coefficient	0.067	[−]
Wave breaking	CONSTANT	
. Wave breaking α	1	[−]
. Wave breaking γ	0.73	[−]

4.3. VALIDATION IN DEEP WATER

In Pezij (2015), the SCALOOST model setup was previously calibrated and validated for measured water level and wave data in 2013 and 2014. The modelled water levels and wave heights inside and outside of the basin, including at the Marollegat, were further validated for the new measured data in January 2016. The results are shown in Appendix B. The use of astronomic forcing as the offshore boundary conditions resulted in small differences of up to 10 cm between measured and modelled water levels, usually only at the low water levels.

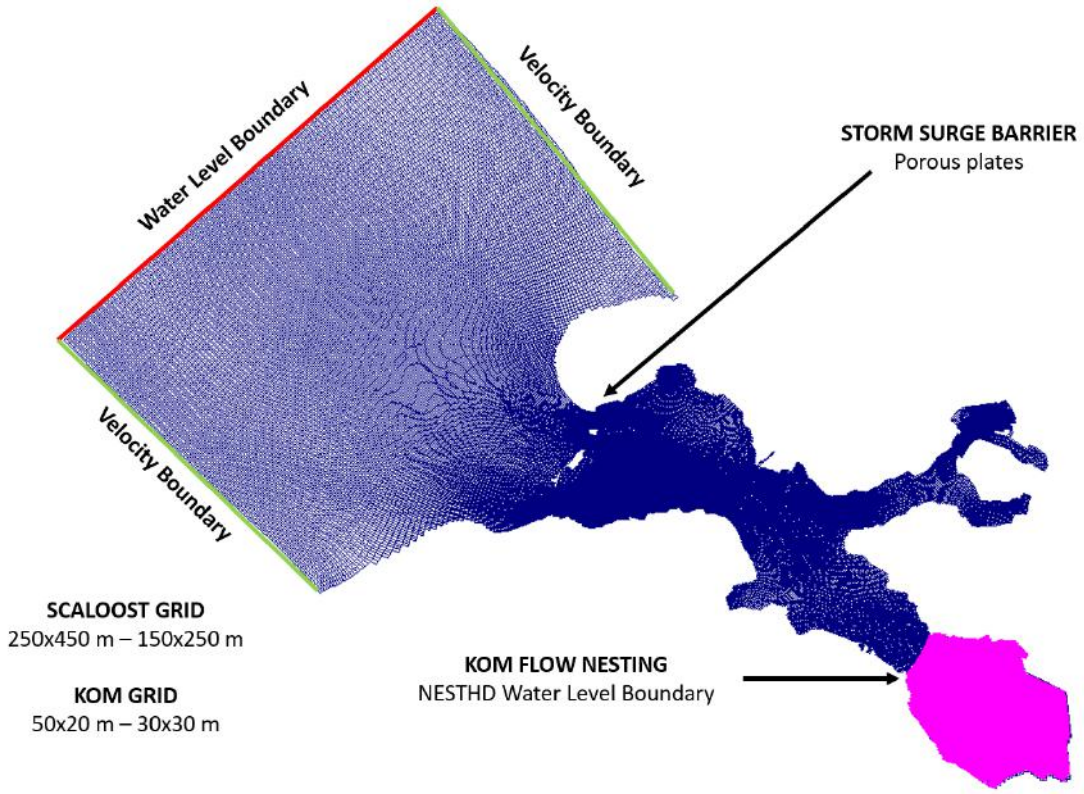

FIGURE 4.1: DELFT3D FLOW GRIDS FOR SCALOOST AND THE KOM.

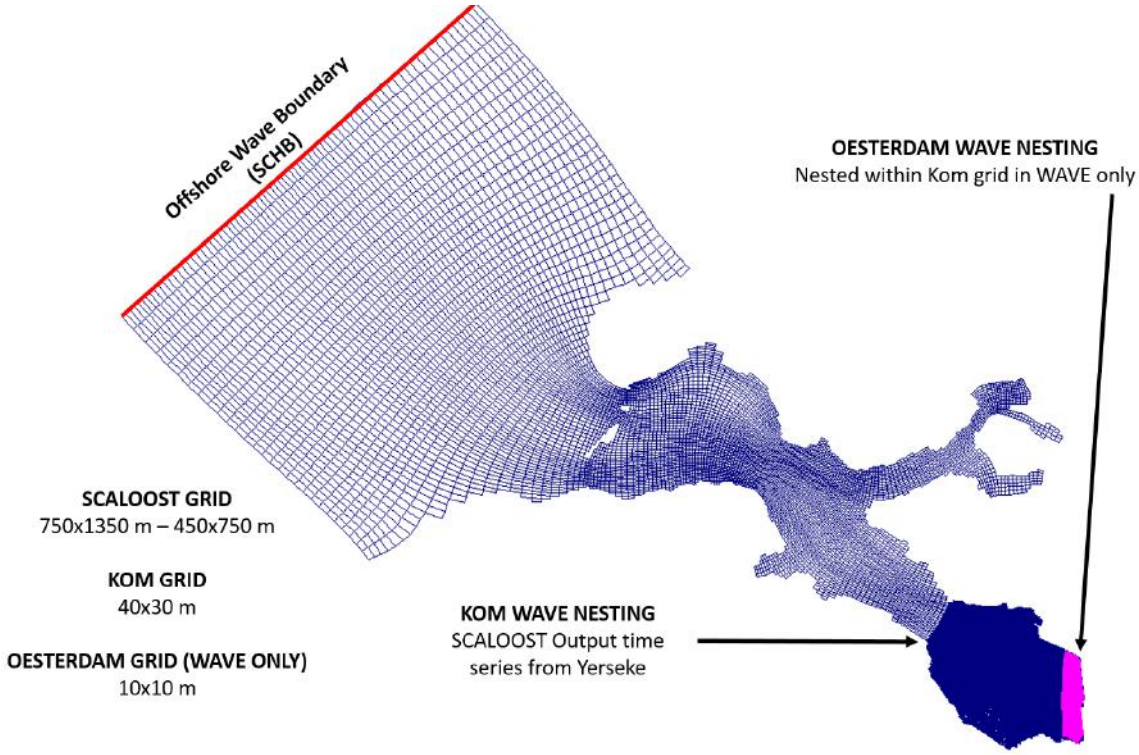

FIGURE 4.2: DELFT3D WAVE GRIDS FOR SCALOOST, THE KOM, AND THE OESTERDAM.

4.4. PARTIAL VALIDATION AT THE OESTERDAM

As explained in Section 3.3, the calibration/validation of wave heights at the Oesterdam is done by converting model results to pressure at the pressure box locations. Due to the limitations of this method, mainly the neglect of the high frequency tails of the spectra, it is considered a partial validation. Two calibration periods were chosen: February/March 2014 and March/April 2014. The chosen validation period is from January 7th to 13th, 2016. Several output points were used for the T1 and T2 simulations, in addition to a transect for detailed analyses (Figure 4.3).

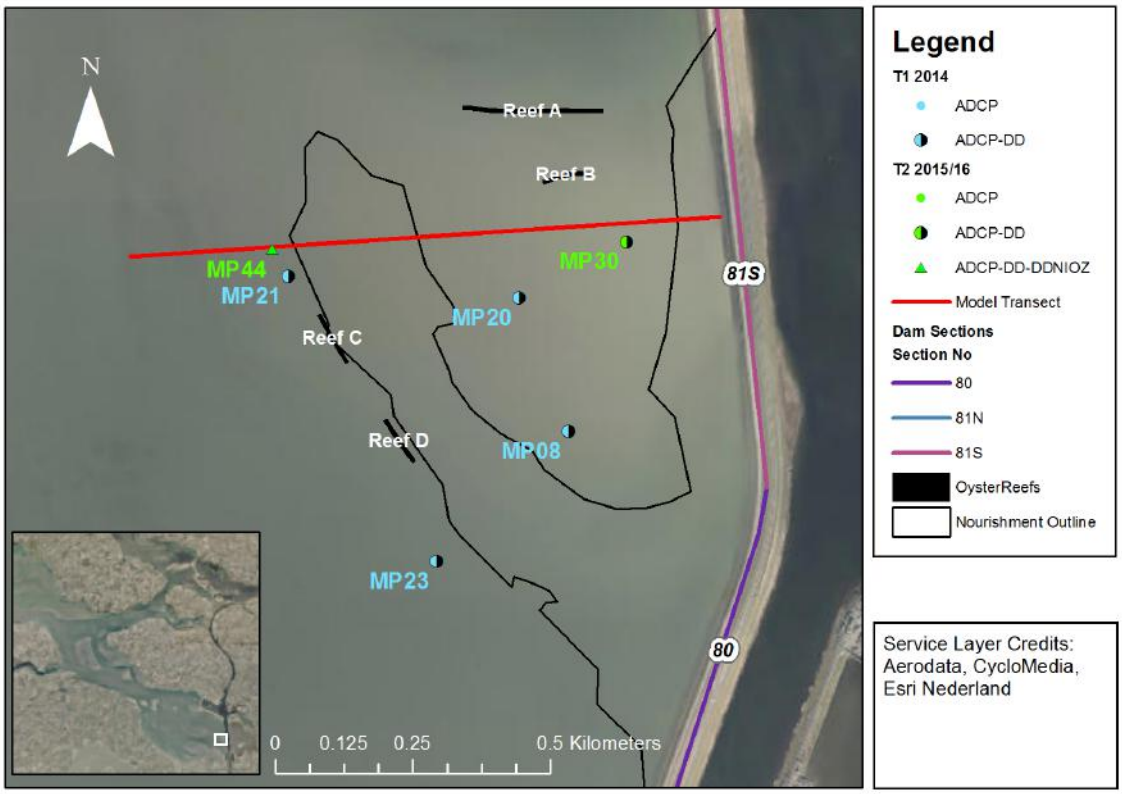

FIGURE 4.3: MODEL OUTPUT LOCATIONS AROUND THE NOURISHMENT.

A test simulation was done with the same parameters used in Pezij (2015). The results for the T1 calibration periods is shown in Figure 4.4. The figure shows generally well-predicted wave pressures at the pressure boxes except at MP20 and MP21. In addition, a small underestimation of wave periods was observed during the higher wave events. To investigate the discrepancy of wave pressures at MP20 and MP21, the wave spectra were plotted in Figure 4.5. A significant amount of wave energy was observed in the modelled surface spectra at high frequencies which induce negligible wave-induced pressure. Improving the prediction of mean wave period (in other words, increasing the lower-frequency energy) would improve the prediction of wave pressure. However, better knowledge of model sensitivity to input parameters is needed before the wave periods are calibrated.

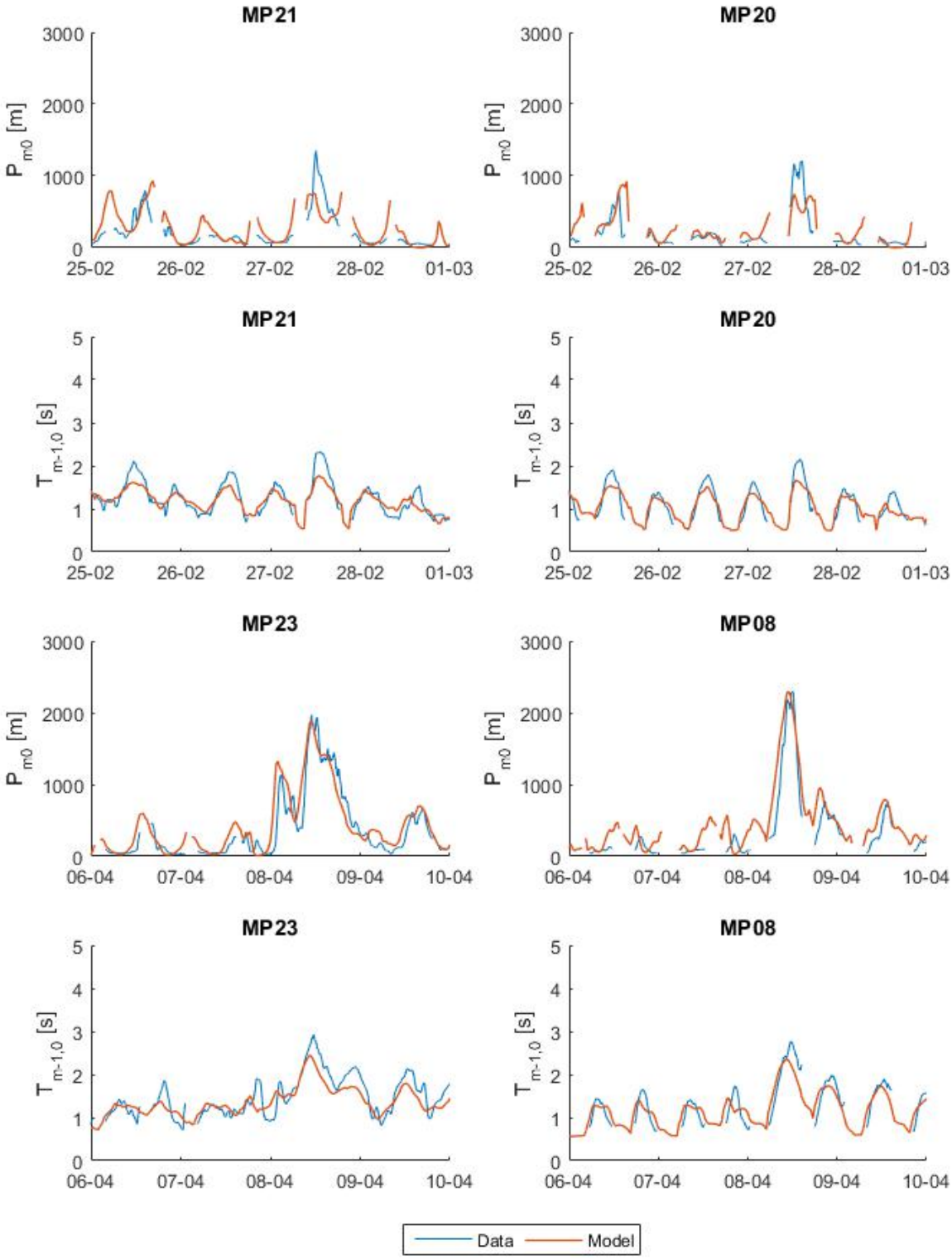

FIGURE 4.4: T1 OESTERDAM INITIAL MODEL RESULTS.

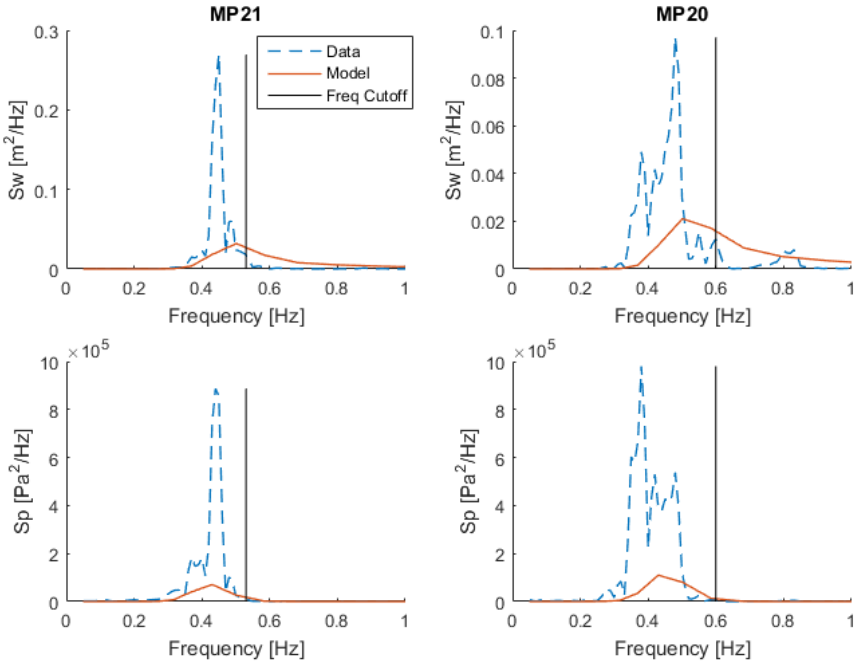

FIGURE 4.5: T1 OESTERDAM INITIAL WAVE SPECTRA (DEFAULT PARAMETERS) AT MP20 (OUTSIDE HOOK) AND MP21 (INSIDE HOOK) ON FEBRUARY 27 AT 2PM. THE BLACK LINES INDICATE THE FREQUENCY CUTOFF CORRESPONDING TO $z/L = 0.5$.

4.4.1. SENSITIVITY ANALYSIS

A simple sensitivity analysis was conducted in order to gain insight into the sensitivity of simulated wave parameters, especially the wave period, to several input parameters. A 22 hour time period on April 8, 2014 was chosen for the sensitivity analysis. Preliminary sensitivity tests on various SWAN parameters resulted in the following list of sensitive parameters. The results are shown in Figure 4.6.

- Wind speed (for reference)
- powst : Komen whitecapping parameter (base = default = 2)
- cds2 : Komen whitecapping linear scaling term (base = 2.5e-5, default = 2.36e-5)
- Delta : Komen whitecapping parameter (base = 0.5, default = 0)
- JONSWAP bed roughness coefficient (base = 0.05, default = 0.067)
- Cnl4 : Quadruplet interaction linear scaling term (base = default = 3e7)
- gamma : Depth-induced breaking parameter (base = 0.7, default = 0.73)

The results show that the most sensitive parameter is always the wind speed, and the wave heights are generally more sensitive to model input than the wave periods. Given that the standard deviation of the measured 10 minute wind speed is 10-15% of the mean 10 minute wind speed, wind gust could cause differences in wave height for the same measured mean. However, the effects of gust may also be insignificant over the 30 minute time intervals that are modelled.

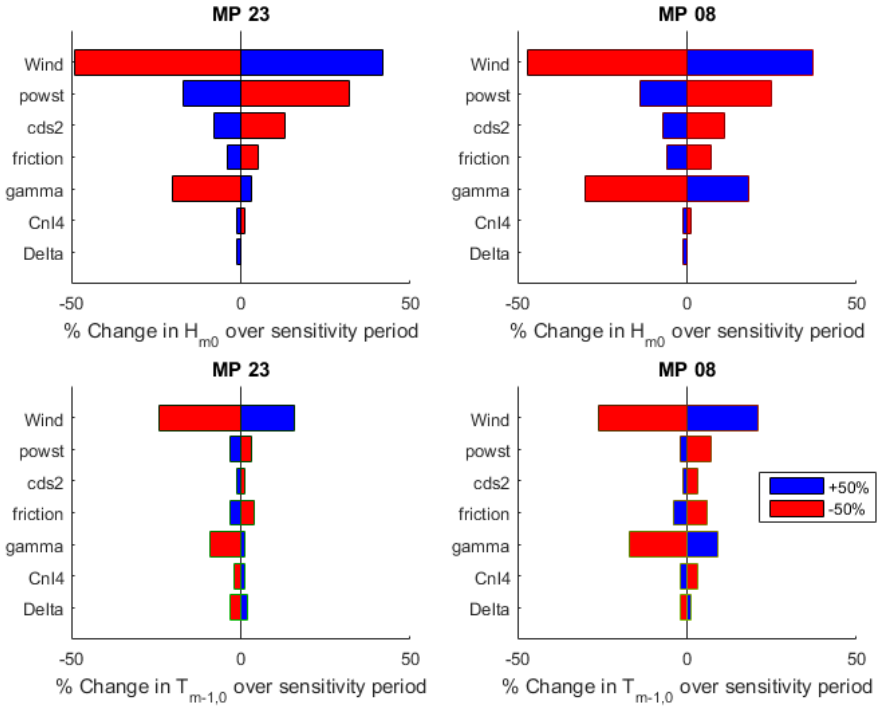

FIGURE 4.6: TORNADO DIAGRAMS OF SWAN PARAMETERS SHOWING THE SENSITIVITY OF WAVE HEIGHT AND PERIOD AT THE NOURISHMENT LOCATION.

An interesting result is the sensitivity of wave period to the quadruplet Cnl4 parameter. It appears that the average wave period decreases at MP08 with increasing Cnl4. The opposite is seen at MP23. This suggests that the quadruplet scaling term may have a complex effect on the spectral moments, especially if they are calculated using the full spectral range of up to 2 Hz. Gorman & Neilson (1999) notes that the quadruplet interaction source term not only transfers high frequency energy to lower frequencies, but also to very high frequencies above 1 Hz.

4.4.2. CALIBRATION OF WAVE PERIODS

From the sensitivity analysis, the parameter which affects wave period but has very little effect on the wave height was determined to be the quadruplet scaling term Cnl4. While the delta term also shows similar sensitivity, the range is much less liberal than that of Cnl4[1]. An increase in Cnl4 term increases the transfer of high frequency energy to the lower frequency part of the spectrum, visualized in Figure 2.4. However, an increase in Cnl4 does not always increase the mean wave period, as shown in the result for MP08 in Figure 4.6. Test simulations were done with the quadruplet interaction term (Cnl4) scaled up by a factor of 5. With a Cnl4 of 1.5e8[2], the modelled wave pressures and wave periods show a closer match with the data (Figure 4.7).

[1] The choice of delta is limited to the range between 0 and 1, while Cnl4 is simply a scaling term.
[2] The default value in SWAN is Cnl4 = 3e7

The effect of changing the scaling term may have unexpected consequences under different hydrodynamic conditions. In addition, the use of a scaling term for a complex process such as quadruplet interactions must be backed with a strong understanding of the quadruplet implementation in SWAN. It has been shown from the SCALOOST results that the wave heights and periods are well represented in the model in deep water. Furthermore, the discrepancy in wave pressures at MP20 and MP21 were mostly due to the fact that they were very short waves. Therefore, mindful of the application of the model to design conditions, the new quadruplet scaling term was not implemented. The results for the T2 period also show reasonable agreement, and are shown in Appendix B.

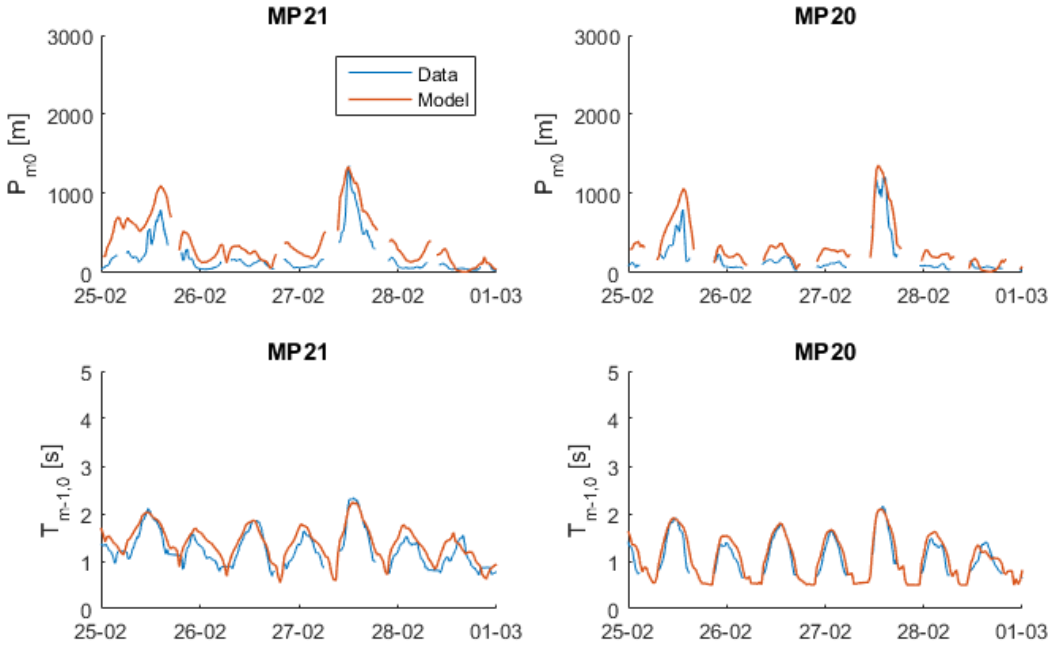

FIGURE 4.7: T1 OESTERDAM SIMULATIONS WITH CALIBRATED WAVE PERIODS USING SCALED UP QUADRUPLET INTERACTIONS. LEFT: OUTSIDE HOOK. RIGHT: INSIDE HOOK.

4.4.3. CALIBRATION OF CURRENT VELOCITIES

The calibration of current velocities is done independently of the wave parameters. The assumption is that the currents have a negligible effect on the wave heights. This assumption is tested in Section 4.5. The FLOW bottom roughness was used to calibrate the current velocities to the measurements on the Oesterdam nourishment. The best results were observed from a roughness value of 0.015. This is approximately half of the value used by Pezij (2015).

The results show a consistent under-prediction of current velocities at MP23 (Figure 4.8). In Chapter 3, it was noted that the southern part of the nourishment hook contained visibly finer material than the northern part. Ideally, a spatially varying roughness field would be implemented with a lower manning's n around the MP23/MP08 area. However, it was not implemented with the assumption that modelled currents have negligible effect on the waves (further explored in Section 4.5). Appendix B includes the validation of the T2 current measurements.

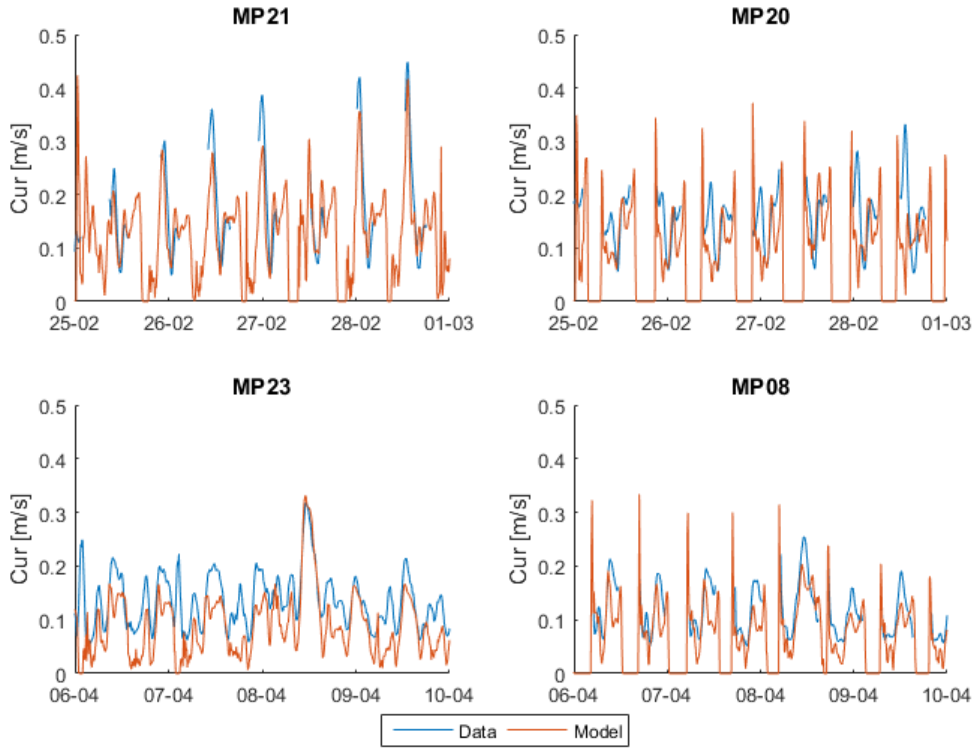

FIGURE 4.8: T1 OESTERDAM MODELLED CURRENTS. LEFT: OUTSIDE HOOK. RIGHT: INSIDE HOOK.

4.5. WAVE-CURRENT INTERACTION

The sensitivity of the simulated wave height to simulated currents relative to wind forcing were explored. The results are shown in Figure 4.9. It was speculated that currents in the Kom have a negligible effect on the wave heights, partially because of small current velocities and partially because of the near-perpendicular angle between them. However, the near-perpendicular angle may not play a large role as the modelled currents rapidly change in direction during the tidal cycle (Figure 4.10). It should be noted that the simulated waves with 'no wind' still included wind-generated waves from the Eastern Scheldt as a boundary condition. Without wind-wave generation in the Eastern Scheldt, no waves would reach the Oesterdam.

4.6. WAVE ATTENUATION OVER THE HOOK

The wave attenuation over the hook was explored by plotting the difference in wave height over each transect, as shown in Figure 4.11. It appears that the model simulates wave attenuation to the same order of magnitude when it comes to the difference in wave height over the hook at the shallow water depths. However, the model does not show as much wave growth at larger depths as is observed in the data.

The model results for a selected time point were visualized along a transect shown in Figure 4.3. It is apparent in Figure 4.12 that attenuation occurs over the hook at high water and only recovers after a large distance of wave growth. The effect of the hook immediately landward appears to be overstated in the model. On the other hand, the data points do have considerable scatter, even at deeper water depths, so it is difficult to say whether or not a net wave growth is expected at high water. The model does capture the diminishing effect of the hook at deeper water depths.

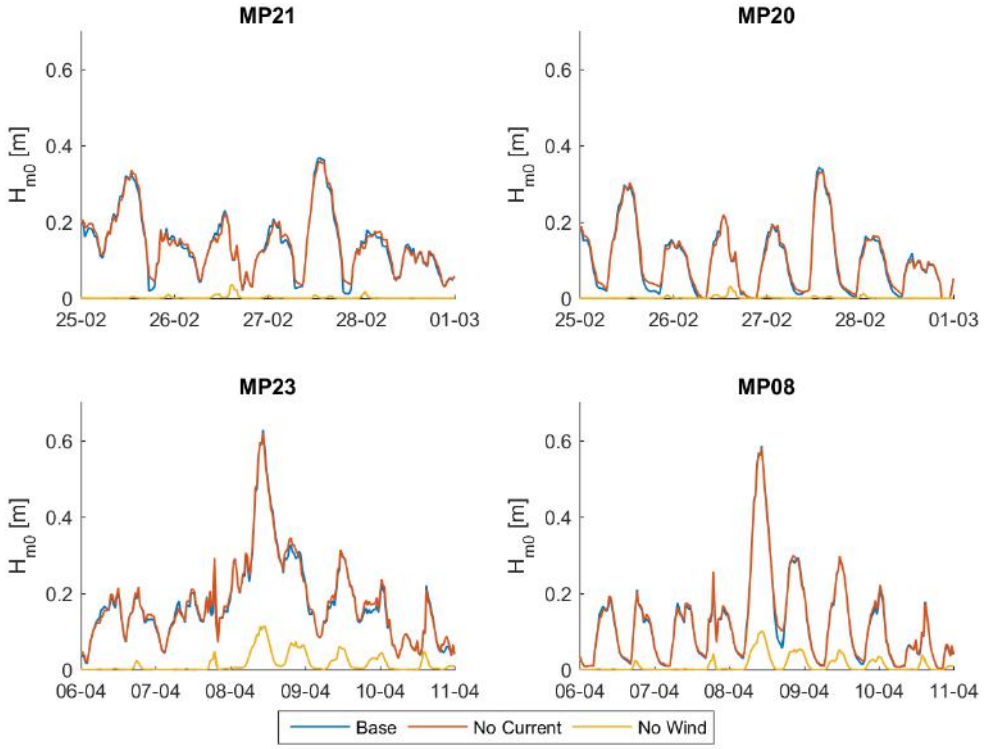

FIGURE 4.9: SENSITIVITY OF WAVE HEIGHT TO SIMULATED CURRENTS AND WIND FORCING.

In Figure 4.12, it is observed that at low water, the approaching waves are dissipated by both bottom friction (just outside of the hook) and by depth-induced breaking (on the inside of the hook). While the waves are very small once they reach inside the hook, the area is more or less dry which explains the wave breaking. At mean water, the dissipation over the hook is due to friction, and some wind-wave growth is responsible for partially recovering the wave height by the time it reaches the dam foot. At high water, a near full recovery of the wave height is observed by the time the waves reach the dam foot, at which point the waves are further damped by breaking and bottom friction.

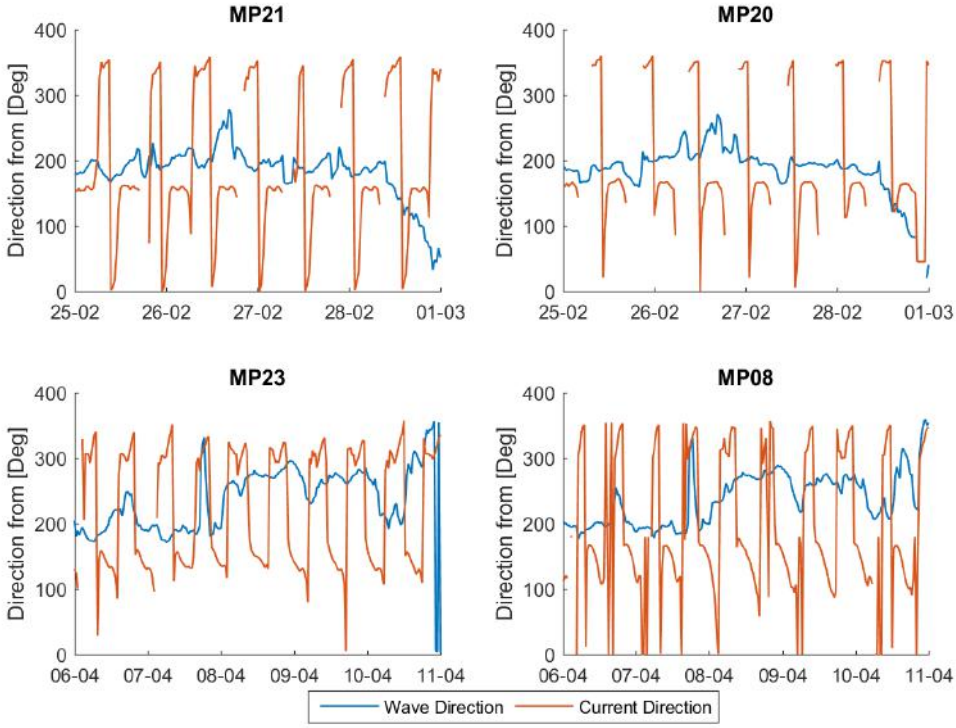

FIGURE 4.10: WAVE AND CURRENT DIRECTIONS DURING THE T1 PERIOD. BOTH CONVENTIONS ARE NAUTICAL.

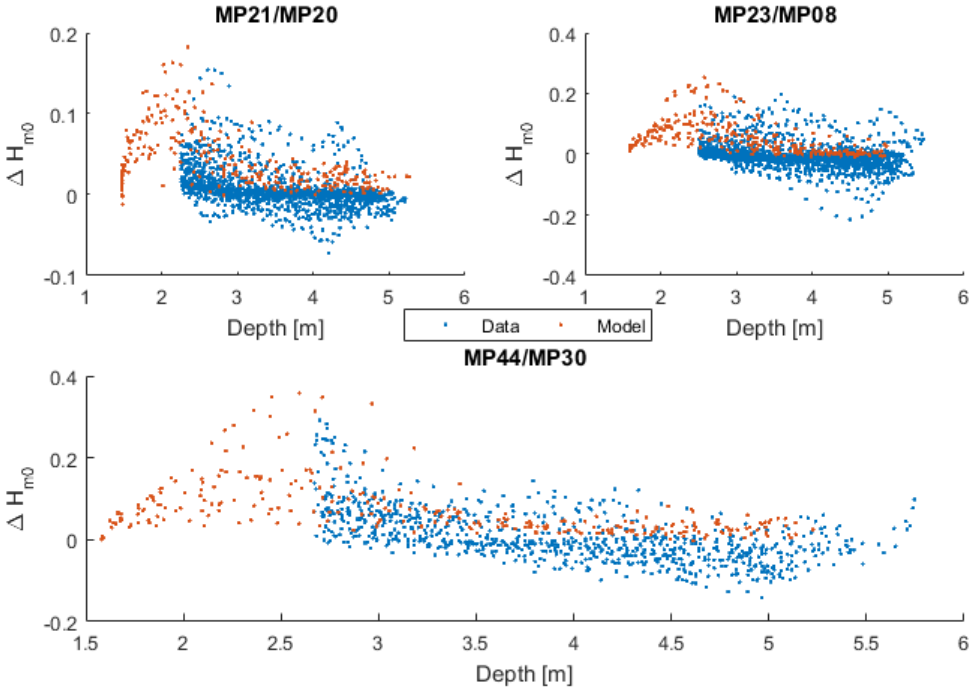

FIGURE 4.11: WAVE ATTENUATION/GROWTH OVER THE NOURISHMENT HOOK. POSITIVE VALUES INDICATE ATTENUATION, NEGATIVE VALUES INDICATE GROWTH.

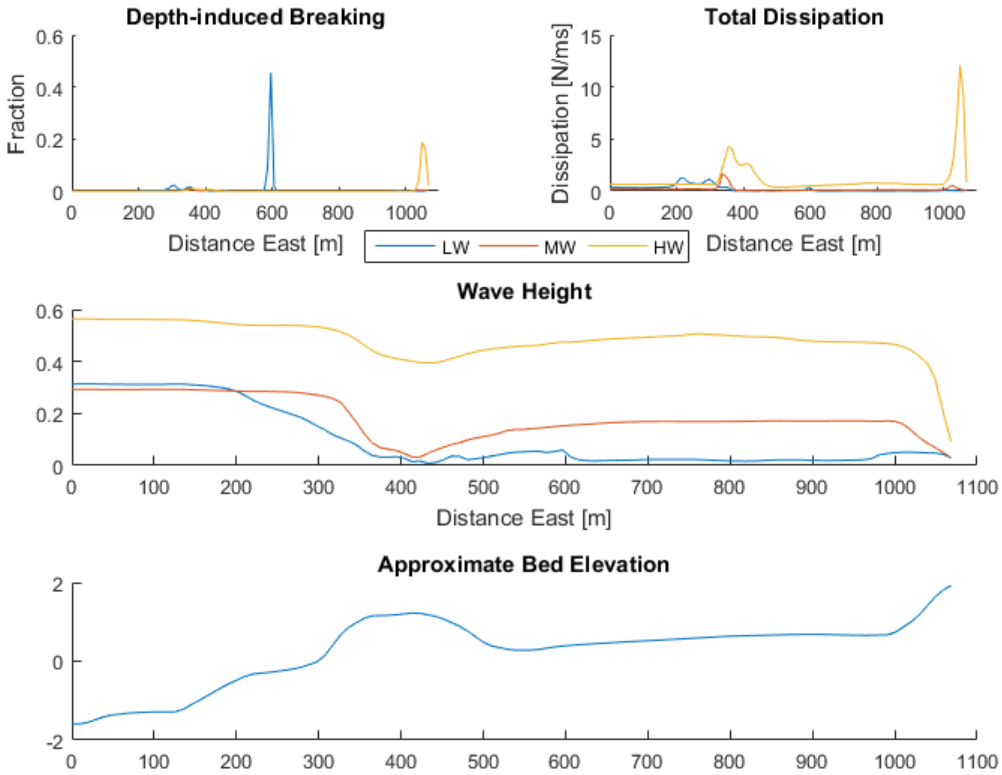

FIGURE 4.12: MODELLED WAVE ATTENUATION ALONG NORTHERN TRANSECT DURING HIGH WATER, MEAN WATER, AND LOW WATER IN APRIL 2014.

5

PROJECTIONS OF TIDAL FLAT EROSION

Projections of erosion in the Kom and at the Oesterdam tidal flat are done in order to estimate the design wave loads in future time scenarios. The projections are prepared mindful of the fact that they are intended for input into Delft3D bathymetric grids. Some simplifications are therefore made, as described below. Between 1990 and 2010, the Oesterdam tidal flat eroded at an average rate of 1.25-2.5 cm/year based on vaklodingen survey data (De Ronde et al., 2013). However, the vaklodingen data is much lower resolution than RTK data surveys. De Graaf (2012) estimated a lower bound erosion rate of 0.5 cm/yr based on RTK measurements on other flats. The results from Section 3.6 were used to project an upper bound and lower bound erosion rate at the Oesterdam.

5.1. ASSUMPTIONS AND LIMITATIONS

Linear trends are used for the erosion projections in this thesis. Conceptually, the rate of morphological change in a natural system that is out of morphological equilibrium can be described by an exponential decay curve (Bosboom & Stive, 2015). However, this curve represents long time scales. On an annual or decadal time scale, the curve can be represented as linear. Also, the concept of morphological equilbrium may not strictly apply to the Eastern Scheldt, since the dimensions of the cross-sectional area are fixed due to the storm surge barrier. In any case, a linear trend is conservative since conceptually, the erosion is expected to slow down over time.

High erosion rates measured at the nourishment hook and foot are assumed to be redistributed within the flat, while any overall volume loss is due to sediment demand from the channels. From linear regression of seven post-nourishment bathymetric surveys over 2.5 years, the sediment demand from the channels is estimated to cause **1.3 to 2.1 cm / year** of erosion from the Oesterdam flat. Conceptually, the post-nourishment erosion rate is expected to be faster than the pre-nourishment rate as the flat is further from the equilibrium state. However, the rates are applied to both the nourishment and no-nourishment scenarios due to the lack of data. It may also be argued that the change in equilibrium state is not large enough to significantly change the erosion rate.

Erosion projections are presented for the overall flat and individual elements such as the hook and foot. However, the implementation of these projections in bathymetry causes irregular steps. Instead of smoothing the boundaries between the elements, implementation of differential erosion is not done for the Delft3D bathymetry grids. Instead, the average erosion rate is applied to the entire nourishment. A progressive smoothing is implemented and is assumed to capture the spreading of the nourishment (see Section 5.3).

Erosion trends on other intertidal flats in the Eastern Scheldt are mentioned in Section 2.3.1. However, no projections are made outside of the Oesterdam flat area. The reason is twofold. First, the implementation of more uncertain erosion trends in other areas increases the number of required scenarios for wave modelling. Second, the main research question focuses on the relative effect of the nourishment and this analysis is possible without consideration of erosion in other areas, which would be the same in the nourishment and no-nourishment scenarios. However, there may be some problems with this assumption, which is further explored in Chapter 7.

5.2. PROJECTIONS

Based on the results of the trend analysis, an upper and lower bound erosion projection was calculated for the nourishment and no-nourishment scenarios. The fast erosion case was calculated by implementing the upper bound (95% confidence interval) erosion rate for each element. The slow erosion case was calculated by using the lower bound (95% confidence interval) erosion rate for each element.

The nourishment hook and foot both erode at a much faster rate than the sheltered area in between. In reality, the sediment is expected to spread out over the flat. This follows the general behavior of erosion at the high areas and deposition at the lower areas, which is described in Pezij (2015). This was approximated in the projections by truncating any further erosion of the individual elements when the bed level reached the projected average bed level for the flat. The results are shown in Figure 5.1.

For the no-nourishment scenario, the erosion trends calculated for the overall flat post-nourishment were used since they were similar to the pre-nourishment estimated trends by De Graaf (2012). However, perhaps a better estimate would be to use the pre-nourishment estimated trends because the lower bound rate is slower than the post-nourishment lower bound. In any case, a faster erosion rate is conservative. The results will show an identical erosion rate in the nourishment and no-nourishment scenarios once their sediment spreads out over the flat.

5.3. IMPLEMENTATION INTO DELFT3D BATHYMETRY

In order to avoid introducing further irregularities in the model bathymetry, a simple approach was taken to implement the erosion projections into the Delft3D model bathymetry. The projected erosion rates were subtracted from the whole of the smallest (nested) Oesterdam grid. In addition, a smoothing tool was used in order to represent the future spreading of the nourishment by 2080 (shown in Figure 5.2). Since the grid is square with a relatively uniform resolution, unequal smoothing was avoided.

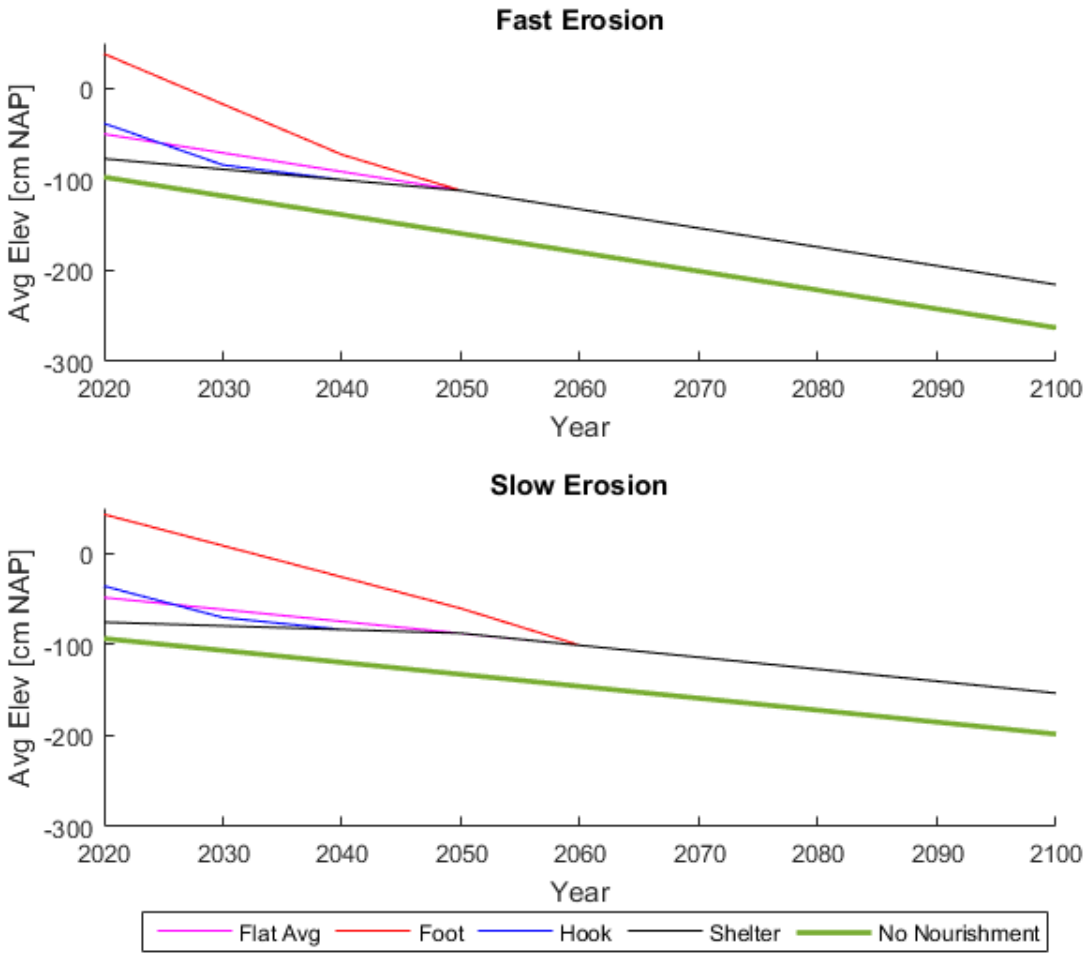

FIGURE 5.1: PROJECTIONS OF BED ELEVATION CHANGES UNTIL 2100.

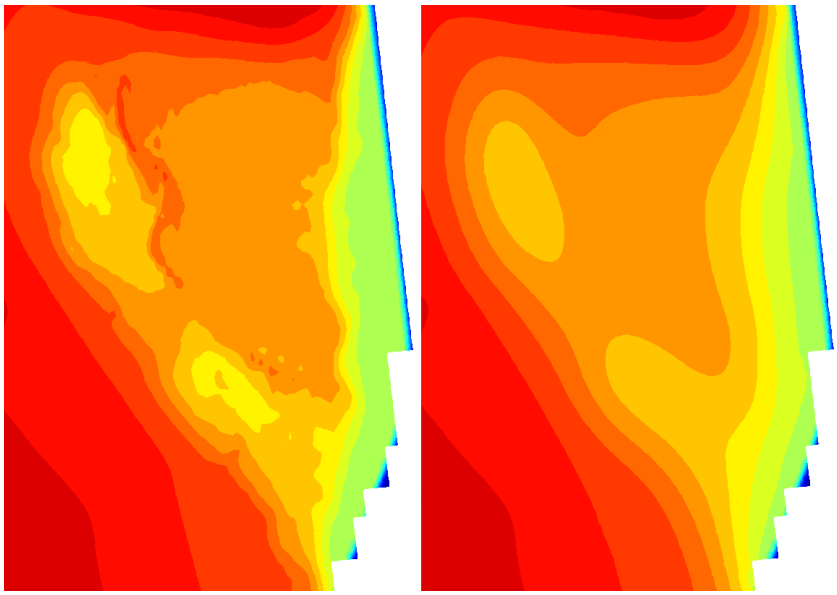

FIGURE 5.2: ESTIMATED NOURISHMENT SPREADING FROM 2020 TO 2080 IN DELFT3D USING A SMOOTHING FUNCTION IN QUICKIN. THE VISUALIZATION DOES NOT INCLUDE THE OVERALL EROSION FROM THE FLAT AREA.

6

PROJECTIONS OF DESIGN WAVE LOADS

The projections of erosion at the Oesterdam were used to calculate the projected design wave loads for the failure mechanisms of block failure, asphalt revetment failure, and overtopping (see Table 2.3 for boundary conditions). A fast erosion rate and a slow erosion rate were implemented in the projections. In addition to the nourishment and no-nourishment scenario, a 'flat nourishment' scenario was added in order to explore the effect of the irregular nourishment shape. The results and limitations are discussed below.

6.1. MODELLING SCENARIOS

Sections 80 and 81S of the Oesterdam are directly behind the Oesterdam flat and are the only ones assessed in this study. Figure 6.2 shows the time points for the decadal safety assessment performed using the erosion projections, wave model, and safety calculations. A nourishment, no-nourishment, and flat nourishment scenario are analyzed (Figure 6.1). The flat nourishment scenario is implemented as a hypothetical nourishment where the Oesterdam flat is raised by 0.45m, which is the average increase in elevation after the real nourishment. This scenario can give insight into the effect of the irregular shape of the real nourishment versus a *'flat'* nourishment that has roughly the same volume.

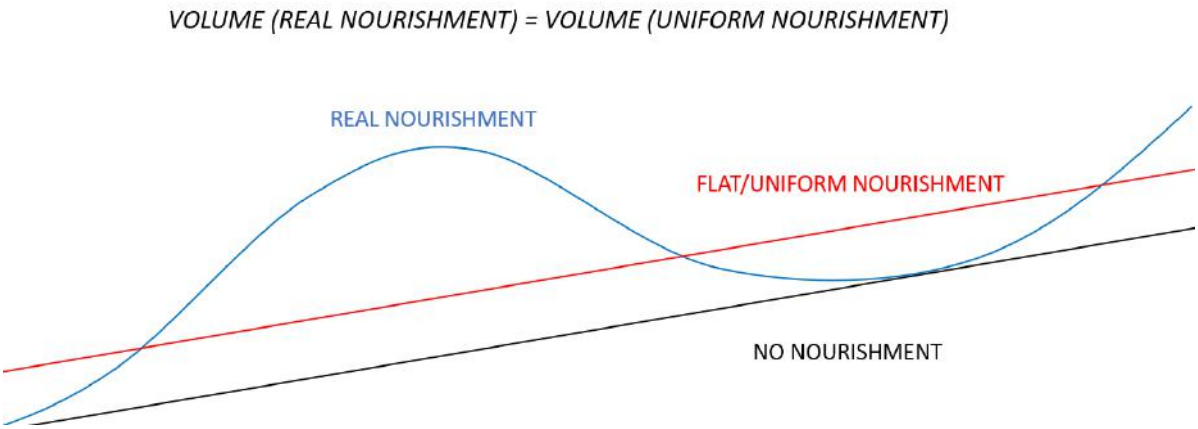

FIGURE 6.1: SCHEMATIZED EAST-WEST CROSS SECTIONS OF THE BED PROFILE IN FRONT OF THE OESTERDAM (NOT TO SCALE). NOURISHMENT, NO-NOURISHMENT, AND UNIFORM NOURISHMENT SCENARIOS FOR DESIGN WAVE LOAD PROJECTIONS.

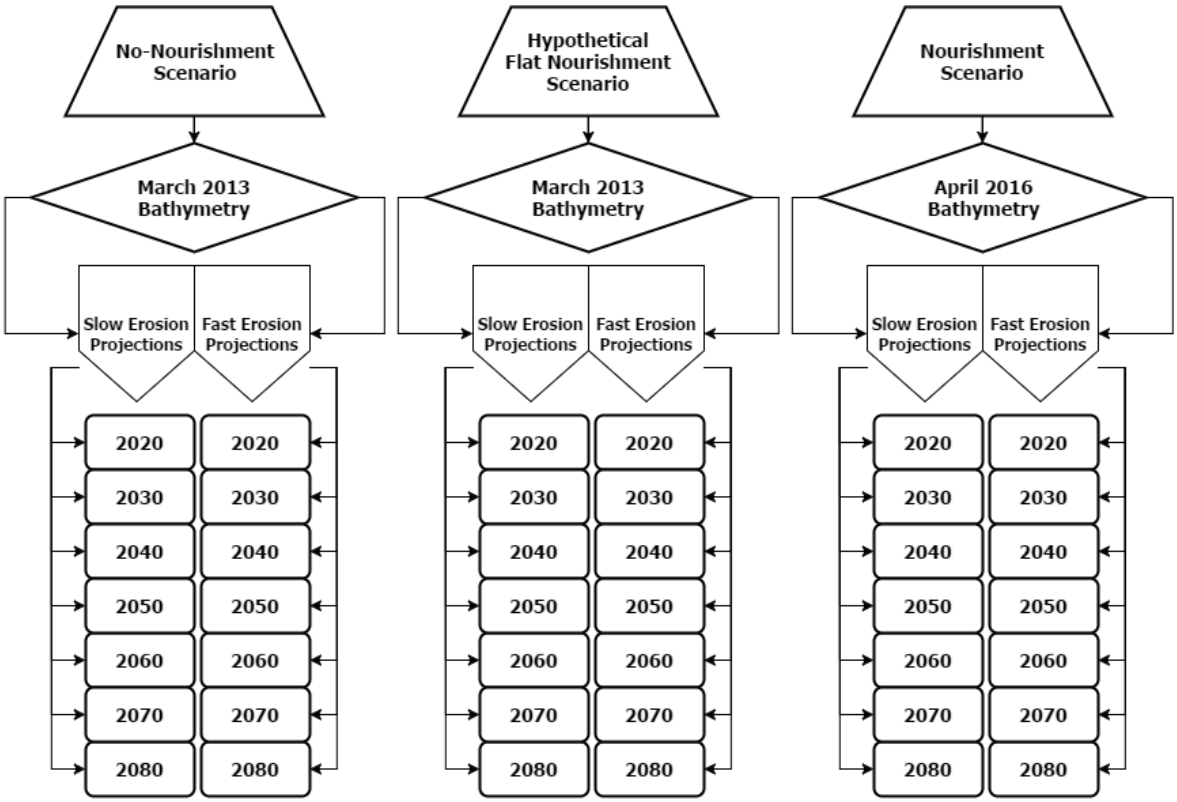

FIGURE 6.2: SCENARIOS FOR SIMULATION OF DESIGN CONDITIONS AT THE OESTERDAM.

6.2. HYDRAULIC BOUNDARY CONDITIONS

For input into the calculations of wave load on the Oesterdam, the wave conditions at the toe of the dam must be calculated. Based on the results from Chapter 4, it was concluded that a standalone stationary WAVE model (SWAN) is appropriate for the simulation of a design storm at the Oesterdam. A WAVE model was run for each erosion scenario and wind forcing/water level scenario. The hydraulic boundary conditions for each time point and scenario are described in Table 2.3.

6.2.1. MODEL SETUP

A double-nested WAVE grid was used for the simulations, using the SCALOOST grid, Kom, and Oesterdam grids together in one setup (Figure 4.2). In addition, each simulation contained 20 time points, one for each wind/water level input combination. The default SWAN parameters described in Chapter 4 were used.

6.2.2. OUTPUT POINTS

Five output points for each dam section were used to extract wave parameters. A load function (see Section 6.2.3) was used to narrow down the worst combination of wind speed/direction and the worst point for each dam section. However, output points had to be reduced to only include 80C-81C. This was because the resulting wave conditions at the other points did not show significant difference in the nourishment and no-nourishment scenarios. This observation showed that the wave damping effect of the nourishment under design conditions is limited to the area directly east of it, and up to 100 meters inside the nourishment footprint.

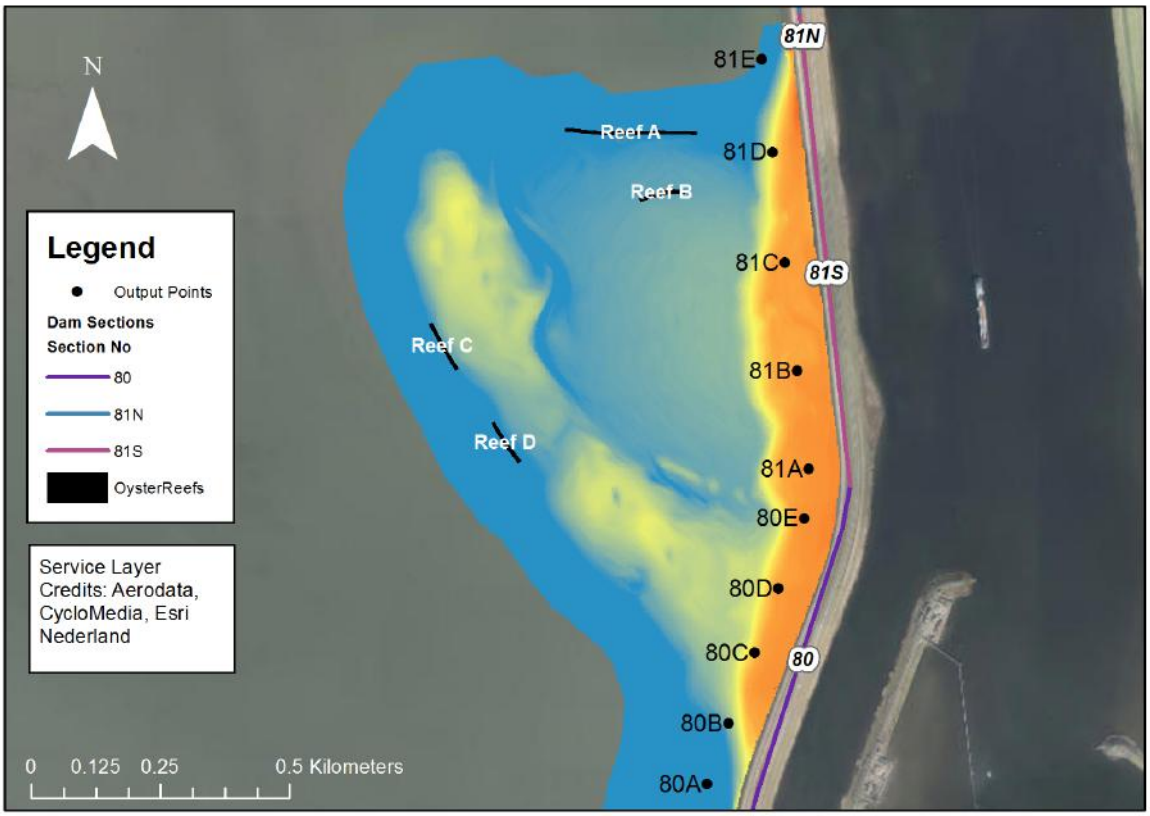

FIGURE 6.3: WAVE MODEL OUTPUT LOCATIONS AT THE DAM FOOT FOR INPUT INTO STRUCTURAL SAFETY CALCULATIONS. THE POINTS ARE LOCATED 30-50M FROM THE DAM FOOT.

6.2.3. NORMATIVE LOAD FUNCTION

The normative load function for a particular failure mechanism is a rough representation of how each wave parameter affects the wave load. It was used to determine which combination of wind speed/direction (Table 2.3) resulted in the most extreme wave load, without calculating the actual wave loads. Typical load functions are shown in Equations (6.1) to (6.3). In Arnold (2007), the normative load function for block failure and asphalt revetment failure is Z3. For overtopping, the equations in Pullen et al. (2007) show a relationship between the square of the wave height and the overtopping. Therefore, Z3 (Equation (6.3)) is assumed to be normative for all considered failure mechanisms[1].

$$Z1 = H_s T_{m-1,0} \tag{6.1}$$

$$Z2 = H_s T_{m-1,0}^2 \tag{6.2}$$

$$Z3 = H_s^2 T_{m-1,0} \tag{6.3}$$

Where:

H_s = Design wave height [m]

$T_{m-1,0}$ = Design mean wave period [s]

[1] The normative load function need not be linearly related to the actual wave load. It can simply be a rough representation of how the wave height and wave period affect the wave load, calculated using the equations in Section 2.4.2. The influence of wave direction on the load functions is not considered in this work.

6.2.4. ESTIMATION OF WAVE LOADS

Instead of a safety assessment, this thesis examines the design wave loads using the equations described in Section 2.4.2. They are implemented using the schematized geometry of the Oesterdam, following the example of De Graaf (2012). The design parameters are shown in Figure 6.4, with no corrections for roughness. The design water level is set as 4 m NAP. A similar value of 3.95 m was used in a previous safety assessment, even for the lower parts of the revetment (Van der Vliet, 2010). The wave loads were normalized for a robust analysis of the projected changes (Equations (6.4) to (6.6)). As described in Section 2.4.2, the required asphalt thickness is a linear function of the wave height for the range of wave heights and for the slope considered. Since the absolute wave loads are not analyzed, no distinction is made between the different asphalt layers and the different block layers.

$$WLA = \frac{H_{m0}}{H_{m0,2013,no-nourishment}} \tag{6.4}$$

$$WLB = \frac{D}{D_{2013,no-nourishment}} \tag{6.5}$$

$$WLC = \frac{q}{q_{2013,no-nourishment}} \tag{6.6}$$

Where:

WLA = Normalized wave load for asphalt revetment [−]

WLB = Normalized wave load for block revetment, from Equation (2.6) [−]

WLC = Normalized wave load for overtopping, from Equation (2.4) [−]

H_{m0} = Design wave height [m]

D = Required block thickness [m]

q = Overtopping rate [l/m/s]

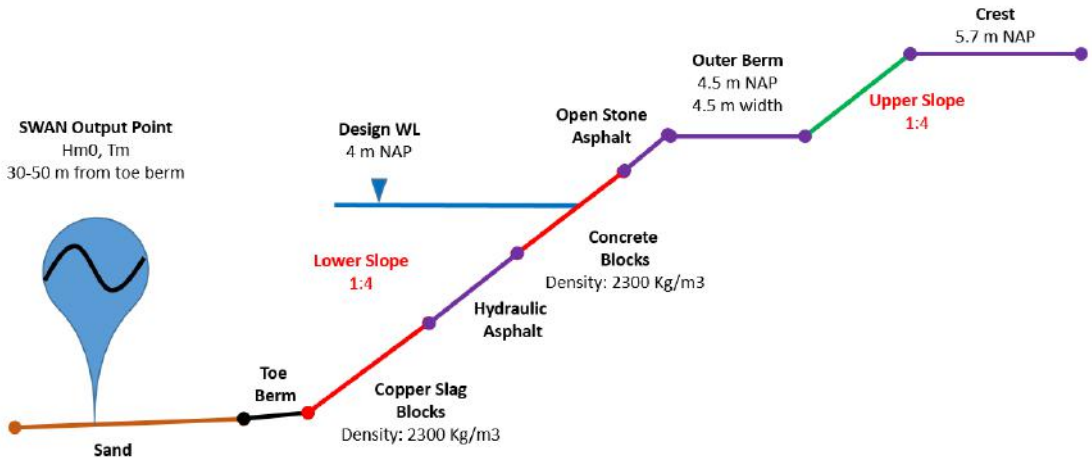

FIGURE 6.4: SIMPLIFIED GEOMETRY AND CHARACTERISTICS USED IN THE CALCULATION OF DESIGN WAVE LOADS ON THE OESTERDAM SECTIONS 80 AND 81S (NOT TO SCALE).

6.3. PROPAGATION OVER THE FLAT

In order to get a deeper insight into the effect of the nourishment on the waves approaching the Oesterdam during a design storm, the model results from the 2020 fast erosion time point were exported into an east-west transect at the northern end of the hook. First, the influence of the water level is plotted in Figure 6.5. Second, a comparison of the three nourishment scenarios at the 4m water level is plotted in Figure 6.6. What is clear from both figures is that depth-induced wave breaking only plays a significant role at the 0m and 1m water levels. While there is some wave breaking in all scenarios, the fraction of breaking waves is less than 1% for the 4m water level.

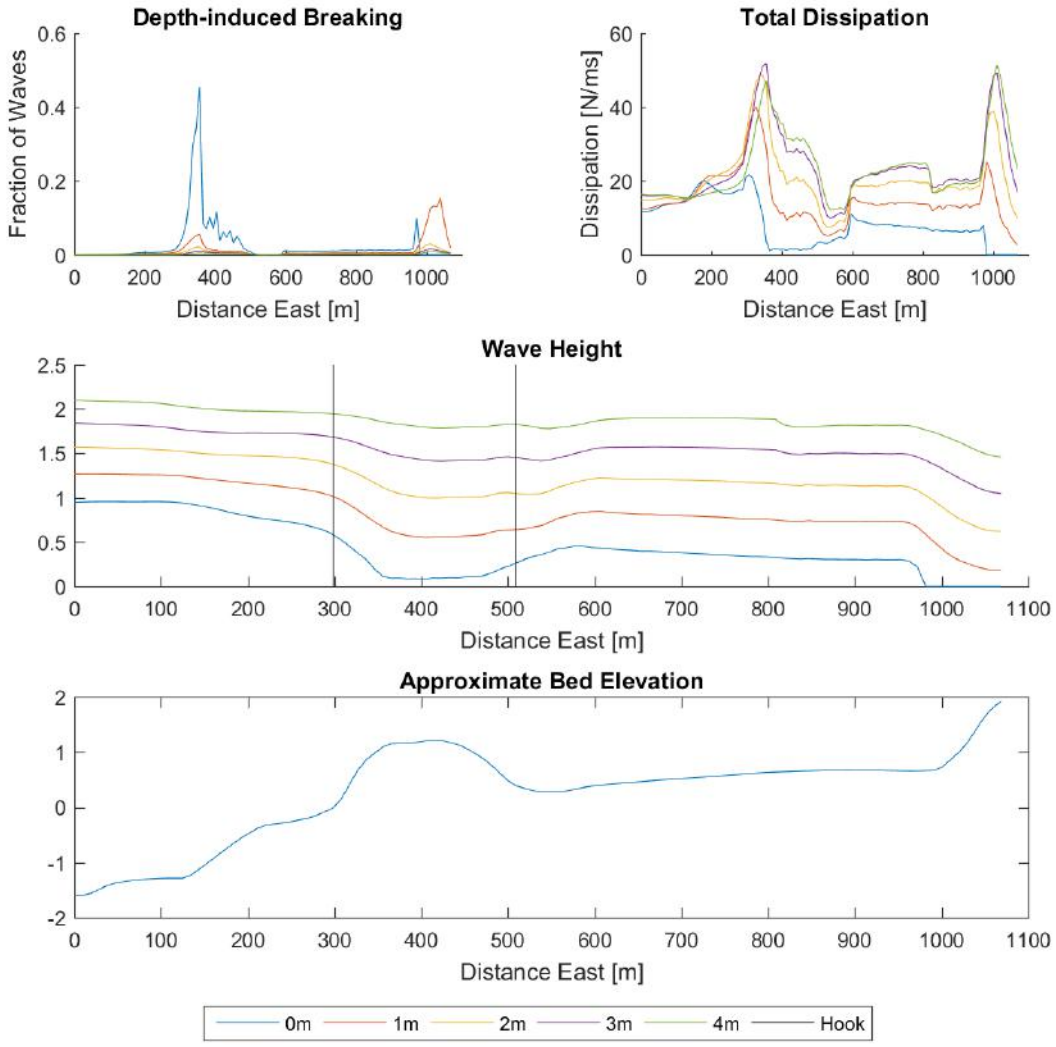

FIGURE 6.5: WAVE DISSIPATION AND GROWTH OVER THE OESTERDAM FLAT FOR THE REAL NOURISHMENT SCENARIO. 2020 FAST EROSION TIME POINT.

An interesting insight from Figure 6.6 is the limited influence of the nourishment hook. While the hook does dissipate the waves (mostly via bottom friction), wind-wave growth in the sheltered area over a distance of 300m recovers the wave height to match the no-nourishment scenario. The difference between the wave heights at the Oesterdam between the nourishment and no-nourishment scenarios is entirely due to the nourishment foot.

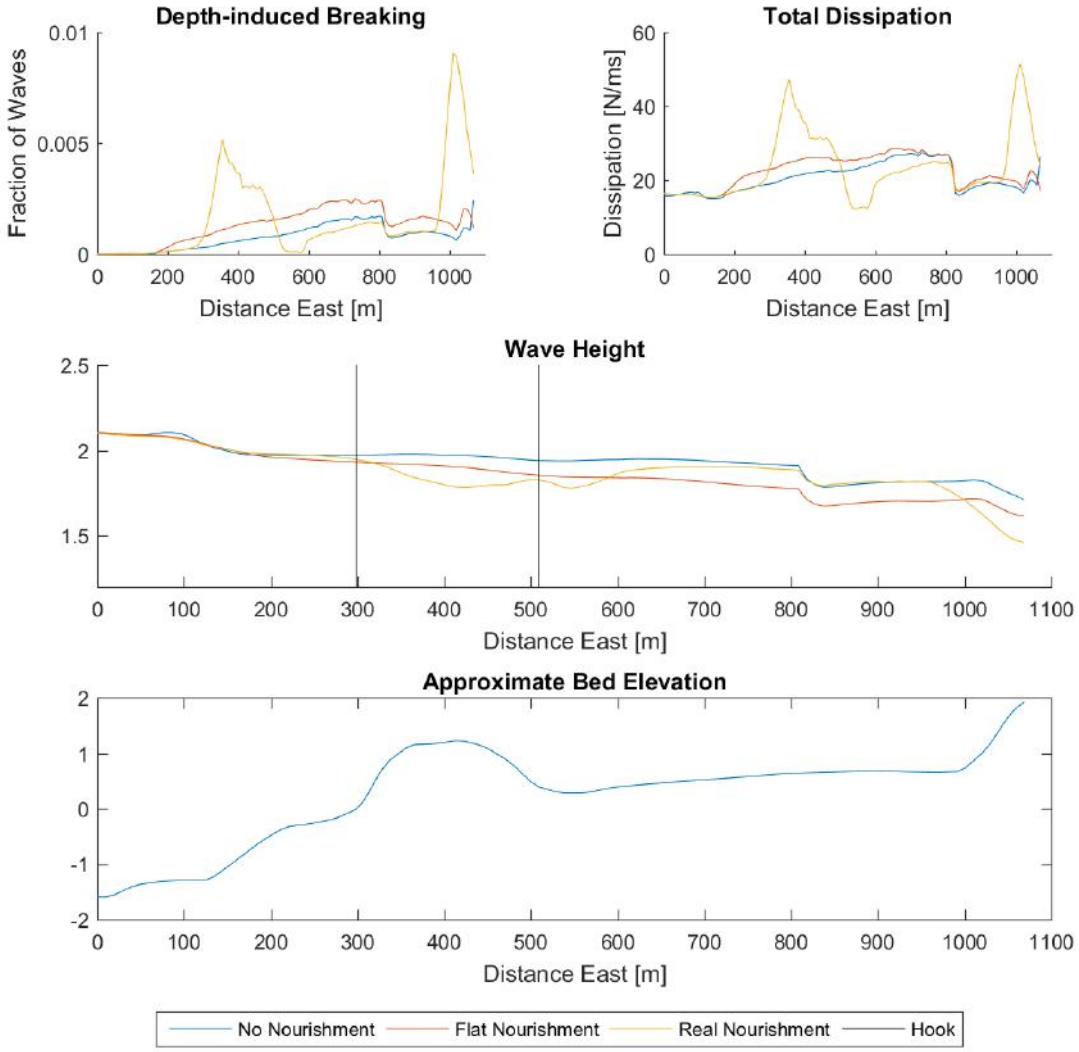

FIGURE 6.6: WAVE DISSIPATION AND GROWTH OVER THE OESTERDAM FLAT DURING DESIGN CONDITIONS AT THE 4M WATER LEVEL. 2020 FAST EROSION TIME POINT.

At all points along the nourishment at the 4 m design water level, wave height attenuation is mainly due to bottom friction, as the fraction of breaking waves is very small. Since the nourishment foot is only about 50-100m wide, there is not much distance for bottom friction to act to dissipate the waves. However, the narrow strip at the foot is more effective at dissipating waves than a uniformly distributed nourishment with the same volume.

6.4. PROJECTED DESIGN WAVE LOADS

Figure 6.7 shows the projected normalized wave loads for Section 81S of the Oesterdam. Figure 6.7 shows the results in tabular format. What is immediately apparent is the rapid change in the overtopping loads relative to the asphalt and block loads. This could be because the calculated overtopping in 2013 results in a wave run-up that is just above the crest. Beyond 2013, the wave overtopping is projected to increase as a multiple of the increased wave height, which increases slowly (up to 16 percent by 2080).

In all cases, the nourishment reduces the projected design wave load increase by 50%. However, this difference is small for the wave loads on the asphalt and block revetments. The projected increase in the wave loads is only 9-16 percent without the nourishment. The hypothetical uniform nourishment also shows smaller wave loads than the no-nourishment scenario, but has a weaker effect on the wave damping than the real nourishment. This is consistent with the findings of Chapter 4 and Section 6.3, which show that the nourishment foot is more effective at wave damping than an alternative flat nourishment. Appendix C includes the hydraulic boundary conditions in tabular format.

TABLE 6.1: PERCENT INCREASE IN (NORMALIZED) DESIGN WAVE LOADS FROM 2013 TO 2080.

Scenario	Asphalt [%]	Blocks [%]	Overtopping [%]
No-nourishment	12-16	9-12	102-142
Flat nourishment	7-13	5-9	56-105
Real nourishment	3-9	2-6	18-57

For the overtopping loads, the projected increases are more or less linear in time. However, the wave loads on the asphalt and block revetments start to level off in 2060-2080, which could indicate that the structural erosion at the toe weakens its influence on wave damping. It can be seen that the faster erosion scenario slightly reduces the difference between the nourishment and no-nourishment scenario at 2080. This observation brings up an important consideration from the erosion projections. Since the erosion in the Kom was not projected, the period of influence may be overestimated since more erosion reduces it. However, the additional effect of erosion in the Kom would only add a few percent to the design wave loads projected in 2080.

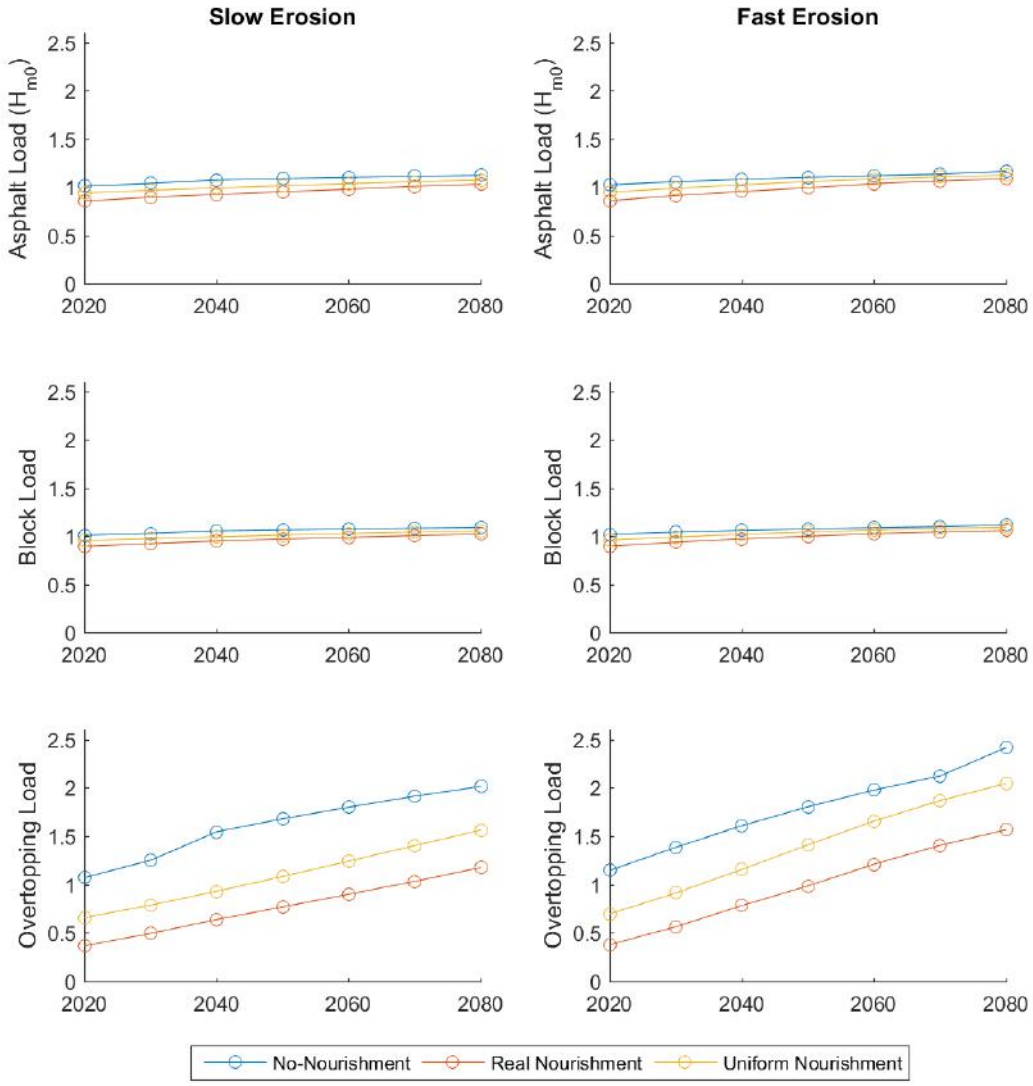

FIGURE 6.7: PROJECTED (NORMALIZED) DESIGN WAVE LOADS FOR THE ASPHALT REVETMENTS, BLOCK REVETMENTS, AND FOR OVERTOPPING USING A DESIGN WATER LEVEL OF 4 M. SECTION 81S OF THE OESTERDAM.

7

DISCUSSION

In Section 1.2, three main research questions were presented, each with several sub-questions. The sub-questions are addressed in this section. The three main research questions are addressed in Chapter 8.

7.1. MORPHOLOGY

Question 1.a) What are the historical trends in morphological development of the tidal flats in the Eastern Scheldt?

Following the completion of the Eastern Scheldt storm surge barrier in 1987, the erosion of several intertidal areas has been measured using methods of variable resolution and accuracy. Higher resolution RTK bathymetric surveys are considered more accurate than surveys compiled in the vaklodingen dataset, but cover less area. Erosion rates estimated using successive RTK surveys intertidal areas range from 0.6 cm/yr at the Galgeplaat to 1.1 cm/yr at the Dortsman, both just outside the Kom. Erosion rates estimated from the vaklodingen dataset reach up to 3 cm/yr in some intertidal areas.

Question 1.b) How has the nourishment developed since November 2013?

The most significant development following the Oesterdam nourishment is the formation of a small ebb channel and ebb-tidal shoal north of the nourishment hook. In 2015/2016, a second channel appears to have formed, resulting in some the sedimentation of the first channel. Both the hook and the foot have spread and widened, with erosion at the high parts and sedimentation on the edges. Some erosion was also observed in the sheltered area, to a lesser degree.

Question 1.c) What are the erosion trends, and what is the strength of those trends?

The estimated erosion rate post-nourishment was 3.4-5.5 cm/yr for the foot, 3.4-4.6 cm/yr for the hook, and 0.4-1.2 cm/yr for the sheltered area. The average erosion rate was estimated to be 1.3-2.1 cm/yr. The ranges were estimated based on the 95% confidence interval of the average erosion rate calculated from linear regression. There are two issues with the estimated trends. First, only seven surveys were available for use in the trend analysis. Second, the surveys were not conducted with the same frequency in the same time points every year. Because of this, seasonal effect bias may have skewed the linear regression.

7.2. OPERATIONAL WAVE CONDITIONS

Question 2.a) What is the applicability of pressure transducers for the measurement of waves at the study site?

The Kom is an environment dominated by fetch-limited wind-waves with peak wave periods of 3 seconds or less during operational conditions. Waves in fetch-limited environments, as confirmed by the surface spectra measured at the Marollegat station, contain gradual high-frequency spectral tails that reach or surpass 1 Hz. Wave energy at 1 Hz creates very little dynamic pressure in the water column. A pressure transducer/pressure box should have a relative submergence less than the deep water limit (d/L < 0.5) in order to read dynamic wave pressure that is above the instrument noise level. In order for a pressure transducer to measure energy at 1 Hz, it must be submerged less than 0.7m below the still water line.

Given that a fixed submergence cannot be achieved in a macro-tidal environment (unless a moving instrument is used), there are several limitations for the use of pressure boxes. If the wave conditions at low and high water levels are desired, two devices can be deployed adjacent to each other with different elevations. Otherwise, the higher frequency tail of the surface spectrum cannot be reliably measured throughout the tidal cycle. This may not be a problem in other environments with long/unlimited fetches where the high frequency tail is much steeper, or in environments with smaller tidal ranges.

Question 2.b) What is the applicability of the selected hydrodynamic model at the study site, under a range of measured hydrodynamic conditions?

The Delft3D FLOW/WAVE model was validated to measured wave pressures (P_{m0}) and wave periods at several locations, including several locations on the Oesterdam nourishment. Due to limitations with the use of pressure box data, the wave pressures were used for calibration and validation. This means that the high frequency tails in the model spectra were not able to be validated over the nourishment. However, gradual high frequency spectral tails are characteristic of fetch-limited wind-waves. In addition, the measured surface spectra at the Marollegat station showed the similar gradual high frequency tails from the model results at the same location. In the model, the processes of bottom friction and wave breaking do not steepen the high-frequency tail. Therefore, can be inferred that the high frequency tail exists in the wave spectra over the Oesterdam nourishment.

Therefore, the Delft3D model is able to reliably simulate wave generation and transformation in the Eastern Scheldt using the default SWAN 40.72AB parameters. A small structural underestimation of wave periods could be improved with different whitecapping or quadruplet parameters, but the quality of the data seen from the measured pressure spectra did not warrant a detailed calibration.

One concern with the use of Delft3D is the calculation of wave overtopping over the Oesterdam. When an extensive shallow foreshore (H/d >=0.5) is present, wave breaking releases bound long waves which contribute to the wave run-up and overtopping. Since SWAN does not simulate long wave generation, a correction factor must be applied to the design wave height and/or wave period that are input into the run-up and overtopping calculations. However, this does not apply to the Oesterdam since at the design water level of 3.95/4 m NAP, the water depth is more than twice the simulated wave height in all scenarios.

While the discrepancy between measured and modelled waves in Pezij (2015) has been explained, it is still unknown why the study of Das (2010) had the same problem with the Galgeplaat. The wave data used for validation was a wave rider bouy located on the edge of the Galgeplaat. It is difficult to speculate as to what the problem was in the model settings or data.

Question 2.c) What are the governing physical processes that affect wave transformation in the Kom and over the nourishment?

The dominant wave processes in the Kom are wind-wave generation, whitecapping, and dissipation by bottom friction. Depth-induced wave breaking does not play a big role as the measured waves were generally smaller than 0.5 m. At high water, very little wave breaking occurs over the Oesterdam nourishment. The Delft3D model results suggest that non-linear four-wave interactions play a significant role in shifting energy from the high frequency tail to the lower frequencies, thus increasing the spectral peak and mean wave period. However, further exploration is needed to determine if this process is important.

Test simulations with no wind input showed that wind-waves generated in the Kom are the dominant influence at the Oesterdam nourishment location, even outside the hook. This is likely due to the irregular shape of the Eastern Scheldt, limiting the fetch from most wave directions.

7.3. DESIGN WAVE CONDITIONS

Question 3.a) Under design conditions, what are the main mechanisms of wave damping?

At the design water level of 4m NAP, the water depths over the Oesterdam nourishment are always more than twice the wave height. At this water level, whitecapping and bed friction are the main mechanisms that limit wind-wave growth. At the lower water levels of 0-2m, depth-induced wave breaking occurs. However, the lower water levels are not presently used for the design of the lower part of the Oesterdam revetment. Therefore, for safety assessments, wave breaking does not play a large role.

Question 3.b) How does the long term erosion of the tidal flats near the Oesterdam affect the wave loads?

For the design water level, the load functions for block failure, asphalt failure, and overtopping increase more or less linearly with time for all scenarios. However, upon further examination, this simply reflects the manner in which the erosion projections were implemented. As it was determined that only the nourishment foot plays a role in wave attenuation in design conditions (wave growth occurs after the hook), the foot erosion rate crucial in the impact of the nourishment.

Since an average erosion rate was applied to the entire flat area with an artificial smoothing of the nourishment, the results may overstate the impact of the nourishment. The calculated erosion rate of the nourishment foot is much faster than the average erosion rate of the flat. The artificial smoothing of the bathymetry does not entirely reflect this rate. Therefore, the impact of the nourishment on the design wave loads may be negligible by the year 2080.

The overtopping discharge increases at a much faster rate than the wave loads on the asphalt and block revetments. Combined with the analysis of De Graaf (2012), the Oesterdam may not be up to the standard for a maximum overtopping discharge of 1 l/m/s. The grassy parts of the cross section are particularly vulnerable to overtopping discharge and may fail under design conditions. This is especially a concern considering the rate at which the overtopping discharge increases due to the erosion of the nourishment. More research is needed into the exact critical overtopping discharge at the Oesterdam, which is likely to be larger than 10 l/m/s.

Question 3.c) What is the sensitivity of the absolute values and relative changes in wave loads over time to changes in the erosion projections?

The difference in results between the slow and fast erosion scenarios is minimal at the high water levels. However, it can be seen that generally, the faster erosion scenario shows less difference between the nourishment and no-nourishment cases by 2080. This difference is very small and for practical purposes, negligible. However, as explained in Section 3.6, the erosion rates may be underestimated due to summer seasonal bias. In addition, erosion projections were not implemented for the rest of the Kom. Therefore, the effect of the nourishment on the design wave loads may be overestimated in both erosion scenarios.

8

CONCLUSIONS

As part of the thesis work, the processing of hydrodynamic and morphological data was used to derive insight into the environmental conditions at the Oesterdam nourishment. The data was used to determine the impact of the nourishment on waves during operational wave conditions. A Delft3D flow/wave model was partially validated over the flat using measured pressure data. The model was then used, in conjunction with erosion projections, to project design wave loads from 2020 to 2080. The three main research questions are addressed below.

8.1. QUESTION 1: MORPHOLOGY

What are the insights gained from the morphological data collected from 2012-2016?

From linear regression of seven post-nourishment bathymetric surveys over 2.5 years, post-nourishment erosion rate at the Oesterdam is estimated to be **1.3 to 2.1 cm / year**. The erosion rates calculated at the higher parts of the nourishment were significantly faster than the other areas on the flat. Much of the erosion is accounted for by spreading within the flat, while some material was calculated to be lost from the flat area. While it is expected that post-nourishment erosion rates are higher than pre-nourishment rates, not enough reliable data (before the nourishment) exists to compare pre- and post-nourishment erosion rates.

8.2. QUESTION 2: OPERATIONAL WAVE CONDITIONS

What is the wave attenuation impact of the nourishment hook in measured environmental conditions?

Wave spectra observed from the Marollegat station in the Kom reflected the fetch-limited character of the waves, with significant wave energy up to frequencies of 1 Hz. It was not possible to analyze the presence of this high frequency energy at the Oesterdam due to the limited applicability of the pressure box instruments for high-frequency waves. At both locations, waves are heavily correlated with local wind speed.

The fetch-limited situation in the Kom does not allow significant wave growth under operational conditions. Even at high water when intertidal areas are submerged, a limited time window exists where some wave growth is noticeable. The wave damping effect of the Oesterdam nourishment is governed by this. Wave damping was observed to be mainly due to bottom friction, as the approach-

ing waves were usually not large enough to break in depths of 1-4 meters. At shallower depths during the ebb tide, wave breaking occurs. At high water, net wave growth over the nourishment was observed, which at lower water levels was hindered due to bottom dissipation.

8.3. QUESTION 3: DESIGN WAVE CONDITIONS

What is the effect of the Oesterdam tidal flat nourishment on the design storm wave loads from 2020 to 2080?

From 2020 to 2080, the Oesterdam nourishment has a small impact on the design wave load functions at the design water level of 4m. The difference between the nourishment and no-nourishment scenarios, with regards to the wave loads on the asphalt and block revetments, is projected to slightly decrease with time. The faster the erosion rate, the faster the difference is reduced by the year 2080. However, the overtopping load increases more or less linearly in time in all nourishment scenarios. In both the slow and fast erosion scenarios, there is still a noticeable impact of the nourishment on the wave loads, but there are several caveats. First, the erosion rates at the Oesterdam may have been underestimated. Second, erosion projections were not implemented for the rest of the Kom. Thus, the impact of the nourishment in the year 2080 may be overrepresented in the results, due to the implementation of the nourishment foot erosion rate. In any case, the overtopping discharge is of particular concern due to the relatively rapid increase with time.

9

RECOMMENDATIONS

The following actions are recommended for further work and research:

- The use of pressure boxes for further data collection may be used, mindful of the limitations detailed in this thesis. If one is to capture high-frequency spectral tail of fetch-limited waves in the Kom, another type of measurement device is required. Examples include step gauges or acoustic sensors. However, other types of devices are more expensive and have their own limitations.
- Further validation of the Delft3D FLOW/WAVE model for larger storms. During the T1 and T2 deployment, relatively small storms were captured which made it difficult to simulate significant wind/wave events.
- Continued RTK bathymetric surveys for at least one decade. For the purposes of long term trend analysis, one must be careful to choose time points in the year that are consistent. Bathymetric surveys taken in the winter cannot be used in a trend analysis which include surveys in the summer, unless those winter surveys are done every year. Otherwise, there will be a seasonal bias that will skew the trend analysis. It is recommended that surveys are conducted once in February and once in august every year for the purposes of long term trend analysis. Other analysis may require more frequent surveys.
- The use of the validated hydrodynamic model in order to simulate annual erosion in the Kom, furthering the work of Pezij (2015).
- More detailed safety assessment of the Oesterdam, using the official tools of *Steentoets* for block revetments, GOLFKLAP for asphalt, and PC-Overslag for overtopping.
- Investigation into the critical threshold for overtopping at the Oesterdam, beyond which the grass upper slope reaches failure.

REFERENCES

ARCADIS (2009). Legger oesterdam. Technical report, Rijkswaterstaat Zeeland.

Arnold, E. (2007). Detailadvies Oesterdam. Technical report, Svasek, Royal Haskoning, RWS.

Bijlsma, E. (2010). Planbeschrijving Oesterdam zuid [38] Ontw. Verbetering steenbekleding. Technical report, ARCADIS.

Bishop, C. T. & Donelan, M. A. (1987). Measuring waves with pressure transducers. *Coastal Engineering*, 11(4):309–328.

Boersema, M., De Vries, M., Bouma, T., De Paiva, J., Pesch, C., Van den Brink, A., Ysebaerd, T., Paree, E., & Van der Werf, J. (2014). Projectplan zandhonger suppletieprojecten: Deelproject: Monitoring veiligheidsbuffer Oesterdam. Technical report, Centre of Expertise Delta Technology.

Boersema, M., Stronkhorst, J., Ysebaert, T., Van der Werf, J., Bouma, T., Pesch, C., & Vader, P. (2015a). Projectplan: Variantenstudie en monitoring: Zandsuppletie roggenplaat. Technical report, Centre of Expertise Delta Technology.

Boersema, M., Ysebaert, T., Bouma, T., Paree, E., Van der Werf, J., De Paiva, J., Van den Brink, A., Pesch, C., & Van Heuvel, T. (2015b). Zandhonger suppletieprojecten: Deelproject: Evaluatie monitoring veiligheidsbuffer Oesterdam eerste jaar na aanleg. Technical report, Center of Expertise Delta Technology.

Boersema, M., Ysebaert, T., Bouma, T., Paree, E., Van der Werf, J., De Paiva, J., Van den Brink, A., Pesch, C., & Van Heuvel, T. (2016). Oesterdam safety buffer: Ecological and morphological development of a sand nourishment - two years after realization: Draft progress report. Technical report, Centre of Expertise Delta Technology.

Booij, N., Ris, R. C., & Holthuijsen, L. H. (1999). A third-generation wave model for coastal regions: 1. Model description and validation. *Journal of Geophysical Research*, 104(C4):7649–7666.

Bosboom, J. & Stive, M. (2015). *Coastal Dynamics I*. Delft Academic Press.

Breteler, M. (2014). SnelStartGids Steentoets2014. Technical report, Deltares, Delft.

Cavaleri, L., Alves, J. H. G. M., Ardhuin, F., Babanin, A., Banner, M., Belibassakis, K., Benoit, M., Donelan, M., Groeneweg, J., Herbers, T. H. C., Hwang, P., Janssen, P. A. E. M., Janssen, T., Lavrenov, I. V., Magne, R., Monbaliu, J., Onorato, M., Polnikov, V., Resio, D., Rogers, W. E., Sheremet, A., McKee Smith, J., Tolman, H. L., van Vledder, G., Wolf, J., & Young, I. (2007). Wave modelling - The state of the art. *Progress in Oceanography*, 75(4):603–674.

CEM (2002). Chapter 3: Estimation of nearshore waves. In *Coastal Engineering Manual*, volume 1100. US Army Corps of Engineers.

CEM (2008). Chapter 1: Water wave mechanics. In *Coastal Engineering Manual*, volume 1100. US Army Corps of Engineers.

Das, I. (2010). *Morphodynamic modelling of the Galgeplaat*. Master thesis, Delft University of Technology.

Davidse, M., Hart, R., De Looff, A., Montauban, C., Van de Ven, M., & Wichman, B. (2010). State of the art: Asfaltdijkbekledingen. Technical report, STOWA, RWS, Amersfoort.

De Bok, C. (2001). Long-Term Morphology of the Eastern Scheldt. Technical report, Rijkswaterstaat.

De Graaf, L. (2012). *Nourishing intertidal foreshore; Improving safety and nature*. Master thesis, Delft University of Technology.

De Looff, A. K., Hart, R. t., Montauban, K., & van de Ven, M. F. (2006). Golfklap a Model To Determine the Impact of Waves on Dike Structures With an Asphaltic Concrete Layer. Technical report, RWS-NPC-TUD, Delft.

De Ronde, J., Mulder, J., Van Duren, L., & Ysebaert, T. (2013). Eindadvies ANT Oosterschelde. Technical report, Rijkswaterstaat WVL.

Deltares (2014a). Delft3D-FLOW: User Manual. Technical report, Deltares, Delft.

Deltares (2014b). Delft3D-WAVE: User Manual: Hydro-Morphodynamics: Version 3.05.34160. Technical report, Deltares, Delft.

Eelkema, M. (2013). *Eastern Scheldt inlet morphodynamics*. Doctoral thesis, Delft University of Technology.

Gorman, R. M. & Neilson, C. G. (1999). Modelling shallow water wave generation and transformation in an intertidal estuary. *Coastal Engineering*, 36(3):197–217.

Hasselmann, K., Barnett, T. P., Bouws, E., Carlson, H., Cartwright, D. E., Enke, K., Ewing, J. A., Gienapp, H., Hasselmann, D. E., Kruseman, P., Meerburg, A., Muller, P., Olbers, D. J., Richter, K., Sell, W., & Walden, H. (1973). Measurements of Wind-Wave Growth and Swell Decay during the Joint North Sea Wave Project (JONSWAP). *Ergnzungsheft zur Deutschen Hydrographischen Zeitschrift Reihe*, A(8)(80):p.95.

Hasselmann, S., Hasselmann, K., Allender, J. H., & Barnett, T. P. (1985). Computations and Parameterizations of the Nonlinear Energy Transfer in a Gravity-Wave Specturm. Part II: Parameterizations of the Nonlinear Energy Transfer for Application in Wave Models. *Journal of Physical Oceanography*, 15(11):1378–1392.

Holthuijsen, L. H. (2007). *Waves in Oceanic and Coastal Waters*. Cambridge University Press, Cambridge, UK.

Janssen, P. (1991). Quasi-linear Theory of Wind-Wave Generation Applied to Wave Forecasting. *Journal of Physical Oceanography*, 21(11):1631–1642.

Komen, G. J., Cavaleri, L., Donelan, M., Hasselmann, K., Hasselmann, S., & Janssen, P. (1994). *Dynamics and Modelling of Ocean Waves*.

Komen, G. J., Hasselmann, K., & Hasselmann, K. (1984). On the Existence of a Fully Developed Wind-Sea Spectrum. *Journal of Physical Oceanography*, 14(8):1271–1285.

Lee, D.-Y. & Wang, H. (1984). Measurement of surface waves from subsurface gage. In *Coastal Engineering Proceedings*, pages 271–286.

Louters, T., van den Berg, J., & Mulder, J. (1998). Geomorphological changes of the Oosterschelde tidal system during and after the implementation of the delta project. *Journal of Coastal Research*, 14(3):1134–1151.

Miles, J. (1957). On the generation of surface waves by shear flows. *Journal of Fluid Mechanics*, 3(2):185–204.

Oosterlo, P. (2015). *A method to calculate the probability of dike failure due to wave overtopping, including the infragravity waves and morphological changes*. Master thesis, TU Delft.

Pandian, P., Emmanuel, O., Ruscoe, J., Side, J., Harris, R., Kerr, S., & Bullen, C. (2010). An overview of recent technologies on wave and current measurement in coastal and marine applications. *Journal of Oceanography and Marine Science*, 1(1):1–10.

Pezij, M. (2015). *Understanding the morphological development of the Oesterdam nourishment*. Master thesis, University of Twente.

Phillips, O. (1957). On the generation of waves by turbulent wind. *Journal of Fluid Mechanics*, 2(5):417–445.

Pilarczyk, K. W. (2003). Design of revetments. Technical report, Rijkswaterstaat, Delft, The Netherlands.

Pullen, T., Allsop, N., Bruce, T., Kortenhaus, A., Schüttrumpf, H., & Van der Meer, J. (2007). EurOtop: Wave Overtopping of Sea Defences and Related Structures: Assesment manual. Technical report, EurOTop.

Roelvink, D., van Dongeren, A., McCall, R., Hoonhout, B., van Rooijen, A., van Geer, P., de Vet, L., Nederhoff, K., & Quataert, E. (2015). XBeach Technical Reference: Kingsday Release. Technical report, Deltares, Delft.

Royal Haskoning & Svasek Hydraulics (2011). Handleiding hydraulische detailadviezen Oosterschelde en Westerschelde 2011: Deel 2 van 3: Achtergrond detailadviezen. Technical report, Rijkswaterstaat.

Salmon, J. & Holthuijsen, L. H. (2011). Re-scaling the Battjes-Janssen model for depth-induced wave-breaking. In *Proc. 12th Int. Workshop on Wave Hindcasting and Forecasting*, Hawaii.

Santinelli, G. & De Ronde, J. (2012). Volume analysis on RTK profiles of the Eastern Scheldt. Technical report, Deltares, Delft.

Slomp, R. (2012). Flood Risk and Water Management in the Netherlands. Technical report, Rijkswaterstaat.

Stelling, G. S. & Zijlema, M. (2003). An accurate and effcient finite-difference algorithm for non-hydrostatic free-surface flow with application to wave propagation. *International Journal For Numerical Methods In Fluids*, 43(May 2002):1–23.

The SWAN Team (2008). SWAN User Manual. SWAN Cycle III version 40.72A. Technical report, TU Delft, Delft.

TU Delft (2016). SWASH user manual: SWASH version 3.14A. Technical report, TU Delft, Delft.

Van der Meer, J. (2002). Technisch Rapport Golfoploop en Golfoverslag bij Dijken. Technical report, TAW, Delft.

Van der Vliet, C. (2010). Ontwerpnota Oesterdam Zuid [38]: Geplande jaar van uitvoering: 2012. Technical report, Projectbureau Zeeweringen.

Van der Westhuysen, A. J., Zijlema, M., & Battjes, J. A. (2007). Nonlinear saturation-based whitecapping dissipation in SWAN for deep and shallow water. *Coastal Engineering*, 54(2):151–170.

van Leeuwen, B., van den Boomgaard, M., & van de Rest, P. (2014). Herbepaling golftransmissie Oosterscheldekering. Technical report, Svasek Hydraulics.

Van Zanten, E. (2012). Monitoringsplan Zandhongerproeven 2013-2018. Technical Report december 2012, Rijkswaterstaat.

Verhagen, H., D'Angremond, K., & van Roode, F. (2012). *Breakwaters and closure dams*. VSSD, Delft, The Netherlands, 2nd edition.

Wenneker, I. (2014). Nauwkeurigheid golfmetingen petten: Analyse van verschillen tussen golfmetingen met drukdozen, stappenbaken, S4's en capdraden. Technical report, Rijkswaterstaat, Deltares.

Wigley, T., Santer, B., & Lanzante, J. (2006). Appendix A: Statistical issues regarding trends. In *Temperature Trends in the Lower Atmosphere Understanding and Reconciling Differences*, pages 129–139.

Young, I. & Verhagen, L. (1996). The growth of fetch limited waves in water of finite depth. Part 1. Total energy and peak frequency. *Coastal Engineering*, 29:47–78.

A

DATA ANALYSIS

PRESSURE BOX DATA

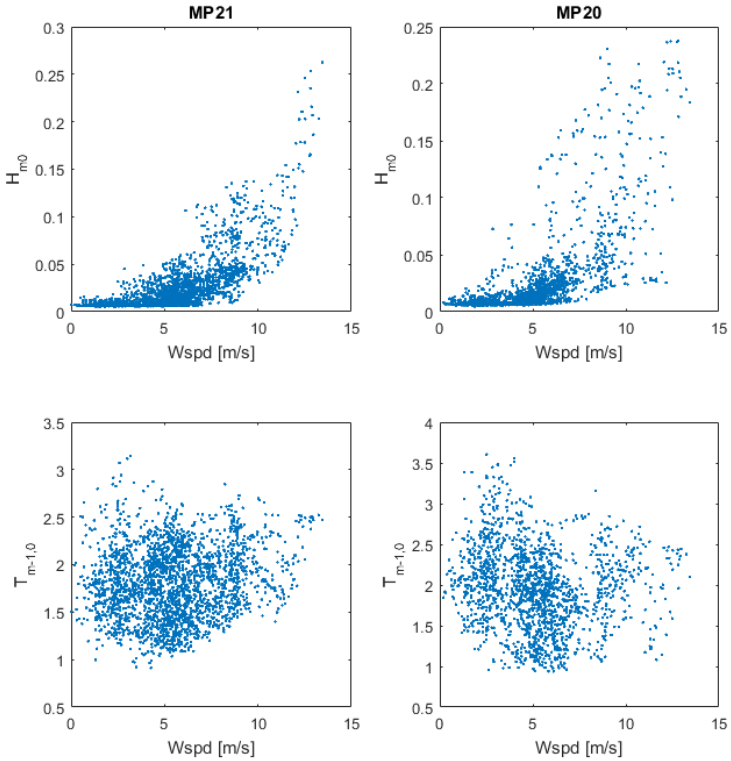

FIGURE A.1: WIND SPEED AT MAROLLEGAT AND WAVES AT MP21 AND MP20.

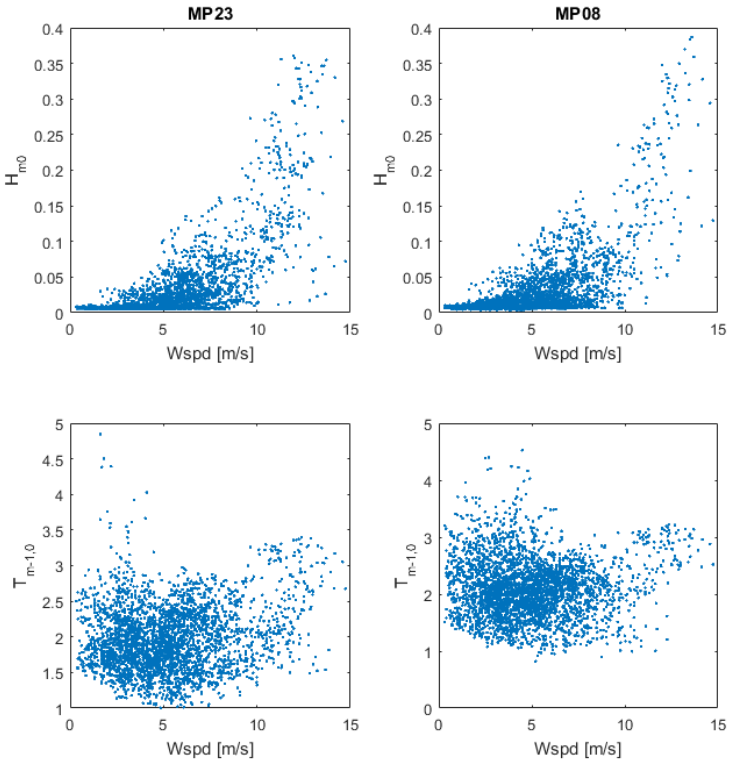

FIGURE A.2: WIND SPEED AT MAROLLEGAT AND WAVES AT MP23 AND MP08.

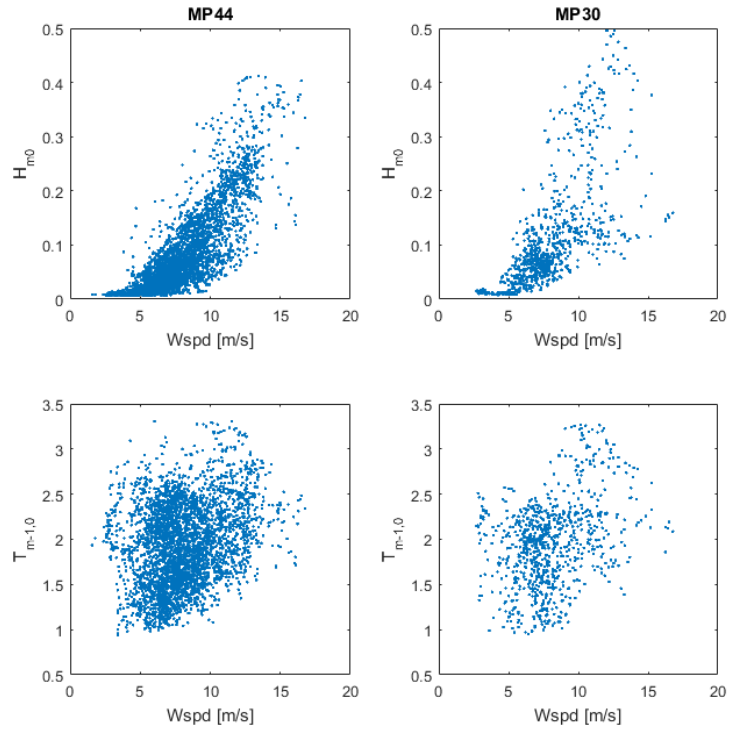

FIGURE A.3: WIND SPEED AT MAROLLEGAT AND WAVES AT MP44 AND MP30.

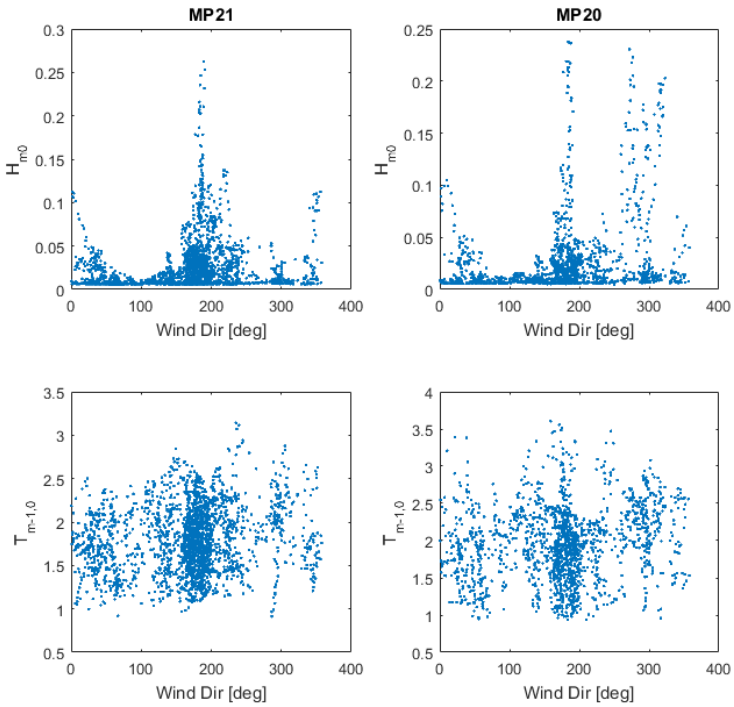

FIGURE A.4: WIND DIRECTION AT MAROLLEGAT AND WAVES AT MP21 AND MP20.

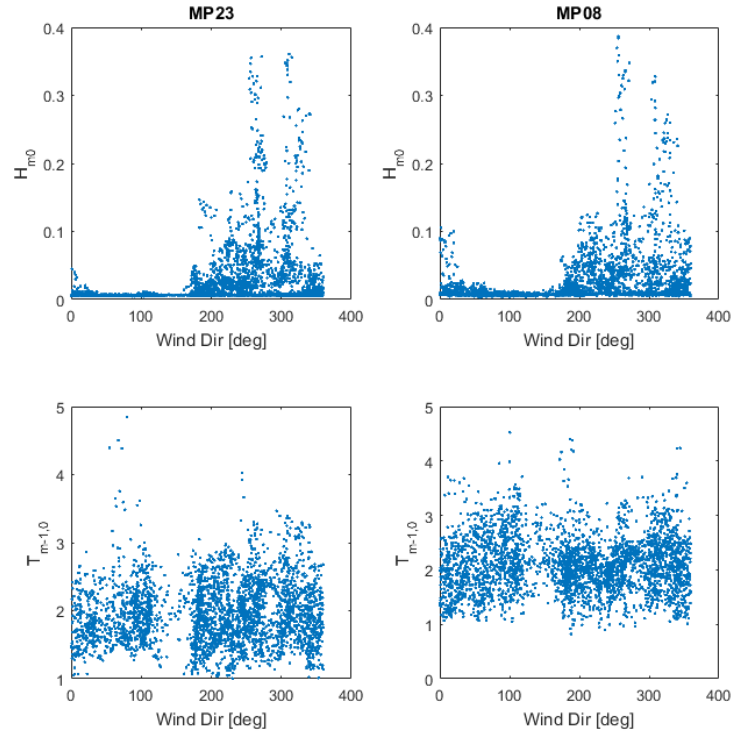

FIGURE A.5: WIND DIRECTION AT MAROLLEGAT AND WAVES AT MP23 AND MP08.

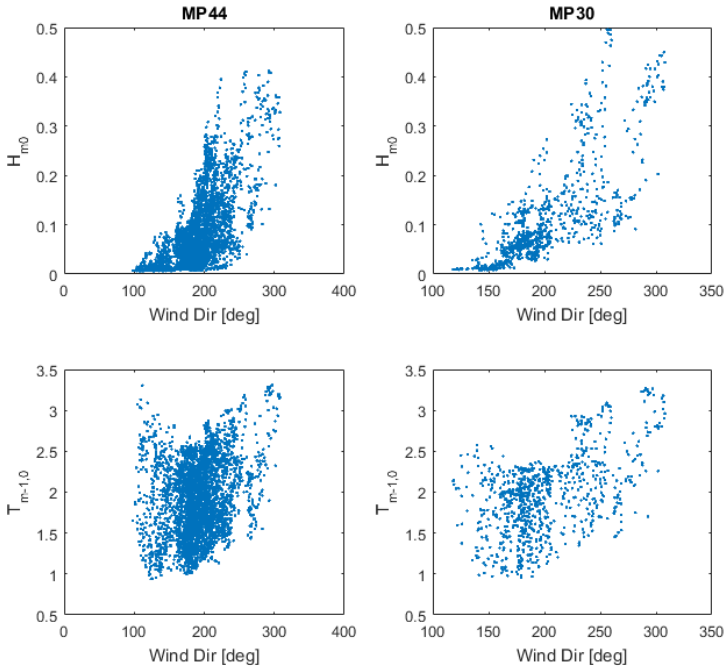

FIGURE A.6: WIND DIRECTION AT MAROLLEGAT AND WAVES AT MP44 AND MP30.

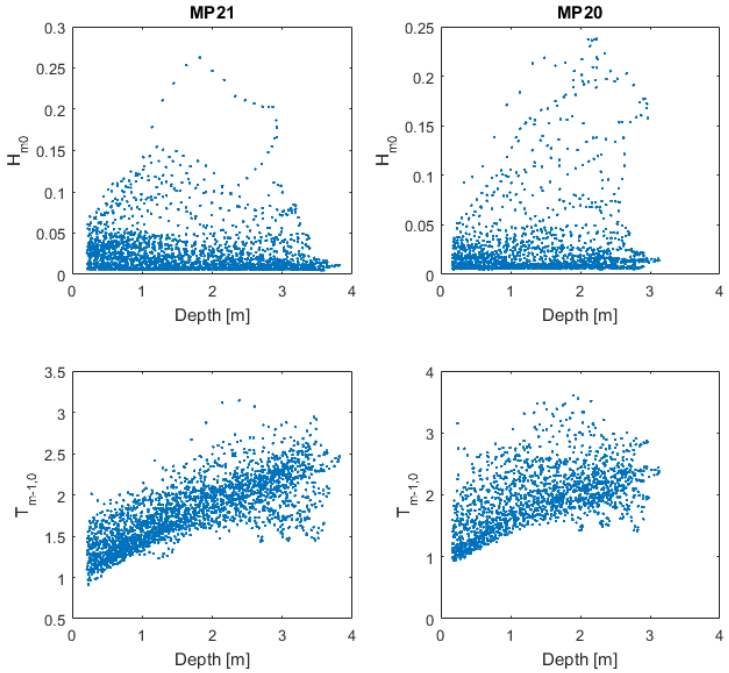

FIGURE A.7: WATER DEPTH AND WAVES AT MP21 AND MP20.

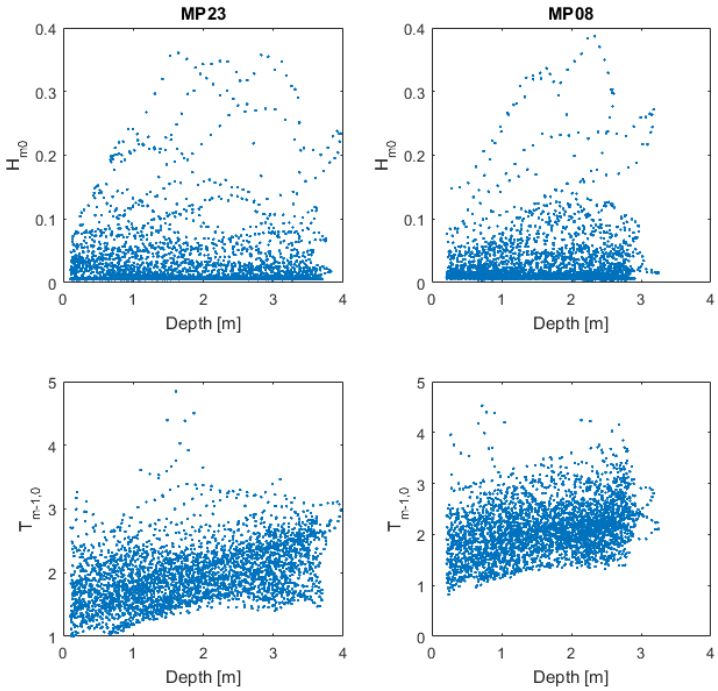

FIGURE A.8: WATER DEPTH AND WAVES AT MP23 AND MP08.

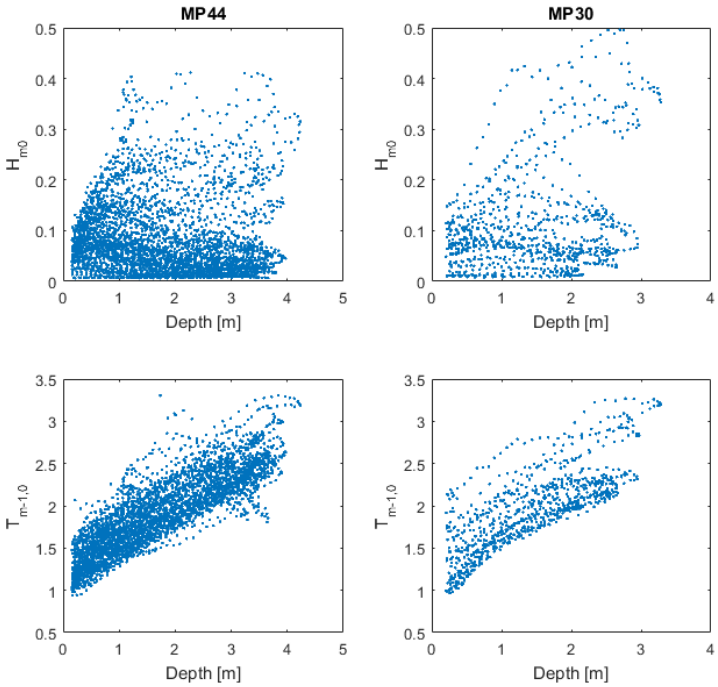

FIGURE A.9: WATER DEPTH AND WAVES AT MP44 AND MP30.

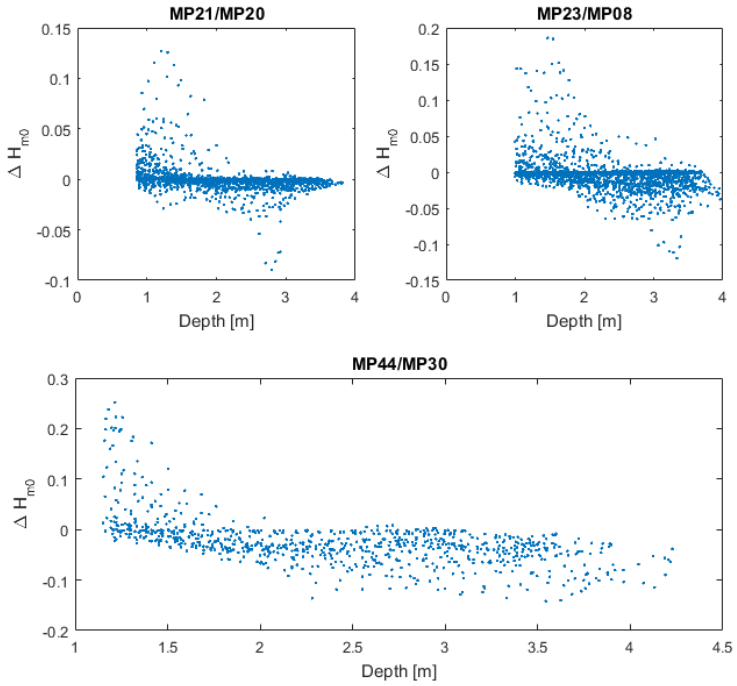

FIGURE A.10: WAVE ATTENUATION OVER THE NOURISHMENT HOOK AS A FUNCTION OF WATER DEPTH.

TIME SERIES PLOTS

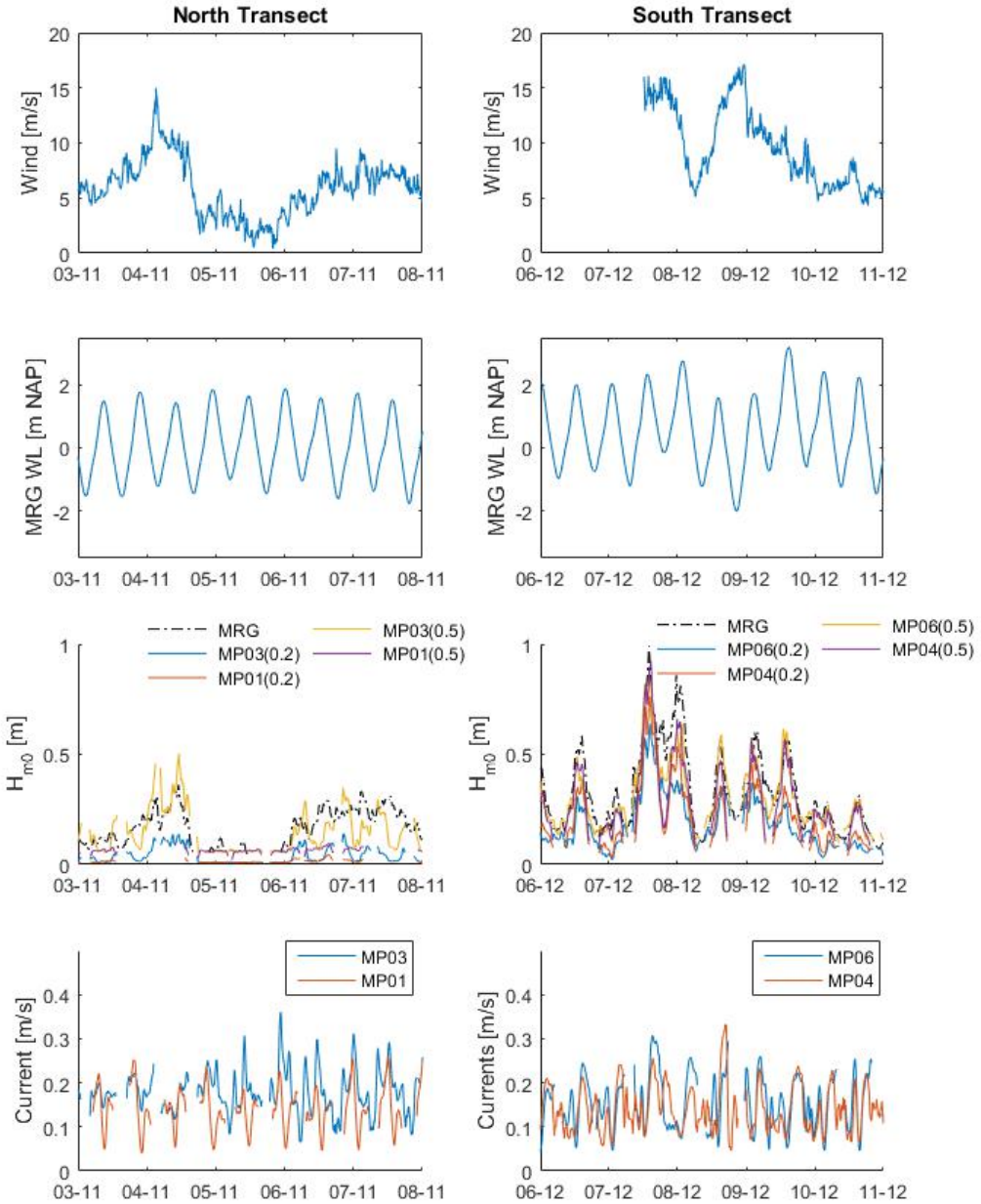

FIGURE A.11: T0 PROCESSED WAVE AND CURRENT DATA.

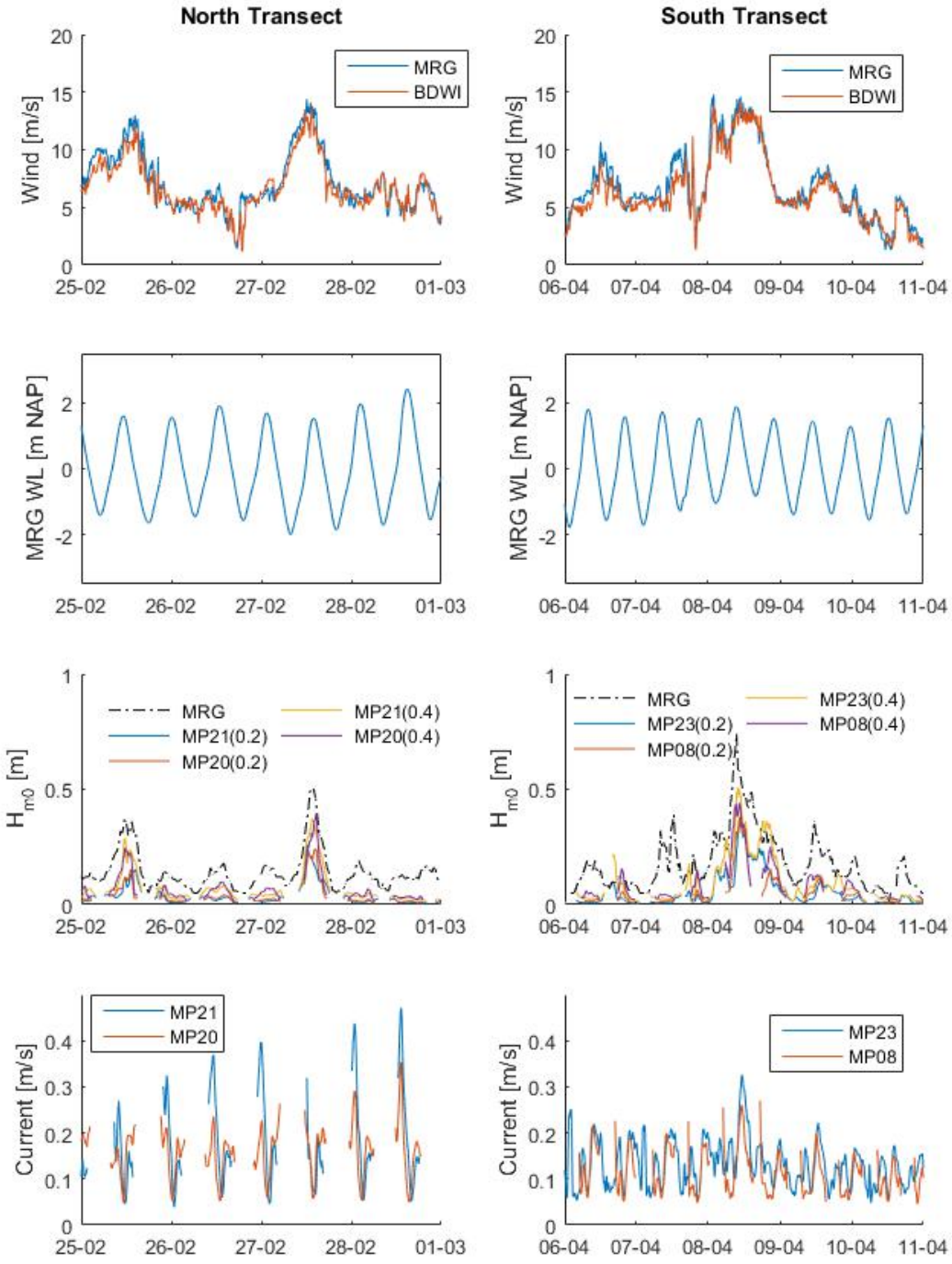

FIGURE A.12: T1 PROCESSED WAVE AND CURRENT DATA.

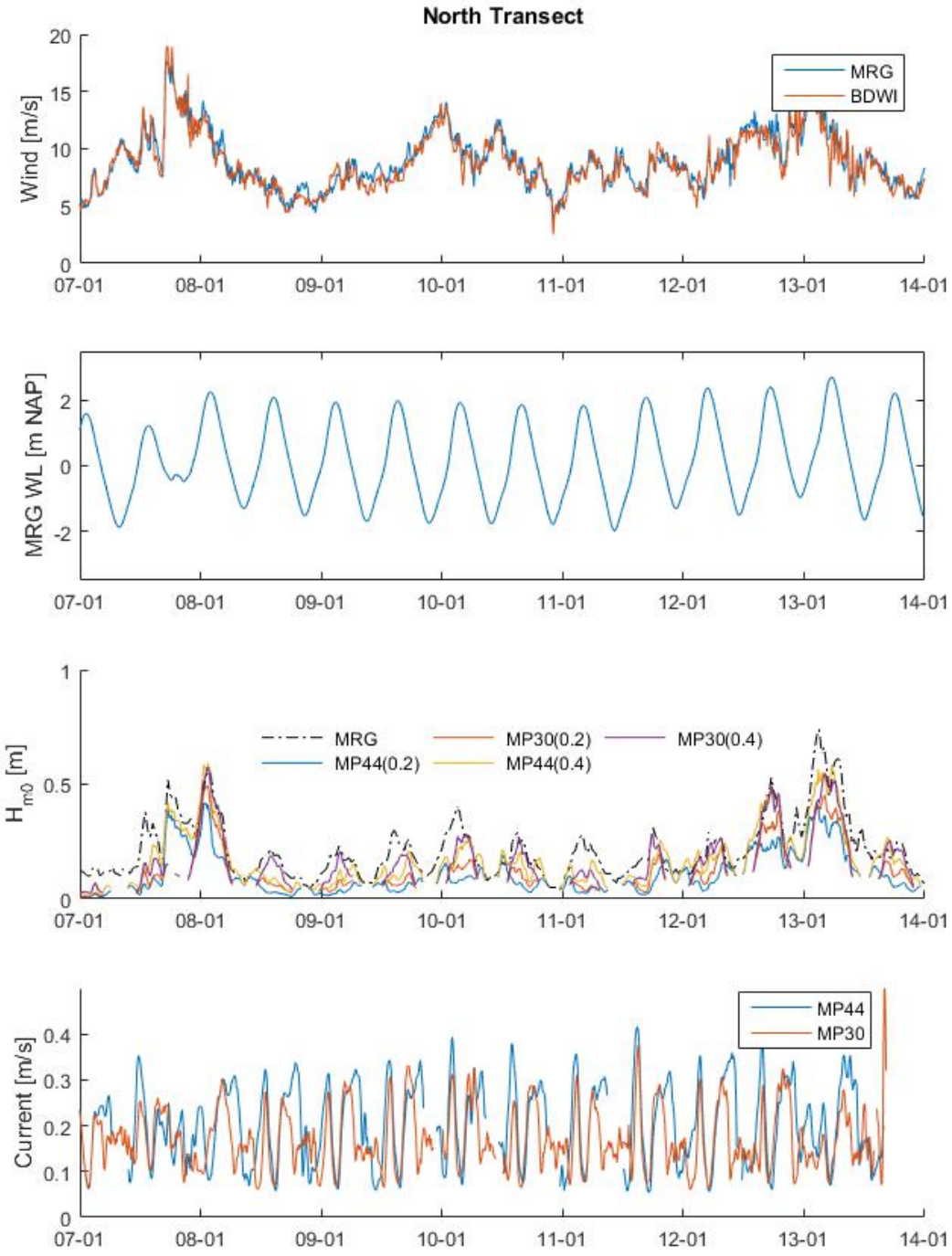

FIGURE A.13: T2 PROCESSED WAVE AND CURRENT DATA.

ADCP CURRENTS

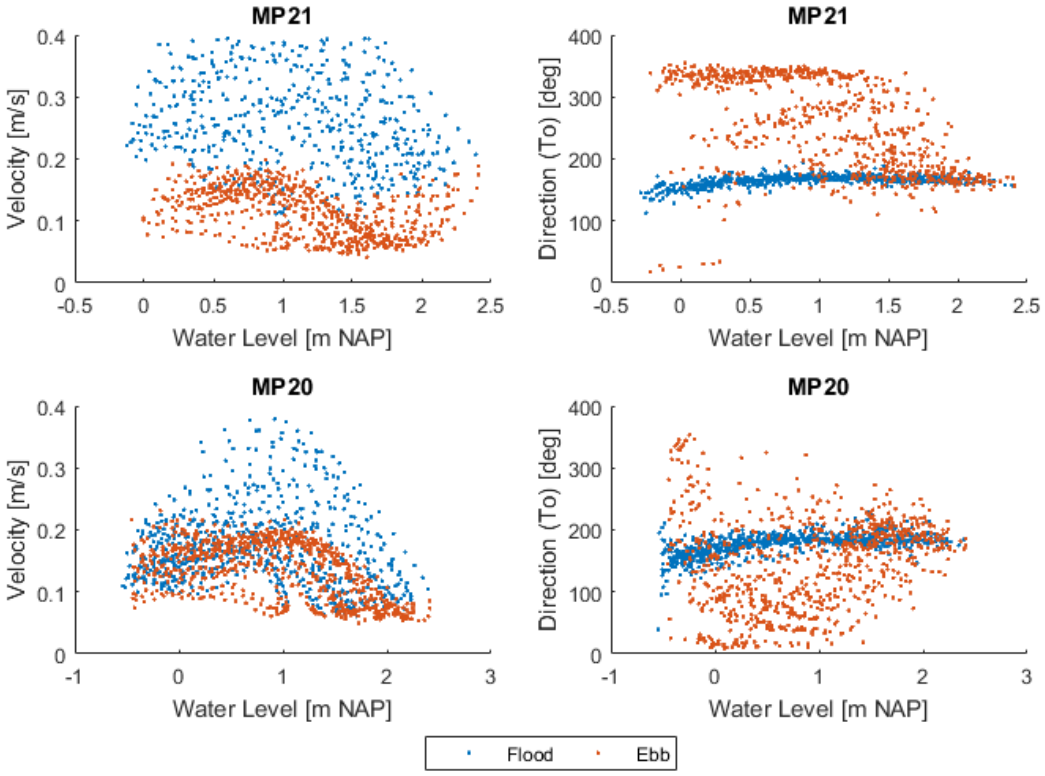

FIGURE A.14: CURRENTS DURING FLOOD AND EBB TIDE AT MP21 AND MP20.

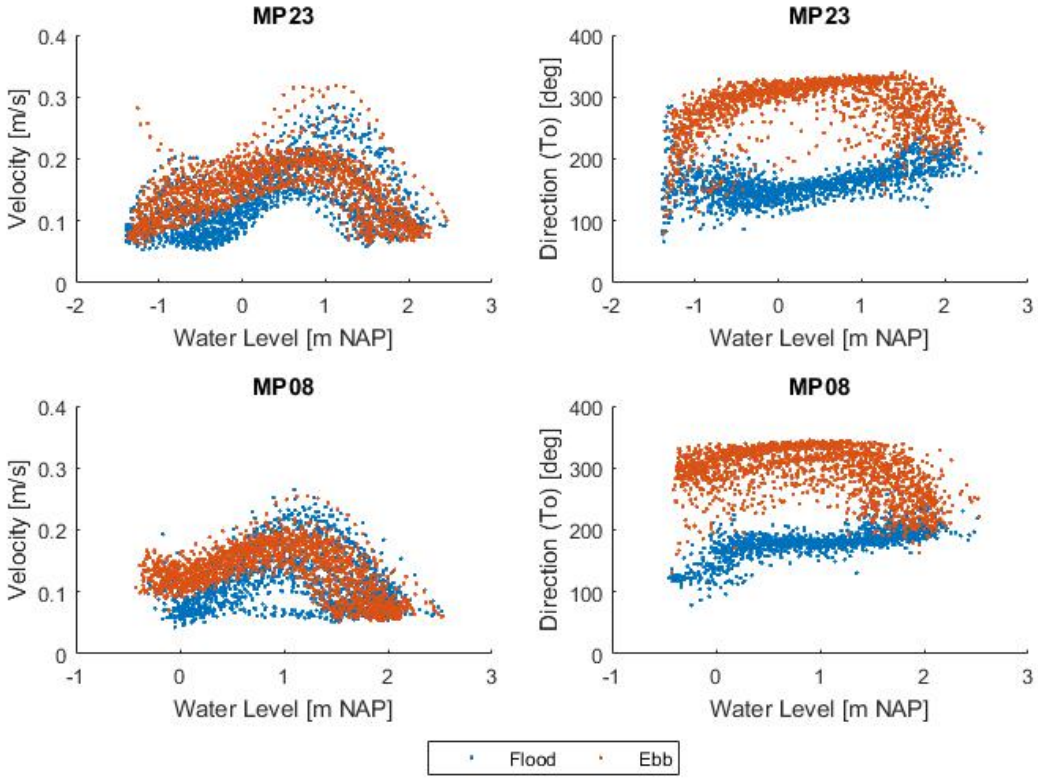

FIGURE A.15: CURRENTS DURING FLOOD AND EBB TIDE AT MP23 AND MP08.

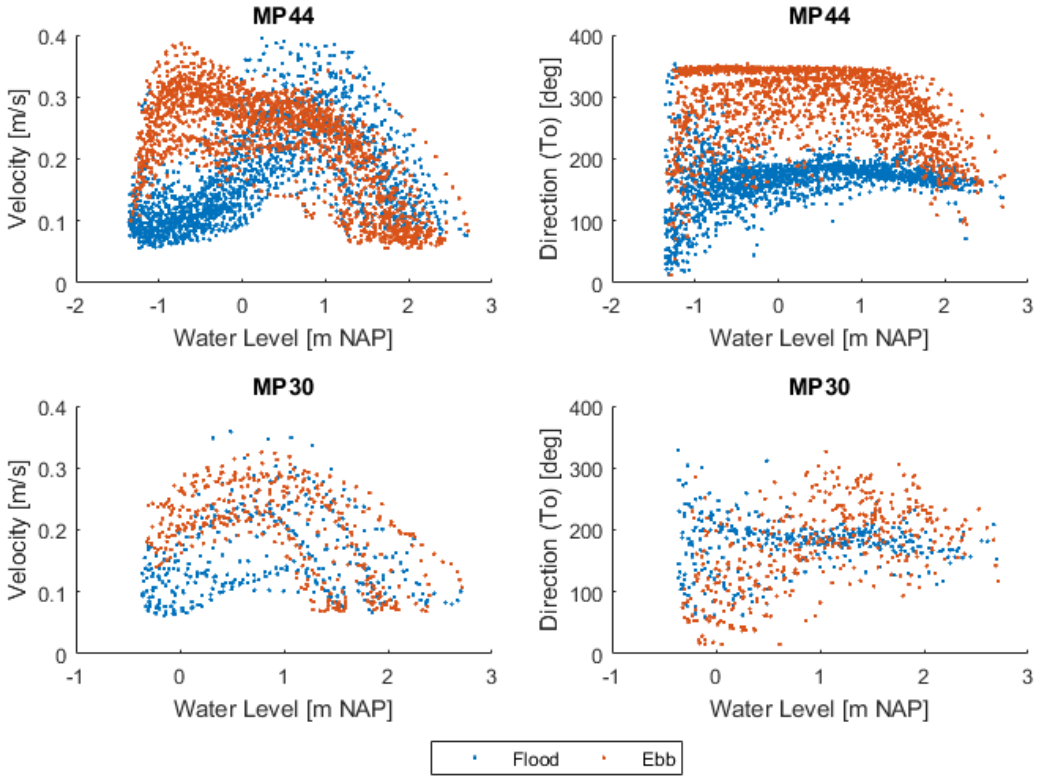

FIGURE A.16: CURRENTS DURING FLOOD AND EBB TIDE AT MP44 AND MP30.

TREND ANALYSIS PLOTS

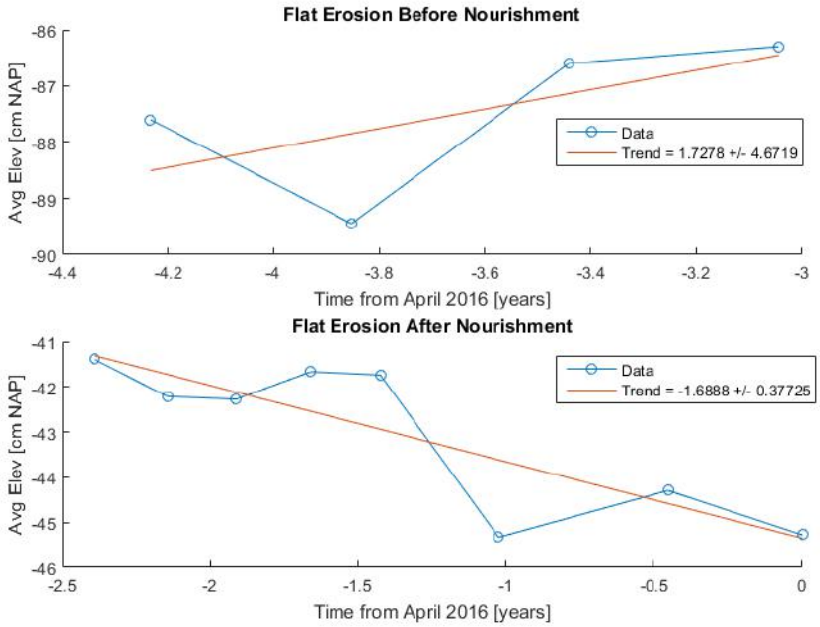

FIGURE A.17: TREND ANALYSIS OF THE OVERALL OESTERDAM FLAT EROSION BASED ON RTK SURVEYS.

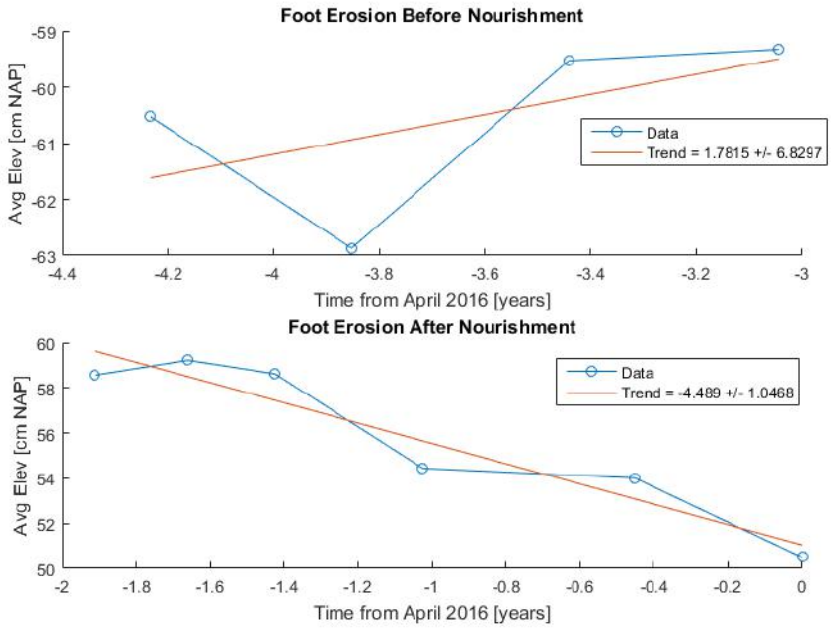

FIGURE A.18: TREND ANALYSIS OF THE NOURISHMENT FOOT EROSION BASED ON RTK SURVEYS.

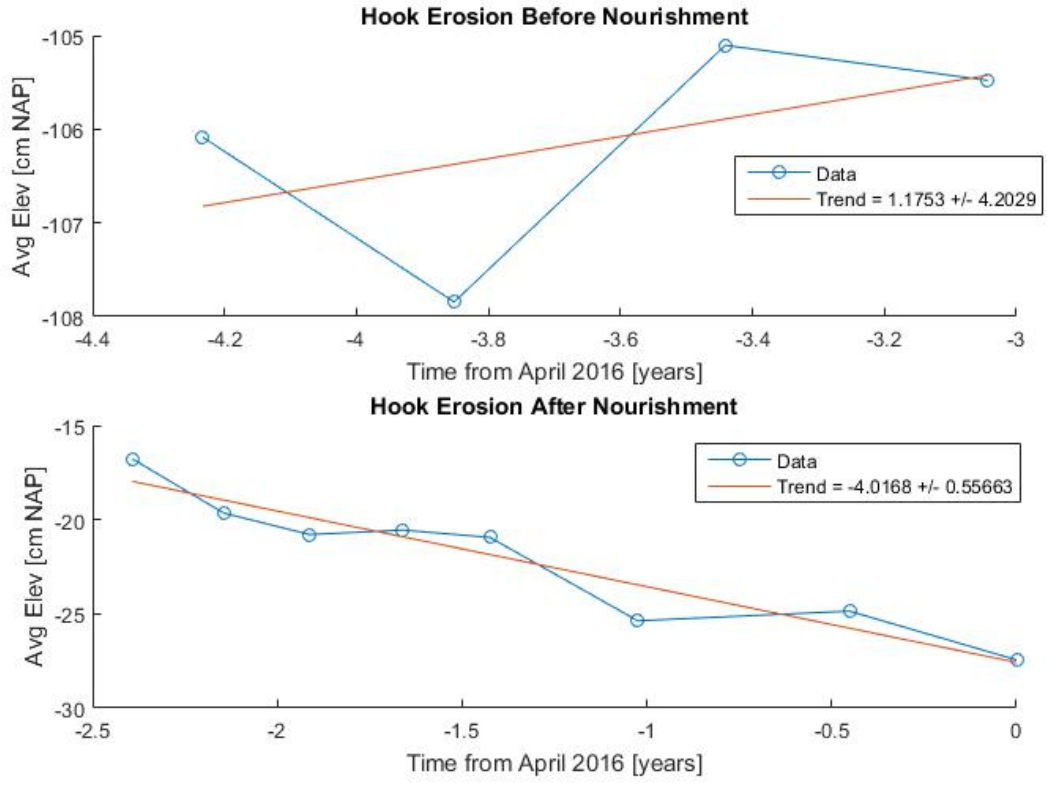

FIGURE A.19: TREND ANALYSIS OF THE NOURISHMENT HOOK EROSION BASED ON RTK SURVEYS.

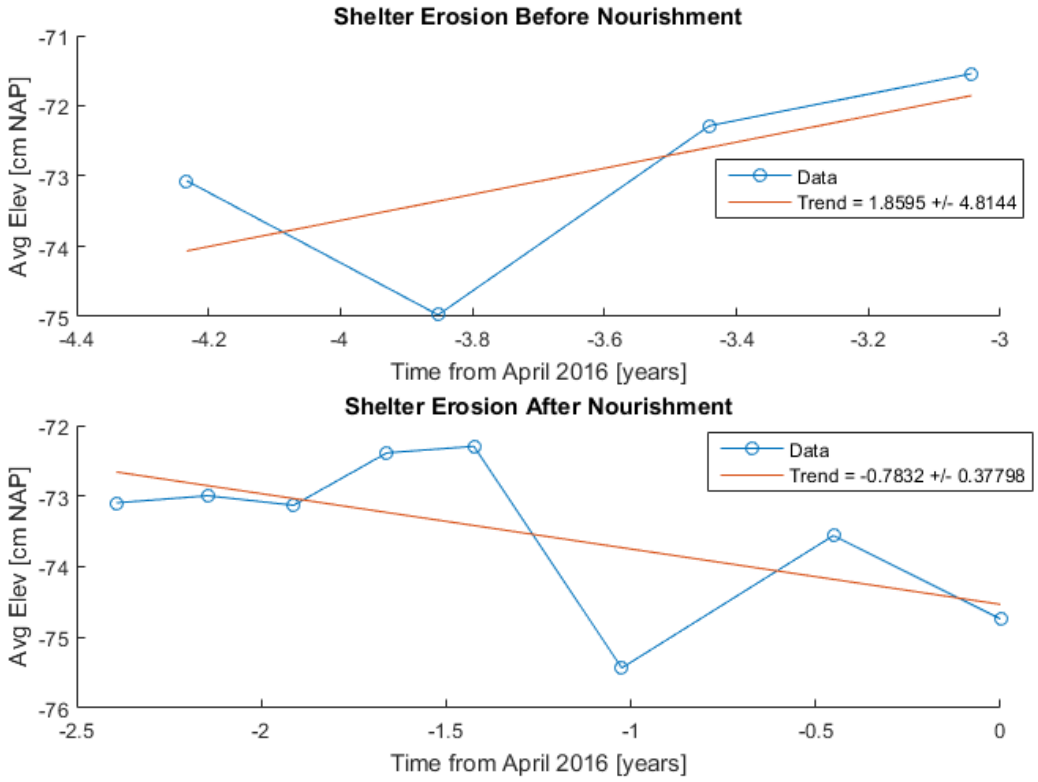

FIGURE A.20: TREND ANALYSIS OF EROSION IN THE SHELTERED AREA BETWEEN THE NOURISHMENT HOOK AND FOOT, BASED ON RTK SURVEYS.

B

DELFT3D MODELLING

SCALOOST MODEL VALIDATION

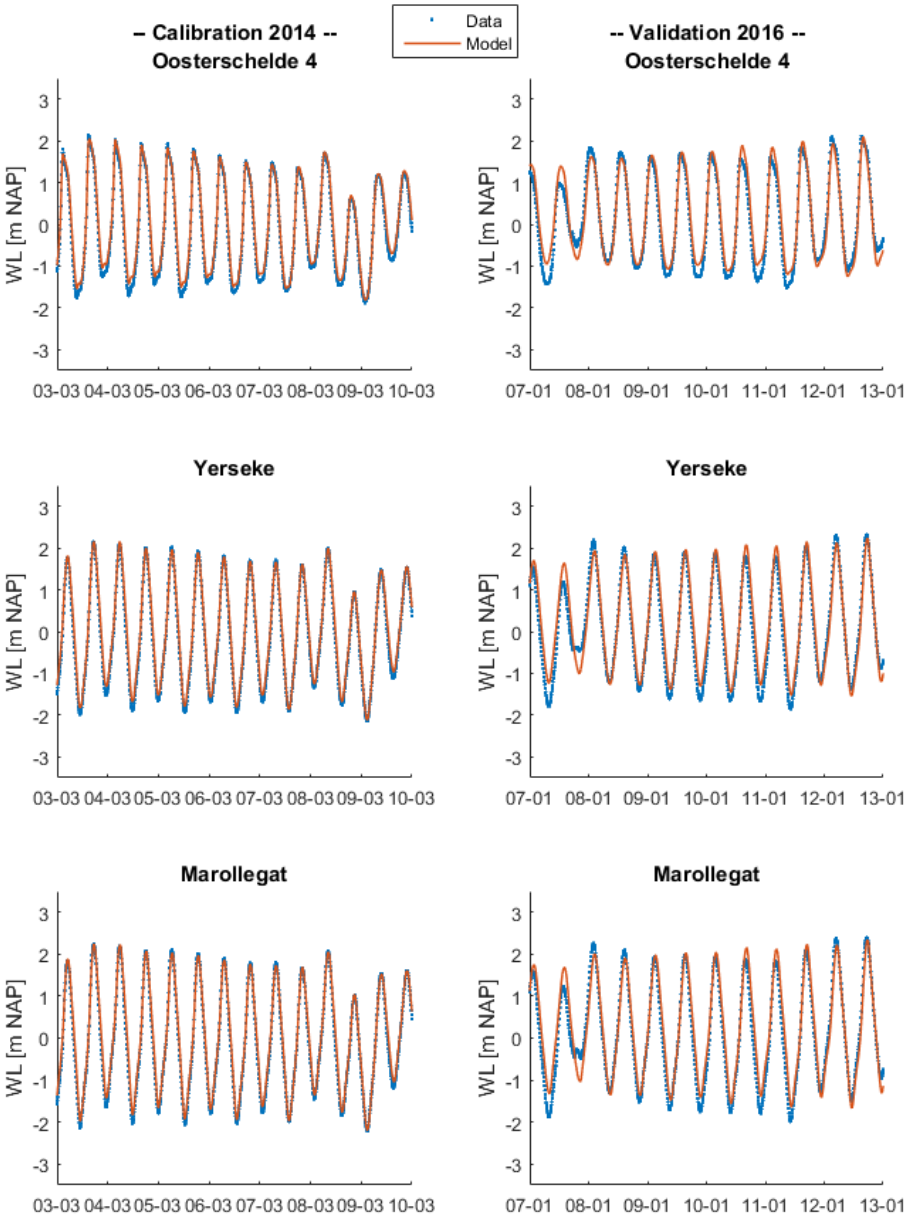

FIGURE B.1: CALIBRATION AND VALIDATION OF THE SCALOOST MODEL AGAINST MEASURED WATER LEVELS.

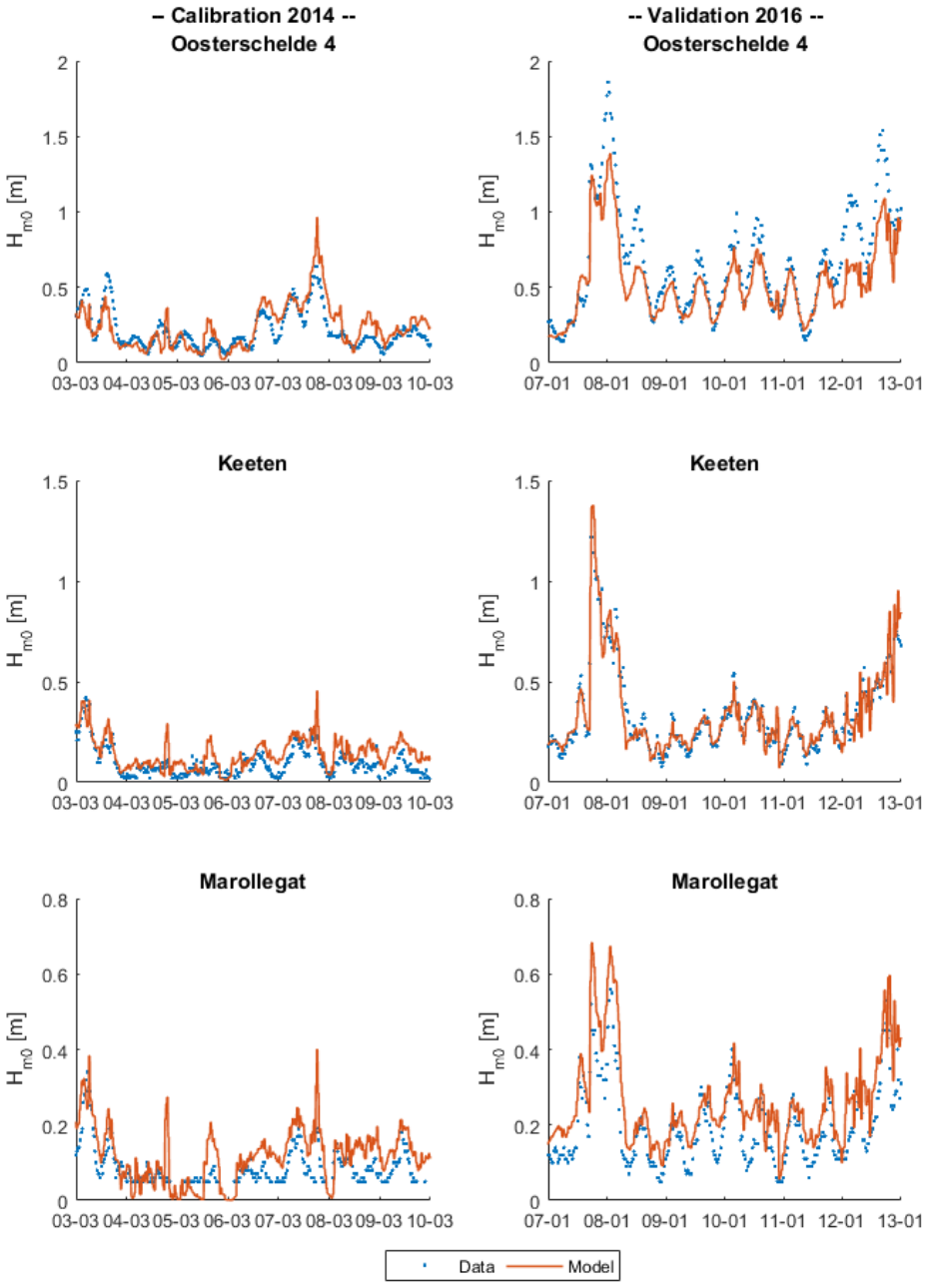

FIGURE B.2: CALIBRATION AND VALIDATION OF THE SCALOOST MODEL AGAINST MEASURED WAVES.

PARTIAL VALIDATION AT THE OESTERDAM

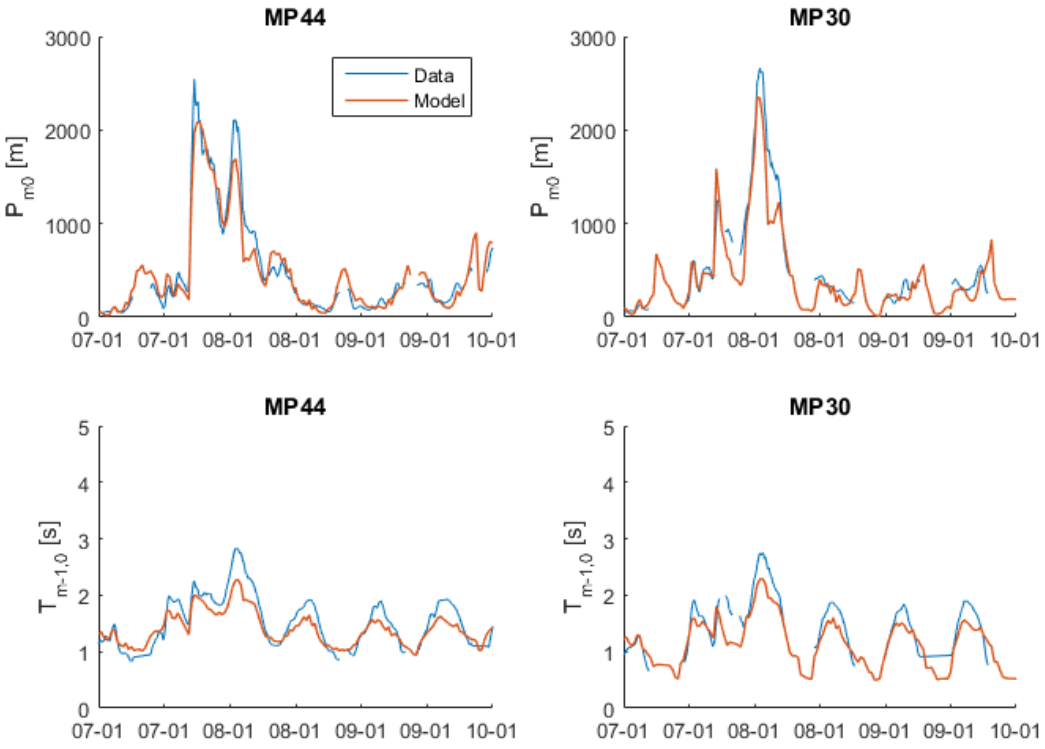

FIGURE B.3: T2 KOM RESULTS WITH DEFAULT SWAN PARAMETERS.

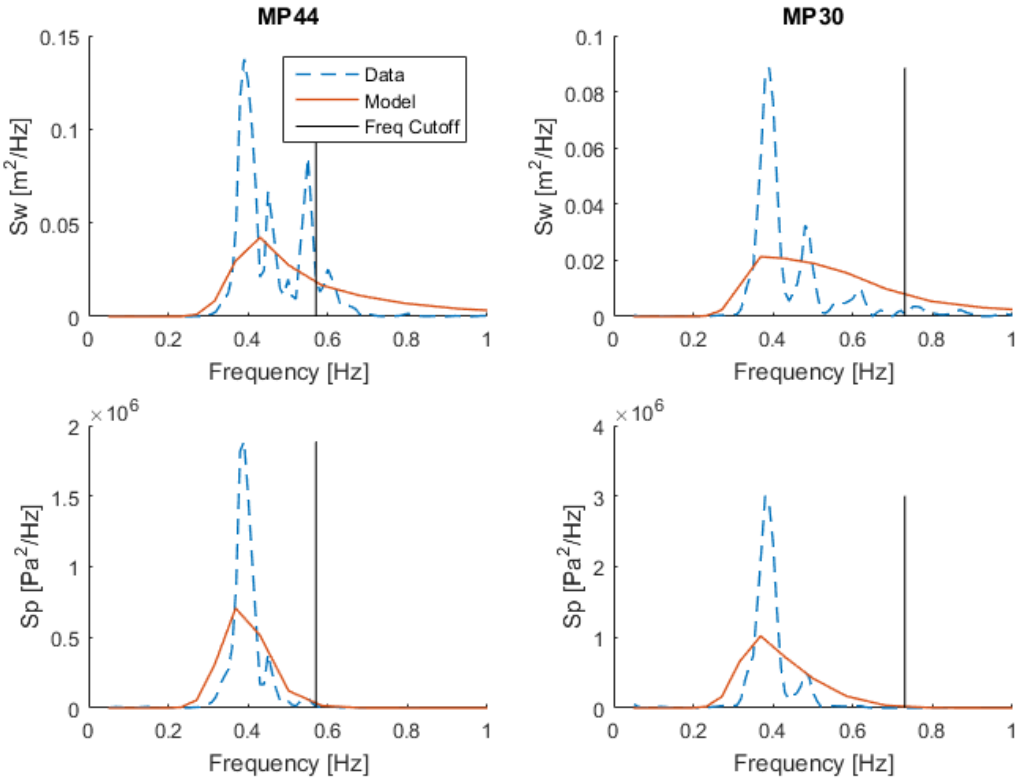

FIGURE B.4: T2 KOM RESULTS WITH DEFAULT SWAN PARAMETERS. JANUARY 8, 12AM

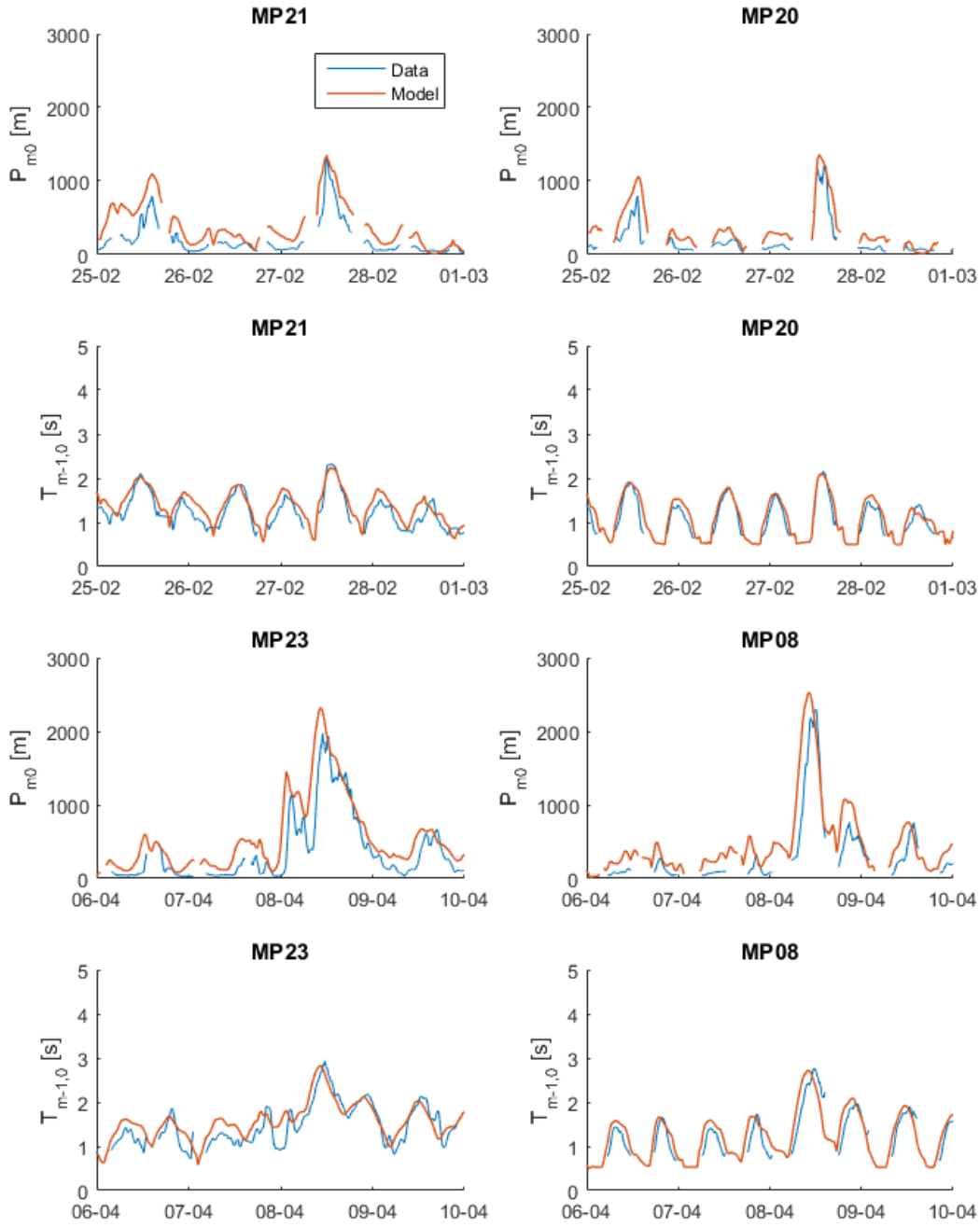

FIGURE B.5: T1 KOM RESULTS WITH SCALED UP QUADRUPLET INTERACTIONS: CNL4 = 1.5E8.

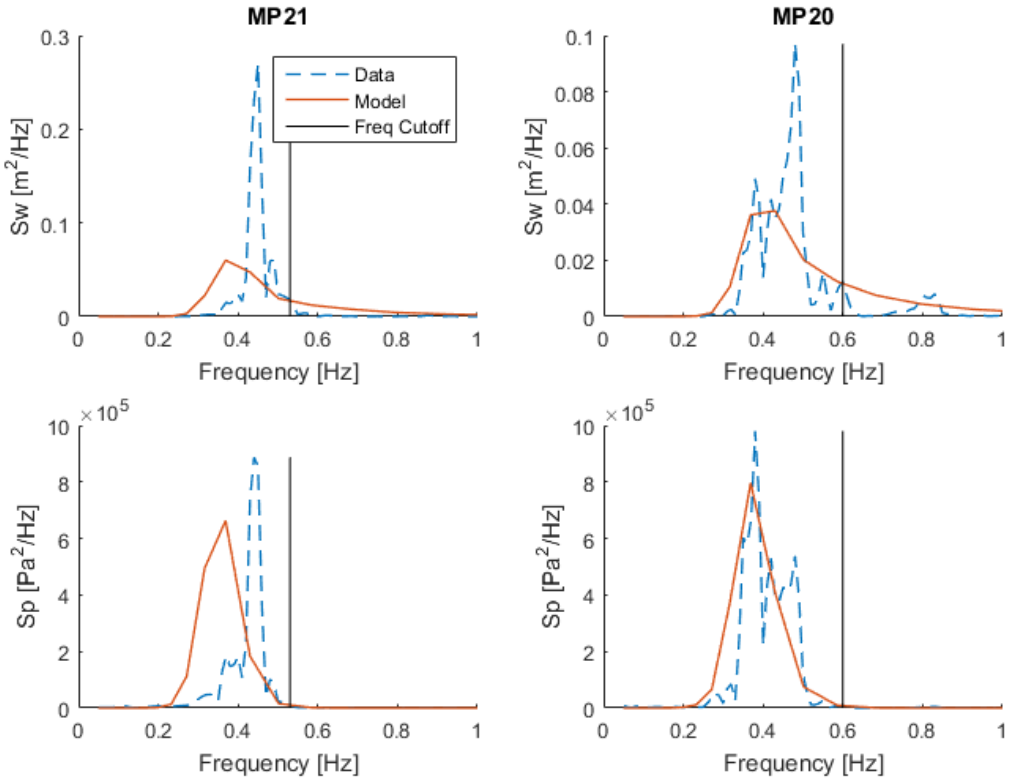

FIGURE B.6: T1 KOM RESULTS WITH SCALED UP QUADRUPLET INTERACTIONS: CNL4 = 1.5E8. FEB 27, 2014 14:00:00

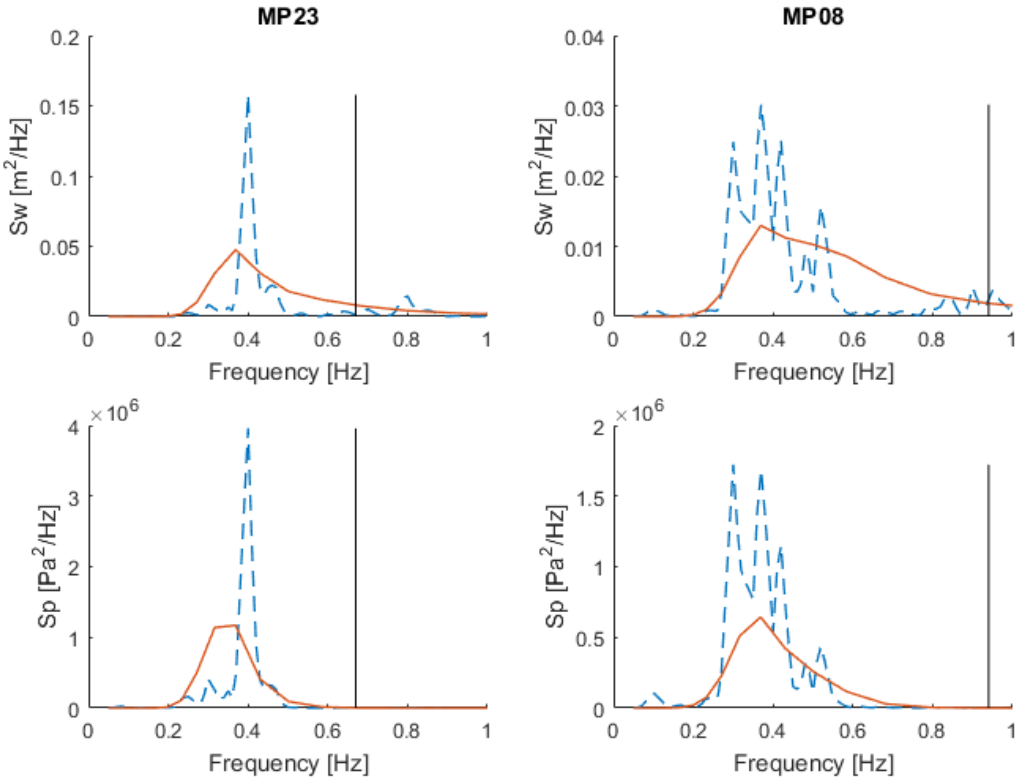

FIGURE B.7: T1 KOM RESULTS WITH SCALED UP QUADRUPLET INTERACTIONS: CNL4 = 1.5E8. APRIL 8, 2014, 1PM

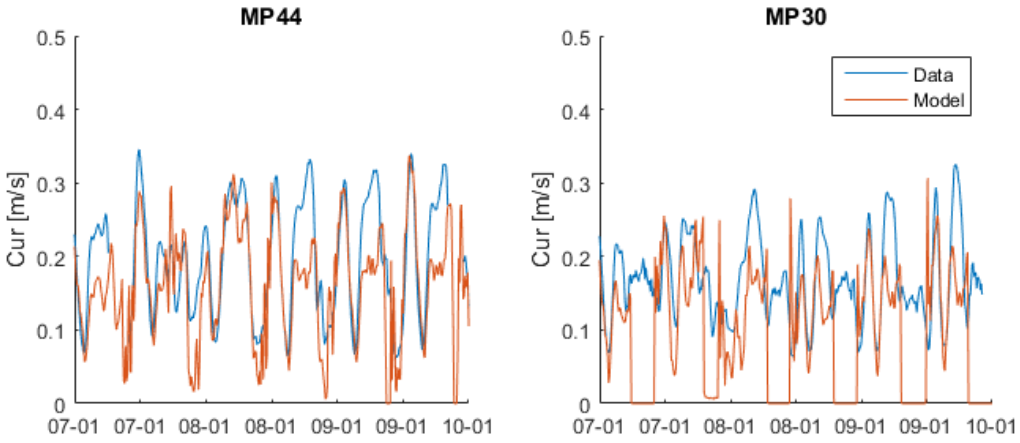

FIGURE B.8: T2 OESTERDAM MODELLED CURRENTS.

C

DESIGN WAVE LOADS

The cross sections of the Oesterdam were obtained from Van der Vliet (2010) and Bijlsma (2010).

Figuur 2

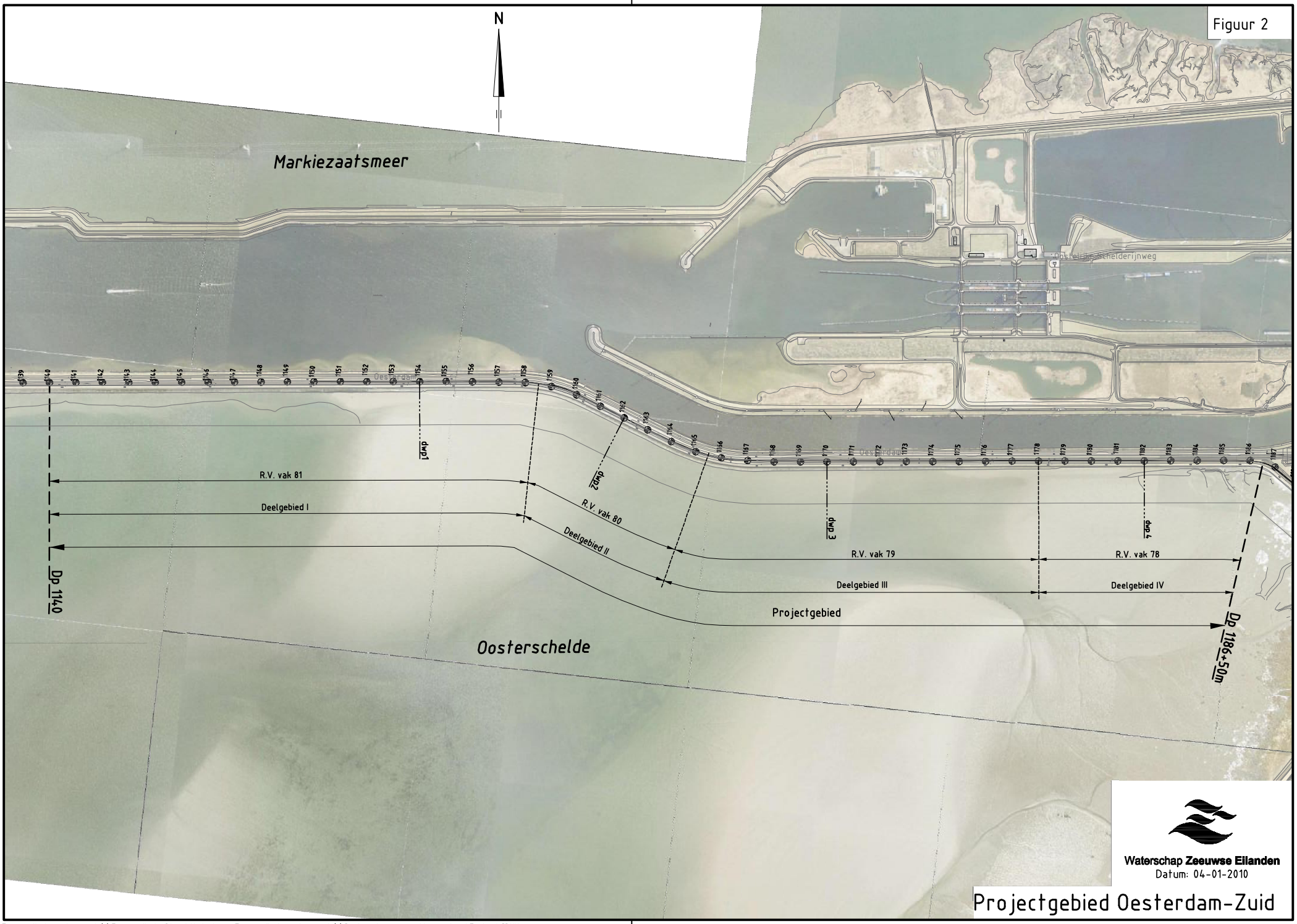

Projectgebied Oesterdam-Zuid

Waterschap Zeeuwse Eilanden
Datum: 04-01-2010

Topografische ondergrond: (c) Topografische Dienst Kadaster
Kadastrale ondergrond: (c) Kadaster, Middelburg
Topografische ondergrond: (c) Regionaal samenwerkingsverband Zeeland GBKN

FILENAME: G:\TEKENING\ZEEKERINGEN\OESTERDAM ZUID\ONTWNOTA-PROJGEB-OESTERDAM-ZUID.DWG
PLOTDATUM: 1/1/2010 23:55

Figuur 8

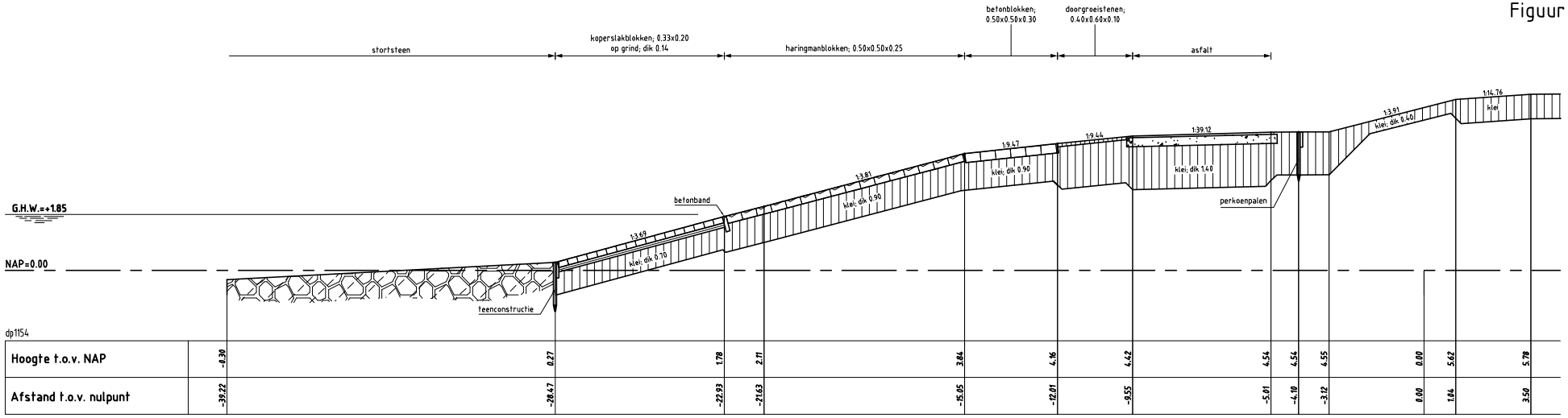

Hoogte t.o.v. NAP	-0.30	0.27	1.78	2.11	3.84	4.16	4.42	4.54	4.54	4.55	0.00	5.62	5.78		
Afstand t.o.v. nulpunt	-39.22	-28.47	-22.93	-21.63	-15.05	-12.01	-9.55	-5.01	-4.10	-3.12	0.00	1.04	3.50		

DWARSPROFIEL 1 bestaand

schaal 1:100

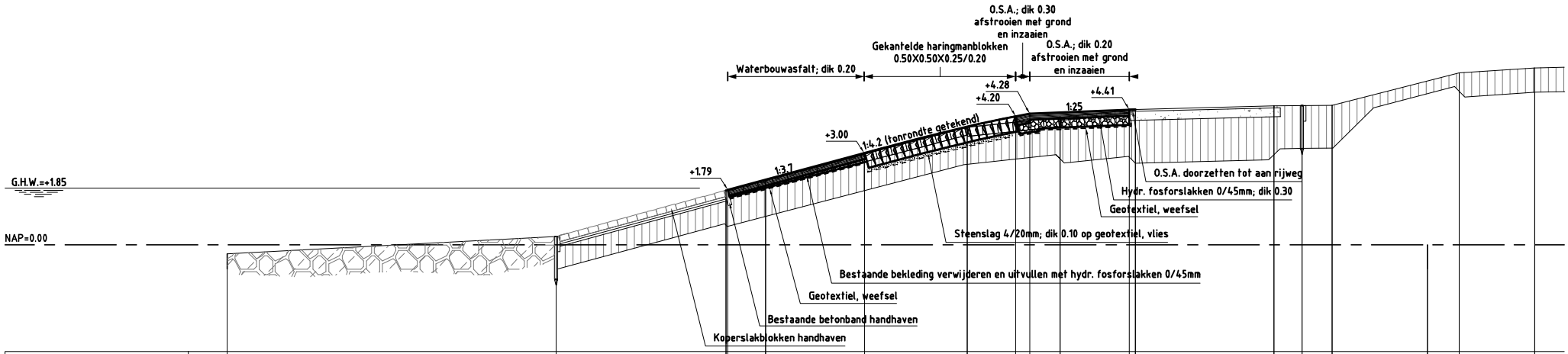

Hoogte t.o.v. NAP	-0.30	0.27	1.78	2.11	3.84	4.16	4.42	4.54	4.54	4.55	0.00	5.62	5.78		
Afstand t.o.v. nulpunt	-39.22	-28.47	-22.93	-21.63	-15.05	-12.01	-9.55	-5.01	-4.10	-3.12	0.00	1.04	3.50		
Nieuwe hoogte t.o.v. NAP			1.79		3.00		4.20	4.28		4.41					
Nieuwe afstand t.o.v. nulpunt			-22.87		-18.39		-13.46	-13.01		-9.74		0.00			

DWARSPROFIEL 1 nieuw

van dp1139+50m tot dp1158+50m VARIANT 4

schaal 1:100

Waterschap **Zeeuwse Eilanden**

Datum: 21-12-2009

Oesterdam Zuid

FILENAME: G:\TEKENING\ZEEWERKEN\OESTERDAM ZUID\ONTWERP\T-DWP-OESTERDAM ZUID.DWA/DWG
PLOTDATUM: 1/6/2010 4:10:15

Figuur 9

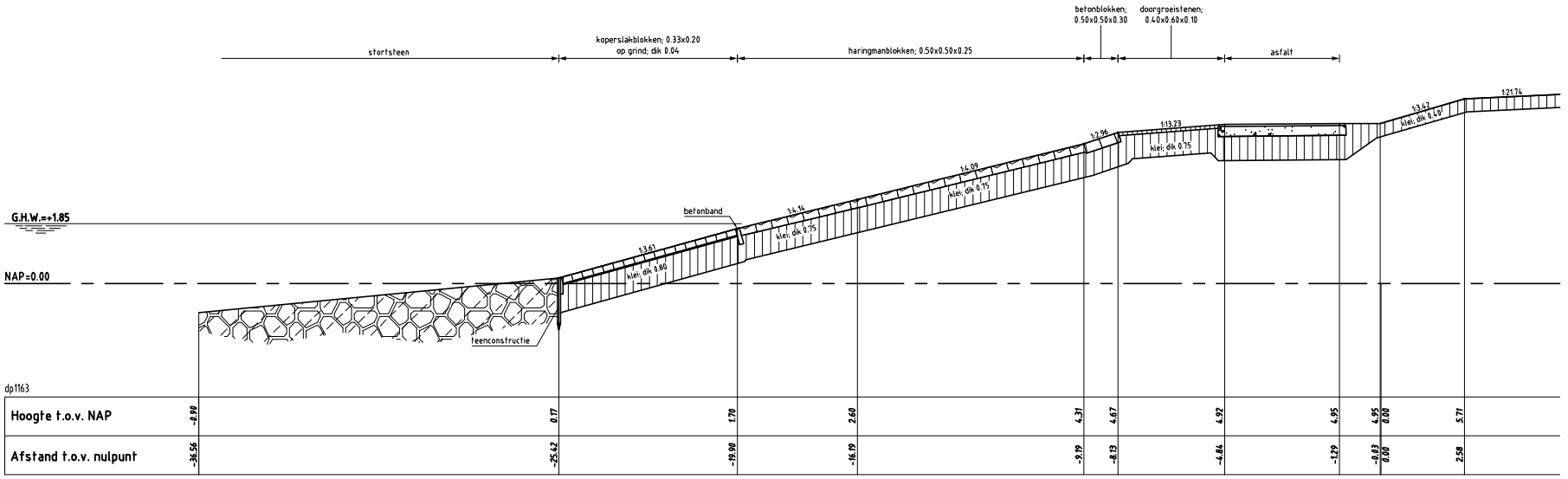

Hoogte t.o.v. NAP	-0.90	0.17	1.70	2.60	4.31	4.67	4.92	4.95	4.95	0.00	5.71	
Afstand t.o.v. nulpunt	-36.56	-25.42	-19.90	-16.19	-9.19	-8.13	-4.84	-1.29	-0.03	0.00	2.58	

DWARSPROFIEL 2 bestaand

schaal 1:100

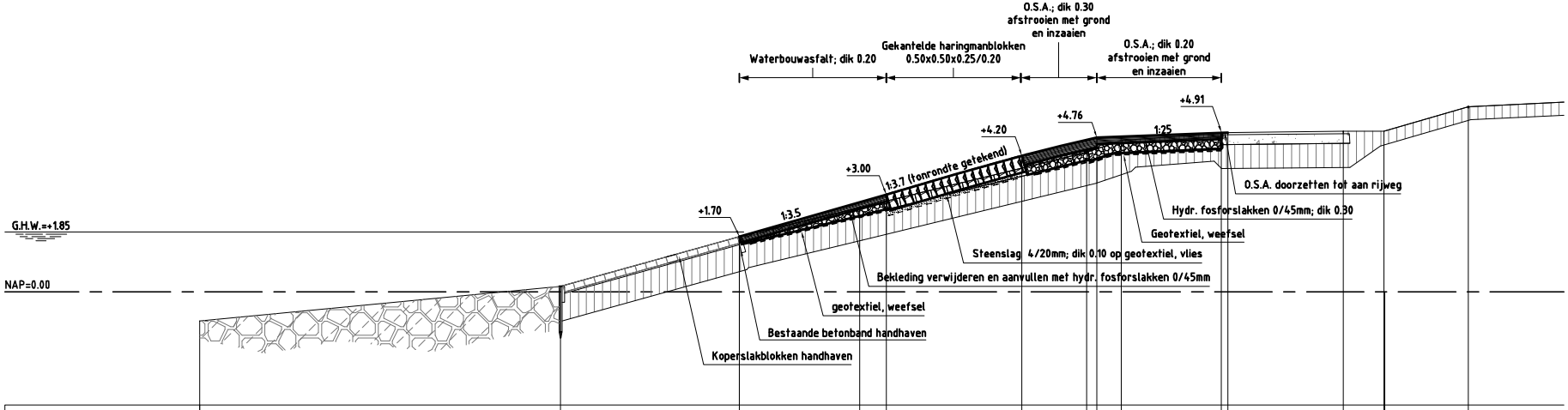

Hoogte t.o.v. NAP	-0.90	0.17	1.70	2.60	4.31	4.67	4.92	4.95	4.95	0.00	5.71	
Afstand t.o.v. nulpunt	-36.56	-25.42	-19.90	-16.19	-9.19	-8.13	-4.84	-1.29	-0.03	0.00	2.58	
Nieuwe hoogte t.o.v. NAP			1.70	3.00	4.20	4.76	4.91					
Nieuwe afstand t.o.v. nulpunt			-19.90	-15.38	-11.19	-8.88	-5.04			0.00		

DWARSPROFIEL 2 nieuw

van dp1158+50m tot dp1165+50m VARIANT 4

schaal 1:100

Waterschap Zeeuwse Eilanden

Datum: 21-12-2009

Oesterdam Zuid

FILENAME: G:\TEKENING\ZEEWERKEN\OESTERDAM ZUID\ONTWERP\T-DWP-OESTERDAM ZUID.DWA/DWG
PLOTDATUM: 1/6/2010 4:12:17

DESIGN WAVE LOAD TABLES

The design wave loads were calculated using the SWAN model using an array of water levels, wind speeds, and wind directions. The projected design wave loads were calculated for the years 2020-2080. At each point along the Oesterdam, the wave load was calculated for each wind direction (and associated wind speed). The Z3 load function ($H_{m0}^2 T_m$) was used to determine the normative wind direction/speed. While the Z0 load function (H_{m0}) was used for asphalt and Z3 for the other failure mechanisms, Z3 is also

no_fast 2020

Point	Hs [m]					Tmm10 [s]					Water Depth [m]					Wind Direction [deg]					Wave Direction [deg]				
Design WL	0m	1m	2m	3m	4m	0m	1m	2m	3m	4m	0m	1m	2m	3m	4m	0m	1m	2m	3m	4m	0m	1m	2m	3m	4m
80A	0.62	1.01	1.33	1.62	1.87	2.59	3.17	3.6	3.95	4.29	1.33	2.33	3.33	4.33	5.33	285	285	285	300	300	289	293	296	302	301
80B	0.59	0.98	1.31	1.62	1.87	2.51	3.13	3.59	3.98	4.31	1.27	2.27	3.27	4.27	5.27	285	285	285	300	300	286	291	295	301	301
80C	0.54	0.95	1.29	1.59	1.87	2.39	3.03	3.57	3.97	4.33	1.16	2.16	3.16	4.16	5.16	270	270	285	300	300	278	281	294	301	301
80D	0.53	0.93	1.28	1.6	1.91	2.28	2.99	3.57	4.02	4.41	1.18	2.18	3.18	4.18	5.18	270	270	285	300	300	272	277	291	299	299
80E	0.38	0.81	1.19	1.53	1.87	2.01	2.86	3.52	4.02	4.43	0.79	1.79	2.79	3.79	4.79	270	270	285	300	300	273	277	291	299	299
81A	0.3	0.75	1.13	1.49	1.84	1.83	2.78	3.48	4	4.42	0.63	1.63	2.63	3.63	4.63	270	270	285	300	300	275	279	292	300	300
81B	0.22	0.68	1.09	1.46	1.81	1.62	2.72	3.47	3.98	4.4	0.51	1.51	2.51	3.51	4.51	270	270	285	300	300	280	287	297	305	304
81C	0.27	0.72	1.13	1.49	1.82	1.93	2.91	3.58	4.01	4.4	0.61	1.61	2.61	3.61	4.61	315	285	285	285	300	322	307	305	303	306
81D	0.33	0.8	1.21	1.56	1.87	2.47	3.3	3.74	4.1	4.43	0.61	1.61	2.61	3.61	4.61	300	300	285	300	300	305	307	302	304	302
81E	0.68	1.06	1.4	1.7	1.94	2.66	3.38	3.81	4.12	4.41	1.67	2.67	3.67	4.67	5.67	285	285	285	300	300	297	301	299	301	300

no2_fast

Point	Hs [m]					Tmm10 [s]					Water Depth [m]					Wind Direction [deg]					Wave Direction [deg]				
Design WL	0m	1m	2m	3m	4m	0m	1m	2m	3m	4m	0m	1m	2m	3m	4m	0m	1m	2m	3m	4m	0m	1m	2m	3m	4m
80A	0.44	0.87	1.25	1.57	1.81	2.32	3.07	3.54	3.91	4.28	0.92	1.92	2.92	3.92	4.92	270	285	285	285	300	278	287	291	293	300
80B	0.4	0.82	1.21	1.53	1.8	2.22	2.98	3.49	3.93	4.3	0.82	1.82	2.82	3.82	4.82	270	285	285	300	300	278	286	290	298	299
80C	0.34	0.78	1.16	1.5	1.78	2.07	2.86	3.44	3.91	4.31	0.71	1.71	2.71	3.71	4.71	270	270	285	300	300	278	278	290	299	299
80D	0.33	0.76	1.14	1.47	1.79	1.9	2.74	3.35	3.91	4.35	0.73	1.73	2.73	3.73	4.73	270	270	270	300	300	272	274	279	297	298
80E	0.16	0.63	1.04	1.39	1.74	1.57	2.55	3.26	3.89	4.38	0.34	1.34	2.34	3.34	4.34	270	270	270	300	300	272	275	279	298	298
81A	0.09	0.56	0.98	1.35	1.7	1.44	2.43	3.22	3.82	4.37	0.18	1.18	2.18	3.18	4.18	270	270	270	285	300	273	277	281	292	300
81B	0	0.48	0.91	1.29	1.66	0	2.3	3.19	3.84	4.34	0	1.06	2.06	3.06	4.06	270	270	270	300	300		284	288	304	304
81C	0.07	0.51	0.95	1.34	1.69	1.48	2.62	3.38	3.93	4.37	0.16	1.16	2.16	3.16	4.16	315	315	300	300	300	330	321	313	310	307
81D	0.11	0.6	1.04	1.43	1.76	1.6	3.09	3.67	4.06	4.41	0.16	1.16	2.16	3.16	4.16	270	285	300	300	300	289	303	307	305	303
81E	0.56	0.97	1.35	1.66	1.89	2.7	3.46	3.87	4.17	4.43	1.14	2.14	3.14	4.14	5.14	285	285	285	300	300	301	304	303	303	301

nour_fast

Point	Hs [m]					Tmm10 [s]					Water Depth [m]					Wind Direction [deg]					Wave Direction [deg]				
Design WL	0m	1m	2m	3m	4m	0m	1m	2m	3m	4m	0m	1m	2m	3m	4m	0m	1m	2m	3m	4m	0m	1m	2m	3m	4m
80A	0.59	1.01	1.31	1.59	1.82	2.6	3.12	3.56	3.92	4.3	1.27	2.27	3.27	4.27	5.27	300	270	285	285	300	295	283	293	294	300
80B	0.34	0.78	1.17	1.5	1.76	2.45	3.1	3.53	3.92	4.32	0.51	1.51	2.51	3.51	4.51	270	285	285	285	300	269	278	284	288	296
80C	0	0.35	0.82	1.25	1.63	0	2.56	3.34	3.92	4.32	0	0.53	1.53	2.53	3.53	270	285	270	300	300		281	282	296	297
80D	0	0.23	0.71	1.17	1.6	0	2.2	3.35	4	4.47	0	0.31	1.31	2.31	3.31	270	285	270	300	300		293	289	298	298
80E	0	0.13	0.62	1.06	1.48	0	2.11	3.13	3.85	4.33	0	0.26	1.26	2.26	3.26	270	315	270	300	300		290	283	293	296
81A	0	0.14	0.6	1.04	1.46	0	2.01	3.04	3.78	4.3	0	0.27	1.27	2.27	3.27	270	285	270	300	300		281	282	294	296
81B	0	0.16	0.63	1.07	1.49	0	2.03	3.11	3.83	4.35	0	0.3	1.3	2.3	3.3	270	285	270	300	300		285	285	298	299
81C	0	0.18	0.65	1.11	1.53	0	2.2	3.29	3.93	4.39	0	0.31	1.31	2.31	3.31	270	285	270	300	300		296	293	303	302
81D	0	0.51	0.99	1.41	1.75	0	3.08	3.67	4.06	4.43	0	0.76	1.76	2.76	3.76	270	285	285	285	300		302	300	298	300
81E	0.78	1.15	1.47	1.71	1.9	3.18	3.62	3.9	4.15	4.41	1.56	2.56	3.56	4.56	5.56	285	285	285	300	300	299	300	298	301	299

no_slow

Point	Hs [m]					Tmm10 [s]					Water Depth [m]					Wind Direction [deg]					Wave Direction [deg]				
Design WL	0m	1m	2m	3m	4m	0m	1m	2m	3m	4m	0m	1m	2m	3m	4m	0m	1m	2m	3m	4m	0m	1m	2m	3m	4m
80A	0.6	1	1.32	1.61	1.84	2.56	3.16	3.59	3.95	4.29	1.29	2.29	3.29	4.29	5.29	285	285	285	300	300	289	292	296	302	301
80B	0.57	0.97	1.3	1.61	1.84	2.46	3.12	3.58	3.98	4.32	1.23	2.23	3.23	4.23	5.23	270	285	285	300	300	280	290	295	301	301
80C	0.53	0.94	1.28	1.58	1.84	2.36	3.02	3.56	3.97	4.34	1.12	2.12	3.12	4.12	5.12	270	270	285	300	300	278	281	294	301	301
80D	0.51	0.92	1.27	1.59	1.87	2.25	2.97	3.55	4.01	4.41	1.14	2.14	3.14	4.14	5.14	270	270	285	300	300	272	277	291	299	300
80E	0.36	0.8	1.17	1.52	1.84	1.96	2.83	3.5	4	4.44	0.75	1.75	2.75	3.75	4.75	270	270	285	300	300	273	277	291	299	300
81A	0.28	0.73	1.12	1.48	1.81	1.79	2.75	3.46	3.98	4.43	0.59	1.59	2.59	3.59	4.59	270	270	285	300	300	275	279	292	300	301
81B	0.2	0.66	1.07	1.44	1.79	1.58	2.69	3.45	3.97	4.41	0.47	1.47	2.47	3.47	4.47	270	270	285	300	300	279	286	297	305	304
81C	0.25	0.7	1.11	1.48	1.79	1.88	2.88	3.57	4	4.41	0.57	1.57	2.57	3.57	4.57	315	285	285	285	300	322	307	305	303	306
81D	0.3	0.78	1.2	1.55	1.84	2.47	3.28	3.73	4.09	4.42	0.57	1.57	2.57	3.57	4.57	315	300	285	300	300	309	307	302	304	302
81E	0.67	1.04	1.39	1.69	1.9	2.62	3.37	3.8	4.12	4.4	1.63	2.63	3.63	4.63	5.63	285	285	285	300	300	297	301	299	301	300

no2_slow

Point	Hs [m]					Tmm10 [s]					Water Depth [m]					Wind Direction [deg]					Wave Direction [deg]				
Design WL	0m	1m	2m	3m	4m	0m	1m	2m	3m	4m	0m	1m	2m	3m	4m	0m	1m	2m	3m	4m	0m	1m	2m	3m	4m
80A	0.43	0.85	1.24	1.56	1.8	2.29	3.05	3.53	3.91	4.28	0.88	1.88	2.88	3.88	4.88	270	285	285	285	300	278	287	291	293	299
80B	0.38	0.81	1.2	1.52	1.79	2.18	2.96	3.48	3.93	4.3	0.78	1.78	2.78	3.78	4.78	270	285	285	300	300	278	286	290	298	299
80C	0.32	0.77	1.15	1.49	1.77	2.03	2.84	3.42	3.9	4.31	0.67	1.67	2.67	3.67	4.67	270	270	285	300	300	278	278	289	298	299
80D	0.31	0.75	1.13	1.46	1.78	1.86	2.72	3.34	3.9	4.35	0.69	1.69	2.69	3.69	4.69	270	270	270	300	300	272	274	279	297	298
80E	0.14	0.61	1.02	1.37	1.72	1.54	2.51	3.24	3.87	4.37	0.3	1.3	2.3	3.3	4.3	270	270	270	300	300	272	275	279	298	298
81A	0.07	0.54	0.96	1.34	1.69	1.42	2.39	3.19	3.81	4.36	0.14	1.14	2.14	3.14	4.14	270	270	270	285	300	272	277	281	292	300
81B	0	0.46	0.9	1.28	1.65	0	2.25	3.16	3.82	4.33	0	1.02	2.02	3.02	4.02	270	270	270	300	300		284	288	304	304
81C	0.06	0.49	0.93	1.32	1.68	1.46	2.58	3.36	3.91	4.36	0.12	1.12	2.12	3.12	4.12	270	315	300	300	300	289	321	313	310	307
81D	0.08	0.58	1.03	1.42	1.75	1.47	3.06	3.66	4.05	4.4	0.12	1.12	2.12	3.12	4.12	270	285	300	300	300	288	303	307	305	303
81E	0.53	0.96	1.34	1.65	1.88	2.65	3.44	3.87	4.17	4.43	1.1	2.1	3.1	4.1	5.1	300	285	285	300	300	305	304	303	303	301

nour_slow

Point	Hs [m]					Tmm10 [s]					Water Depth [m]					Wind Direction [deg]					Wave Direction [deg]				
Design WL	0m	1m	2m	3m	4m	0m	1m	2m	3m	4m	0m	1m	2m	3m	4m	0m	1m	2m	3m	4m	0m	1m	2m	3m	4m
80A	0.59	1	1.3	1.58	1.82	2.59	3.11	3.52	3.91	4.3	1.25	2.25	3.25	4.25	5.25	300	270	270	285	300	295	283	286	294	300
80B	0.33	0.78	1.16	1.5	1.76	2.43	3.1	3.53	3.92	4.31	0.49	1.49	2.49	3.49	4.49	270	285	285	285	300	269	278	284	288	296
80C	0	0.34	0.82	1.24	1.63	0	2.54	3.33	3.91	4.32	0	0.51	1.51	2.51	3.51	270	285	270	300	300		281	282	296	297
80D	0	0.21	0.71	1.16	1.6	0	2.02	3.33	3.99	4.47	0	0.29	1.29	2.29	3.29	270	285	270	300	300		293	289	298	298
80E	0	0.13	0.61	1.06	1.47	0	1.92	3.12	3.85	4.33	0	0.24	1.24	2.24	3.24	270	285	270	300	300		282	283	293	296
81A	0	0.13	0.6	1.04	1.46	0	1.99	3.03	3.77	4.3	0	0.25	1.25	2.25	3.25	270	285	270	300	300		281	282	294	296
81B	0	0.15	0.62	1.06	1.49	0	2.02	3.09	3.83	4.35	0	0.28	1.28	2.28	3.28	270	285	270	300	300		284	285	298	299
81C	0	0.17	0.64	1.1	1.53	0	2.12	3.28	3.91	4.39	0	0.29	1.29	2.29	3.29	270	285	270	285	300		296	294	298	302
81D	0	0.5	0.98	1.41	1.75	0	3.07	3.67	4.06	4.42	0	0.74	1.74	2.74	3.74	270	285	285	285	300		302	300	298	300
81E	0.78	1.14	1.45	1.71	1.9	3.17	3.61	3.9	4.15	4.41	1.54	2.54	3.54	4.54	5.54	285	285	300	300	300	299	300	302	301	299

no_fast 2030

Point	Hs [m]					Tmm10 [s]					Water Depth [m]					Wind Direction [deg]					Wave Direction [deg]				
Design WL	0m	1m	2m	3m	4m	0m	1m	2m	3m	4m	0m	1m	2m	3m	4m	0m	1m	2m	3m	4m	0m	1m	2m	3m	4m
80A	0.71	1.08	1.4	1.66	1.9	2.71	3.22	3.61	3.97	4.3	1.54	2.54	3.54	4.54	5.54	285	300	285	300	300	290	300	296	302	301
80B	0.67	1.05	1.37	1.66	1.9	2.63	3.19	3.64	4	4.32	1.48	2.48	3.48	4.48	5.48	285	285	300	300	300	287	292	301	301	301
80C	0.63	1.01	1.35	1.64	1.91	2.51	3.14	3.62	4	4.35	1.37	2.37	3.37	4.37	5.37	270	285	300	300	300	278	291	301	301	301
80D	0.62	1.01	1.34	1.66	1.95	2.43	3.08	3.63	4.06	4.43	1.39	2.39	3.39	4.39	5.39	270	270	300	300	300	273	278	299	300	300
80E	0.47	0.9	1.27	1.6	1.92	2.2	2.97	3.55	4.07	4.46	1	2	3	4	5	270	270	270	300	300	274	278	283	300	300
81A	0.4	0.83	1.22	1.56	1.89	2.04	2.92	3.52	4.05	4.45	0.84	1.84	2.84	3.84	4.84	270	270	270	300	300	276	280	283	301	301
81B	0.32	0.77	1.17	1.53	1.87	1.85	2.88	3.55	4.03	4.43	0.71	1.71	2.71	3.71	4.71	270	270	285	300	300	281	287	297	305	304
81C	0.36	0.81	1.21	1.56	1.87	2.19	3.05	3.64	4.03	4.42	0.82	1.82	2.82	3.82	4.82	315	285	285	285	300	322	307	305	302	306
81D	0.42	0.89	1.29	1.63	1.91	2.73	3.38	3.78	4.09	4.44	0.82	1.82	2.82	3.82	4.82	315	300	285	285	300	310	307	301	298	301
81E	0.76	1.13	1.48	1.75	1.97	2.83	3.45	3.84	4.12	4.42	1.87	2.87	3.87	4.87	5.87	285	285	285	285	300	299	300	298	296	300

no2_fast

Point	Hs [m]					Tmm10 [s]					Water Depth [m]					Wind Direction [deg]					Wave Direction [deg]				
Design WL	0m	1m	2m	3m	4m	0m	1m	2m	3m	4m	0m	1m	2m	3m	4m	0m	1m	2m	3m	4m	0m	1m	2m	3m	4m
80A	0.53	0.95	1.31	1.6	1.86	2.46	3.14	3.58	3.95	4.28	1.12	2.12	3.12	4.12	5.12	270	285	285	300	300	278	288	292	300	299
80B	0.49	0.9	1.27	1.58	1.85	2.38	3.06	3.54	3.96	4.3	1.03	2.03	3.03	4.03	5.03	270	285	285	300	300	278	287	291	299	299
80C	0.44	0.87	1.23	1.55	1.84	2.25	2.96	3.5	3.95	4.32	0.92	1.92	2.92	3.92	4.92	270	270	285	300	300	278	279	291	299	299
80D	0.42	0.84	1.21	1.54	1.85	2.1	2.86	3.43	3.97	4.37	0.94	1.94	2.94	3.94	4.94	270	270	270	300	300	272	275	280	298	298
80E	0.26	0.72	1.12	1.46	1.81	1.77	2.7	3.36	3.96	4.4	0.55	1.55	2.55	3.55	4.55	270	270	270	300	300	272	276	280	298	298
81A	0.18	0.65	1.06	1.41	1.77	1.6	2.6	3.33	3.93	4.39	0.39	1.39	2.39	3.39	4.39	270	270	270	300	300	274	278	282	300	300
81B	0.11	0.58	1	1.37	1.74	1.44	2.51	3.31	3.91	4.37	0.26	1.26	2.26	3.26	4.26	270	270	270	300	300	278	285	288	305	304
81C	0.15	0.62	1.03	1.41	1.76	1.67	2.73	3.49	3.98	4.38	0.37	1.37	2.37	3.37	4.37	315	285	300	300	300	323	308	312	310	307
81D	0.21	0.69	1.13	1.5	1.83	2.19	3.21	3.74	4.09	4.44	0.37	1.37	2.37	3.37	4.37	300	285	300	300	300	306	303	307	304	302
81E	0.65	1.05	1.42	1.71	1.95	2.88	3.53	3.91	4.18	4.45	1.35	2.35	3.35	4.35	5.35	285	285	285	300	300	302	304	302	303	301

nour_fast

Point	Hs [m]					Tmm10 [s]					Water Depth [m]					Wind Direction [deg]					Wave Direction [deg]				
Design WL	0m	1m	2m	3m	4m	0m	1m	2m	3m	4m	0m	1m	2m	3m	4m	0m	1m	2m	3m	4m	0m	1m	2m	3m	4m
80A	0.68	1.06	1.35	1.61	1.84	2.74	3.16	3.58	3.95	4.31	1.47	2.47	3.47	4.47	5.47	300	270	285	300	300	295	283	293	300	300
80B	0.4	0.85	1.22	1.53	1.79	2.54	3.11	3.57	3.98	4.32	0.64	1.64	2.64	3.64	4.64	270	270	285	300	300	271	274	286	295	297
80C	0	0.47	0.91	1.33	1.7	0	2.7	3.47	3.96	4.34	0	0.79	1.79	2.79	3.79	270	270	300	300	300		276	295	297	298
80D	0	0.37	0.85	1.29	1.7	0	2.53	3.45	4.03	4.49	0	0.63	1.63	2.63	3.63	270	270	270	285	300		287	288	293	298
80E	0	0.3	0.76	1.19	1.58	0	2.3	3.31	3.91	4.38	0	0.5	1.5	2.5	3.5	270	270	270	285	300		287	286	291	296
81A	0	0.28	0.72	1.15	1.56	0	2.18	3.25	3.91	4.37	0	0.47	1.47	2.47	3.47	270	270	270	300	300		288	286	296	297
81B	0	0.31	0.74	1.17	1.59	0	2.22	3.27	3.93	4.41	0	0.52	1.52	2.52	3.52	270	270	270	300	300		289	287	298	299
81C	0	0.33	0.79	1.24	1.63	0	2.43	3.43	3.98	4.41	0	0.55	1.55	2.55	3.55	270	270	270	285	300		295	294	298	302
81D	0	0.64	1.11	1.5	1.82	0	3.23	3.75	4.13	4.45	0	1.09	2.09	3.09	4.09	270	285	285	300	300		302	300	302	300
81E	0.82	1.2	1.51	1.74	1.92	3.28	3.64	3.93	4.17	4.42	1.61	2.61	3.61	4.61	5.61	285	300	285	300	300	299	303	297	300	299

no_slow

Point	Hs [m]					Tmm10 [s]					Water Depth [m]					Wind Direction [deg]					Wave Direction [deg]				
Design WL	0m	1m	2m	3m	4m	0m	1m	2m	3m	4m	0m	1m	2m	3m	4m	0m	1m	2m	3m	4m	0m	1m	2m	3m	4m
80A	0.66	1.04	1.36	1.64	1.89	2.64	3.19	3.61	3.96	4.29	1.42	2.42	3.42	4.42	5.42	285	285	300	300	300	290	293	302	302	301
80B	0.63	1.01	1.34	1.63	1.89	2.57	3.16	3.62	3.99	4.32	1.36	2.36	3.36	4.36	5.36	285	285	300	300	300	286	291	301	301	301
80C	0.58	0.98	1.32	1.61	1.89	2.45	3.07	3.6	3.99	4.34	1.25	2.25	3.25	4.25	5.25	270	270	300	300	300	278	282	301	301	301
80D	0.57	0.97	1.3	1.63	1.92	2.35	3.03	3.6	4.04	4.41	1.27	2.27	3.27	4.27	5.27	270	270	285	300	300	272	277	292	300	300
80E	0.42	0.85	1.22	1.56	1.89	2.09	2.91	3.56	4.04	4.44	0.88	1.88	2.88	3.88	4.88	270	270	285	300	300	273	278	291	299	300
81A	0.34	0.79	1.17	1.52	1.86	1.93	2.84	3.52	4.02	4.44	0.72	1.72	2.72	3.72	4.72	270	270	285	300	300	275	280	292	301	301
81B	0.27	0.72	1.12	1.49	1.83	1.72	2.79	3.52	4.01	4.41	0.6	1.6	2.6	3.6	4.6	270	270	285	300	300	280	287	297	305	304
81C	0.31	0.76	1.16	1.53	1.84	2.06	2.97	3.62	4.01	4.41	0.7	1.7	2.7	3.7	4.7	315	285	285	285	300	322	307	305	302	306
81D	0.37	0.84	1.24	1.6	1.89	2.62	3.34	3.78	4.07	4.43	0.7	1.7	2.7	3.7	4.7	315	300	300	285	300	310	307	306	299	302
81E	0.72	1.09	1.43	1.73	1.95	2.73	3.41	3.83	4.11	4.42	1.76	2.76	3.76	4.76	5.76	285	285	285	285	300	298	301	299	297	300

no2_slow

Point	Hs [m]					Tmm10 [s]					Water Depth [m]					Wind Direction [deg]					Wave Direction [deg]				
Design WL	0m	1m	2m	3m	4m	0m	1m	2m	3m	4m	0m	1m	2m	3m	4m	0m	1m	2m	3m	4m	0m	1m	2m	3m	4m
80A	0.48	0.9	1.28	1.59	1.84	2.38	3.1	3.56	3.92	4.28	1.01	2.01	3.01	4.01	5.01	270	285	285	285	300	278	288	292	293	299
80B	0.44	0.86	1.24	1.55	1.83	2.3	3.02	3.52	3.95	4.29	0.91	1.91	2.91	3.91	4.91	270	285	285	300	300	278	287	291	298	299
80C	0.38	0.82	1.2	1.52	1.82	2.15	2.9	3.47	3.93	4.31	0.8	1.8	2.8	3.8	4.8	270	270	285	300	300	278	278	290	299	299
80D	0.37	0.8	1.17	1.5	1.82	1.99	2.79	3.39	3.94	4.36	0.82	1.82	2.82	3.82	4.82	270	270	270	300	300	272	274	279	298	298
80E	0.2	0.67	1.07	1.42	1.77	1.65	2.62	3.31	3.92	4.38	0.43	1.43	2.43	3.43	4.43	270	270	270	300	300	272	276	280	298	298
81A	0.13	0.6	1.01	1.37	1.74	1.5	2.51	3.27	3.89	4.37	0.27	1.27	2.27	3.27	4.27	270	270	270	300	300	273	278	282	300	300
81B	0.07	0.52	0.95	1.33	1.7	1.4	2.4	3.25	3.87	4.34	0.15	1.15	2.15	3.15	4.15	270	270	270	300	300	275	285	288	304	304
81C	0.11	0.55	0.98	1.37	1.72	1.56	2.7	3.43	3.95	4.37	0.25	1.25	2.25	3.25	4.25	315	315	300	300	300	326	321	313	310	307
81D	0.16	0.64	1.08	1.46	1.8	1.94	3.14	3.7	4.07	4.43	0.25	1.25	2.25	3.25	4.25	270	285	300	300	300	293	303	307	305	303
81E	0.6	1.01	1.38	1.68	1.93	2.78	3.49	3.89	4.18	4.45	1.23	2.23	3.23	4.23	5.23	285	285	285	300	300	301	304	302	303	301

nour_slow

Point	Hs [m]					Tmm10 [s]					Water Depth [m]					Wind Direction [deg]					Wave Direction [deg]				
Design WL	0m	1m	2m	3m	4m	0m	1m	2m	3m	4m	0m	1m	2m	3m	4m	0m	1m	2m	3m	4m	0m	1m	2m	3m	4m
80A	0.64	1.03	1.33	1.59	1.83	2.68	3.15	3.57	3.94	4.3	1.37	2.37	3.37	4.37	5.37	300	270	285	300	300	295	283	293	299	300
80B	0.35	0.81	1.19	1.51	1.77	2.47	3.09	3.55	3.97	4.32	0.55	1.55	2.55	3.55	4.55	270	270	285	300	300	271	274	285	294	297
80C	0	0.43	0.87	1.3	1.67	0	2.62	3.43	3.95	4.34	0	0.69	1.69	2.69	3.69	270	270	300	300	300		275	295	297	297
80D	0	0.33	0.81	1.25	1.66	0	2.43	3.4	4	4.48	0	0.54	1.54	2.54	3.54	270	270	270	285	300		286	288	293	298
80E	0	0.26	0.71	1.15	1.54	0	2.19	3.25	3.88	4.36	0	0.4	1.4	2.4	3.4	270	270	270	285	300		288	286	291	296
81A	0	0.24	0.68	1.12	1.52	0	2.06	3.18	3.86	4.36	0	0.38	1.38	2.38	3.38	270	270	270	285	300		288	286	291	297
81B	0	0.27	0.7	1.14	1.55	0	2.09	3.2	3.87	4.39	0	0.43	1.43	2.43	3.43	270	270	270	285	300		288	287	293	299
81C	0	0.29	0.75	1.2	1.6	0	2.31	3.38	3.95	4.4	0	0.46	1.46	2.46	3.46	270	270	270	285	300		295	294	298	302
81D	0	0.6	1.07	1.47	1.8	0	3.17	3.72	4.11	4.44	0	1	2	3	4	270	285	285	300	300		302	301	302	301
81E	0.78	1.16	1.49	1.73	1.91	3.24	3.64	3.92	4.16	4.42	1.52	2.52	3.52	4.52	5.52	285	285	285	300	300	298	300	298	300	299

no_fast 2040

Point	Hs [m]					Tmm10 [s]					Water Depth [m]					Wind Direction [deg]					Wave Direction [deg]				
Design WL	0m	1m	2m	3m	4m	0m	1m	2m	3m	4m	0m	1m	2m	3m	4m	0m	1m	2m	3m	4m	0m	1m	2m	3m	4m
80A	0.79	1.14	1.44	1.69	1.93	2.8	3.27	3.64	3.99	4.31	1.75	2.75	3.75	4.75	5.75	285	300	285	300	300	291	301	296	302	302
80B	0.75	1.11	1.42	1.69	1.93	2.73	3.25	3.67	4.02	4.33	1.68	2.68	3.68	4.68	5.68	285	300	300	300	300	288	300	302	301	301
80C	0.72	1.08	1.4	1.68	1.94	2.62	3.21	3.67	4.03	4.36	1.58	2.58	3.58	4.58	5.58	270	285	300	300	300	278	292	302	302	301
80D	0.71	1.07	1.4	1.71	1.98	2.55	3.19	3.69	4.09	4.44	1.6	2.6	3.6	4.6	5.6	270	285	300	300	300	273	289	300	301	300
80E	0.57	0.98	1.33	1.66	1.96	2.37	3.08	3.64	4.11	4.48	1.21	2.21	3.21	4.21	5.21	270	270	285	300	300	274	279	292	300	300
81A	0.49	0.92	1.28	1.63	1.94	2.24	3.04	3.63	4.1	4.47	1.05	2.05	3.05	4.05	5.05	270	270	285	300	300	276	281	293	301	301
81B	0.42	0.85	1.24	1.59	1.92	2.09	3.01	3.63	4.08	4.45	0.92	1.92	2.92	3.92	4.92	270	270	285	300	300	283	288	297	305	304
81C	0.45	0.89	1.28	1.62	1.91	2.41	3.18	3.7	4.06	4.43	1.03	2.03	3.03	4.03	5.03	315	285	285	285	300	321	306	304	302	305
81D	0.53	0.97	1.37	1.68	1.94	2.86	3.45	3.82	4.11	4.44	1.03	2.03	3.03	4.03	5.03	300	300	285	285	300	306	307	300	298	301
81E	0.84	1.2	1.53	1.78	1.99	2.97	3.51	3.88	4.14	4.42	2.08	3.08	4.08	5.08	6.08	285	285	285	285	300	299	300	298	296	299

no2_fast

Point	Hs [m]					Tmm10 [s]					Water Depth [m]					Wind Direction [deg]					Wave Direction [deg]				
Design WL	0m	1m	2m	3m	4m	0m	1m	2m	3m	4m	0m	1m	2m	3m	4m	0m	1m	2m	3m	4m	0m	1m	2m	3m	4m
80A	0.62	1.03	1.37	1.64	1.89	2.61	3.19	3.61	3.97	4.29	1.33	2.33	3.33	4.33	5.33	285	285	285	300	300	286	289	293	300	300
80B	0.58	0.98	1.33	1.62	1.88	2.5	3.12	3.58	3.98	4.31	1.23	2.23	3.23	4.23	5.23	270	285	285	300	300	278	288	292	299	299
80C	0.53	0.95	1.3	1.6	1.88	2.4	3.04	3.55	3.98	4.34	1.13	2.13	3.13	4.13	5.13	270	270	285	300	300	278	279	292	300	300
80D	0.52	0.92	1.27	1.59	1.9	2.27	2.96	3.53	4.01	4.4	1.15	2.15	3.15	4.15	5.15	270	270	285	300	300	272	276	289	299	299
80E	0.36	0.8	1.18	1.53	1.87	1.97	2.83	3.48	4.02	4.44	0.76	1.76	2.76	3.76	4.76	270	270	285	300	300	273	277	289	299	299
81A	0.28	0.74	1.12	1.49	1.84	1.8	2.76	3.44	4	4.43	0.6	1.6	2.6	3.6	4.6	270	270	285	300	300	275	279	291	300	300
81B	0.21	0.67	1.07	1.45	1.8	1.59	2.7	3.43	3.98	4.4	0.47	1.47	2.47	3.47	4.47	270	270	285	300	300	280	286	297	305	304
81C	0.25	0.7	1.11	1.48	1.81	1.9	2.9	3.58	4.03	4.41	0.58	1.58	2.58	3.58	4.58	315	300	300	300	300	323	314	312	309	306
81D	0.31	0.78	1.21	1.57	1.87	2.48	3.32	3.77	4.08	4.45	0.58	1.58	2.58	3.58	4.58	300	300	285	285	300	305	307	302	299	302
81E	0.74	1.13	1.48	1.75	1.97	3.03	3.57	3.94	4.17	4.45	1.55	2.55	3.55	4.55	5.55	285	285	285	285	300	302	304	301	298	300

nour_fast

Point	Hs [m]					Tmm10 [s]					Water Depth [m]					Wind Direction [deg]					Wave Direction [deg]				
Design WL	0m	1m	2m	3m	4m	0m	1m	2m	3m	4m	0m	1m	2m	3m	4m	0m	1m	2m	3m	4m	0m	1m	2m	3m	4m
80A	0.76	1.1	1.39	1.66	1.89	2.79	3.22	3.61	3.95	4.31	1.65	2.65	3.65	4.65	5.65	285	285	285	285	300	289	291	293	294	300
80B	0.47	0.91	1.27	1.57	1.84	2.63	3.14	3.6	4	4.32	0.81	1.81	2.81	3.81	4.81	270	270	285	300	300	272	276	287	296	297
80C	0	0.57	1.01	1.41	1.77	0	2.84	3.56	4	4.36	0	1.03	2.03	3.03	4.03	270	270	300	300	300		278	296	297	298
80D	0	0.5	0.95	1.37	1.77	0	2.7	3.53	4.08	4.5	0	0.89	1.89	2.89	3.89	270	270	270	300	300		285	287	298	299
80E	0	0.42	0.87	1.28	1.67	0	2.58	3.43	3.99	4.4	0	0.75	1.75	2.75	3.75	270	270	270	300	300		288	287	297	297
81A	0	0.39	0.83	1.25	1.65	0	2.48	3.38	3.98	4.41	0	0.7	1.7	2.7	3.7	270	270	270	300	300		288	286	296	297
81B	0	0.41	0.85	1.26	1.67	0	2.49	3.4	4	4.43	0	0.74	1.74	2.74	3.74	270	270	270	300	300		290	287	299	299
81C	0	0.45	0.91	1.33	1.71	0	2.72	3.54	4.02	4.43	0	0.81	1.81	2.81	3.81	270	270	270	285	300		294	294	298	301
81D	0.26	0.75	1.2	1.59	1.89	2.45	3.34	3.8	4.12	4.47	0.36	1.36	2.36	3.36	4.36	270	300	285	285	300	296	305	300	297	300
81E	0.86	1.24	1.55	1.78	1.97	3.34	3.66	3.95	4.15	4.43	1.66	2.66	3.66	4.66	5.66	285	285	285	285	300	298	298	297	295	299

no_slow

Point	Hs [m]					Tmm10 [s]					Water Depth [m]					Wind Direction [deg]					Wave Direction [deg]				
Design WL	0m	1m	2m	3m	4m	0m	1m	2m	3m	4m	0m	1m	2m	3m	4m	0m	1m	2m	3m	4m	0m	1m	2m	3m	4m
80A	0.77	1.12	1.43	1.68	1.92	2.78	3.26	3.63	3.98	4.31	1.69	2.69	3.69	4.69	5.69	285	300	285	300	300	290	301	296	302	301
80B	0.73	1.1	1.41	1.68	1.92	2.7	3.23	3.66	4.01	4.33	1.62	2.62	3.62	4.62	5.62	285	300	300	300	300	287	300	302	301	301
80C	0.69	1.06	1.39	1.67	1.93	2.59	3.19	3.66	4.02	4.36	1.52	2.52	3.52	4.52	5.52	270	285	300	300	300	278	292	302	302	301
80D	0.68	1.06	1.38	1.69	1.97	2.52	3.13	3.67	4.08	4.44	1.54	2.54	3.54	4.54	5.54	270	270	300	300	300	273	279	300	300	300
80E	0.54	0.95	1.31	1.64	1.95	2.32	3.05	3.63	4.1	4.47	1.15	2.15	3.15	4.15	5.15	270	270	285	300	300	274	279	292	300	300
81A	0.46	0.89	1.26	1.61	1.93	2.19	3	3.61	4.09	4.47	0.99	1.99	2.99	3.99	4.99	270	270	285	300	300	276	281	293	301	301
81B	0.39	0.83	1.22	1.57	1.91	2.02	2.98	3.61	4.07	4.45	0.86	1.86	2.86	3.86	4.86	270	270	285	300	300	282	288	297	305	304
81C	0.43	0.87	1.26	1.61	1.9	2.35	3.15	3.69	4.05	4.43	0.97	1.97	2.97	3.97	4.97	315	285	285	285	300	322	306	305	302	305
81D	0.5	0.95	1.35	1.67	1.93	2.81	3.43	3.81	4.1	4.44	0.96	1.96	2.96	3.96	4.96	300	300	285	285	300	306	307	301	298	301
81E	0.82	1.18	1.52	1.78	1.98	2.93	3.49	3.87	4.13	4.42	2.02	3.02	4.02	5.02	6.02	285	285	285	285	300	299	300	298	296	299

no2_slow

Point	Hs [m]					Tmm10 [s]					Water Depth [m]					Wind Direction [deg]					Wave Direction [deg]				
Design WL	0m	1m	2m	3m	4m	0m	1m	2m	3m	4m	0m	1m	2m	3m	4m	0m	1m	2m	3m	4m	0m	1m	2m	3m	4m
80A	0.54	0.95	1.32	1.61	1.86	2.47	3.15	3.58	3.95	4.28	1.14	2.14	3.14	4.14	5.14	270	285	285	300	300	278	289	292	300	299
80B	0.5	0.91	1.28	1.58	1.85	2.39	3.07	3.54	3.96	4.3	1.04	2.04	3.04	4.04	5.04	270	285	285	300	300	278	287	291	299	299
80C	0.44	0.87	1.24	1.55	1.85	2.27	2.96	3.5	3.95	4.32	0.94	1.94	2.94	3.94	4.94	270	270	285	300	300	278	279	291	299	299
80D	0.43	0.85	1.22	1.54	1.86	2.11	2.87	3.44	3.97	4.37	0.96	1.96	2.96	3.96	4.96	270	270	270	300	300	272	275	280	298	298
80E	0.27	0.72	1.12	1.46	1.81	1.78	2.71	3.37	3.96	4.41	0.56	1.56	2.56	3.56	4.56	270	270	270	300	300	273	276	280	298	298
81A	0.19	0.65	1.06	1.42	1.78	1.61	2.62	3.33	3.94	4.4	0.41	1.41	2.41	3.41	4.41	270	270	270	300	300	274	278	282	300	300
81B	0.12	0.58	1	1.38	1.74	1.45	2.52	3.32	3.91	4.37	0.28	1.28	2.28	3.28	4.28	270	270	270	300	300	278	285	288	305	304
81C	0.16	0.62	1.04	1.41	1.76	1.68	2.74	3.5	3.98	4.39	0.39	1.39	2.39	3.39	4.39	315	285	300	300	300	323	308	312	310	307
81D	0.22	0.7	1.13	1.5	1.83	2.21	3.22	3.74	4.09	4.44	0.38	1.38	2.38	3.38	4.38	300	285	300	300	300	305	303	307	304	302
81E	0.65	1.06	1.43	1.71	1.95	2.89	3.53	3.91	4.18	4.45	1.36	2.36	3.36	4.36	5.36	285	285	285	300	300	302	304	302	302	301

nour_slow

Point	Hs [m]					Tmm10 [s]					Water Depth [m]					Wind Direction [deg]					Wave Direction [deg]				
Design WL	0m	1m	2m	3m	4m	0m	1m	2m	3m	4m	0m	1m	2m	3m	4m	0m	1m	2m	3m	4m	0m	1m	2m	3m	4m
80A	0.68	1.07	1.36	1.61	1.87	2.75	3.17	3.59	3.95	4.3	1.48	2.48	3.48	4.48	5.48	300	270	285	300	300	295	283	293	300	300
80B	0.39	0.84	1.22	1.54	1.81	2.53	3.11	3.57	3.98	4.31	0.64	1.64	2.64	3.64	4.64	270	270	285	300	300	272	275	286	295	297
80C	0	0.49	0.93	1.35	1.72	0	2.72	3.49	3.98	4.35	0	0.86	1.86	2.86	3.86	270	270	300	300	300		276	295	297	297
80D	0	0.42	0.88	1.31	1.72	0	2.54	3.45	4.03	4.48	0	0.72	1.72	2.72	3.72	270	270	270	285	300		283	287	293	298
80E	0	0.34	0.79	1.22	1.61	0	2.38	3.35	3.94	4.38	0	0.58	1.58	2.58	3.58	270	270	270	285	300		288	287	292	297
81A	0	0.31	0.76	1.19	1.59	0	2.27	3.29	3.92	4.39	0	0.53	1.53	2.53	3.53	270	270	270	285	300		288	287	292	297
81B	0	0.33	0.78	1.2	1.61	0	2.29	3.29	3.93	4.4	0	0.57	1.57	2.57	3.57	270	270	270	285	300		289	288	293	299
81C	0	0.37	0.83	1.27	1.66	0	2.53	3.47	3.99	4.42	0	0.64	1.64	2.64	3.64	270	270	270	285	300		294	294	298	302
81D	0	0.67	1.14	1.52	1.86	0	3.24	3.75	4.13	4.46	0	1.19	2.19	3.19	4.19	270	285	285	300	300		302	300	302	300
81E	0.79	1.18	1.51	1.74	1.96	3.28	3.65	3.94	4.17	4.43	1.49	2.49	3.49	4.49	5.49	285	285	285	300	300	298	299	297	300	299

no_fast 2050

Point	Hs [m]					Tmm10 [s]					Water Depth [m]					Wind Direction [deg]					Wave Direction [deg]				
Design WL	0m	1m	2m	3m	4m	0m	1m	2m	3m	4m	0m	1m	2m	3m	4m	0m	1m	2m	3m	4m	0m	1m	2m	3m	4m
80A	0.86	1.19	1.47	1.72	1.95	2.88	3.31	3.68	4	4.32	1.95	2.95	3.95	4.95	5.95	300	300	300	300	300	299	302	303	302	302
80B	0.83	1.17	1.46	1.72	1.95	2.81	3.3	3.69	4.04	4.34	1.89	2.89	3.89	4.89	5.89	285	300	300	300	300	289	301	302	302	301
80C	0.79	1.14	1.45	1.72	1.97	2.74	3.29	3.71	4.05	4.37	1.78	2.78	3.78	4.78	5.78	285	300	300	300	300	287	301	302	302	302
80D	0.79	1.14	1.46	1.75	2.01	2.66	3.25	3.73	4.12	4.45	1.8	2.8	3.8	4.8	5.8	270	285	300	300	300	274	290	301	301	301
80E	0.65	1.04	1.39	1.71	2	2.51	3.19	3.7	4.14	4.49	1.41	2.41	3.41	4.41	5.41	270	285	285	300	300	275	289	293	301	300
81A	0.58	0.99	1.36	1.69	1.98	2.41	3.12	3.7	4.14	4.49	1.25	2.25	3.25	4.25	5.25	270	270	285	300	300	277	281	294	301	301
81B	0.51	0.93	1.32	1.66	1.96	2.3	3.13	3.7	4.12	4.47	1.13	2.13	3.13	4.13	5.13	270	285	285	300	300	284	296	298	305	304
81C	0.55	0.97	1.35	1.68	1.97	2.53	3.29	3.76	4.09	4.4	1.23	2.23	3.23	4.23	5.23	300	300	285	285	285	315	312	304	301	299
81D	0.63	1.05	1.43	1.73	1.99	3	3.49	3.86	4.12	4.41	1.23	2.23	3.23	4.23	5.23	300	300	285	285	285	307	307	299	297	295
81E	0.92	1.27	1.58	1.82	2.03	3.09	3.54	3.91	4.15	4.39	2.29	3.29	4.29	5.29	6.29	285	285	285	285	285	300	299	297	295	294

no2_fast

Point	Hs [m]					Tmm10 [s]					Water Depth [m]					Wind Direction [deg]					Wave Direction [deg]				
Design WL	0m	1m	2m	3m	4m	0m	1m	2m	3m	4m	0m	1m	2m	3m	4m	0m	1m	2m	3m	4m	0m	1m	2m	3m	4m
80A	0.71	1.1	1.42	1.67	1.91	2.72	3.23	3.63	3.98	4.3	1.54	2.54	3.54	4.54	5.54	285	285	285	300	300	286	290	293	300	300
80B	0.66	1.05	1.38	1.66	1.91	2.63	3.18	3.64	4	4.32	1.44	2.44	3.44	4.44	5.44	285	285	300	300	300	285	289	299	300	300
80C	0.62	1.02	1.36	1.65	1.91	2.52	3.09	3.6	4.01	4.35	1.33	2.33	3.33	4.33	5.33	270	270	285	300	300	277	280	292	300	300
80D	0.61	0.99	1.33	1.65	1.94	2.41	3.03	3.62	4.05	4.42	1.35	2.35	3.35	4.35	5.35	270	270	300	300	300	273	276	298	299	299
80E	0.46	0.88	1.25	1.59	1.92	2.17	2.93	3.56	4.07	4.46	0.96	1.96	2.96	3.96	4.96	270	270	285	300	300	273	277	290	299	299
81A	0.38	0.82	1.2	1.56	1.89	2.01	2.87	3.54	4.06	4.46	0.8	1.8	2.8	3.8	4.8	270	270	285	300	300	276	279	292	301	300
81B	0.31	0.75	1.15	1.52	1.86	1.81	2.82	3.53	4.03	4.43	0.68	1.68	2.68	3.68	4.68	270	270	285	300	300	281	286	297	305	304
81C	0.35	0.79	1.2	1.55	1.86	2.14	3.04	3.63	4.03	4.42	0.78	1.78	2.78	3.78	4.78	315	300	285	285	300	322	314	305	302	306
81D	0.41	0.88	1.29	1.63	1.91	2.72	3.4	3.81	4.1	4.46	0.78	1.78	2.78	3.78	4.78	300	300	285	285	300	306	307	302	298	301
81E	0.82	1.2	1.54	1.79	1.99	3.16	3.61	3.96	4.18	4.45	1.76	2.76	3.76	4.76	5.76	285	285	285	285	300	303	303	300	297	300

nour_fast

Point	Hs [m]					Tmm10 [s]					Water Depth [m]					Wind Direction [deg]					Wave Direction [deg]				
Design WL	0m	1m	2m	3m	4m	0m	1m	2m	3m	4m	0m	1m	2m	3m	4m	0m	1m	2m	3m	4m	0m	1m	2m	3m	4m
80A	0.83	1.17	1.43	1.69	1.92	2.85	3.21	3.63	3.96	4.31	1.84	2.84	3.84	4.84	5.84	285	270	285	285	300	289	283	293	294	300
80B	0.55	0.97	1.33	1.61	1.87	2.69	3.21	3.62	4.02	4.33	0.99	1.99	2.99	3.99	4.99	270	285	285	300	300	273	284	289	297	298
80C	0.19	0.65	1.09	1.49	1.83	2.07	2.94	3.63	4.04	4.38	0.25	1.25	2.25	3.25	4.25	270	270	300	300	300	268	279	297	298	298
80D	0.1	0.59	1.04	1.45	1.84	1.56	2.87	3.62	4.11	4.51	0.13	1.13	2.13	3.13	4.13	270	270	285	300	300	278	286	293	299	299
80E	0	0.52	0.97	1.37	1.74	0	2.77	3.53	4.04	4.43	0	1	2	3	4	270	270	270	300	300		288	287	297	298
81A	0	0.48	0.94	1.34	1.72	0	2.68	3.49	4.04	4.44	0	0.93	1.93	2.93	3.93	270	270	270	300	300		288	286	297	297
81B	0	0.5	0.95	1.36	1.74	0	2.68	3.51	4.05	4.45	0	0.96	1.96	2.96	3.96	270	270	270	300	300		289	286	299	299
81C	0	0.55	1.01	1.42	1.78	0	2.92	3.64	4.06	4.44	0	1.06	2.06	3.06	4.06	270	270	285	285	300		293	299	297	301
81D	0.36	0.84	1.29	1.65	1.93	2.64	3.41	3.84	4.14	4.47	0.59	1.59	2.59	3.59	4.59	270	300	285	285	300	296	305	299	297	300
81E	0.9	1.27	1.58	1.8	1.99	3.38	3.67	3.97	4.16	4.43	1.74	2.74	3.74	4.74	5.74	285	285	285	285	300	298	298	296	294	299

no_slow

Point	Hs [m]					Tmm10 [s]					Water Depth [m]					Wind Direction [deg]					Wave Direction [deg]				
Design WL	0m	1m	2m	3m	4m	0m	1m	2m	3m	4m	0m	1m	2m	3m	4m	0m	1m	2m	3m	4m	0m	1m	2m	3m	4m
80A	0.82	1.16	1.45	1.7	1.93	2.82	3.29	3.64	3.99	4.31	1.82	2.82	3.82	4.82	5.82	285	300	285	300	300	291	302	296	302	302
80B	0.78	1.13	1.44	1.7	1.93	2.76	3.27	3.68	4.02	4.33	1.75	2.75	3.75	4.75	5.75	285	300	300	300	300	288	300	302	302	301
80C	0.75	1.1	1.42	1.69	1.95	2.65	3.23	3.68	4.04	4.37	1.65	2.65	3.65	4.65	5.65	270	285	300	300	300	278	293	302	302	301
80D	0.73	1.09	1.42	1.72	1.99	2.59	3.21	3.7	4.1	4.45	1.67	2.67	3.67	4.67	5.67	270	285	300	300	300	273	289	300	301	300
80E	0.6	1	1.35	1.67	1.97	2.42	3.12	3.67	4.12	4.48	1.28	2.28	3.28	4.28	5.28	270	270	285	300	300	275	280	292	300	300
81A	0.52	0.94	1.31	1.65	1.95	2.3	3.08	3.65	4.11	4.48	1.12	2.12	3.12	4.12	5.12	270	270	285	300	300	277	281	293	301	301
81B	0.45	0.88	1.27	1.62	1.94	2.16	3.06	3.66	4.09	4.46	0.99	1.99	2.99	3.99	4.99	270	270	285	300	300	283	288	298	305	304
81C	0.48	0.92	1.3	1.64	1.94	2.48	3.22	3.72	4.07	4.4	1.1	2.1	3.1	4.1	5.1	315	285	285	285	285	321	306	304	302	299
81D	0.56	1	1.39	1.7	1.98	2.91	3.47	3.83	4.11	4.41	1.1	2.1	3.1	4.1	5.1	300	300	285	285	285	306	307	300	297	295
81E	0.87	1.22	1.55	1.8	2.01	3.02	3.52	3.89	4.14	4.39	2.15	3.15	4.15	5.15	6.15	285	285	285	285	285	299	300	297	296	294

no2_slow

Point	Hs [m]					Tmm10 [s]					Water Depth [m]					Wind Direction [deg]					Wave Direction [deg]				
Design WL	0m	1m	2m	3m	4m	0m	1m	2m	3m	4m	0m	1m	2m	3m	4m	0m	1m	2m	3m	4m	0m	1m	2m	3m	4m
80A	0.59	1	1.35	1.63	1.88	2.57	3.17	3.6	3.96	4.29	1.27	2.27	3.27	4.27	5.27	285	285	285	300	300	285	289	293	300	300
80B	0.55	0.96	1.32	1.61	1.87	2.47	3.1	3.57	3.97	4.31	1.17	2.17	3.17	4.17	5.17	270	285	285	300	300	278	288	292	299	299
80C	0.5	0.92	1.28	1.58	1.87	2.37	3.02	3.54	3.97	4.33	1.07	2.07	3.07	4.07	5.07	270	270	285	300	300	278	279	292	299	299
80D	0.49	0.9	1.25	1.58	1.89	2.22	2.93	3.51	4	4.39	1.09	2.09	3.09	4.09	5.09	270	270	285	300	300	272	276	289	298	299
80E	0.33	0.78	1.17	1.51	1.85	1.91	2.8	3.43	4	4.43	0.7	1.7	2.7	3.7	4.7	270	270	270	300	300	273	277	281	298	299
81A	0.25	0.71	1.11	1.47	1.82	1.74	2.72	3.4	3.98	4.42	0.54	1.54	2.54	3.54	4.54	270	270	270	300	300	275	279	282	300	300
81B	0.18	0.64	1.05	1.42	1.78	1.54	2.65	3.39	3.96	4.39	0.41	1.41	2.41	3.41	4.41	270	270	270	300	300	279	286	288	305	304
81C	0.22	0.68	1.09	1.47	1.8	1.83	2.85	3.56	3.98	4.4	0.52	1.52	2.52	3.52	4.52	315	300	300	285	300	323	314	312	303	306
81D	0.28	0.76	1.19	1.54	1.86	2.41	3.29	3.75	4.11	4.45	0.51	1.51	2.51	3.51	4.51	300	300	285	300	300	305	307	303	304	302
81E	0.71	1.11	1.47	1.74	1.96	2.99	3.55	3.93	4.17	4.45	1.49	2.49	3.49	4.49	5.49	285	285	285	285	300	302	304	301	298	300

nour_slow

Point	Hs [m]					Tmm10 [s]					Water Depth [m]					Wind Direction [deg]					Wave Direction [deg]				
Design WL	0m	1m	2m	3m	4m	0m	1m	2m	3m	4m	0m	1m	2m	3m	4m	0m	1m	2m	3m	4m	0m	1m	2m	3m	4m
80A	0.74	1.1	1.38	1.65	1.89	2.77	3.18	3.6	3.95	4.31	1.59	2.59	3.59	4.59	5.59	285	270	285	285	300	288	283	293	294	300
80B	0.43	0.87	1.26	1.56	1.83	2.58	3.17	3.59	4	4.32	0.74	1.74	2.74	3.74	4.74	270	285	285	300	300	272	282	287	296	297
80C	0	0.56	0.99	1.4	1.76	0	2.82	3.55	4	4.37	0	1.01	2.01	3.01	4.01	270	270	300	300	300		277	296	297	298
80D	0	0.49	0.94	1.36	1.76	0	2.67	3.5	4.07	4.48	0	0.88	1.88	2.88	3.88	270	270	270	300	300		284	287	298	298
80E	0	0.41	0.87	1.28	1.67	0	2.57	3.42	3.99	4.41	0	0.76	1.76	2.76	3.76	270	270	270	300	300		288	288	297	298
81A	0	0.38	0.83	1.25	1.65	0	2.47	3.37	3.98	4.42	0	0.69	1.69	2.69	3.69	270	270	270	300	300		287	287	296	297
81B	0	0.4	0.84	1.26	1.66	0	2.47	3.39	3.99	4.42	0	0.72	1.72	2.72	3.72	270	270	270	300	300		289	287	299	299
81C	0	0.45	0.91	1.33	1.71	0	2.7	3.53	4.01	4.43	0	0.82	1.82	2.82	3.82	270	270	270	285	300		294	294	298	301
81D	0.24	0.73	1.19	1.57	1.88	2.37	3.31	3.78	4.12	4.47	0.35	1.35	2.35	3.35	4.35	270	300	285	285	300	295	306	300	297	300
81E	0.79	1.19	1.53	1.77	1.97	3.31	3.66	3.95	4.15	4.43	1.5	2.5	3.5	4.5	5.5	285	300	285	285	300	297	302	296	295	299

no_fast 2060

Point	Hs [m]					Tmm10 [s]					Water Depth [m]					Wind Direction [deg]					Wave Direction [deg]				
Design WL	0m	1m	2m	3m	4m	0m	1m	2m	3m	4m	0m	1m	2m	3m	4m	0m	1m	2m	3m	4m	0m	1m	2m	3m	4m
80A	0.92	1.24	1.51	1.74	1.97	2.93	3.35	3.7	4.02	4.32	2.16	3.16	4.16	5.16	6.16	300	300	300	300	300	300	303	303	303	302
80B	0.9	1.23	1.5	1.75	1.97	2.9	3.35	3.72	4.05	4.34	2.1	3.1	4.1	5.1	6.1	300	300	300	300	300	298	302	303	302	302
80C	0.87	1.21	1.5	1.75	1.99	2.83	3.35	3.74	4.07	4.38	1.99	2.99	3.99	4.99	5.99	285	300	300	300	300	289	302	303	303	302
80D	0.86	1.2	1.51	1.79	2.04	2.76	3.35	3.77	4.14	4.46	2.01	3.01	4.01	5.01	6.01	270	300	300	300	300	275	300	301	301	301
80E	0.74	1.11	1.46	1.76	2.03	2.64	3.28	3.75	4.17	4.5	1.62	2.62	3.62	4.62	5.62	270	285	285	300	300	276	291	293	301	301
81A	0.67	1.07	1.42	1.74	2.01	2.57	3.21	3.75	4.17	4.5	1.46	2.46	3.46	4.46	5.46	270	270	285	300	300	278	281	294	302	302
81B	0.6	1	1.38	1.71	2	2.49	3.28	3.79	4.15	4.48	1.33	2.33	3.33	4.33	5.33	270	300	300	300	300	285	305	306	305	304
81C	0.64	1.05	1.42	1.73	2	2.71	3.38	3.8	4.11	4.41	1.44	2.44	3.44	4.44	5.44	300	300	285	285	285	314	312	303	301	298
81D	0.72	1.13	1.49	1.77	2.01	3.12	3.5	3.88	4.14	4.41	1.44	2.44	3.44	4.44	5.44	300	285	285	285	285	307	301	299	296	294
81E	1	1.33	1.62	1.84	2.04	3.18	3.58	3.93	4.16	4.4	2.49	3.49	4.49	5.49	6.49	285	285	285	285	285	300	299	296	295	294

no2_fast

Point	Hs [m]					Tmm10 [s]					Water Depth [m]					Wind Direction [deg]					Wave Direction [deg]				
Design WL	0m	1m	2m	3m	4m	0m	1m	2m	3m	4m	0m	1m	2m	3m	4m	0m	1m	2m	3m	4m	0m	1m	2m	3m	4m
80A	0.79	1.16	1.46	1.7	1.94	2.81	3.27	3.65	4	4.31	1.74	2.74	3.74	4.74	5.74	285	285	285	300	300	287	291	294	301	300
80B	0.74	1.12	1.43	1.69	1.93	2.73	3.23	3.67	4.02	4.33	1.65	2.65	3.65	4.65	5.65	285	285	300	300	300	285	291	300	300	300
80C	0.71	1.08	1.4	1.69	1.95	2.62	3.18	3.66	4.03	4.36	1.54	2.54	3.54	4.54	5.54	270	285	300	300	300	277	290	300	301	301
80D	0.69	1.06	1.39	1.7	1.98	2.53	3.15	3.67	4.08	4.44	1.56	2.56	3.56	4.56	5.56	270	285	300	300	300	273	287	299	300	300
80E	0.55	0.96	1.32	1.66	1.96	2.34	3.04	3.64	4.11	4.48	1.17	2.17	3.17	4.17	5.17	270	270	285	300	300	274	278	291	299	300
81A	0.48	0.9	1.28	1.62	1.94	2.21	2.99	3.63	4.1	4.49	1.01	2.01	3.01	4.01	5.01	270	270	285	300	300	276	279	292	301	301
81B	0.4	0.83	1.22	1.58	1.91	2.05	2.98	3.65	4.08	4.45	0.88	1.88	2.88	3.88	4.88	270	285	300	300	300	282	296	305	305	304
81C	0.44	0.87	1.27	1.61	1.9	2.36	3.17	3.7	4.06	4.44	0.99	1.99	2.99	3.99	4.99	315	300	285	285	300	322	313	305	302	305
81D	0.51	0.96	1.36	1.68	1.94	2.86	3.46	3.85	4.12	4.46	0.99	1.99	2.99	3.99	4.99	285	300	285	285	300	301	307	301	298	301
81E	0.9	1.27	1.58	1.82	2.03	3.25	3.64	3.97	4.19	4.41	1.97	2.97	3.97	4.97	5.97	285	285	285	285	285	304	302	299	296	295

nour_fast

Point	Hs [m]					Tmm10 [s]					Water Depth [m]					Wind Direction [deg]					Wave Direction [deg]				
Design WL	0m	1m	2m	3m	4m	0m	1m	2m	3m	4m	0m	1m	2m	3m	4m	0m	1m	2m	3m	4m	0m	1m	2m	3m	4m
80A	0.89	1.22	1.47	1.72	1.94	2.89	3.23	3.65	3.98	4.32	2.02	3.02	4.02	5.02	6.02	285	270	285	285	300	289	283	294	294	300
80B	0.63	1.03	1.38	1.65	1.9	2.76	3.25	3.65	4.03	4.33	1.17	2.17	3.17	4.17	5.17	270	285	285	300	300	274	286	290	298	299
80C	0.31	0.74	1.18	1.56	1.88	2.25	3.11	3.69	4.07	4.4	0.48	1.48	2.48	3.48	4.48	270	300	300	300	300	271	294	298	298	299
80D	0.24	0.69	1.13	1.53	1.89	1.98	3.02	3.68	4.14	4.52	0.35	1.35	2.35	3.35	4.35	270	270	285	300	300	274	286	293	299	299
80E	0.16	0.62	1.06	1.45	1.81	1.84	2.96	3.62	4.08	4.45	0.24	1.24	2.24	3.24	4.24	270	270	285	300	300	289	288	292	298	298
81A	0.12	0.59	1.02	1.43	1.79	1.75	2.89	3.63	4.08	4.46	0.17	1.17	2.17	3.17	4.17	270	270	300	300	300	285	288	297	297	298
81B	0.13	0.6	1.04	1.44	1.81	1.76	2.88	3.62	4.09	4.47	0.19	1.19	2.19	3.19	4.19	270	270	285	300	300	285	288	292	300	300
81C	0.19	0.66	1.11	1.5	1.86	1.97	3.09	3.71	4.09	4.42	0.3	1.3	2.3	3.3	4.3	270	270	285	285	285	294	293	298	297	295
81D	0.45	0.93	1.36	1.7	1.98	2.87	3.47	3.87	4.15	4.43	0.81	1.81	2.81	3.81	4.81	300	300	285	285	285	306	305	299	296	294
81E	0.95	1.31	1.61	1.82	2	3.42	3.69	3.98	4.17	4.43	1.85	2.85	3.85	4.85	5.85	285	285	285	285	300	298	297	295	294	298

no_slow

Point	Hs [m]					Tmm10 [s]					Water Depth [m]					Wind Direction [deg]					Wave Direction [deg]				
Design WL	0m	1m	2m	3m	4m	0m	1m	2m	3m	4m	0m	1m	2m	3m	4m	0m	1m	2m	3m	4m	0m	1m	2m	3m	4m
80A	0.85	1.19	1.47	1.72	1.95	2.88	3.31	3.67	4	4.32	1.95	2.95	3.95	4.95	5.95	300	300	300	300	300	299	302	303	302	302
80B	0.83	1.17	1.46	1.72	1.95	2.81	3.3	3.69	4.04	4.34	1.88	2.88	3.88	4.88	5.88	285	300	300	300	300	289	301	302	302	301
80C	0.79	1.14	1.45	1.72	1.97	2.74	3.28	3.71	4.05	4.37	1.78	2.78	3.78	4.78	5.78	285	300	300	300	300	287	301	302	302	302
80D	0.78	1.14	1.45	1.75	2.01	2.66	3.24	3.73	4.12	4.45	1.8	2.8	3.8	4.8	5.8	270	285	300	300	300	274	290	301	301	301
80E	0.65	1.04	1.39	1.71	1.99	2.51	3.18	3.7	4.14	4.49	1.41	2.41	3.41	4.41	5.41	270	285	285	300	300	275	289	293	301	300
81A	0.58	0.99	1.35	1.68	1.97	2.41	3.12	3.69	4.14	4.49	1.25	2.25	3.25	4.25	5.25	270	270	285	300	300	277	280	294	301	301
81B	0.51	0.93	1.32	1.66	1.96	2.3	3.13	3.7	4.12	4.47	1.12	2.12	3.12	4.12	5.12	270	285	285	300	300	284	296	298	305	304
81C	0.55	0.96	1.35	1.68	1.97	2.53	3.29	3.76	4.09	4.4	1.23	2.23	3.23	4.23	5.23	300	300	285	285	285	315	312	304	301	299
81D	0.62	1.05	1.43	1.73	1.99	3	3.49	3.85	4.12	4.41	1.23	2.23	3.23	4.23	5.23	300	300	285	285	285	307	307	299	297	295
81E	0.92	1.27	1.58	1.82	2.03	3.09	3.54	3.91	4.15	4.39	2.28	3.28	4.28	5.28	6.28	285	285	285	285	285	300	299	297	295	294

no2_slow

Point	Hs [m]					Tmm10 [s]					Water Depth [m]					Wind Direction [deg]					Wave Direction [deg]				
Design WL	0m	1m	2m	3m	4m	0m	1m	2m	3m	4m	0m	1m	2m	3m	4m	0m	1m	2m	3m	4m	0m	1m	2m	3m	4m
80A	0.65	1.05	1.39	1.65	1.9	2.65	3.2	3.61	3.97	4.29	1.4	2.4	3.4	4.4	5.4	285	285	285	300	300	286	290	293	300	300
80B	0.61	1.01	1.35	1.64	1.89	2.54	3.14	3.59	3.99	4.31	1.3	2.3	3.3	4.3	5.3	270	285	285	300	300	278	289	292	299	299
80C	0.56	0.97	1.32	1.61	1.89	2.45	3.05	3.57	3.99	4.34	1.2	2.2	3.2	4.2	5.2	270	270	285	300	300	277	279	292	300	300
80D	0.55	0.94	1.29	1.61	1.91	2.32	2.97	3.55	4.03	4.4	1.22	2.22	3.22	4.22	5.22	270	270	285	300	300	272	276	290	299	299
80E	0.39	0.83	1.2	1.55	1.89	2.04	2.85	3.51	4.04	4.45	0.83	1.83	2.83	3.83	4.83	270	270	285	300	300	273	276	290	299	299
81A	0.31	0.76	1.15	1.51	1.86	1.87	2.78	3.48	4.02	4.44	0.67	1.67	2.67	3.67	4.67	270	270	285	300	300	275	278	291	300	300
81B	0.24	0.69	1.1	1.47	1.82	1.66	2.72	3.47	4	4.41	0.54	1.54	2.54	3.54	4.54	270	270	285	300	300	280	286	297	305	304
81C	0.28	0.73	1.15	1.51	1.83	1.99	2.95	3.59	4	4.41	0.65	1.65	2.65	3.65	4.65	315	300	285	285	300	322	314	306	303	306
81D	0.34	0.82	1.24	1.59	1.89	2.57	3.35	3.78	4.09	4.45	0.65	1.65	2.65	3.65	4.65	300	300	285	285	300	306	307	302	299	301
81E	0.77	1.16	1.5	1.77	1.98	3.08	3.58	3.95	4.17	4.45	1.63	2.63	3.63	4.63	5.63	285	285	285	285	300	303	304	301	297	300

nour_slow

Point	Hs [m]					Tmm10 [s]					Water Depth [m]					Wind Direction [deg]					Wave Direction [deg]				
Design WL	0m	1m	2m	3m	4m	0m	1m	2m	3m	4m	0m	1m	2m	3m	4m	0m	1m	2m	3m	4m	0m	1m	2m	3m	4m
80A	0.78	1.12	1.41	1.67	1.9	2.81	3.23	3.62	3.96	4.31	1.71	2.71	3.71	4.71	5.71	285	285	285	285	300	288	291	293	294	300
80B	0.48	0.91	1.29	1.59	1.85	2.62	3.18	3.61	4.01	4.32	0.85	1.85	2.85	3.85	4.85	270	285	285	300	300	273	283	289	296	298
80C	0.12	0.62	1.05	1.45	1.8	1.85	2.9	3.6	4.03	4.38	0.16	1.16	2.16	3.16	4.16	270	270	300	300	300	268	278	296	297	298
80D	0	0.56	0.99	1.41	1.8	0	2.79	3.57	4.09	4.49	0	1.03	2.03	3.03	4.03	270	270	285	300	300		285	292	299	298
80E	0	0.49	0.93	1.34	1.72	0	2.7	3.49	4.02	4.43	0	0.92	1.92	2.92	3.92	270	270	270	300	300		290	288	298	298
81A	0	0.46	0.9	1.31	1.7	0	2.62	3.45	4.01	4.43	0	0.85	1.85	2.85	3.85	270	270	270	300	300		289	286	297	297
81B	0	0.47	0.91	1.32	1.71	0	2.62	3.46	4.02	4.44	0	0.87	1.87	2.87	3.87	270	270	270	300	300		290	287	299	299
81C	0	0.52	0.98	1.39	1.75	0	2.85	3.58	4.04	4.44	0	0.98	1.98	2.98	3.98	270	270	270	285	300		294	293	297	301
81D	0.3	0.79	1.24	1.61	1.91	2.5	3.36	3.81	4.13	4.47	0.49	1.49	2.49	3.49	4.49	270	300	285	285	300	296	305	300	297	300
81E	0.81	1.21	1.55	1.78	1.98	3.33	3.67	3.97	4.16	4.43	1.53	2.53	3.53	4.53	5.53	285	285	285	285	300	297	298	296	295	298

no_fast

2070

Point	Hs [m]					Tmm10 [s]					Water Depth [m]					Wind Direction [deg]					Wave Direction [deg]				
Design WL	0m	1m	2m	3m	4m	0m	1m	2m	3m	4m	0m	1m	2m	3m	4m	0m	1m	2m	3m	4m	0m	1m	2m	3m	4m
80A	0.99	1.29	1.54	1.77	1.99	2.98	3.37	3.71	4.03	4.33	2.37	3.37	4.37	5.37	6.37	300	300	300	300	300	301	304	304	303	302
80B	0.96	1.28	1.54	1.78	1.99	2.97	3.39	3.74	4.07	4.35	2.3	3.3	4.3	5.3	6.3	300	300	300	300	300	300	303	303	302	302
80C	0.94	1.26	1.54	1.78	2.01	2.91	3.4	3.77	4.09	4.39	2.2	3.2	4.2	5.2	6.2	285	300	300	300	300	290	303	303	303	302
80D	0.93	1.26	1.56	1.83	2.06	2.85	3.41	3.81	4.16	4.47	2.22	3.22	4.22	5.22	6.22	270	300	300	300	300	276	301	302	302	301
80E	0.82	1.18	1.5	1.8	2.05	2.76	3.35	3.83	4.18	4.51	1.83	2.83	3.83	4.83	5.83	270	285	300	300	300	276	292	301	301	301
81A	0.76	1.13	1.48	1.78	2.03	2.7	3.33	3.84	4.19	4.5	1.67	2.67	3.67	4.67	5.67	270	285	300	300	300	279	292	302	302	302
81B	0.69	1.08	1.45	1.76	2.03	2.65	3.37	3.84	4.17	4.48	1.54	2.54	3.54	4.54	5.54	270	300	300	300	300	286	305	306	305	304
81C	0.73	1.13	1.48	1.77	2.02	2.86	3.42	3.84	4.12	4.41	1.65	2.65	3.65	4.65	5.65	300	285	285	285	285	314	305	303	300	298
81D	0.81	1.2	1.55	1.8	2.03	3.2	3.53	3.91	4.14	4.41	1.65	2.65	3.65	4.65	5.65	300	285	285	285	285	307	300	298	296	294
81E	1.07	1.38	1.66	1.87	2.06	3.25	3.61	3.94	4.17	4.4	2.7	3.7	4.7	5.7	6.7	285	285	285	285	285	300	298	296	295	294

no2_fast

Point	Hs [m]					Tmm10 [s]					Water Depth [m]					Wind Direction [deg]					Wave Direction [deg]				
Design WL	0m	1m	2m	3m	4m	0m	1m	2m	3m	4m	0m	1m	2m	3m	4m	0m	1m	2m	3m	4m	0m	1m	2m	3m	4m
80A	0.87	1.23	1.5	1.73	1.96	2.87	3.3	3.66	4.01	4.31	1.95	2.95	3.95	4.95	5.95	285	285	285	300	300	288	292	294	301	301
80B	0.82	1.19	1.47	1.72	1.95	2.81	3.27	3.69	4.03	4.33	1.85	2.85	3.85	4.85	5.85	285	285	300	300	300	287	291	301	301	300
80C	0.79	1.15	1.45	1.73	1.97	2.71	3.26	3.7	4.06	4.38	1.75	2.75	3.75	4.75	5.75	270	300	300	300	300	277	299	301	301	301
80D	0.77	1.13	1.45	1.75	2.01	2.64	3.21	3.72	4.11	4.45	1.77	2.77	3.77	4.77	5.77	270	285	300	300	300	273	288	300	300	300
80E	0.64	1.04	1.39	1.71	2	2.49	3.14	3.7	4.14	4.5	1.38	2.38	3.38	4.38	5.38	270	270	285	300	300	275	278	292	300	300
81A	0.57	0.98	1.35	1.69	1.98	2.39	3.11	3.7	4.15	4.5	1.22	2.22	3.22	4.22	5.22	270	270	285	300	300	277	280	293	301	301
81B	0.5	0.92	1.3	1.65	1.96	2.27	3.09	3.72	4.12	4.47	1.09	2.09	3.09	4.09	5.09	270	270	300	300	300	284	287	306	305	304
81C	0.52	0.96	1.34	1.67	1.96	2.55	3.26	3.75	4.09	4.41	1.2	2.2	3.2	4.2	5.2	315	300	285	285	285	321	313	304	301	299
81D	0.61	1.04	1.43	1.73	1.99	3	3.5	3.88	4.14	4.42	1.2	2.2	3.2	4.2	5.2	285	300	285	285	285	302	307	300	297	295
81E	0.98	1.34	1.63	1.85	2.04	3.33	3.66	3.98	4.2	4.42	2.17	3.17	4.17	5.17	6.17	285	285	285	285	285	304	301	298	296	294

nour_fast

Point	Hs [m]					Tmm10 [s]					Water Depth [m]					Wind Direction [deg]					Wave Direction [deg]				
Design WL	0m	1m	2m	3m	4m	0m	1m	2m	3m	4m	0m	1m	2m	3m	4m	0m	1m	2m	3m	4m	0m	1m	2m	3m	4m
80A	0.94	1.26	1.5	1.74	1.96	2.91	3.25	3.66	3.99	4.33	2.22	3.22	4.22	5.22	6.22	285	270	285	285	300	289	283	294	294	301
80B	0.7	1.1	1.43	1.69	1.92	2.8	3.28	3.67	4.05	4.34	1.36	2.36	3.36	4.36	5.36	270	285	285	300	300	274	287	291	298	299
80C	0.41	0.84	1.26	1.62	1.93	2.42	3.23	3.74	4.1	4.41	0.69	1.69	2.69	3.69	4.69	270	300	300	300	300	273	296	298	299	300
80D	0.34	0.77	1.21	1.6	1.94	2.22	3.19	3.73	4.16	4.52	0.57	1.57	2.57	3.57	4.57	270	300	285	300	300	277	299	293	299	299
80E	0.27	0.72	1.15	1.53	1.86	2.12	3.1	3.69	4.1	4.47	0.48	1.48	2.48	3.48	4.48	270	285	285	300	300	290	293	293	299	299
81A	0.24	0.69	1.12	1.51	1.85	2.03	3.04	3.68	4.11	4.47	0.4	1.4	2.4	3.4	4.4	270	270	285	300	300	288	287	291	298	298
81B	0.25	0.7	1.13	1.52	1.87	2.04	3.04	3.7	4.12	4.48	0.42	1.42	2.42	3.42	4.42	270	270	285	300	300	289	287	293	300	300
81C	0.3	0.76	1.2	1.58	1.91	2.26	3.22	3.76	4.11	4.42	0.53	1.53	2.53	3.53	4.53	270	285	285	285	285	294	298	298	296	295
81D	0.56	1.01	1.43	1.74	2.01	2.97	3.52	3.9	4.16	4.43	1.01	2.01	3.01	4.01	5.01	285	300	285	285	285	301	304	298	295	294
81E	1	1.35	1.64	1.84	2.03	3.44	3.69	3.99	4.18	4.4	1.97	2.97	3.97	4.97	5.97	285	285	285	285	285	298	296	295	294	293

no_slow

Point	Hs [m]					Tmm10 [s]					Water Depth [m]					Wind Direction [deg]					Wave Direction [deg]				
Design WL	0m	1m	2m	3m	4m	0m	1m	2m	3m	4m	0m	1m	2m	3m	4m	0m	1m	2m	3m	4m	0m	1m	2m	3m	4m
80A	0.9	1.23	1.49	1.73	1.96	2.91	3.33	3.69	4.01	4.32	2.08	3.08	4.08	5.08	6.08	300	300	300	300	300	299	303	303	303	302
80B	0.88	1.21	1.49	1.74	1.96	2.85	3.33	3.71	4.05	4.34	2.02	3.02	4.02	5.02	6.02	285	300	300	300	300	290	302	303	302	302
80C	0.84	1.18	1.48	1.74	1.98	2.8	3.32	3.73	4.07	4.38	1.91	2.91	3.91	4.91	5.91	285	300	300	300	300	288	302	303	302	302
80D	0.83	1.17	1.49	1.78	2.03	2.72	3.32	3.76	4.14	4.46	1.93	2.93	3.93	4.93	5.93	270	300	300	300	300	275	299	301	301	301
80E	0.71	1.08	1.43	1.74	2.02	2.59	3.25	3.73	4.16	4.5	1.54	2.54	3.54	4.54	5.54	270	285	285	300	300	275	290	293	301	301
81A	0.64	1.04	1.4	1.72	2	2.51	3.18	3.73	4.16	4.49	1.38	2.38	3.38	4.38	5.38	270	270	285	300	300	278	281	294	302	301
81B	0.57	0.98	1.35	1.69	1.99	2.42	3.21	3.77	4.14	4.47	1.25	2.25	3.25	4.25	5.25	270	285	300	300	300	285	296	306	305	304
81C	0.61	1.02	1.39	1.71	1.99	2.64	3.35	3.79	4.1	4.41	1.36	2.36	3.36	4.36	5.36	300	300	285	285	285	314	312	304	301	298
81D	0.68	1.1	1.47	1.75	2.01	3.08	3.49	3.87	4.13	4.41	1.36	2.36	3.36	4.36	5.36	300	285	285	285	285	307	301	299	296	295
81E	0.97	1.3	1.61	1.83	2.04	3.15	3.56	3.92	4.16	4.4	2.41	3.41	4.41	5.41	6.41	285	285	285	285	285	300	299	297	295	294

no2_slow

Point	Hs [m]					Tmm10 [s]					Water Depth [m]					Wind Direction [deg]					Wave Direction [deg]				
Design WL	0m	1m	2m	3m	4m	0m	1m	2m	3m	4m	0m	1m	2m	3m	4m	0m	1m	2m	3m	4m	0m	1m	2m	3m	4m
80A	0.7	1.09	1.42	1.67	1.91	2.72	3.23	3.63	3.98	4.3	1.53	2.53	3.53	4.53	5.53	285	285	285	300	300	286	290	293	300	300
80B	0.66	1.05	1.38	1.66	1.91	2.63	3.17	3.64	4	4.32	1.43	2.43	3.43	4.43	5.43	285	285	300	300	300	285	289	299	300	300
80C	0.62	1.02	1.36	1.64	1.91	2.51	3.09	3.6	4.01	4.35	1.33	2.33	3.33	4.33	5.33	270	270	285	300	300	277	280	292	300	300
80D	0.6	0.99	1.32	1.65	1.94	2.4	3.03	3.61	4.05	4.42	1.35	2.35	3.35	4.35	5.35	270	270	300	300	300	273	276	298	299	299
80E	0.45	0.88	1.25	1.59	1.92	2.17	2.92	3.56	4.07	4.46	0.96	1.96	2.96	3.96	4.96	270	270	285	300	300	273	277	290	299	299
81A	0.38	0.82	1.2	1.56	1.89	2.01	2.87	3.54	4.06	4.46	0.8	1.8	2.8	3.8	4.8	270	270	285	300	300	275	279	292	301	300
81B	0.3	0.75	1.15	1.51	1.86	1.81	2.82	3.53	4.03	4.43	0.67	1.67	2.67	3.67	4.67	270	270	285	300	300	281	286	297	305	304
81C	0.34	0.79	1.19	1.55	1.86	2.14	3.04	3.63	4.03	4.42	0.78	1.78	2.78	3.78	4.78	315	300	285	285	300	322	314	305	302	306
81D	0.41	0.87	1.29	1.63	1.91	2.71	3.4	3.81	4.1	4.46	0.78	1.78	2.78	3.78	4.78	300	300	285	285	300	306	307	302	298	301
81E	0.82	1.2	1.54	1.79	1.99	3.16	3.61	3.96	4.18	4.45	1.76	2.76	3.76	4.76	5.76	285	285	285	285	300	303	303	300	297	300

nour_slow

Point	Hs [m]					Tmm10 [s]					Water Depth [m]					Wind Direction [deg]					Wave Direction [deg]				
Design WL	0m	1m	2m	3m	4m	0m	1m	2m	3m	4m	0m	1m	2m	3m	4m	0m	1m	2m	3m	4m	0m	1m	2m	3m	4m
80A	0.82	1.17	1.43	1.69	1.92	2.85	3.21	3.63	3.96	4.31	1.82	2.82	3.82	4.82	5.82	285	270	285	285	300	288	283	293	294	300
80B	0.53	0.96	1.33	1.62	1.87	2.66	3.21	3.63	4.02	4.33	0.96	1.96	2.96	3.96	4.96	270	285	285	300	300	274	285	289	297	298
80C	0.22	0.67	1.11	1.5	1.84	2.09	2.95	3.65	4.05	4.4	0.3	1.3	2.3	3.3	4.3	270	270	300	300	300	269	279	297	298	298
80D	0.14	0.61	1.05	1.46	1.84	1.74	2.87	3.61	4.11	4.5	0.18	1.18	2.18	3.18	4.18	270	270	285	300	300	275	286	292	299	299
80E	0.06	0.55	0.99	1.39	1.76	1.45	2.81	3.56	4.05	4.44	0.08	1.08	2.08	3.08	4.08	285	270	285	300	300	287	289	293	298	298
81A	0	0.52	0.96	1.37	1.75	0	2.73	3.53	4.05	4.45	0	1.01	2.01	3.01	4.01	270	270	285	300	300		288	291	297	298
81B	0	0.53	0.97	1.38	1.76	0	2.72	3.55	4.05	4.45	0	1.02	2.02	3.02	4.02	270	270	285	300	300		289	292	299	300
81C	0.09	0.58	1.03	1.44	1.81	1.6	2.95	3.64	4.06	4.41	0.14	1.14	2.14	3.14	4.14	270	270	285	285	285	288	293	298	297	295
81D	0.36	0.84	1.28	1.65	1.95	2.66	3.4	3.84	4.14	4.43	0.62	1.62	2.62	3.62	4.62	300	300	285	285	285	306	305	299	297	295
81E	0.84	1.24	1.57	1.8	1.99	3.36	3.68	3.98	4.17	4.44	1.57	2.57	3.57	4.57	5.57	285	285	285	285	300	297	297	295	294	298

no_fast 2080

Point	Hs [m]					Tmm10 [s]					Water Depth [m]					Wind Direction [deg]					Wave Direction [deg]				
Design WL	0m	1m	2m	3m	4m	0m	1m	2m	3m	4m	0m	1m	2m	3m	4m	0m	1m	2m	3m	4m	0m	1m	2m	3m	4m
80A	1.06	1.34	1.6	1.82	2.04	3.02	3.39	3.73	4.05	4.33	2.57	3.57	4.57	5.57	6.57	300	300	300	300	300	303	304	304	303	302
80B	1.04	1.34	1.59	1.83	2.04	3.02	3.42	3.75	4.08	4.35	2.51	3.51	4.51	5.51	6.51	300	300	300	300	300	301	303	303	303	302
80C	1	1.32	1.6	1.84	2.06	3.01	3.43	3.78	4.11	4.39	2.4	3.4	4.4	5.4	6.4	300	300	300	300	300	300	303	303	303	302
80D	0.99	1.32	1.62	1.89	2.12	2.97	3.45	3.84	4.18	4.47	2.42	3.42	4.42	5.42	6.42	285	300	300	300	300	288	301	302	302	301
80E	0.9	1.24	1.57	1.86	2.11	2.87	3.44	3.86	4.2	4.51	2.03	3.03	4.03	5.03	6.03	270	300	300	300	300	277	301	302	302	301
81A	0.84	1.2	1.54	1.84	2.09	2.82	3.43	3.87	4.2	4.51	1.87	2.87	3.87	4.87	5.87	270	300	300	300	300	279	301	303	302	302
81B	0.78	1.16	1.53	1.82	2.07	2.8	3.44	3.85	4.18	4.48	1.75	2.75	3.75	4.75	5.75	270	300	285	300	300	286	306	299	305	304
81C	0.82	1.2	1.54	1.8	2.04	2.98	3.47	3.87	4.14	4.44	1.85	2.85	3.85	4.85	5.85	285	285	285	285	300	306	304	302	300	304
81D	0.9	1.28	1.59	1.83	2.06	3.24	3.56	3.92	4.17	4.45	1.85	2.85	3.85	4.85	5.85	285	285	285	300	300	302	299	297	301	300
81E	1.13	1.44	1.69	1.89	2.08	3.3	3.63	3.96	4.19	4.43	2.91	3.91	4.91	5.91	6.91	285	285	285	300	300	299	297	295	300	299

no2_fast

Point	Hs [m]					Tmm10 [s]					Water Depth [m]					Wind Direction [deg]					Wave Direction [deg]				
Design WL	0m	1m	2m	3m	4m	0m	1m	2m	3m	4m	0m	1m	2m	3m	4m	0m	1m	2m	3m	4m	0m	1m	2m	3m	4m
80A	0.94	1.27	1.52	1.76	1.98	2.93	3.35	3.7	4.03	4.32	2.16	3.16	4.16	5.16	6.16	300	300	300	300	300	297	301	302	301	301
80B	0.9	1.24	1.51	1.75	1.97	2.85	3.34	3.72	4.05	4.34	2.06	3.06	4.06	5.06	6.06	285	300	300	300	300	288	300	301	301	301
80C	0.87	1.21	1.5	1.76	2	2.78	3.32	3.73	4.08	4.38	1.95	2.95	3.95	4.95	5.95	270	300	300	300	300	278	300	302	302	301
80D	0.85	1.19	1.5	1.79	2.04	2.74	3.31	3.76	4.14	4.46	1.97	2.97	3.97	4.97	5.97	270	300	300	300	300	274	298	301	301	301
80E	0.73	1.11	1.44	1.76	2.04	2.62	3.22	3.78	4.17	4.51	1.58	2.58	3.58	4.58	5.58	270	270	300	300	300	275	279	300	301	300
81A	0.66	1.06	1.42	1.74	2.02	2.54	3.2	3.76	4.18	4.51	1.42	2.42	3.42	4.42	5.42	270	270	285	300	300	278	281	294	302	301
81B	0.59	0.99	1.37	1.71	2	2.46	3.24	3.78	4.15	4.48	1.3	2.3	3.3	4.3	5.3	270	300	300	300	300	285	305	306	305	304
81C	0.63	1.03	1.41	1.72	2	2.66	3.35	3.8	4.11	4.41	1.4	2.4	3.4	4.4	5.4	300	300	285	285	285	314	312	304	301	298
81D	0.7	1.13	1.49	1.76	2.01	3.11	3.51	3.9	4.15	4.42	1.4	2.4	3.4	4.4	5.4	300	285	285	285	285	307	301	299	296	294
81E	1.06	1.39	1.66	1.87	2.06	3.36	3.68	3.98	4.2	4.42	2.38	3.38	4.38	5.38	6.38	285	285	285	285	285	303	300	297	295	294

nour_fast

Point	Hs [m]					Tmm10 [s]					Water Depth [m]					Wind Direction [deg]					Wave Direction [deg]				
Design WL	0m	1m	2m	3m	4m	0m	1m	2m	3m	4m	0m	1m	2m	3m	4m	0m	1m	2m	3m	4m	0m	1m	2m	3m	4m
80A	0.99	1.27	1.53	1.77	1.97	2.93	3.33	3.68	4	4.33	2.41	3.41	4.41	5.41	6.41	285	300	285	285	300	290	299	294	294	301
80B	0.77	1.15	1.46	1.72	1.94	2.88	3.34	3.73	4.06	4.35	1.54	2.54	3.54	4.54	5.54	285	300	300	300	300	283	295	298	299	300
80C	0.5	0.93	1.33	1.68	1.96	2.57	3.32	3.77	4.12	4.42	0.91	1.91	2.91	3.91	4.91	270	300	300	300	300	276	296	299	300	300
80D	0.43	0.87	1.29	1.67	1.98	2.45	3.27	3.77	4.18	4.52	0.79	1.79	2.79	3.79	4.79	270	285	285	300	300	282	293	293	300	299
80E	0.38	0.82	1.24	1.6	1.91	2.37	3.21	3.74	4.13	4.48	0.71	1.71	2.71	3.71	4.71	270	285	285	300	300	291	293	293	299	299
81A	0.35	0.79	1.21	1.58	1.9	2.3	3.18	3.73	4.13	4.48	0.64	1.64	2.64	3.64	4.64	270	285	285	300	300	289	291	292	298	299
81B	0.36	0.8	1.22	1.59	1.92	2.3	3.17	3.75	4.14	4.48	0.64	1.64	2.64	3.64	4.64	270	270	285	300	300	290	286	293	300	300
81C	0.41	0.86	1.28	1.64	1.95	2.5	3.32	3.81	4.13	4.42	0.76	1.76	2.76	3.76	4.76	270	285	285	285	285	293	298	298	296	295
81D	0.65	1.09	1.49	1.78	2.03	3.08	3.56	3.93	4.17	4.43	1.21	2.21	3.21	4.21	5.21	285	300	285	285	285	301	304	297	295	294
81E	1.05	1.39	1.67	1.86	2.05	3.47	3.7	3.99	4.19	4.41	2.1	3.1	4.1	5.1	6.1	285	285	285	285	285	297	296	294	293	293

no_slow

Point	Hs [m]					Tmm10 [s]					Water Depth [m]					Wind Direction [deg]					Wave Direction [deg]				
Design WL	0m	1m	2m	3m	4m	0m	1m	2m	3m	4m	0m	1m	2m	3m	4m	0m	1m	2m	3m	4m	0m	1m	2m	3m	4m
80A	0.94	1.26	1.51	1.75	1.97	2.95	3.35	3.7	4.02	4.32	2.21	3.21	4.21	5.21	6.21	300	300	300	300	300	300	303	303	303	302
80B	0.91	1.24	1.51	1.76	1.97	2.92	3.36	3.72	4.06	4.35	2.15	3.15	4.15	5.15	6.15	300	300	300	300	300	299	302	303	302	302
80C	0.89	1.22	1.51	1.76	2	2.85	3.36	3.74	4.08	4.38	2.04	3.04	4.04	5.04	6.04	285	300	300	300	300	289	302	303	303	302
80D	0.88	1.21	1.52	1.8	2.04	2.79	3.36	3.78	4.15	4.46	2.06	3.06	4.06	5.06	6.06	270	300	300	300	300	275	300	301	302	301
80E	0.76	1.13	1.47	1.77	2.03	2.67	3.3	3.76	4.17	4.5	1.67	2.67	3.67	4.67	5.67	270	285	285	300	300	276	291	294	301	301
81A	0.69	1.09	1.44	1.75	2.01	2.6	3.24	3.77	4.17	4.5	1.51	2.51	3.51	4.51	5.51	270	270	285	300	300	278	281	294	302	302
81B	0.63	1.02	1.4	1.73	2.01	2.53	3.3	3.81	4.16	4.48	1.38	2.38	3.38	4.38	5.38	270	300	300	300	300	285	305	306	305	304
81C	0.66	1.06	1.43	1.74	2.01	2.75	3.4	3.81	4.12	4.41	1.49	2.49	3.49	4.49	5.49	300	300	285	285	285	314	312	303	301	298
81D	0.74	1.15	1.51	1.78	2.02	3.14	3.51	3.89	4.14	4.41	1.49	2.49	3.49	4.49	5.49	300	285	285	285	285	307	301	298	296	294
81E	1.01	1.34	1.63	1.85	2.05	3.2	3.58	3.93	4.16	4.4	2.54	3.54	4.54	5.54	6.54	285	285	285	285	285	300	298	296	295	294

no2_slow

Point	Hs [m]					Tmm10 [s]					Water Depth [m]					Wind Direction [deg]					Wave Direction [deg]				
Design WL	0m	1m	2m	3m	4m	0m	1m	2m	3m	4m	0m	1m	2m	3m	4m	0m	1m	2m	3m	4m	0m	1m	2m	3m	4m
80A	0.76	1.14	1.45	1.69	1.93	2.78	3.25	3.64	3.99	4.3	1.66	2.66	3.66	4.66	5.66	285	285	285	300	300	287	291	294	301	300
80B	0.71	1.1	1.41	1.68	1.92	2.7	3.21	3.66	4.01	4.32	1.57	2.57	3.57	4.57	5.57	285	285	300	300	300	285	290	300	300	300
80C	0.67	1.06	1.39	1.67	1.93	2.58	3.13	3.62	4.02	4.36	1.46	2.46	3.46	4.46	5.46	270	270	285	300	300	277	280	293	300	300
80D	0.66	1.03	1.37	1.68	1.96	2.49	3.11	3.65	4.07	4.43	1.48	2.48	3.48	4.48	5.48	270	285	300	300	300	273	286	299	300	300
80E	0.51	0.93	1.29	1.63	1.95	2.28	3	3.61	4.1	4.48	1.09	2.09	3.09	4.09	5.09	270	270	285	300	300	274	277	291	299	300
81A	0.44	0.87	1.25	1.6	1.93	2.14	2.95	3.59	4.09	4.48	0.93	1.93	2.93	3.93	4.93	270	270	285	300	300	276	279	292	301	301
81B	0.37	0.8	1.2	1.56	1.89	1.96	2.91	3.59	4.06	4.44	0.8	1.8	2.8	3.8	4.8	270	270	285	300	300	282	287	297	305	304
81C	0.4	0.84	1.24	1.59	1.89	2.28	3.12	3.67	4.05	4.43	0.91	1.91	2.91	3.91	4.91	315	300	285	285	300	322	313	305	302	305
81D	0.47	0.93	1.34	1.66	1.93	2.79	3.44	3.83	4.11	4.46	0.91	1.91	2.91	3.91	4.91	285	300	285	285	300	301	307	301	298	301
81E	0.87	1.24	1.57	1.81	2.02	3.22	3.63	3.96	4.19	4.41	1.89	2.89	3.89	4.89	5.89	285	285	285	285	285	304	303	299	296	295

nour_slow

Point	Hs [m]					Tmm10 [s]					Water Depth [m]					Wind Direction [deg]					Wave Direction [deg]				
Design WL	0m	1m	2m	3m	4m	0m	1m	2m	3m	4m	0m	1m	2m	3m	4m	0m	1m	2m	3m	4m	0m	1m	2m	3m	4m
80A	0.86	1.2	1.45	1.71	1.93	2.87	3.23	3.64	3.97	4.32	1.94	2.94	3.94	4.94	5.94	285	270	285	285	300	288	283	293	294	300
80B	0.58	1	1.36	1.64	1.89	2.71	3.24	3.65	4.03	4.33	1.07	2.07	3.07	4.07	5.07	270	285	285	300	300	274	286	290	298	298
80C	0.29	0.72	1.16	1.54	1.88	2.19	3.08	3.68	4.07	4.41	0.44	1.44	2.44	3.44	4.44	270	300	300	300	300	271	293	297	298	299
80D	0.21	0.67	1.11	1.51	1.88	1.92	2.96	3.65	4.12	4.51	0.32	1.32	2.32	3.32	4.32	270	270	285	300	300	272	286	293	299	299
80E	0.15	0.62	1.05	1.45	1.8	1.81	2.92	3.61	4.07	4.46	0.24	1.24	2.24	3.24	4.24	270	270	285	300	300	289	289	293	298	299
81A	0.12	0.59	1.02	1.42	1.79	1.71	2.87	3.59	4.07	4.46	0.17	1.17	2.17	3.17	4.17	270	270	285	300	300	284	288	291	297	298
81B	0.12	0.59	1.03	1.43	1.8	1.72	2.85	3.61	4.08	4.46	0.17	1.17	2.17	3.17	4.17	270	270	285	300	300	284	288	292	300	300
81C	0.18	0.65	1.09	1.49	1.85	1.94	3.05	3.68	4.08	4.41	0.29	1.29	2.29	3.29	4.29	270	270	285	285	285	294	292	298	297	295
81D	0.42	0.9	1.33	1.68	1.97	2.78	3.44	3.86	4.15	4.43	0.74	1.74	2.74	3.74	4.74	300	300	285	285	285	306	305	299	296	294
81E	0.86	1.26	1.59	1.81	2.01	3.38	3.69	3.99	4.18	4.4	1.63	2.63	3.63	4.63	5.63	285	285	285	285	285	297	297	295	294	293

DESIGN CHARTS FOR ASPHALT REVETMENTS

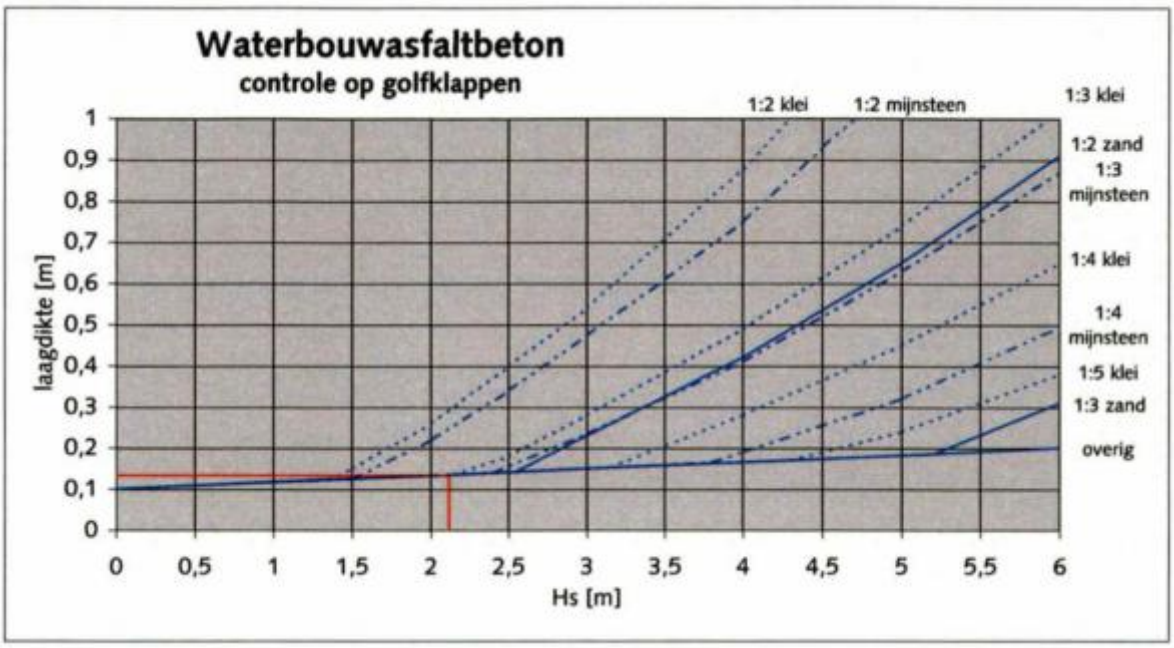

FIGURE C.1: DESIGN CHART FOR HYDRAULIC ASPHALT USED IN VAN DER VLIET (2010).

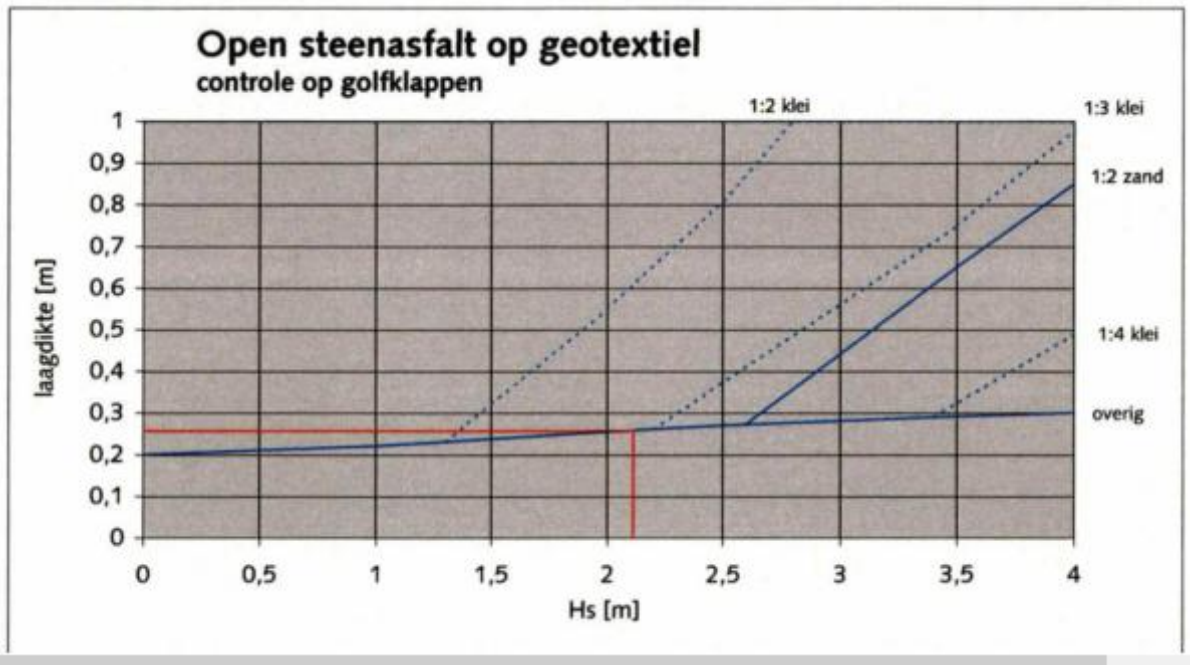

FIGURE C.2: DESIGN CHART FOR OPEN STONE ASPHALT USED IN VAN DER VLIET (2010).

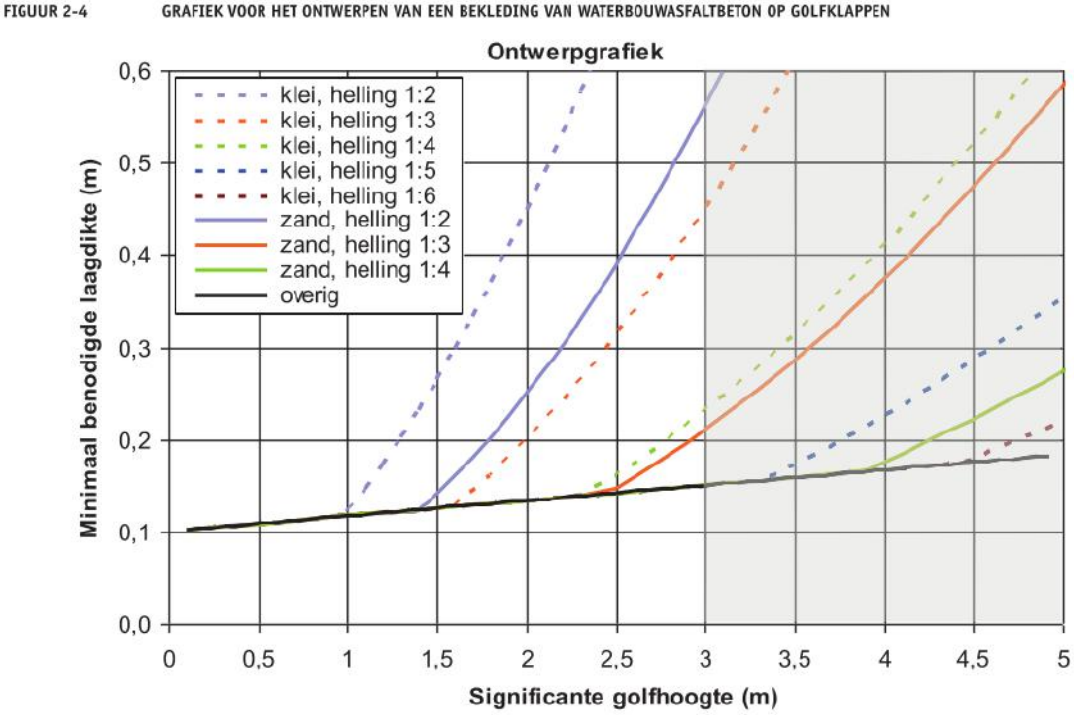

FIGURE C.3: DESIGN CHART FOR HYDRAULIC ASPHALT USED IN DAVIDSE ET AL. (2010).

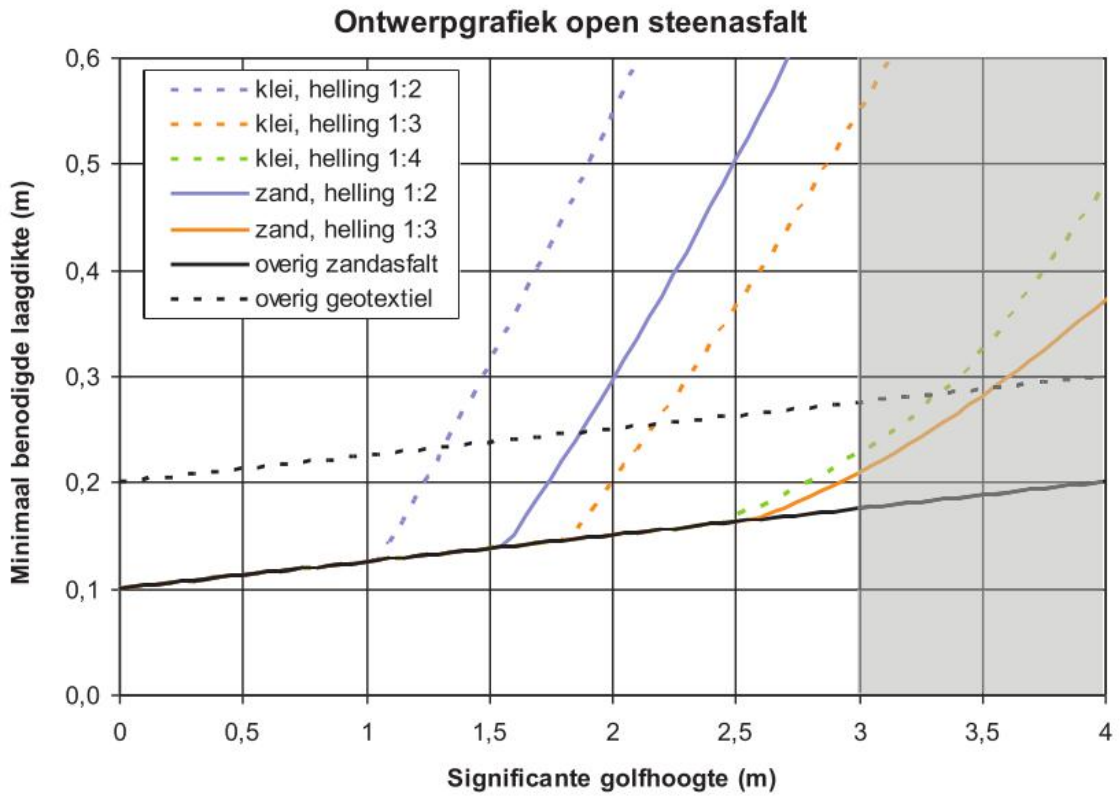

FIGURE C.4: DESIGN CHART FOR OPEN STONE ASPHALT USED IN DAVIDSE ET AL. (2010).

WAVE LOAD PLOTS

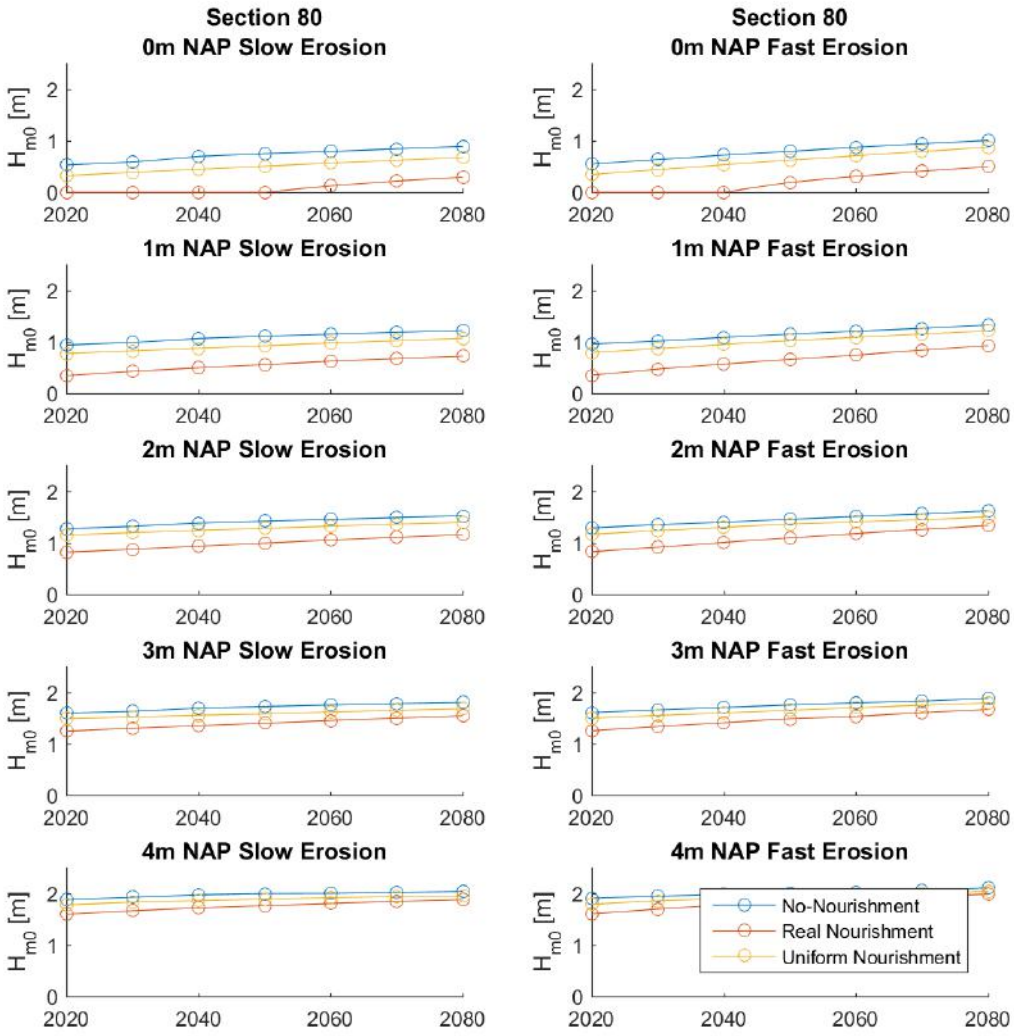

FIGURE C.5: LOAD FUNCTION Z0=HS. PROJECTED TO 2080 IN THE SLOW AND FAST EROSION PROJECTION SCENARIOS. SECTION 80 OF THE OESTERDAM.

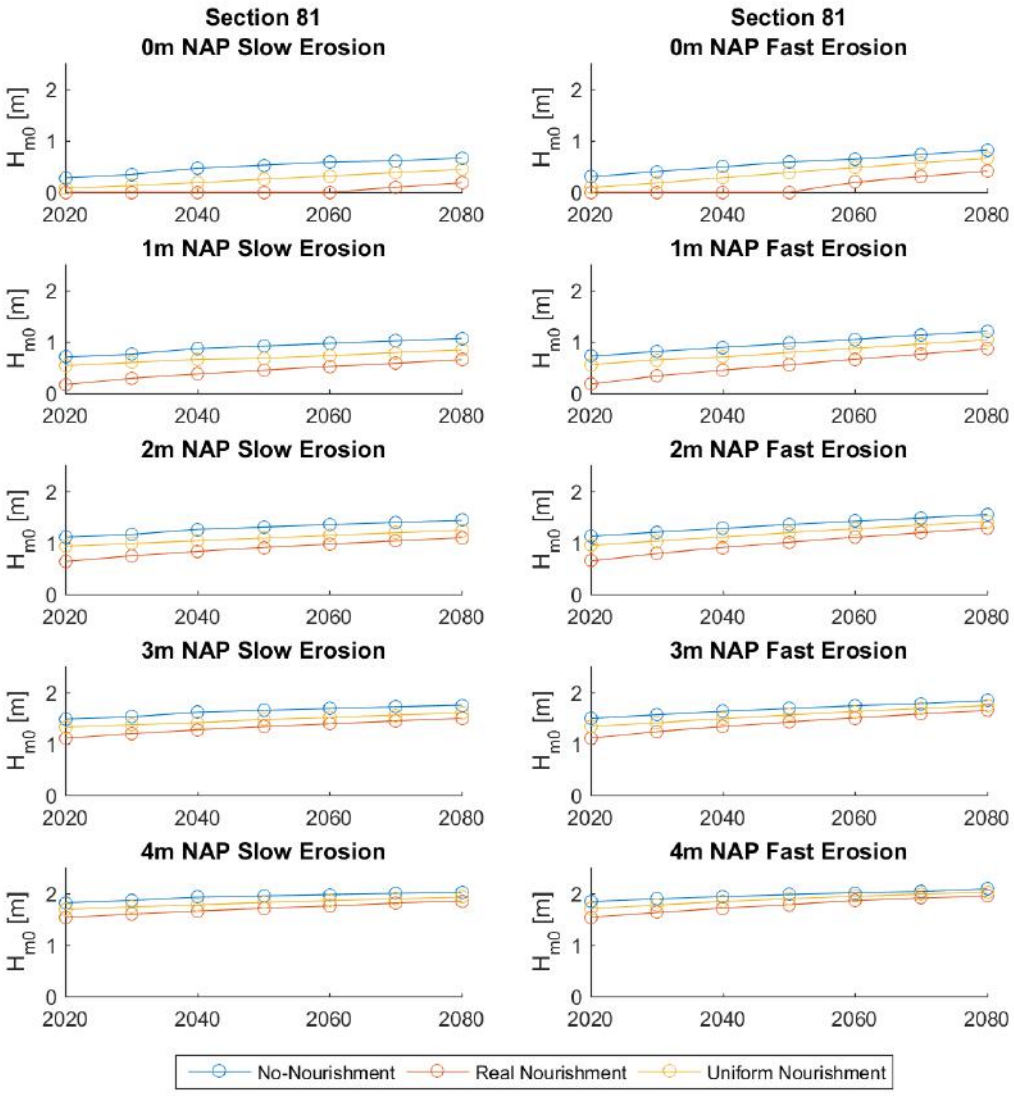

FIGURE C.6: LOAD FUNCTION Z0=HS. PROJECTED TO 2080 IN THE SLOW AND FAST EROSION PROJECTION SCENARIOS. SECTION 81S OF THE OESTERDAM.

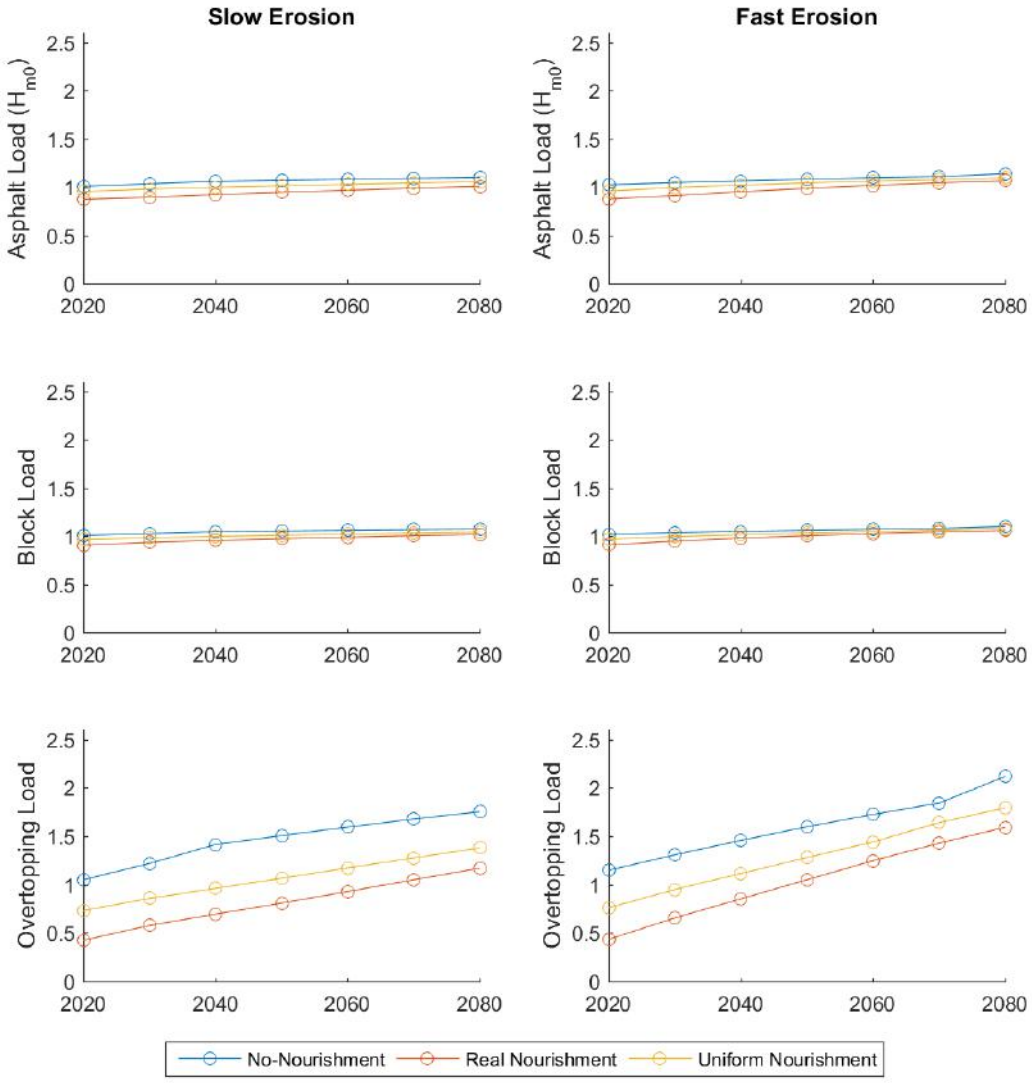
Slow Erosion
Fast Erosion
Asphalt Load (H_{m0})
Block Load
Overtopping Load
2020
2040
2060
2080
No-Nourishment
Real Nourishment
Uniform Nourishment

FIGURE C.7